In vitro osteogenic differentiation of mesenchymal stem cells

By

Jamie Mollentze

15086128

Submitted in the fulfilment of the requirements for the degree in

Master of Science (Medical Immunology)

In the faculty of Health Sciences,

Department of Immunology, School of Medicine,

University of Pretoria

2022

Supervisor: Prof. Michael S. Pepper

Co-Supervisor: Dr. Chrisna Durandt

Contact Information

MSc Candidate

Jamie Mollentze

Student number: 15086128

E-mail: *u15086128@tuks.co.za*

Supervisor

Prof. M.S. Pepper

Institute for Cellular and Molecular Medicine, Department of Immunology

Faculty of Health Sciences, University of Pretoria

E-mail: *michael.pepper@up.ac.za*

Co-Supervisor

Dr. C. Durandt

Institute for Cellular and Molecular Medicine, Department of Immunology

Faculty of Health Sciences, University of Pretoria

E-mail: *chrisna.durandt@up.ac.za*

Declaration of Originality

I, **Jamie Mollentze,** hereby declare that this dissertation entitled:

In vitro osteogenic differentiation of mesenchymal stem cells

which I herewith submit to the University of Pretoria for the Degree of Master of Science in Human Physiology, is my own original work and has never been submitted for any academic award to any other tertiary institution for any degree.

Date: 20 October 2022   **Signature:** Jamie Mollentze

Research Outputs

Articles

Jamie Mollentze, Chrisna Durandt, Michael S. Pepper, "An *In Vitro* and *In Vivo* Comparison of Osteogenic Differentiation of Human Mensenchymal Stromal/Stem Cells", Stem Cells International, vol. 2021, Article ID 9919361, 23 pages, 2021. https://doi.org/10.1155/2021/9919361.

Poster

2022: University of Pretoria's Faculty Day
Human alternatives to foetal bovine serum suitable for osteogenic differentiation of adipogenic-derived stem/stromal cells

Acknowledgments

To my supervisor, Prof Pepper; thank you for making me a part of the Institute of Cellular and Molecular Medicine and for the opportunity to take part in the exciting research of regenerative medicine. Thank you for all the guidance along the way and keeping my best interests at heart. I remember coming to see you in my matric year as I was so fascinated with the idea of stem cells, and you set me on my academic journey. After 3 years of undergraduate and 1 year of honours studies I finally ended up where I always dreamt, I was going to be. Thank you for the continuous support and for making my dream a reality.

To my co-supervisor, Dr Chrisna Durandt, your guidance and support through these last few years is truly appreciated. You have always grounded me and kept reminding me to stick to my basics when I had wild ideas. Thank you for teaching me the ins and outs of the complicated world of flow cytometry.

Mrs Candice Murdoch, you truly helped me complete this Master's degree. From listening to all my failures to helping me come up with solutions to most of my problems. Thank you for helping me with concentration calculations when my brain was so tired that it couldn't even comprehend a simple $C_1V_1=C_2V_2$ calculation.

Thank you to Carolina Strydom at SANBS for all the help in collection Platelet-rich Plasma as well as the willing donors that donated their platelets.

I would like to thank the South African Medical Research Council (SAMRC), who provided the financial support for this research project.

To my colleagues: Aurona Gerber, Candice Murdoch, Candice Herd, Candice Hendricks, Priyanka Dhanraj and Rachel Giles. I appreciate all the tea breaks, lunch breaks and brainstorming sessions.

To my best friend, Kinosha Moodley. Thank you for being you. Thank you for keeping me sane through the tough times. Thank you for all the sleepovers and the late-night chats. Thank you for all the presentations you listened to and all the documents you proofread. You have taught me to never give up and keep pushing no matter what. You are such a strong and inspiring woman, and I will always strive to be as strong as you.

To my mom, dad, and sister. No words can describe the support you have given me through this journey. Thank you for checking up on me when I was spending late nights at the lab. To all the tears of joy and heart break when my "selltjies" died or got infected with fungus. Thank you for letting me drag you with to the lab from time to time just to keep me company. Thank you for all the proofreads and making sense of all my gibberish. Thank you for listening to every one of my presentations. Thank you, thank you thank you!

To the love of my life, rock and my other best friend, Hannes. Thank you for always believing in me supporting me no matter what. You are always able to put a smile on my face. Thank you for letting me unload on you, no matter how big or small the weight. Your always celebrated my wins, comforted me through my failures and got just as frustrated with me when my experiments did not work out. You always kept me level-headed and kept me focused on the end goal whenever there was doubt. Thank you for everything, love you always!

Table of Contents

List of Figures

Chapter 2: Literature Review

Chapter 3: Isolation of primary ASCs

Chapter 4: Optimal Osteogenic Differentiations Medium

Chapter 5: Human Alternative to Foetal Bovine Serum

List of Tables

List of Equations

Abbreviations, Symbols and Units

Abbreviation	Definition
3D	Three-Dimensional
7AAD	7-Aminoactinomycin D
ALP	Alkaline phosphatase
APC	Allophycocyanin
APC Cy7	Allophycocyanin cayanin dye -7 tandem conjugate
ARS	Alizarin Red S
ASCs	Adipose-derived stromal/stem cells
Atf4	Activating transcription factor 4
BM	Bone marrow
β-ME	Beta-mercaptoethanol
BM-MSCs	Bone marrow-derived MSCs
BMP	Bone morphogenetic protein
BP	Band-pass
BSP	Bone sialoprotein
BV421	Brilliant violet 421
CD	Cluster of differentiation
CGM	Complete growth medium
Cp/Cq	Crossing point
C_T	Threshold cycle
DAPI	4',6-Diamidino-2-phenylindole
Dkk	Dickopf
Dlx5	Distal less homeobox 5
DMEM	Dulbecco's Modified Eagle Medium
Dmp1	Dentin matrix acidic phosphoprotein 1
DMSO	Dimethyl sulfoxide
dNTP	Deoxynucleoside triphosphates
ECM	Extracellular matrix
ESCs	Embryonic stem cells
FBS	Foetal bovine serum
FFP	Freshly frozen plasma
FGF	Fibroblast growth factor
FITC	Fluorescein Isothiocyanate
FL	Fluorescence channel
FRZB	Frizzled-related protein
FSC	Forward scatter
gDNA	Genomic DNA
GMP	Good Manufacturing Practice
HA	Hydroxyapatite
HLA	Human leukocyte antigen
HOXB7	Homeobox protein Hox-B7
HS	Human serum
HSCs	Haematopoietic stem cell

ICMM	Institute for Cellular and Molecular Medicine	
IGF	Insulin-like growth factor	
iPCs	Induced pluripotent stem cells	
ISCT	International Society for Cellular Therapy	
KO	Krome Orange	
LPL	Lipoprotein lipase	
M-CSF	Macrophage-colony stimulating factor	
Min	Minutes	
ml	Millilitre	
mRNA	Messenger RNA	
MSCs	Mesenchymal stromal/stem cells	
nm	Nanometer	
NRT	No reverse transcriptase	
NTC	No template control	
OA	Ostheoarthritis	
OCN	Osteocalcin	
OPG	Osteoprotegerin	
Opn	Osteopontin	
OSX	Osterix	
PBS	Phosphate-buffered saline	
PC5	Phycoerythrin-Cyanin 5	
PDGF	Platelet-derived growth factor	
PE	Phycoerythrin	
Pen/strep	Penicilin/streptomycin	
pHPL	Pooled human platelet lysate	
PPARγ	Peroxisome proliferator-activated receptor	
PPP	Platelet-poor plasma	
PRP	Platelet-rich plasma	
RANK/L	Receptor activator of nuclear factor kappa-B/ligand	
RIN	RNA integrity number	
RNA	Ribonucleic acid	
RT-qPCR	Quantitative reverse transcription polymerase chain reaction	
RUNX2	Runt-related transcription factor 2	
s	Seconds	
SANBS	South African National Blood Service	
SD	Standard deviation	
SEM	Standard error of mean	
SIBLING	Small integrin-binding ligand N-linked glycoprotein	
SVF	Stromal vascular fraction	
TBP	Tata binding protein	
Tm	Prmer melting temperature	
UC-MSCs	Ubilical cord derived MSCs	
v/v	Volume/volume	
VDC	Vybrant® DyeCycle™	
VEGF	Vascular endothelial growth factor	

vs.	Versus	
w/v	Weight/volume	
YWHAZ	Tyrosine 3-monooxygenase/tryptophan 5-monooxygenase activation protein, zeta	
Greek Symbols		
α	Alpha	
β	Beta	
γ	Gamma	
μ	Micro	

Chapter 1: Executive Summary

The use of adipose-derived stromal/stem cells (ASCs) continues to increase in the field of regenerative medicine and other clinical applications. Adipose tissue can be collected in a less invasive procedure, when compared to bone marrow aspirations, from patients undergoing cosmetic liposuction or abdominoplasty procedures either as an aspirate or as intact tissue. Adipose tissue is seen as medical waste that would otherwise been discarded. ASCs are seen as the one of the most promising stem cell populations for tissue regeneration as they can be harvested with relative ease, can yield large quantities, grow under standard cell culture conditions, differentiate into multiple lineages, and secrete various cytokines.

One of the clinical applications of ASCs is their role in enhancement of bone regeneration. To achieve osteogenic differentiation of ASCs, the ASCs are exposed to a differentiation cocktail containing β-glycerophosphate, ascorbate-2-phosphate and dexamethasone. Currently there is no consensus regarding the most optimal osteogenic differentiation medium for *in vitro* osteogenic differentiation of mesenchymal stromal/stem cells (MSCs), and the concentrations of the stimulating factors vary amongst published osteogenic induction media. It is for this reason we tested 3 previously published osteogenic differentiation media with varying concentrations of β-glycerophosphate, ascorbate-2-phosphate and dexamethasone. The success of the different differentiation cocktails was assessed using two osteogenic assays namely Alizarin Red S (ARS) and alkaline phosphatase (ALP) which were used to quantify the amount of calcified product and ALP enzyme activity respectively. Of the three differentiation media, one differentiation medium that produced the best osteogenic differentiation was chosen for further downstream testing.

Foetal bovine serum (FBS) has been the gold standard for medium supplementation when expanding ASCs *ex vivo* despite the many disadvantages associated with its use, such as batch-to-batch variability, the presence of xenogenic proteins, possibility of zoonotic disease transmission, and ethical concerns regarding animal welfare to name a few. Furthermore, for ASCs to be used in a clinical setting, they need to comply with Good Manufacturing Practice (GMP) guidelines, which strongly advise against the use of FBS in clinical-grade cell therapy products. For this reason, researchers and clinicians continue to seek optimal and GMP

compliant alternatives to FBS. Human alternatives to FBS will not only overcome FBS-associated disadvantages, but also more accurately mimic the environmental niche thus making the cell therapy product more physiologically compatible and consequently more reliable when applied clinically.

The current study explored the use of two human alternatives to FBS namely platelet-rich plasma (PRP) and pooled human platelet lysate (pHPL) for use in osteogenic differentiation of ASCs *in vitro*. ASCs were expanded and differentiated in medium supplemented with either FBS, PRP or pHPL. Again, the two osteogenic assays, ARS and ALP were used to determine the success of osteogenic differentiation. To examine the kinetics of osteogenic gene expression, RNA was isolated at 4 time points during the differentiation period (days 0, 7, 14 and 21) and quantitative reverse transcription polymerase chain reaction (RT-qPCR) was performed. We found that both human alternatives were superior to FBS supplemented medium in terms of the amount of calcified bone product produced and the rate at which osteogenesis occurred. RT-qPCR data revealed that cells grown in FBS take longer to switch from a proliferative to an osteogenic differentiation state. Results revealed that PRP and pHPL are effective substitutes to FBS when differentiating ASCs into osteoblasts, and that this can effectively be assessed in the therapeutic setting.

The aim of this study is to optimize and standardize protocols to differentiate MSCs into osteoblasts.

The objectives of this study include:
1. To isolate MSCs from adipose tissue.
2. To establish standardized quantitative assays for osteoblast differentiation of MSCs *in vitro* using microscopy and gene expression.
3. To test a range of different osteogenic differentiation media to determine which medium is optimal for ASC-induced osteogenesis using microscopy and gene expression.
4. To test two human alternatives to FBS including platelet rich plasma and pooled human platelet lysate, to determine which is optimal for MSC-induced osteogenesis using microscopy and gene expression.

5. To differentiate MSCs from adipose tissue into osteoblasts using the optimal osteogenic medium and the optimal human alternative.

Chapter 2: Literature Review

Disclosure

Parts of this literature review has been published as a review article in Stem Cells International Journal. The sections that were copied verbatim from the review are indicated using italic font.

Jamie Mollentze, Chrisna Durandt, Michael S. Pepper, "An In Vitro and In Vivo Comparison of Osteogenic Differentiation of Human Mesenchymal Stromal/Stem Cells", Stem Cells International, vol. 2021, Article ID 9919361, 23 pages, 2021. https://doi.org/10.1155/2021/9919361.

Author contributions

Jamie Mollentze: Writing- Original draft preparation, Investigation, Visualization.
Chrisna Durandt: Writing- Review and editing.
Michael S. Pepper: Writing- Review and editing.

2.1. Defining stem cells

Stem cells are unspecialized cells which simultaneously possess self-renewal and differentiation ability. For this reason, stem cells have been the focus of cell based therapy in the field of regenerative medicine [1]. Regenerative medicine makes use of the ability of stem cells to differentiate into various cell types, replacing damaged or dysfunctional cells at the site of injury, and in doing so, restoring the function and structure of the damaged tissue or organ [2]. The stem cells received from donors used in regenerative medicine can either be autologous or allogeneic. Autologous refers to stem cells that are taken from an individual and later given back to that same individual whereas allogeneic refers to stem cells taken from a donor whose human leukocyte antigen (HLA) has an acceptable level of compatibility to that of the patient i.e. a relative or a person found on a donor registry [3,4].

The term 'potency' refers to the ability of stem cells to differentiate into multiple lineages. There are four potency levels: totipotent, pluripotent, multipotent and unipotent, listed from

most to least potent. Totipotent cells give rise to all embryonic and extra-embryonic cells and are derived from zygotes/blastomeres [5]. Pluripotent stem cells are derived from blastocysts and are termed "master cells" as they can differentiate into any cells of the three embryonic germ layers [6]. Multipotent stem cells can be described as cells that reside in a specific site, e.g. bone-marrow, and are only able to differentiate into a restricted number of cell types. Both haematopoietic stem cells (HSCs) and MSCs are examples of multipotent stem cells [7,8]. Lastly, cells whose differentiation is limited to one cell type and which have limited self-renewing ability, such as germ line stem cells responsible for sperm production, are known as unipotent stem cells [6]. Table 2.1 compares features of totipotent, pluripotent, multipotent and unipotent stem cells.

From a therapeutic perspective, stem cells are divided into two categories: pluripotent stem cells and adult stem cells. Pluripotent cells include embryonic stem cells (ESCs) and induced pluripotent stem cells (iPSCs). Embryonic stem cells are usually isolated from the inner cell mass of a pre-implantation blastocyst obtained during *in vitro* fertilization [9]. Induced pluripotent stem cells (iPCs) are adult stem cells that have been genetically reprogrammed *in vitro* into pluripotent stem cells [10]. Briefly, iPSCs are produced by taking somatic cells and reprogramming them to express Myc, Oct3/4, Sox2 and Klf4. By encoding these transcription factors, the somatic cells are converted into pluripotent stem cells. Induced pluripotent stem cells are very similar to ESCs at the cellular level as they also have a self-renewing ability and the ability to differentiate into the three different germ lines, however iPSCs have less ethical concerns than ESCs [11].

Adult stem cells are found throughout the body in a variety of tissues and organs. Adult stem cells can either be multipotent or unipotent. As mentioned before, multipotent adult stem cells are able to differentiate into various cell types of the mesodermal layer [12]. Unipotent adult stem cells are only able to repair or replace damaged tissue of the same origin as the adult stem cell, i.e. satellite cells found in skeletal muscle can only differentiate into skeletal muscle cells as seen in muscle regeneration [13]. MSCs, HSCs and neural stem cells are three examples of multipotent adult stem cells. In this study, we will be investigating mesenchymal stromal/stem cells.

Table 2.1 Comparison of stem cell potency.

	Totipotent	Pluripotent	Multipotent	Unipotent
Terminology	Toti = Whole	Pluri = Many	Multi = Several	Uni = One
Relative potency	High	Medium	Low	Very low
Cell types	Any cell type	Any cells of the three germ lines	Limited number of cell types	Only differentiate into one specific cell type
Origin	Cells of zygote	Inner cell mass of blastocyst	Multiple tissues	Multiple tissues
Expression of pluripotent genes	++++	+++	++	+
Expression of lineage specific genes	+	++	+++	++++
Advantages of use in research	Isolation and culture process is relatively easy	Isolation and growth process is relatively easy	Less ethical concerns	Less ethical concerns
Disadvantages of use in research	Ethical limitations	Ethical limitations and concerns of teratoma formation	Limited differentiation ability, difficult to isolate	Limited differentiation ability
Examples	Zygotes/Blastomeres	Embryonic and induced pluripotent stem cells	Mesenchymal, haematopoietic, neural stem cells, and satellite cells	Germline stem cells that produce sperm in the testes

2.2. Mesenchymal stem/stromal cells

MSCs contain a population of multipotent adult stem cells capable of differentiating into cell types of mesodermal origin [14]. *MSCs were initially isolated from bone marrow (BM) and are in this setting referred to as bone marrow-derived MSCs (BM-MSC)*[15]. *Since then, human MSCs have been isolated from various foetal and adult tissues, such as adipose tissue* [16], *the amniotic membrane* [17], *amniotic fluid* [18], *placental and foetal membranes* [19], *umbilical cord lining membrane* [20], *the endometrium* [21], *dental tissue* [22], *menstrual blood* [23], *peripheral blood* [24], *skin* [25], *synovial fluid* [26], *Wharton's jelly* [27] *and others.*

It is well accepted that isolated MSC populations are heterogeneous, containing both stem cells and mature stromal cells. Even though the terms mesenchymal stem cells and mesenchymal stromal cells are used interchangeably [14], *there are distinct differences between the two. Mesenchymal stem cells possess the ability to self-renew and differentiate, demonstrating the functionality of true stem cells, while the term 'mesenchymal stromal cells' refer to a heterogeneous populations of progenitor cells at various stages of maturation. Directly after isolation, the isolated cell population may also contain differentiated cells present in the tissue microenvironment such as endothelial cells, pericytes, fibroblasts and immune cells, as well as various haematopoietic cells* [28–30].

2.2.1. Characterization of MSCs

All MSCs, independent of their source, should adhere to minimal criteria recommended by the International Society for Cellular Therapy (ISCT). These include (a) the ability to adhere to plastic; (b) the expression of a specific set of cell surface markers such as cluster of differentiation (CD)73, CD90, CD105 or CD13 and the lack of CD14, CD19, CD31, CD45 and human leukocyte antigen (HLA)-DR; and (c) the ability to differentiate into at least adipocytes, osteoblasts and chondrocytes in vitro [31]. *Many studies have suggested that the expression of CD34 is variable and therefore MSCs can either be positive or negative for CD34* [31–33]. *Currently, there is no cell surface protein specific to MSCs and MSCs isolated from different sources may differ regarding cell surface protein expression profiles. Table 2.2*

summarizes the different cell surface markers that are associated with MSCs isolated from different tissue sites.

Table 2.2 Cell surface markers expressed by MSCs isolated from different tissues.

Source	Cell Surface Marker		Reference
	Positive	Negative	
Adipose tissue	CD10, CD13, CD29, CD34, CD44, CD49e, CD59, CD71, CD73, CD90, CD105, CD166, CD200, HLA-ABC	CD11b, CD14, CD19, CD31, CD34, CD45, CD56, CD146, CD235a, Stro1, HLA-DR	[16,34–37]
Amniotic membrane and fluid	CD29, CD44, CD73, CD90, CD105, SH2-4 HLA-ABC	CD11b, CD10, CD14, CD19, CD20, CD34, CD45, CD79a, HLA-DR	[18,38–40]
Bone marrow	CD29, CD44, CD73, CD90, CD105, CD271, Stro-1	CD14, CD34, CD45, HLA-DR	[31,35,41,42]
Dental tissue	CD29, CD34, CD44, CD73, CD90, CD105, CD105, CD117, CD166, Stro1	CD11b, CD14, CD19, CD31, CD34, CD45, CD79a, CD146, HLA-DR	[22,41,43,44]
Endometrium	CD44, CD49d, CD479f, CD73, CD90, CD105, CD146	CD14, CD19, CD34, CD45, HLA-DR	[21,45]
Peripheral blood	CD29, CD73, CD90, CD105, CD106, CD146, CD166,	CD34, CD45, CD133	[24,46,47]
Placental and foetal membrane	CD29, CD73, CD90, CD105	CD34, CD45	[19]
Skin	CD29, CD44, CD73, CD90, CD105, CD166	CD14, CD34, CD45, HLA-DR	[25,48]
Synovial fluid	CD44, CD73, CD90, CD105, CD147, Stro-1	CD11b, CD14, CD19, CD31, CD34, CD45, CD79a, CD106, HLA-DR	[26,39]
Umbilical cord lining membrane	CD29, CD44, CD73, CD90, CD105, CD106, HLA-I	CD14, CD31, CD34, CD45, HLA-DR	[16,20,49]
Wharton's jelly within umbilical cord	CD73, CD90, CD105	CD14, CD19, CD34, CD45, CD79, HLA-DR	[27,50]

2.2.2. Adipose derived stem/stromal cells

MSCs were initially isolated from bone marrow and has been the standard practice for many years, but this might not be the most optimal source from which to harvest MSCs for future clinical applications as bone marrow aspirations are known to be highly invasive and painful [15,51,52]. The invasive nature of bone marrow aspirations does not adhere to the criteria set by Gimble *et al.* 2017 [53]. Gimble *et al.* 2017 states that; (1) the harvesting process should be done through a minimally invasive process, (2) MSCs should be harvested in large

therapeutic quantities, (3) that MSCs used in regenerative medicine should show multilineage potential, (4) the transplantation of these cells must be done under safe and effientient protocols that minimizes the risk of pathogen exposure in both autologous and allogeneic conditions, and lastly (5) the manufactured cells should adhere to current GMP guidelines.

Zuk *et al.* 2001 [54] characterized the first ASCs, which are MSCs that have been harvested from adipose tissue, in 2001 and together with the work of Gimble *et al.* 2017 suggests that adipose tissues is a more acceptable source of MSCs as large quantities can be isolated from resected fat or lipoaspirates from cosmetic surgeries. Adipose-derived stromal/stem cells exhibit similar characteristics as BM-derived MSCs, such as multipotent differentiation potential and plastic adherent properties [53,55]. Adipose-derived stromal cells are specifically isolated from the stromal vascular fraction (SVF) [34]. The SVF is a component of lipoaspirate that is obtained by enzymatically digesting adipose tissue with collagenase, washing the tissue with phosphate-buffered saline (PBS) and collecting the cells by centrifugation. The SVF contains a wide range of cells including ASCs, HSCs, endothelial cells, fibroblasts, erythrocytes and immune cells such as monocytes, macrophages and lymphocytes [34].

2.3. Alternative serum supplementation

A limit to in vitro cell culturing is the use of foetal bovine/calf serum (FBS/FCS) as a supplement to cell culture medium to ensure optimal cell proliferation [56]. *Although commonly used, FBS/FCS-supplemented growth media are associated with number of disadvantages. First, FBS/FCS shows batch-to-batch variation due to the variable composition of the product, and thus results are often not reproducible* [57]. *Furthermore, FBS/FCS is xenogeneic and contains bovine proteins that can potentially elicit an immune response in humans* [58]. *The transmission of zoonotic diseases is also a possibility and thus also a primary concern when culturing cells in FBS/FCS; cells that have been cultured in FBS/FCS can therefore not be used clinically* [59].

Due to the disadvantages associated with FBS/FCS, the use of human blood products in cell culture medium as alternatives to animal serum is becoming increasingly popular [60,61]. *In short, blood is separated by centrifugation into its components i.e., platelets, growth*

factors, fibrin, etc., which are separated from erythrocytes [62]. *Some of these blood products include human serum (HS), platelet-rich plasma (PRP), platelet-poor plasma (PPP), fresh frozen plasma (FFP) and human platelet lysate (HPL).*

Both human serum and plasma are the liquid portion of whole blood. The difference between serum and plasma is the presence of clotting factors. *Human serum (HS) is produced by taking whole blood donated by a patient, allowing it to clot after which the clotted blood is centrifuged to produce serum that is devoid of platelets, erythrocytes and leukocytes* [63]. *Plasma is also produced by centrifuging whole blood containing an anti-coagulant to produce the non-cellular liquid part of whole blood known as plasma* [64].

It has been reported that ASC cultures maintained in HS, the cells show an extended lifespan, accelerated growth and clonogenic potential. Furthermore, it has been reported that there are no differential potential and senescence marker expression differences observed between cells cultured in FBS and cells cultured in HS [65]. However, one of the disadvantages that have been associated with HS is the limited availability of large quantities of autologous HS. This limitation can be overcome by pooling HS from different patients to produce large quantities of allogeneic HS for clinical applications. To ensure that the product is acceptable for clinical applications, blood banks perform strict quality checks as well as disease screening before releasing allogeneic HS [66].

Two human alternatives can be prepared from plasma: PRP and PPP. The difference is the concentration of platelets present in the product. *Platelets are anucleated, disc-shaped cell fragments that play a role in cell growth, differentiation and tissue regeneration* [67]. *When preparing PRP, whole blood is centrifuged and the supernatant (plasma) is centrifuged again* (high-speed centrifugation) *to collect a platelet pellet, the platelet pellet is then re-suspended in a smaller volume of plasma to produce PRP* [68]. *Alternatively, PRP can be collected via apheresis* [69]. *PPP is prepared by removing platelets from the plasma obtained from whole blood.* PPP thus has low levels of platelet-derived growth factor (PDGF) and will usually require the addition of growth factors [70]. Both PRP and PPP have been shown to increase ASC proliferation compared to FBS, and are considered to be an alternative to FBS [70,71]. *Fresh frozen plasma (FFP) is obtained by rapidly freezing plasma separated from whole blood*

at -65°C [72]. Mitra *et al.* 2014 determined that ASCs maintained in low glucose Dulbecco's Modified Eagle Medium (DMEM), with 5% (v/v) of FFP, resulted in a higher ASC proliferation rate than ASCs grown in FBS supplemented medium [72].

Lastly, to produce HPL, PRP is submitted to several freeze-thaw cycles to rupture the platelets releasing growth factors, followed by centrifugation to remove cell debris [69]. *The various human alternatives provide unique advantages and disadvantages with regard to culturing MSCs in vitro by providing suitable growth factors and ensuring genomic stability* [64]. ASCs cultured in HPL also show increased cell proliferation and differentiation rate when compared to FBS [73]. It has also been reported that ASCs cultured in HPL show neither chromosomal abnormalities nor any changes in immunophenotype [74].

2.4. Osteogenic differentiation

Osteogenesis can be divided into intramembranous and endochondral ossification processes. Intramembranous ossification occurs in the craniofacial bones and clavicle and involves the direct differentiation of MSCs into osteocytes to form bone, while endochondral ossification involves the differentiation of MSCs into chondrocytes to form cartilage, which then forms a template for bone formation. Endochondral ossification is responsible for the formation of the long, short and irregular bones that form part of the axial and appendicular skeleton [75].

Bone is a highly dynamic tissue and involves the constant build up and breakdown of bone tissue known as bone remodelling. Bone is composed of both cells (osteocytes, osteoblasts and osteoclasts) and an extracellular matrix that is mineralized by the deposition of calcium hydroxyapatite [76]. *Bone matrix homeostasis is monitored and maintained by mature bone cells known as osteocytes* [77]. *When matrix microdamage occurs, such as in a fracture, disruption of osteocyte canaliculi leads to the paracrine release of cytokines and other mediators by osteocytes, attracting osteoclasts to the site of injury/defect* [78,79]. *Osteoclastogenesis (osteoclast differentiation) from mononuclear osteoclast precursors can also be induced by the secretion of receptor activator of nuclear factor kappa-B ligand (RANKL) and macrophage-colony stimulating factor (M-CSF) by surrounding stromal and osteoblast cells* [80,81]. *Osteoclasts secrete a collagen digesting enzyme and an acidic hydrogen ion mixture that dissolves the calcium phosphate in the defective bone tissue, a process known as*

bone resorption [82]*. Once the defective bone tissue is cleaned out, macrophage-like cells smooth the resorbed bone tissue in preparation for matrix deposition* [81]*. Osteoclasts then recruit bone-forming cells termed osteoblasts before they undergo apoptosis. Osteoblasts are responsible for synthesizing components of the bone matrix, such as type I collagen, proteoglycan and alkaline phosphatase (ALP), to name a few* [76]*. By balancing bone resorption and bone formation, bone homeostasis is maintained (Figure 1).*
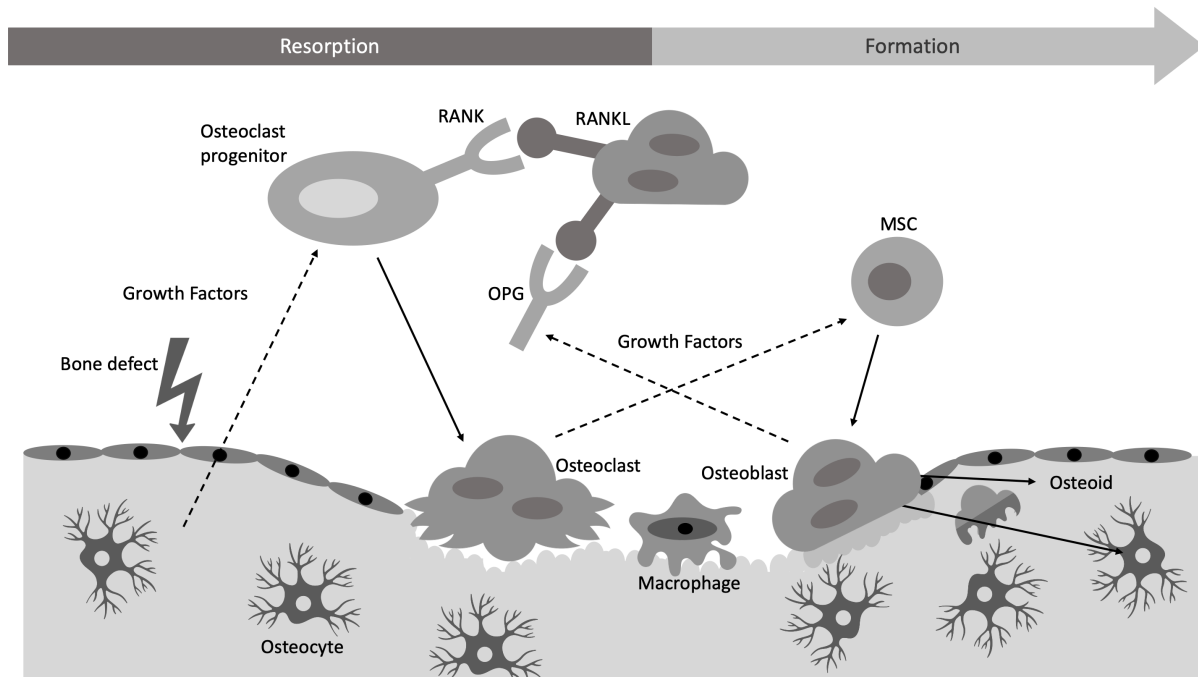
Figure 2.1. Schematic representation of the bone remodelling process. Solid lines indicate differentiation and dotted lines indicate stimulation. Osteocytes within bone tissue stimulate osteoclast progenitor cells to differentiates into osteoclasts. Osteoblasts can also stimulate osteoclast progenitor cells through RANK/RANKL binding. Once the defective bone tissue is cleared, macrophage-like cells smooth the resorbed bone tissue. Before undergoing apoptosis, osteoclasts recruit osteoblasts for matrix deposition. Osteoblasts stimulate the release of osteoprotegerin (OPG) that acts as a soluble decoy and inhibits osteoclast differentiation. Adapted from Wittkowske et al. [81], Bone remodelling cycle, https://creativecommons.org/licenses/by/4.0/legalcode http://creativecommons.org/licenses/by/4.0/]. MSC, Mesenchymal stroma/stem cell; RANK, Receptor activator of nuclear factor kappa-B; RANKL, Receptor activator of nuclear factor kappa-B ligand; OPG, osteoprotegerin. Mollentze *et al*. 2021.

2.4.1. Transcriptional genes involved in osteogenesis

Osteogenesis is controlled by a wide range of stimulators and inhibitors, which occur both at the transcriptional level and through extracellular signalling pathways. Runt-related transcription factor 2 (RUNX2) is an essential transcription factor that controls the differentiation of MSCs into osteoblasts [83]*. Additionally, osteogenesis is regulated through changes in the osteoprotegerin (OPG)/ RANKL ratio. RANKL binds to RANK, found on the*

surface of pre-osteoclasts, to induce differentiation of pre-osteoclasts into mature osteoclasts in the presence of M-CSF, leading to bone resorption [76]. Osteoclast differentiation needs to be blocked in order for osteoblast differentiation to occur; this happens through the secretion of OPG that acts as a soluble decoy receptor, which binds to RANKL, blocking RANKL/RANK interactions and thereby inhibiting osteoclast differentiation (Figure 2.1).

2.4.1.1. RUNX2: Master regulator of osteogenic transcription

RUNX2 is the main molecular regulator responsible for the differentiation of MSCs into preosteoblasts and is expressed early to promote osteogenesis and inhibit adipogenesis and chondrogenesis [84]. RUNX2 regulates many downstream osteogenic genes such as Osterix (Osx), osteocalcin (Ocn), ALP, β-catenin, core binding factor-1α (CBF-1α), bone sialoprotein (BSP), osteonectin, osteopontin (Opn) and type I collagen, to name a few (Figure 2). Furthermore, activation/overexpression of RUNX2 results in a significant decrease in adipogenic related transcription factors and enzymes, peroxisome proliferator-activated receptor (PPARγ) and lipoprotein lipase (LPL) [85]. RUNX2 is downregulated during the later stages of bone maturation [84]. In vitro studies show that RUNX2 also directly regulates synthesis of both OPG and RANKL [86,87]. These findings have been confirmed in vivo [85,88]. Otto et al. [88] showed that a mutation in the RUNX2 gene resulted in a complete absence of osteoblasts, which resulted in turn in a cartilaginous skeleton; RUNX2 deficient mice also die shortly after birth. A later study done by Adhami et al. [89] demonstrated that RUNX2 null mice were born alive and were identical to wildtype mice and only after a month did the RUNX2 null mice display poor growth, weighing 20-25% less than their wildtype counterparts. With closer inspection they found there was a 50% decrease in trabecular number and a 20% decrease in trabecular thickness indicating that the loss of RUNX2 led to significant growth deficits. They also noticed impaired bone mineralization due to a decrease in the average density of hydroxyapatite. Together these findings indicated that RUNX2 is important in bone formation. The difference between the two studies could be explained by differences in the strain of mice used in the respective studies. On the other hand, Zhang et al. [85]

demonstrated that the overexpression of RUNX2 in 4-week-old nude mice resulted in increased mineral deposition.

2.4.1.2. Early-stage osteogenic regulators

Msx2 is a homeobox transcription factor that mainly controls the early stages of osteogenic differentiation but also plays a role in the later stages of osteoblastic mineralization. Ex vivo studies have shown that the expression of Msx2 promoted up-regulation of Osx and ALP, but did not influence the expression of RUNX2 [90]. Cheng et al. [90] demonstrated the ability of Msx2 to regulate osteogenesis through the suppression PPARγ. Ocn, a late stage osteogenic marker, is down-regulated in the early stages of osteogenesis through protein-protein interactions between Msx2 and Ocn [91]. Satokata et al. [92] reported osteoblast deficiency leading to osteoporosis syndromes in Msx2 null mice, supporting the idea that Msx2 plays an important role in osteogenic differentiation. The insulin-like growth factor (IGF) axis regulates both osteoblast and osteoclast differentiation and is one of the most abundant growth factors in bone tissue [93]. Osteocytes upregulate IGF-1 in response to mechanical loading; IGF-1 is thus considered to be an early osteogenic marker [94]. The knockout of IGF-1 in MSCs compromises the osteogenic process in vitro [95]. This study was corroborated by Zhang et al. [96] who showed that bone formation was completely blocked by disrupting the Igf1 gene in mature osteoblasts. Similarly, in vivo, a disruption in the Igf1 gene inhibited periosteal expansion resulting in rodents with smaller body features [97].

Osx and activating transcription factor 4 (Atf4) are located downstream of RUNX2 and are both important transcription factors in osteogenesis. Atf4 regulates osteogenesis through its ability to regulate Ocn and collagen type I. Deletion of Atf4 in mice led to impaired terminal osteoblast differentiation and resulted in severe osteopenia and other defects during skeletal development [98,99]. Osx is a potent bone forming stimulator that is part of the specificity protein 1 family [100]. Osx stimulates osteoblastic differentiation in MSCs through the repression of PPARγ, which inhibits adipogenesis [101]. Several in vivo studies have demonstrated the indispensable function of Osx in osteogenic differentiation [100,102–104]. The importance of Osx was demonstrated by Hilton et al. [102]: inhibition of Osx impairs osteoblast mineralization of cartilage into bone. In vitro studies suggest that Osx is modulated by IGF-I, BMPs, Msx2, and the Wnt signalling pathway [100,103,104]. Overexpression of Osx

in C2C12 cells resulted in increased expression of ALP and Ocn, leading to the calcification of bone tissue [100]. ALP plays an important role in phosphate metabolism by hydrolysing inorganic phosphate to promote matrix calcification, thus playing a key role during osteogenesis [105]. Nakamura et al. [106] overexpressed ALP in wild-type osteoblast cells which resulted in increased expression of osteogenic genes RUNX2, Osx, Ocn, and dentin matrix acidic phosphoprotein 1 (Dmp1), an osteocyte differentiation marker. Consistent with Nakamura et al.'s [106] in vitro study, Narisawa et al. [107] demonstrated that the overexpression of ALP by osteoblasts resulted in an increase in bone mineralization in vivo. ALP-/- mice exhibit long bone and skull fusion defects, and by administering exogenous ALP, the authors were able to increase bone density and the life span of these mice [107–111]. Another early-stage osteogenic marker is COL1A1. Mutations in COL1A1 have been studied extensively in osteogenesis imperfecta, a genetic disorder that results in bone fragility and multiple fractures. COL1A1 is important for the synthesis of collagen type I which is a major component of bone extracellular matrix (ECM), is expressed in all osteoblastic cells throughout osteogenic differentiation, and mutations lead to ineffective or absent differentiation [112,113].

2.4.1.3. Late-stage osteogenic regulators

Transcription factors involved in the later stages of osteogenesis regulate terminal differentiation and are involved in mineralization. Some of the most important late-stage transcription factors are Opn, distal less homeobox 5 (Dlx5), Ocn, OPG and BSP, to name a few. Opn is a matricellular protein that belongs to the small integrin-binding ligand N-linked glycoprotein (SIBLING) family and is involved in mineralization in response to mechanical stress. Chen et al. [114] observed that Opn-/- MSCs form considerably less bone tissue in vitro compared to their wild-type counterparts; however, the same is not true in vivo. Chen et al. [114] suggest that the difference between in vitro and in vivo studies may reflect functional redundancy and that other members of the SIBLING family can compensate for Opn deficiency. Interestingly however, Opn-/- mice did show a higher fat weight/body weight ratio. Dlx5 is another bone inducing transcription factor that plays a role in the later stages of osteogenesis. In vitro studies show that by inhibiting Dlx5, RUNX2 and Osx expression was blocked, suggesting that Dlx5 may be an upstream regulator of RUNX2 and Osx. Dlx5 is also a downstream target of BMP signalling [115]. Additionally, upregulation of Dlx5 did not increase

the osteogenic markers ALP and Ocn in vitro. Other cell culture studies demonstrated however that overexpression of Dlx5 increases expression of Ocn [116]. Dlx5 null osteoblasts display a higher RANKL/OPG ratio, suggesting that Dlx5 deficient osteoblasts are able to induce osteoclastogenesis [117]. Dlx5-deficient mice displayed delayed and abnormal osteogenesis, resulting in severe craniofacial abnormalities as well as a decrease in RUNX2, Osx, Ocn and BSP expression [117,118]. An increase in the number of osteoclasts was observed in the femurs of Dlx5 null mice [119]. Bone defects were also present in Dlx5/Dlx6 double knockout mice, further indicating that Dlx5 plays an important role in bone mineralization [119]. Interestingly, the forced overexpression of Dlx5 in vivo also resulted in reduced bone mineralized matrix deposition despite high levels of RUNX2 and BSP expression, suggesting a block in the later stages of osteogenesis [120].

OPG is expressed by osteoblasts, MSCs and endothelial cells, and can enhance osteogenesis by acting as a decoy receptor for RANKL, inhibiting osteoclastogenesis [121,122]. Both in vitro and in vivo models have demonstrated that OPG levels are inversely related to osteoclastogenesis [123,124]. In an in vitro study, the treatment of undifferentiated MSCs with OPG resulted in the enhancement of osteogenesis [125]. Furthermore, OPG knockout mice demonstrate an increase in bone resorption due to increased osteoclast activity [42].

Ocn and BSP are both non-collagenous proteins found in bone tissue. Ocn is the most abundant, non-collagenous protein in bone tissue, and is used as a biochemical marker for bone formation in vitro and in vivo: an increase in Ocn levels has been associated with an increase in bone mineral density [126]. BSP is found in mineralized tissue such as bone, calcified cartilage and dentin, and makes up approximately 8% of the non-collagenous protein of bone [127]. Although the function of BSP is not yet fully known, it is suspected to play a role in the formation of hydroxyapatite (essential component of healthy bone tissue) [128]. In the absence of BSP in vitro, osteogenic differentiation is negatively impacted. BSP overexpression leads to an increase in osteoblast-related gene expression as well as enhanced mineralization. The opposite is also true; when BSP expression is reduced, there is both a reduction in osteoblast-related gene expression and bone mineralization [129]. In vitro studies have suggested that a lack of BSP reduces osteoprogenitor cell numbers and has a compensatory role on Opn. The BSP-/- phenotype is associated with the upregulation of Opn in an attempt

to rescue the cells. However, the overexpression of Opn is not enough to rescue the cells, and thus bone formation and mineralization does not occur [130,131]. BSP-/- mice demonstrate normal skeletal development; however, they display under-mineralization of long bones [131,132].

2.4.1.4. Additional osteogenic transcription factors

Other transcription factors that are involved in osteogenic differentiation are frizzled-related protein (FRZB), dickopf (Dkk) 2, homeobox protein Hox-B7 (HOXB7), β-catenin and others. FRZB is a Wnt modulator that increases the expression of osteogenic-related markers and calcium deposition. The overexpression of Frzb in MC3T3-E1 cells increases osteogenic activity while the loss of Frzb results in a decrease in osteogenic activity [133]. However, Frzb null mice show an increase in cortical bone thickness [134]. These contrasting results may be explained by the deficiency of FRZB leading to supraphysiological levels of other Wnt modulators such as Dkk1 and Dkk2, that stimulate osteogenesis. Dkk1 and Dkk2 work antagonistically in vivo, where the increased expression of Dkk1 results in a decrease in bone mass while an increase in Dkk2 expression positively stimulates bone formation [135,136].

When the transcription factor HOXB7 is over expressed, osteogenesis is enhanced through the upregulation of RUNX2 [137]. Gao et al. [137] performed both in vitro and in vivo studies to investigate the role of HOXB7 during osteogenic differentiation. In their in vitro studies, the overexpression of HOXB7 enhanced bone mineralization through activation of ALP. HOXB7 overexpression also had an effect on other osteogenic transcription factors and proteins such as RUNX2, osteonectin, collagen type I, BSP and Ocn, leading to the promotion of osteogenesis. In contrast, when HOXB7 was inhibited these transcription factors were downregulated resulting in a decrease in ALP activity that led to a decrease in mineralization. Other HOX genes involved in osteogenesis are HOXa2 and HOXd9. In vivo studies showed that during bone regeneration, HOXa2 is upregulated after bone fracture while HOXd9 is downregulated [138].

The β-catenin protein is multifunctional. One important function is its ability to regulate the transduction of Wnt signalling [139]. The inhibition of β-catenin leads to the inhibition of osteogenesis and the promotion of chondrogenesis [140]. β-catenin is activated by the Wnt

signalling pathway; β-catenin then interacts with LEF/TCF which together increase bone mineralization [141]*. Ex vivo studies have demonstrated the importance of β-catenin in osteoblast mineralization through its downstream regulation of BMP2* [142]*. In an in vivo study, Hill et al. 2005* [143] *knocked-down β-catenin from head and limb mesenchyme in mouse embryos. In the absence of β-catenin, the mutant mice did not form cortical or trabecular bone. Interestingly, the overexpression of β-catenin does not result in an increase in osteoblast number, but rather inhibits chondrogenesis and allows for MSC osteogenesis* [143]*.*

There are several other transcription factors, not discussed in this overview (review), that are involved in osteogenesis. These include matrix extracellular phosphoglycoprotein (MEPE), human high-temperature requirement protein 1 (HTRA1), IGFBP-2, secreted protein acidic and rich in cysteine (SPARC), TMEM119, sclerostin and hypoxia-inducible factor-1α (HIF-1α); for further information, please refer to [144–151]*. The osteogenic process involves a complex network of cells and mediators, and even the slightest disruption of the network leads to defective bone formation (Figure 2.2).*

2.4.2. Signalling pathways involved in osteogenesis

Successful translation of in vitro findings to clinical applications in vivo requires a good understanding of potential differences in events during in vitro and in vivo regulation of osteogenic differentiation. The BMP pathway and the Wnt/β-Catenin signalling pathway are two important extracellular signalling pathways involved in osteogenic differentiation [140,152]*. Several studies have investigated the role of the BMP pathway during in vitro and in vivo osteogenic differentiation and reported on the differences and similarities in extracellular signalling pathways regulating events in these settings. Tsialogiannis et al.* [153] *concluded that the BMP pathway plays an important role during both in vitro and in vivo osteogenic differentiation. The majority of studies looking at the relationship between the Wnt/β-Catenin signalling pathway and bone formation have been done in vivo. Other extracellular signalling pathways that play a role in osteogenesis are the Notch signalling*

pathway, the hedgehog pathway, fibroblast growth factor (FGF), vascular endothelial growth factor (VEGF) and extracellular signal-regulated kinase [154] *(Figure 2.3).*
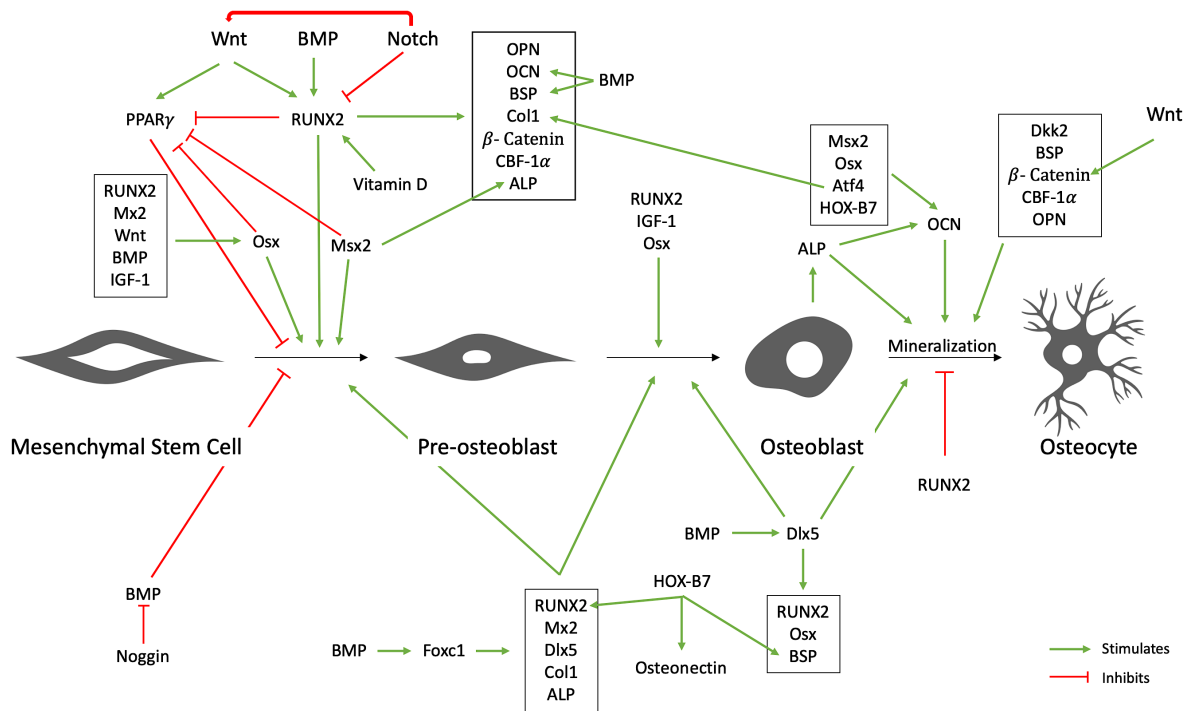
Figure 2.2. Regulation of MSC osteogenic differentiation. Green arrows indicate positive regulation while red lines indicate negative regulation. This figure illustrates the complex network of cells and mediators involved in bone formation. Mesechymal stem cells differentiate into pre-osteoblasts, then into osteoblasts and when osteoblasts become enclosed in the mineralized bone matrix, they are then classified as osteocytes. Mollentze *et al.* 2021.

2.4.2.1. BMP signalling pathway

BMP binds to its receptor, BMPR, found on epithelial cells, which in turn activates the intracellular transcription factor Smad. Smad binds to the master regulator, RUNX2. The Smad-RUNX2 complex induces osteogenesis [155] *(Figure 3). Using various BMP antagonists in vitro, Tsialogiannis et al.* [153] *demonstrated that inhibition of BMP function affects multiple downstream factors, such as RUNX2, BSP and Ocn. The investigators extended their investigation by overexpressing noggin, a BMP antagonist, in transgenic mice, and reported a significant decrease in bone density and bone formation in these animals* [156]. *In contrast, complete knockout of noggin led to irregularly thickened bones and death shortly after birth* [153,157]. *Other BMP antagonists include chordin and gremlin. Multiple in vitro studies have demonstrated that chordin is a strong endochondral ossification stimulator* [158–161].

Zhang et al. [162] *examined the role of chordin in vivo and their results show that BMP-2 enhances maturation of chondrocytes resulting in growth of the growth plate of Hamburger-Hamilton stage 25-27 embryonic chick limbs. When chordin (a BMP antagonist) was expressed ectopically, it resulted in a delayed growth rate of the growth plate by binding to BMP to inhibit BMP's function. From previous in vitro studies it is known that when gremlin-1 is supressed, the expression of osteoblastic genes ALP, BSP, MSX2, OC, OPN, and RUNX2 is significantly increased* [163]. *It was only recently that the role of gremlin was investigated in vivo. Rowan et al.* [164] *explored the effect of Grem 1 deletion in ROSA26CreER-Grem1 flx/flx mice. Although these mice demonstrated normal bone structure, there were other abnormalities present including severe bowel disruption as well as abnormal haematopoiesis. Cyclooxygenase 2 (COX-2) enhances in vitro osteogenic differentiation through initiating the BMP signalling pathway via a positive regulatory loop with BMP9, a potent osteogenic stimulator* [165,166]. *Wang et al.* [166] *demonstrated that COX-2 is critical for orchestrating the BMP/Smad signalling pathway in vitro (Figure 3). Silencing Cox2 down-regulated the expression of RUNX2 and Dlx-5. Similarly, in vivo studies showed that COX-2 knockout mice displayed 98% and 86% reduction in bone formation when they received a bone graft from other COX-2 knockout mice or wild type mice, respectively* [167].

Foxc1 is another important osteogenic regulator that interacts with an osteogenic factor, BMP4. Foxc1 mutant mice display numerous abnormalities related to bone development. The calvarial bones and sternum are absent, the ribs are deformed, and the skull base is reduced in size [168,169]. *The ectopic expression of Foxc1 in C2C12 myoblasts resulted in the rescue of osteogenesis by increasing ALP activity and inducing early osteogenic markers such as RUNX2 and type I collagen* [170]. *Furthermore, Hopkins et al.* [171] *demonstrated that a down-regulation of Foxc1 in C2C12 cells resulted in the inhibition of RUNX2, Msx2 and ALP activity (Figure 3). These investigators suggested that Foxc1 is required for the initiation of osteogenesis but not for the later stages, as they observed a decrease in Foxc1 levels as differentiation proceeded.*

2.4.2.2. Wnt/β-Catenin signalling pathway

Wnt/β-Catenin signalling, also known as the classical or canonical Wnt pathway, is of particular importance as it can either induce or inhibit osteogenesis. This pathway can

regulate the expression of RUNX2 to induce osteogenesis. Alternatively, the Wnt pathway inhibits osteogenesis by altering the OPG/RANKL ratio. The expression of PPARγ is also controlled by the Wnt pathway. PPARγ is the main transcription factor in adipogenesis and therefore its expression needs to be inhibited in order for osteogenesis to occur [104] *(Figure 3).*
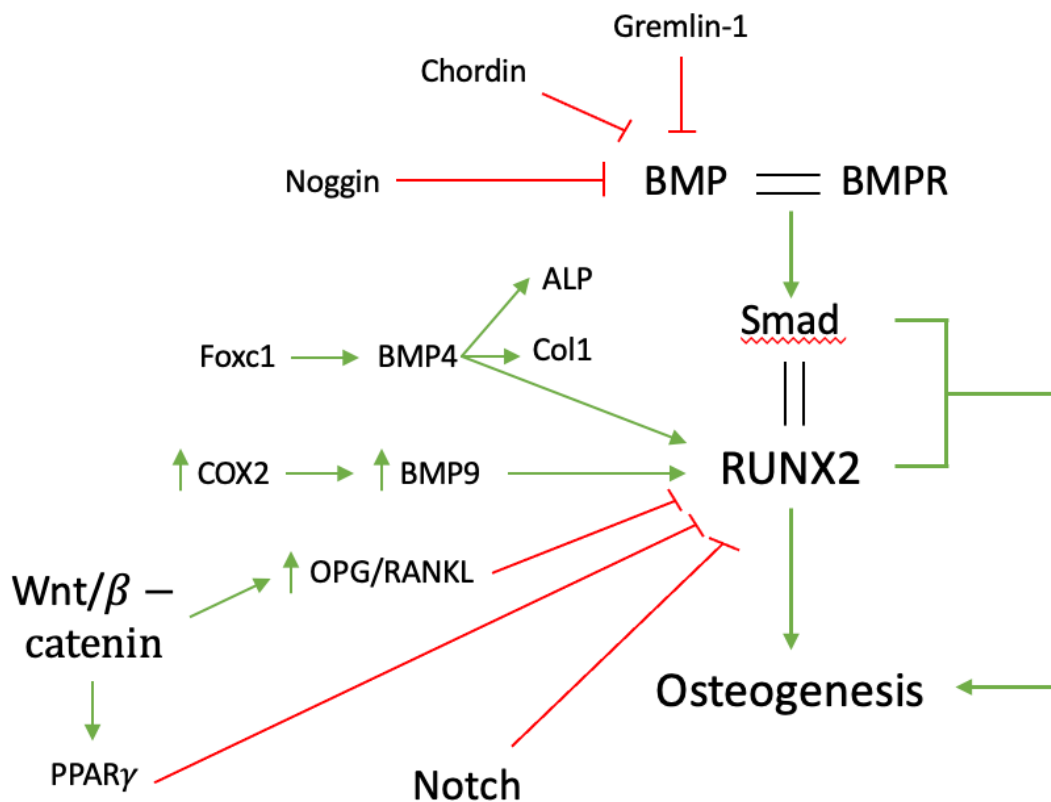
Figure 2.3. Illustration of how various signalling pathways regulate osteogenesis through the master regulator of osteogenesis, RUNX2. Green arrows indicate positive regulation while red lines indicate negative regulation. The main signalling pathways involved in osteogenesis are the BMP pathway which involves the upregulation of the master transcription factor RUNX2. The other important signalling pathway involved is the Wnt signalling pathway. Mollentze *et al.* 2021.

Mice lacking the Lrp5 gene, which codes for a Wnt co-receptor, developed osteopenia, while the overexpression of Lrp5 resulted in high-bone-mass syndromes [172,173]. *Genome-wide association studies in humans revealed an association between multiple mutations in Wnt1 and Wnt16, and early onset osteogenesis imperfecta and osteoporosis; both bone disorders result in brittle bones as well as an increased risk of fractures* [174,175]. *Hilton et al.* [102] *removed all the components of the Notch network in mice, and this resulted in increased bone*

mass and a depleted pool of MSCs in the bone marrow [102]. *The Notch network inhibits osteogenesis through the expression of HEY1 and HEYL transcription factors that directly inhibit RUNX2 (Figure 2.3). Over-expression of Notch-1 in mice inhibited osteogenesis through the inhibition of the Wnt/β-Catenin signalling pathway* [176]. *It is clear that extracellular signalling pathways play a major role in osteogenesis via a complex network of transcription factors. It is therefore important to examine the network as a whole and not separate out specific interactions, as would occur in an in vitro setting.*

2.5. Osteogenic potential of MSCs *In Vitro*

In vitro, MSCs are induced to undergo osteogenic differentiation following exposure to compounds such as β-glycerophosphate, dexamethasone and ascorbate-2-phosphate, that promote cell proliferation and osteogenic differentiation. Although these 3 compounds (β-glycerophosphate, dexamethasone and ascorbate-2-phosphate) are present in all in vitro osteogenic media, there is a lack of consensus regarding the optimal medium for in vitro osteogenic differentiation of MSCs, particularly regarding the concentration of dexamethasone, which varies significantly between studies. Table 2.3 summarises the composition of the osteogenic media used most often. Ascorbic acid and dexamethasone are the main osteogenic inducing factors, and together increase the activity of ALP. Upregulation of ALP activity increases the speed at which bone differentiation occurs [177]. *Ascorbate-2-phosphate is responsible for the synthesis of collagen in the early stages of osteogenesis, while β-glycerophosphate is responsible for mineralization in the later stages* [178,179]. *Along with increasing ALP activity, dexamethasone also regulates the osteogenesis related gene RUNX2* [180].

Various spectrophotometric assays are used to determine the extent of in vitro osteogenic differentiation. Both the Von Kossa assay and the Alizarin Red S (ARS) assay stain for calcium deposits that are present in bone tissue. The Von Kossa assay is a qualitative assay in which calcium is replaced with silver ions (source: silver nitrate solution) to form black/brown deposits that can be analysed under a microscope [181]. *The ARS assay is semi-quantitative in which ARS reacts with calcium to form a red deposit which is extracted using acetic acid. The extracted dye is spectrophotometrically quantified at 405 nm* [182]. *Another assay that is often used to quantify osteogenesis is the ALP assay that also uses spectrophotometry to*

measure the level of ALP activity. In short, 4-nitrophynylphosphate is used as a phosphate substrate for ALP which dephosphorylates 4-nitrophenylphosphate which then turns yellow. This colour change is measured at 405 nm [183].

Table 2.3. Summary of different osteogenic differentiation media reported in the literature.

Reference	Cell Density	Assays /Stains	Passage	Induction time (days)	Basal Culture Medium	FBS	Antibiotics	Dexamethasone (µM)	Ascorbate-2-phosphate (µM)	B-glycero-phosphate (mM)
Cai et al. 2014	NI	Alizarin Red S and ALP	2	21	DMEM-low glucose (lg)	10%	100 units/mL	0.01	155.26	1×10^{-5}
Vieira et al. 2010	NI	Von Kossa	3	21	NI	10%	NI	0.1	50	1×10^{-5}
Nishimura et al. 2015	5×10^5		5	14	DMEM	10%	100 units/mL	0.05	0.0002	10
Bieback et al. 2004	$3.1 \times 10^3/cm^2$	Von Kossa	NI	21	Cell Systems	10%	NI	0.1	50	10
Waterman et al. 2010	3×10^4 cells/well (6-well)	Alizarin Red S	NI	NI	NI	NI	NI	0.1	50	1×10^{-5}
Elashrya et al. 2019	2×10^4 cells/well (6-well)	Alizarin Red S	2-3	NI	DMEM	10%	100 U/mL	0.1	60	10
Li et al. 2015	5 000 cm^2	ALP	NI	NI	DMEM-high glucose	10%	100 U/mL	0.01	155.26	10

Sotiropoulou *et al.* **2006**	NI	Von Kossa	NI	NI	DMEM-lg	10%	50 µg/mL Gentamicin	1	50	10
Rada *et al.* **2011**	NI	Alizarin Red S	NI	21	α-MEM	10%	1%	0.1	155.26	10
Meuleman *et al.* **2006**	NI	Von Kossa	1	14	α-MEM	NI	NI	0.1	60	10
Sasaki *et al.* **2008**	NI	Von Kossa	NI	NI	DMEM	10%	0.1 µM	-	50	10
Zuk *et al.* **2001**	NI	ALP or Von Kossa	1	14	DMEM	10%	1%	1	50	10
Bunnell *et al.* **2008**	NI	Alizarin Red S	NI	14	α-MEM	20%	1%	0.001	50	2
Wagner *et al.* **2005**	1-2 x 10^4 cells/cm^2	ALP or Von Kossa	NI	21	DMEM	10%	-	1	200	10

NI, Not indicated
DMEM, Dulbecco's Modified Eagle's Medium
ALP, Alkaline phosphatase

MSCs isolated from various tissues also differ in their differentiation capabilities [195–198]. This may be due to DNA methylation of key transcription factors. Xu et al. [195] demonstrated that MSCs retain their epigenetic memory and favour either of adipogenic or osteogenic differentiation, depending on their tissue of origin. In BM-MSCs, the CpG island in the RUNX2 promoter is hypomethylated while the CpG island in PPARγ is hypermethylated. The opposite is true in adipose tissue-derived stromal/stem cells (ASCs): the PPARγ promoter is hypomethylated while the RUNX2 promoter is hypermethylated. Pérez-Silos et al. and McLeod et al. [199,200] suggest that MSCs consist of sub-populations that share common features while varying in the expression profile of their cell surface proteins, which can be related to differences in differentiation potential. Cantentin et al. [201] found that UC-MSCs produced significantly more ECM, while stronger staining for type I collagen was observed for BM-MSCs indicating that BM-MSCs have enhanced osteogenic potential when compared to UC-MSCs. UC-MSCs produced molecules that BM-MSCs did not such as type X collagen and the HtrA1 gene product. Umbilical cord MSCs (UC-MSCs) additionally displayed a higher proportion of CD73+ cells. The authors suggest that the difference in CD73 expression and the production of these atypical molecules are the major reason for differences in chondrogenic differentiation potential between BM-MSCs and UC-MSCs.

Other factors that may influence the differentiation capabilities of MSCs include the age of the donor, the health of the donor, culture conditions and method of isolation. Barboni et al. and Xin et al. [202,203] both demonstrated a positive correlation between age and DNA methylation status. Barboni et al. [202] observed a correlation between gestational age of amniotic derived MSCs and global DNA methylation status, which resulted in a decrease in osteogenic differentiation potential. Xin et al. [203] extensively compared DNA methylation status and multi-lineage differential capabilities. An age-related decline in ASC osteogenic differentiation was observed when ASCs from young and old donors were compared. In another study, the differentiation potential of BM-MSCs from patients with osteoarthritis (OA) was compared to MSCs isolated from a control group of a similar age: both the chondrogenic and adipogenic differentiation potential of BM-MSCs from OA patients were significantly decreased compared to controls, while the osteogenic potential was similar when BM-MSCs from OA patients and MSCs from the control group were compared [204].

He et al. [205,206] *demonstrated that the extracellular matrix is important in directing MSCs down a specific lineage: a hydroxyapatite (HA)-collagen matrix was found to be superior to a HA-synthetic hydrogel for osteogenic differentiation. For chondrogenesis, the HA-synthetic hydrogel was preferred over the HA-collagen matrix. The HA-collagen matrix imitated the natural composition of bone and resembled the physical and chemical microenvironment found in the human body, thus favouring osteogenesis. The reason why the HA-synthetic hydrogel was favoured for chondrogenesis is not fully understood, as the HA-synthetic hydrogel does not imitate natural cartilage. Overall, the use of a matrix increased cell proliferation, adhesion, migration and differentiation. The biomechanics of the MSC microenvironment also has an effect on differentiation capabilities. Gungordo et al.* [207] *concluded that rat BM-MSCs progress to an adipogenic lineage under unstrained conditions on a softer polyacrylamide hydrogel film, while rat BM-MSCs seeded on a stiffer polyacrylamide hydrogel and under strained conditions are driven down the osteogenic lineage. The use of animal serum which contains xenoantigens is another culture condition that can affect differentiation potential, specifically osteogenic differentiation* [208,209]. *Okajcekova et al.* [210] *compared three different osteogenic induction media and their differentiation capabilities, of which one was xeno-free. Not only did the xeno-free induction medium result in significantly greater osteogenic differentiation potential compared to the other two, but the morphology of the cells grown in the xeno-free medium changed much earlier than the cells grown in the FBS induction medium: cell proliferation decreased while cell differentiation increased.*

The method of isolation also has an impact on the differentiation capability of MSCs. In a recent study by Walter et al. [211]*, different isolation techniques from the same donor site were compared with regard to osteo-, adipo- and chondrogenic differentiation. MSCs isolated from bone marrow aspiration showed better osteogenic differentiation than MSCs generated through outgrowth from culturing bone chips, which can be attributed to the fact that bone marrow aspiration yields more biomaterial and thus more MSCs. Chondrogenic and adipogenic differentiation, both from MSCs from bone marrow aspiration and MSCs generated through outgrowth from culturing bone chips, was relatively low; the authors*

attribute this to the specific microenvironment of the isolated bone tissue and suggest that this led to MSCs favouring the osteogenic lineage.

Musina et al. [212] compared the osteogenic differentiation potential of MSCs from different tissue sources after a three-week induction period. These investigators reported that BM-MSCs displayed the highest level of osteogenic differentiation, followed by ASCs which showed better osteogenic differentiation capabilities than MSCs isolated from the thymus, skin and placental tissues. Mohamed-Ahmed et al. [213] compared the osteogenic potential of MSCs isolated from bone marrow and adipose tissue and also reported that BM-MSCs possess enhanced osteogenic potential when compared to ASCs. The reason for the difference was attributed in part to increased alkaline phosphatase (ALP) activity and osteogenic gene expression kinetics. Early-stage osteogenic genes such as RUNX2, collagen type I and ALP were expressed as early as day 14 in osteogenic differentiating BM-MSCs, while these genes were only expressed on day 21 in differentiating ASCs. This indicates that BM-MSCs stop proliferation early (day 14) and switch to differentiation and formation of a mature collagenous matrix, while ASCs have an extended proliferation period and only switch to differentiation after day 21, resulting in BM-MSCs having greater mineralization and therefore more bone tissue on day 21 [213]. Shen et al. [196] compared MSCs derived from the amniotic membrane (AM-MSCs), the UC-MSC), the chorionic membrane (CM-MSCs) and the decidua (DC-MSCs) and reported enhanced osteogenic differentiation (based on ARS staining and ALP activity) in AM-MSCs and UC-MSCs when compared to CM-MSCs and DC-MSCs. In terms of gene expression profiles involved in osteogenesis, AM-MSCs and UC-MSCs showed strongly enhanced expression of Ocn compared to CM-MSCs and DC-MSCs. MSCs from all four sources showed the same expression levels of Osx and collagen type I on day 21. Szöke et al. [214] compared the osteogenic potential of MSCs isolated from bone marrow and adipose tissue. They concluded that although ASCs had a higher proliferative capacity and a greater ability to form a collagenous extracellular matrix, their terminal osteogenic differentiation capability was reduced. BM-MSCs expressed a higher level of the late osteogenic markers Ocn and BSP. They further went on to suggest that ASCs may be more suitable for in vitro studies, as their isolation procedure is less invasive than BM-MSCs, and although their terminal differentiation capability is reduced, it is still adequate for in vitro studies, while BM-MSCs may

hold greater potential for in vivo studies as their terminal osteogenic differentiation capability is greater than that of ASCs.

2.6. The use of MSC-derived exosomes for osteogenesis *in vivo*

The ability of MSCs to secrete exosomes, in addition to cytokines and growth factors, contributes to their therapeutic effect [215]. Multiple in vivo studies have demonstrated that very few MSCs engraft at sites of injury when administered intravenously, but rather are filtered out in the lungs; however, they still exhibit a therapeutic effect [216–220]. Other studies have gone on to report that it is in particular the microvesicles/exosomes secreted from MSCs than provide this therapeutic effect [32,221,222]. The therapeutic effect of MSC-derived exosomes has been extensively studied in vivo in a wide range of disease models. Some of these include cardiovascular disease [223–225], renal disease [226–228], neurological complications [229–231], pulmonary disease [232–234], wound healing [235,236], muscle regeneration [237] and many more. With regard to osteogenesis, multiple studies have shown that MSC-derived exosomes can stimulate the osteogenic differentiation process, increasing bone regeneration. Qi et al. [238] demonstrated that exosomes from BM-MSCs from ovariectomized rats stimulated osteogenesis and were able to regenerate bone tissue in a critical-sized calvarial defect. They also found that the increase in osteogenic stimulation was related to the increase in exosome concentration over time. The repair of a critical osteochondral defect in adult immunocompromised rats through the intravenous injection of human embryonic MSC-derived exosomes was demonstrate by Zhang et al. [239]. The use of MSC-derived exosomes in regenerative medicine has gained a great deal of attention as it is an attractive alternative to using MSCs. MSC-derived exosomes are cell-free and are more compatible with a variety of administration routes [239]. Another reason why exosomes are attractive is that they lack major histocompatibility complex (MHC) I/II proteins, and there is therefore no need for immunosuppression [240,241].

2.7. Clinical relevance

Bone is a vital part of the human body that protects and supports various organs, enables mobility, stores minerals and produces cells of the hematopoietic lineage [242]. Bone fractures typically heal without the need for major intervention; however, there are more than 2 million cases worldwide in which patients require bone reconstruction using tissue transplants [243].

Current reconstruction procedures involve autologous bone grafts, allogeneic bone grafts, and artificial metal or ceramic replacements.

Autologous bone grafts are viewed as the gold standard for treating bone defects as they enhance osteogenesis and are less likely to be rejected by the host [244]. However, 10% of bone harvests are associated with major complications, limited supply and donor-site morbidity [245,246]. Allogeneic bone grafts provide an ample source of tissue, but the risk of immune-rejection and the transmission of diseases makes them less ideal [247]. The use of metals as artificial replacements also has limitations such as tissue-host integration, increased risk of infection and wearing out [248]. The brittle nature of ceramic replacements is especially problematic in areas where high stress or torsion is endured [249]. It is thus clear that alternative, more effective options are needed for the treatment of skeletal defects.

2.7.1. The use of cultured MSCs for osteogenesis in vivo

The osteogenic differentiation potential of multipotent MSCs has gained increasing interest in tissue engineering especially when it comes to offering an alternative to overcome the limitations of bone grafts and artificial bone replacements [250]. Multiple in vitro studies have demonstrated that MSCs are able to differentiate into bone tissue, but bone formation is a complex process that involves many cell types, growth factors, cytokines and mechanical stimulation, that all form part of the environmental niche [251]. Therefore, investigation of bone formation in vivo is required to provide a complete understanding of osteogenesis, and also bridges the gap between the use of MSCs in vitro and the clinical use of MSCs for bone repair.

Most studies that have investigated osteogenic differentiation of MSCs in vivo first expanded the cells ex vivo, seeded them onto a scaffold and transplanted the scaffold subcutaneously in an animal model in which osteogenesis was studied [252–254]. For optimal bone regeneration, the biomaterial used as a scaffold should be biocompatible, cost effective, biodegradable and should also induce or improve the osteogenic process. The biological behaviour of MSCs is greatly affected by the surface morphology of the biomaterial which in turn affects the formation of bone tissue [255]. The most common scaffold material being used in tissue engineering is hydroxyapatite, an inorganic material that is naturally found in

bone tissue [256]. *These scaffolds are cast into the desired shape. Another new and attractive method of making scaffolds is the use of 3-dimensional (3D) printing, as it allows for a reproducible design when it comes to pore size* [257]. *Once the scaffolds are transplanted, MSCs differentiate into osteoblasts and form bone tissue.*

Bone remodelling is a complex and highly integrated process, and as described in this overview (review) involves various transcription factors and osteogenic genes and their protein products including cytokines, growth factors, extracellular matrix components and others. The smallest deviations from this well-balanced system can affect bone health and can lead to a number of bone diseases. Bone tissue is a porous, mesh-like network made up of collagen proteins and calcium phosphate minerals and is constantly being replaced throughout life. When the bone remodelling process is defective, this mesh-like structure becomes porous as seen in osteoporosis, leading to brittle bones and fractures.

According to the International Osteoporosis Foundation, over 200 million people are affected by osteoporosis worldwide [258]. *Osteoporosis is associated with low bone mass as well as bone deterioration usually seen with increasing age, and it is thought that osteoporosis results, in part, from a significant decrease in the number of MSCs present in the bone marrow, leading to less new bone formation* [259]. *Osteoporosis is currently treated with drugs that increase bone resorption, but these drugs are associated with multiple adverse effects* [260]. *Stem cell therapy is a potential alternative for the treatment of osteoporosis, reducing the susceptibility to fractures by increasing the MSC pool present within the bone marrow. Wang et al.* [261] *reported increased bone formation, trabecular thickness and overall strength of bone tissue by embedding MSCs into the distal femurs of osteoporotic rabbits. Hsiao et al.* [262] *treated osteoporotic mice by injecting MSCs intravenously. They observed that the MSCs homed to the bone marrow where they increased bone density, rescuing the mice from osteoporosis.*

OA is a degenerative joint disease affecting synovial joints and frequently results in chronic pain [263]. *Currently the treatment of OA involves long-term pain management with the use of pharmacological therapies. Osteotomy can improve alignment, but this therapy is limited as it can decrease the risk of OA but has little effect on degeneration once it has occurred* [264]. *It has been hypothesized that the multipotency properties of MSCs could also benefit*

patients with OA. Currently, there are over 100 documented clinical trials assessing the potential of MSCs for the treatment of OA; however more preclinical work is needed to fully understand the mechanisms behind the potential healing effect of MSCs in OA [263]. Eder et al. [265] comprehensively reviewed the use of both ASCs and BM-MSCs in the treatment of musculoskeletal disorders, including OA. The overall conclusion of these studies is that the use of MSCs (ASCs and BM-MSCs) decreases pain levels and improves healing rates. Eder et al. [265] concluded that MSCs could be used as a therapeutic option in the future treatment of OA, although the field would benefit from large, randomized, blinded clinical investigations.

The repair and reconstruction of large segments of bone, such as fractures displaying non-union or delayed union, and large bone defects, have been a challenge to orthopaedic surgery. MSCs are an attractive therapeutic option for the healing of bone defects due to their ability in vivo to influence the secretion of specific factors by the immune system and through their interaction with other cells [266]. A number of clinical trials have been conducted with the aim of assessing the ability of MSCs to improve fracture healing. In most cases, improved fracture healing rates, decreased pain levels, and improved remodelling have been observed when compared to controls [267–274]. The conclusions that can be drawn from these studies indicate that the use of MSCs could be an important treatment option for larger more difficult bone defects in the future. Many more bone diseases could benefit from bone regeneration therapy, and hence the importance of understanding the osteogenic process in full.

2.8. Rationale for this study

Current trends in tissue engineering and regenerative medicine include the use of MSCs. One of these applications is the use of MSCs to enhance fractured bone tissue healing that would naturally heal over an extensive time period or not heal at all (non-unions). The optimization and standardization of protocols following GMP guideline is needed in the production of cell therapy products to ensure the safety of these cells in a clinical setting. Furthermore, to capitalize on the use of these cells, the mechanism in which the cells differentiate into the different lineages needs to be fully understood. The adipogenic differentiating potential of ASCs has previously been studied in depth at the ICMM and several papers have been published on this subject [275–280]. The ability of MSCs to differentiate into muscle (myogenesis) has been investigated by Ms Simone Grobbelaar, while chondrogenesis and

osteogenesis have also been investigated at the ICMM, but not in as much depth as adipogenesis [281,282]. No standardized protocol for osteogenic differentiation of MSCs and no optimal protocol for the use of growth medium supplemented with human alternative for osteogenic differentiation exists at the ICMM. The ultimate goal of all research projects done at the ICMM is to understand the characteristics of stromal/stem cells better in order to allow for the development of optimal clinical-grade cell therapy products. As described above, differentiation media used for osteogenesis include the use of FBS, a xenogeneic agent, which limits the application of ASC use in a clinical setting. This study aims to establish standard operating protocols that will allow for optimal differentiation of ASCs into osteoblasts, in other words undergo osteogenic differentiation. Factors that will be optimized include which differentiation supplementation cocktail is optimal and which human alternative is optimal as a growth medium supplement for osteogenic differentiation of ASCs. This study will serve as future reference to osteogenic protocols in our laboratory. Reverse transcriptase real-time quantitative polymerase chain reaction (RT-qPCR), microscopy and spectrophotometry are used to quantify osteogenic differentiation of ASCs and to study the expression patterns of a select number of osteogenesis-associated genes at set time points.

Chapter 3: Isolation of ASCs

3.1. Introduction

Mesenchymal stem/stromal cells (MSCs) are characterized as undifferentiated cells that have the ability to proliferate, self-renew and differentiate into many cells types that originate from the mesoderm [1]. MSCs are thus an attractive cell type for regenerative medicine. Multipotent MSCs were originally isolated from bone marrow [15]. Alternative sources of MSCs are being considered due to the highly invasive nature of a bone marrow harvest procedure, the low cell yield obtained and, the decrease in differential potential observed with increasing age of the donor [283,284]. New sources of MSCs are continuously being explored and cells from these new sources are being characterized. Some of these sources include various foetal and adult tissues such as adipose tissue [16], the amniotic membrane [17], amniotic fluid [18], placental and foetal membrane [19], umbilical cord lining membrane [20], the endometrium [21], dental tissue [22], menstrual blood [23], peripheral blood [24], skin [25], synovial fluid [26], Wharton's jelly (umbilical cord) [27] and many others.

The collection of adipose tissue from patients undergoing cosmetic liposuction or abdominoplasty procedures either as an aspirate or as intact excised tissue is viewed as less invasive. The adipose tissue removed during the above-mentioned surgical procedures is usually discarded as medical waste. Adipose tissue is a rich source of MSCs with a higher number of MSCs per volume of tissue when compared to the conventional bone marrow tissue. Adipose-derived stem/stromal cells (ASCs) are seen as one of the most promising stem cell populations for tissue regeneration as they can be harvested with relative ease, and at relatively large quantities, can be expanded and maintained under standard cell culture conditions, have the ability to differentiate into multiple lineages and secrete various cytokines that play a role in maintenance and differentiation of these cells [285–287].

In this chapter, published isolation and culturing methods, with slight modifications, were used and are described below [54].

3.2. Materials, reagents, and equipment

3.2.1. Materials and reagents

All serological pipettes were acquired from NUNC™ (Roskilde site, Kamstrupvej, Denmark). Filter cap culture flasks, 6-well tissue culture plates, and cryovials were manufactured by Greiner (Bio-One GmbH, Frickenhausen, Germany). Sigma Aldrich Chemie (Darmstadt, Germany) supplied the dimethyl sulfoxide (DMSO). Phosphate buffered solution (PBS), penicillin-streptomycin (pen/strep), Dulbecco's Modified Eagle Medium (DMEM), trypsin (0.25%), and foetal bovine serum (FBS) were sourced from Gibco/Invitrogen™ (Carlsbad, California, United States of America (USA)). Microcentrifuge tubes was supplied by the Scientific Group (Johannesburg, South Africa).

3.2.2. Equipment

The following equipment was used: ESCO Class II biological safety cabinet (AC2-4Si), SL 16R centrifuge from Lasec South Africa, NALGENE® Mr Frosty™ Cryo1°C freezing container manufactured by Thermo Fischer Scientific™, Waltham (Massachusetts, USA), CytoFLEX flow cytometer from Beckman Coulter (Miami, FL, USA), Thermo Forma™ CO_2 water jacketed incubator (3111TF) from Thermo Fisher Scientific™ (Waltham, Massachusetts, USA) , Zeiss Axiocam digital camera, and an inverted light microscope (Zeiss Primo Vert) from Carl Zeiss Werke, Göttingen, Germany.

3.3. Methods

The main objective of this chapter is to describe how the primary ASC cultures used in this study were established. The isolation of ASCs from adipose tissue, *ex vivo* expansion of ASCs, maintenance and differentiation of the primary cultures are described in Chapters 4 and 5.

3.3.1. Adipose tissue collection

The lipoaspirate was collected from informed and consenting patients undergoing liposuction or abdominoplasty procedures and who had also given informed consent (See supplementary information). These collections were done in collaboration with Dr Yanke van der Westhuizen

(Lift and Tuck). Additional information that was collected from the donors included age, gender, ethnicity, height, weight, whether the donors smoked, suffered from diabetes, cardiovascular disease, or hypertension. If the donors smoked, suffered from either diabetes, cardiovascular disease, or hypertension, they were excluded from the study.

3.3.1.1. Sample coding

The samples were anonymized by labelling with a specific code as illustrated in Figure 3.1.
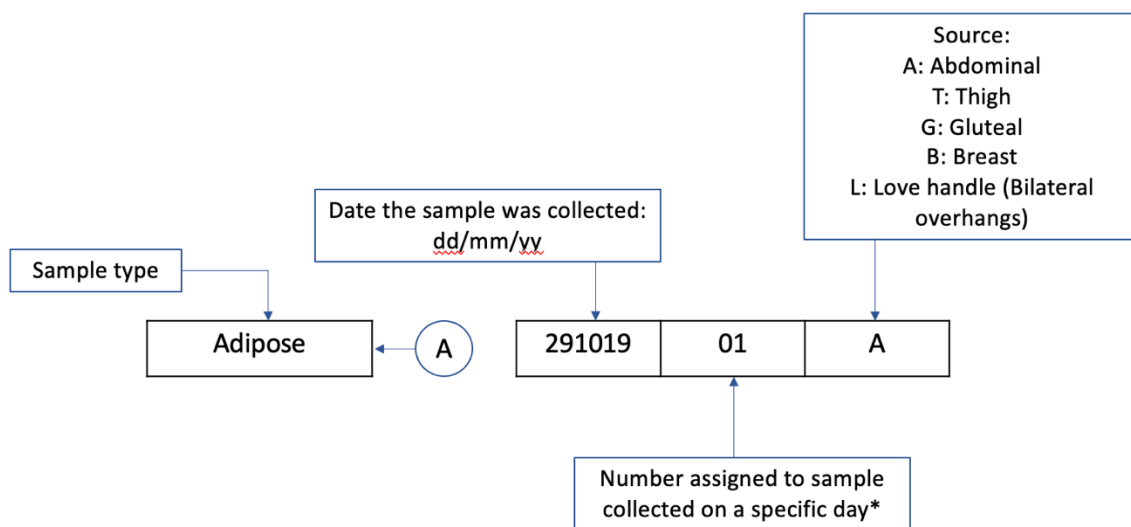
Figure 3.1. Illustration of the coding strategy to keep samples anonymous.

The coding strategy was developed to give each sample a unique identifier while keeping the patients anonymous. *In situations where more than one sample was collected from more than one patient on a given day, different numbers were given to the different patients. E.g., A291019-01A and A291019-02A are samples collected on the same day from two different patients.

3.3.1.2. Screening for HIV, Hepatitis B and C and mycoplasma

All samples were tested for the Human Immunodeficiency virus (HIV), Hepatitis B and Hepatitis C by the South African National Blood Services (SANBS). Mycoplasma testing (nucleic acid testing) was performed by Ms. Candice Murdoch at the Institute for Cellular and Molecular Medicine (ICCM) laboratory. All samples in this study tested negative for HIV, Hepatitis B and C and were free of mycoplasma.

3.3.2. Isolation of primary MSCs

The following protocol was used to isolate MSCs from adipose tissue.

3.3.2.1. Isolation of ASCs from Adipose tissue

The protocol previously described by Zuk et al. [54] was used, with minor modifications, to isolate ASCs from adipose tissue. In short, approximately 25mL of the lipoaspirate was transferred into 50 mL centrifuge tubes. The tubes were then topped up with PBS (2% pen/strep) and centrifuged for 3 minutes (min) at 1660 x g after which the lipid fraction and PBS were aspirated. The compacted adipose tissue was transferred into a new 50 mL tube. If there was a lot of blood contamination, the tissue was again washed with PBS (2% pen/strep), centrifuged and the lipid fraction and PBS again aspirated until no blood contamination was observed. The tubes were weighed, and the volume and the mass of the compacted adipose tissue was recorded to determine the amount of collagenase type I that was needed to digest the tissue. Collagenase type I powder was dissolved in PBS (2% pen/strep) to prepare a 0.1% collagenase type I solution. Before use, the collagenase was filtered through a 0.22µm filter. An equal volume of the 0.1% collagenase type I solution was added to the washed adipose tissue, followed by incubation at 37°C for 45 min in a rotating incubator. After incubation, the tubes were centrifuged for 5 min at 738 x g after which the tubes were shaken vigorously to disrupt the pellet and mix the cells. The cell suspension was then put through a cell strainer (70 µm) to remove any tissue debris and again centrifuged for 5 min at 738 x g. The collagenase solution was neutralized by adding a volume (equal to the volume of collagenase type I solution added) of complete growth medium (CGM, DMEM with 10% FBS and 2% pen/strep). The tube was filled with PBS (2% pen/strep) and centrifuged at 266 x g for 5 min. The supernatant was aspirated, while taking care not to disrupt the cell pellet. The cell pellet was resuspended in a volume of Versalyse™ and incubated at room temperature (RT) for 10 min, after which the tubes were filled with PBS (2% pen/strep) and centrifuged at 266 x g for 5 min. The supernatant was once again removed, the pellet resuspended in PBS (2% pen/strep) and again centrifuged at 266 x g for 5 min. The Versalyse™ step was repeated if red blood cell contamination was visible. The cell suspension was strained using a 70 µm cell strainer to get rid of any remaining tissue debris. The cell strainer

was washed with CGM to optimize cell recovery. Cells were then counted as described below. Cells were plated at 50 000 cells/cm^2 in T75 flasks and maintained at 37°C, 5% CO_2. After 72 hours, the cultures were washed with PBS (2% pen/strep) to remove any non-adherent cells. The isolation process is visually summarised in Figure 3.2.
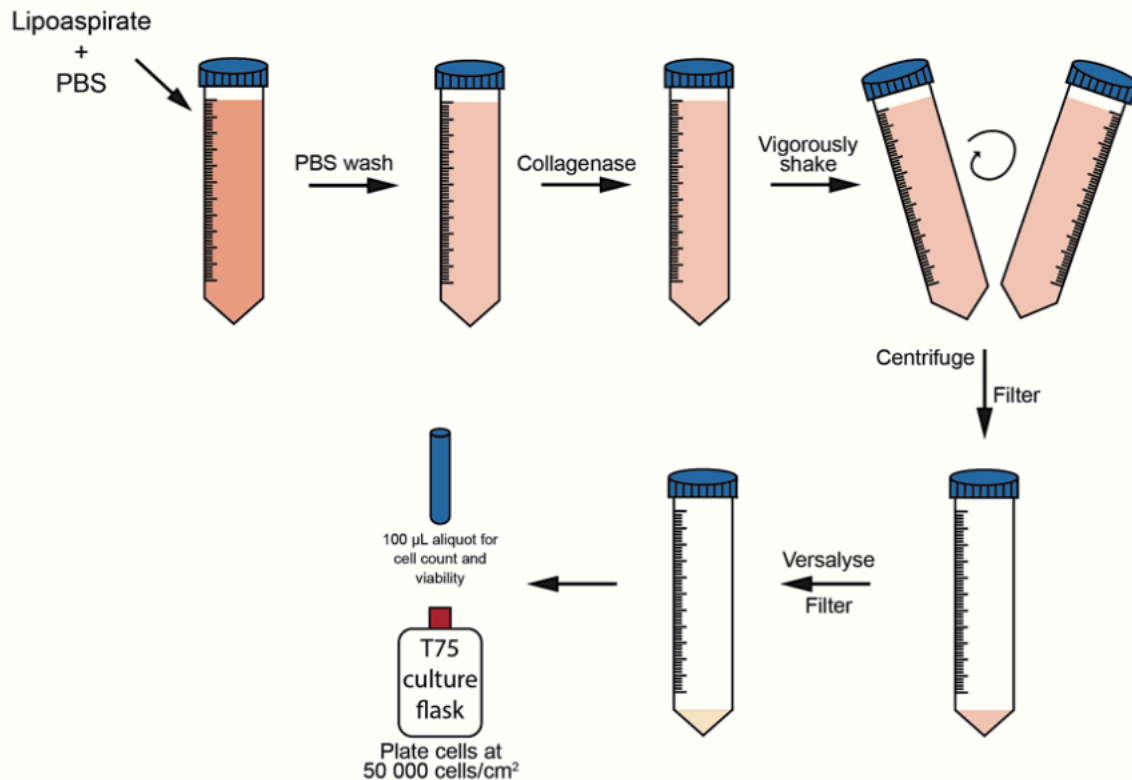
Figure 3.2. Schematic illustration of ASC isolation from lipoaspirate.
Lipoaspirate was washed with PBS to remove any excess blood and lipid fraction. The adipose tissue was then digested with 0.1% type I collagenase solution. The digested adipose tissue was centrifuged and filtered. Versalyse™ was added to the remaining tissue to lyse any residual red blood cells. The cell pellet, also referred to as the stromal vascular fraction (SVF) was resuspended in PBS and an aliquot taken to obtain a cell count and determine the viability of the isolated cells. The SVF was seeded at 50 000 cells/cm^2. (This image was taken from Ms. Simone Grobbelaar's MSc, titled "*In vitro* adipose-derived cell myogenic differentiation").

3.3.3. Flow cytometry

Flow cytometry is a technique used to measure multiple physical and chemical characteristics of a cell. The underlying principle of flow cytometry involves a light beam (commonly a laser beam) that strikes moving particles to cause light scattering and fluorescence emission (Adan et al. 2017). With the use of fluorochrome-labelled monoclonal antibodies and a variety of fluorescent stains, the size, granularity, and fluorescent features of cells can be derived (Wilkerson 2012).

After cells were isolated, they were counted to obtain cell number. Cells were counted on a CytoFlex flow cytometer by transferring 100 µl of the cell suspension to a flow cytometry tube. 7-Aminoactinomycin D was added to the flow cytometry tubes to exclude anucleated cells from the count. Additionally, PBS (1 mL) and 100 µl of Flow-Count™ fluorospheres was added to the flow tube. In the case where 7-AAD/VDC Ruby was not available, DAPI (0.02 µg/ml in molecular grade H_2O) was used and the following additional steps were performed. Paraformaldehyde (4%, 100 µl) was added to the 100 µl cell suspension (before adding PBS and Flow-Count™ fluorospheres) and incubated for 15 min. After incubation 1 µl of DAPI (0.02 µg/ml in molecular grade H_2O) was added to the 200 µl. PBS and Flow-Count™ fluorospheres were then added and the flow tube was analysed on the CytoFLEX cytometer. Analyses was done on a minimum of 5 000 viable MSCs (Figure 3.3). The following equations describes how the absolute cell count was determined.

$$Absolute\ cell\ count\ (\frac{cells}{\mu L}) = \frac{Number\ of\ events\ in\ region\ of\ interest}{Number\ of\ bead\ counts} \times Cal\ factor$$

Equation 3.1. Formula the analysis software uses to calculate absolute cell count (cells/ul) shown in Figure 3.

$$Absolute\ cell\ count\ (Cells) = Absolute\ cell\ count\ \left(\frac{cells}{ul}\right) \times Volume\ of\ cells$$

Equation 3.2. Formula used to calculate absolute cell count (cells).

$$Volume\ of\ cells\ (ul) = Absolute\ cell\ count\ \left(\frac{cells}{ul}\right) \div Number\ of\ cells\ per\ plate$$

Equation 3.3. Formula used to the volume of cells to add to each plate for optimal seeding density of 5000cells/cm².

Figure 3.3. Schematic representation of the flow cytometry protocol, including gating strategies used to determine absolute cell counts and cell viability.

A. Side-scatter versus 7-AAD dot plot used to visualise the viable cells. B. Forward scatter versus side-scatter gated on the viable cells created a P1 gate that was used to determine the cells/ul. C. An event count versus FITC identified the Flow-Count™ fluorospheres. D. FITC versus time gated on FlowCount beads identified the intact fluorospheres. E. The events/ul of P1 population were used to calculate the total cell count (Equation 3.2).

3.3.4. Cell passaging and maintenance

The isolated cells were maintained at 37°C, 5% carbon dioxide (CO_2) in a Thermo Scientific™ water-jacketed CO_2 incubator and were assessed 2-3 times a week during which the culture medium was replaced with fresh CGM. Once the cells reached 80-90% confluency, they were either frozen for later use, plated for experiments, or passaged further depending on the number of cells required for an experiment. To passage cells, cells were first washed with 4 mL pre-warmed PBS (2% pen/strep), and 2-3 mL 0.25% of Trypsin-EDTA was added to the cells for 7 min. The trypsin was neutralized by adding 2-3 mL of CGM to the flask and the content was swirled gently to get all the cells into suspension. The cell suspension was transferred into a 15/50 mL centrifuged tube (each culture in a separate tube) and centrifuged

at 300 x *g* for 5 min. The supernatant was aspirated, and the cell pellet was re-suspended in 2 mL CGM. Cells were seeded at 5000 cells/cm^2 with CGM and the growth medium was replaced every 3-4 days. Excess cells not plated were cryopreserved in cyrogenic medium (CGM supplemented with 10% DMSO) in cryovials by placing the vials in NALGENE® Mr Frosty^{TM} Cryo 1°C freezing container to control the freezing rate. The container was placed in a -80°C freezer overnight, they were then placed in a liquid nitrogen tank for long term storage.

3.3.4.1. Light microscopy

Bright field images were taken of samples to compare the morphology of the primary ASC cultures isolated from lipoaspirates obtained from different patients. The Zeiss Primo Vert inverted light microscope, Zeiss Axiocam digital camera, and ZEN software (version 2.6) was used to capture the images.

3.4. Results

3.4.1. MSCs isolated from adipose tissue

A total of 7 patients' lipoaspirate were collected and processed (Table 3.1). All 7 patients were female between the ages of 33 and 45 (Table 3.1). None of the patients enrolled in the study smoked, suffered from diabetes, cardiovascular disease, or hypertension as this might introduce additional variance. Of the 7 patients, 4 patients were Caucasian (57%), and 3 patients were African (43%) (Table 3.1). The average body mass index (BMI) was calculated as 30.35 (Table 3.1). HIV and hepatitis status were negative for all samples. The volume of adipose tissue processed from each patient ranged from 304 ml – 510 ml (average 433.5 $\pm$ 71.78 ml) (Table 3.1). The number of cells obtained from each isolation was variable and ranged from 29.82 x 10^6 – 224.26 x 10^6 (Average cell yield of 78.09 x10^6 $\pm$ 62.09 x10^6) (Figure 3.4). The majority of the cells isolated from the lipoaspirates displayed a fibroblastic morphology (Figure 9).

Table 3.1. Sample information of adipose-derived stem/stromal cells.

Patient ID	Anatomical position	Collection Date	Patient details			Patient measurements			Amount collected	
			Patient Age	Gender	Patient Ethnicity	Height (m)	Weight (kg)	BMI	Volume (ml)	Weight (g)[3]
A091019	Not specified	09/10/2019	Not recorded	Female	African	1.7	101	34.95	393 ml	336.69
A231019	Not specified	23/20/2019	33-year-old	Female	Caucasian	1.74	88	29.07	304 ml	293.7
A311019-01A	Abdomen	31/10/2019	30-year-old	Female	African	Not recorded	Not recorded	Not recorded	400 ml	Weight not recorded
A311019-02T	Thigh	31/10/2019	39-year-old	Female	Caucasian	1.52	62	26.83	502.5 ml	461.2
A270620-01A	Abdomen	27/06/2020	45-year-old	Female	African	1.57	94	38.14	438 ml	659.09
A150221-01A	Abdomen	15/02/2021	38-year-old	Female	Caucasian	1.68	75	26.57	413 ml	590.9
A150221-01L[1]	Love-handle (Bilateral overhang)	15/02/2021	38-year-old	Female	Caucasian	1.68	75	26.57	Volume not recorded	1418.4[2]
A280621-01B	Back	28/06/2021	39-year-old	Female	Caucasian	1.66	75	27.22	510	639.3
A280621-01R	Arms	28/06/2021	39-year-old	Female	Caucasian	1.66	75	27.22	507.5	712.2

1 A150221-01L is the same patient as A150221-01A just from a different location on the body.
2 Comparing the weight collected from other results, this measurement seems to be an outlier and thus may be incorrect.
3 The empty tube was first weighed. Lipoaspirate samples were then added to the tube and weighed. To determine the weight of the lipoaspirate processed the weight of the empty tube was subtracted from the total weight of the lipoaspirate + tube to obtain only the weight of the lipoaspirate.

The number of nucleated cells obtained per isolation ranged from 29.82 x10^6 – 224.26 x10^6 (Average 76.41 x10^6 $\pm$ 62.09 x10^6). The variance can be attributed to biological variance, amount of adipose tissue processed or due to varying personnel who performed the isolation procedure.
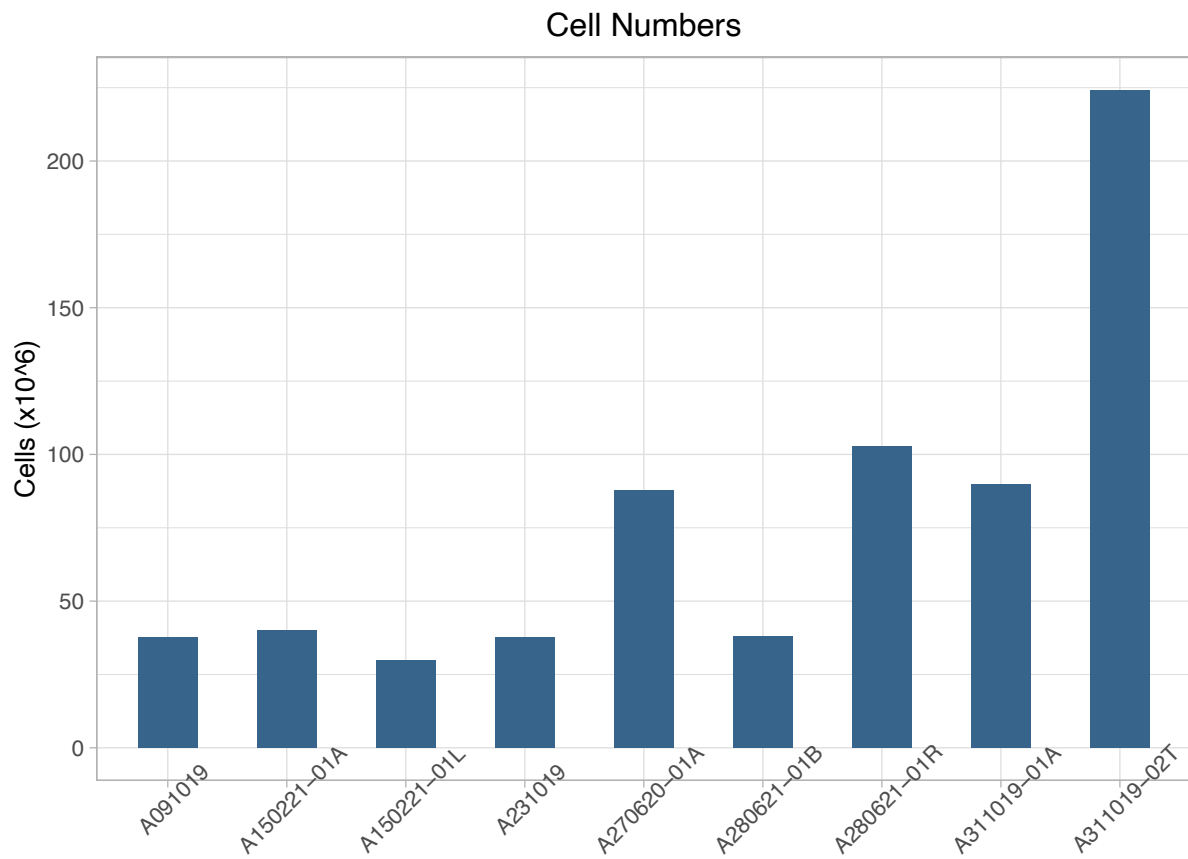
Figure 3.4. Cell yield from each adipose tissue sample.
A311019-02T sample provided the highest yield, while A150221-01L provided the lowest yield of cells.

A091019
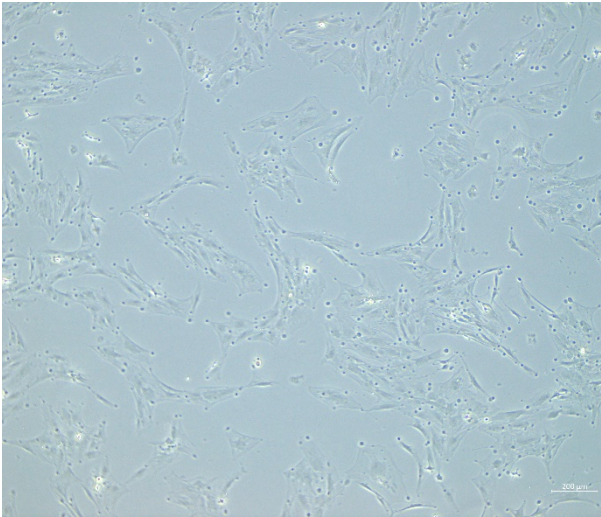
A231019
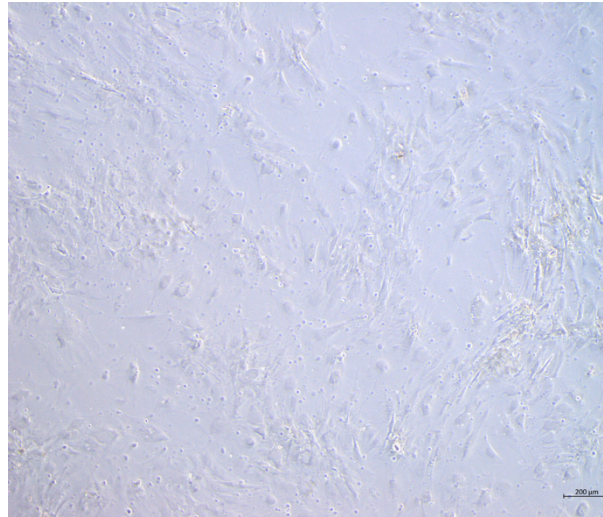
A311019-01A
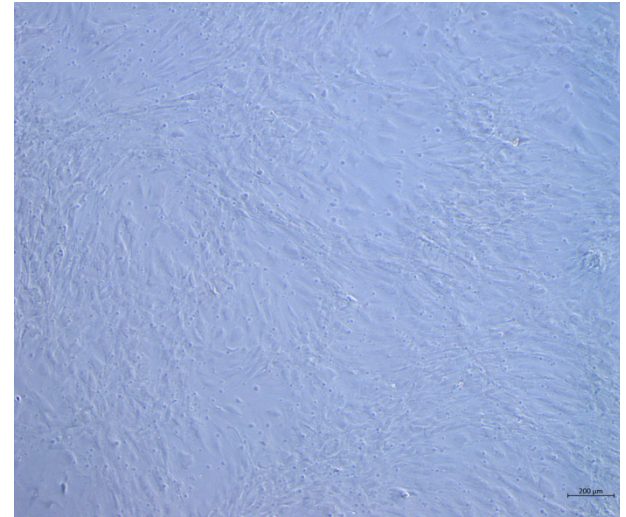
A311019-02T
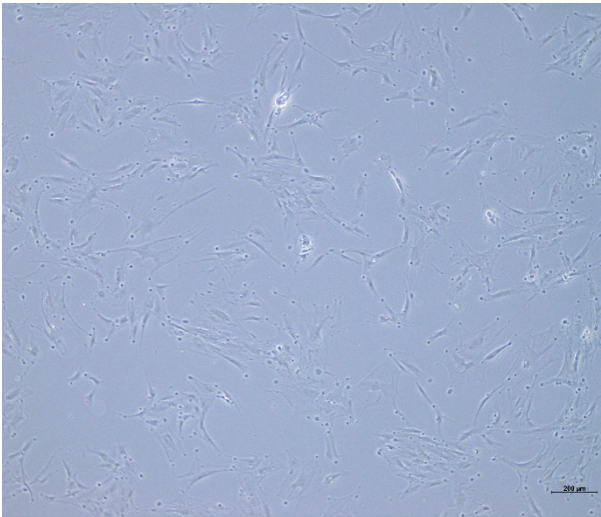
A270620-01A
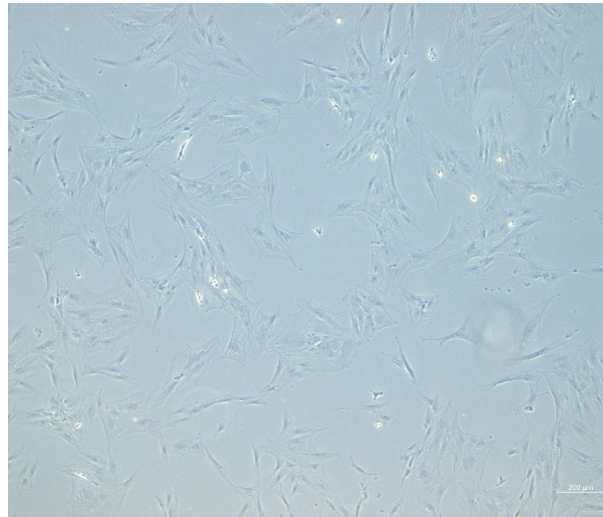
A150221-01A
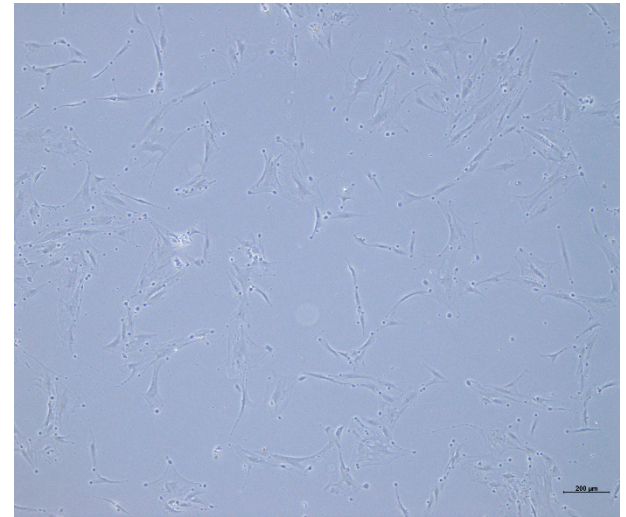
A150221-01L
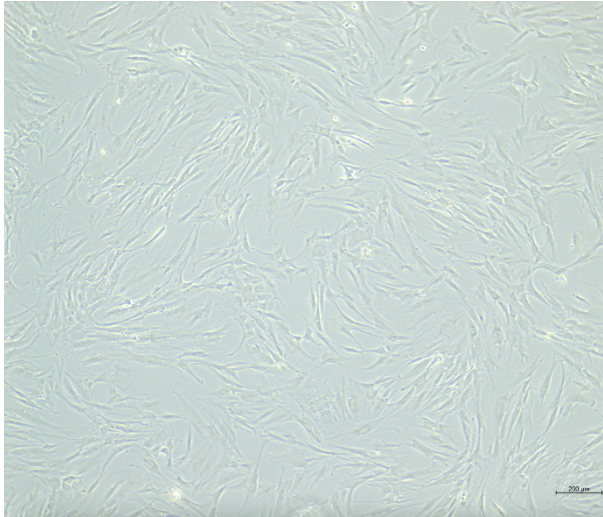
A280621-01B
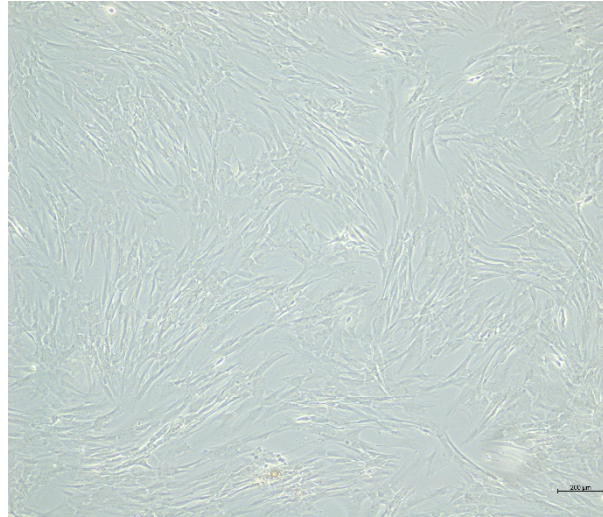
A280621-01R
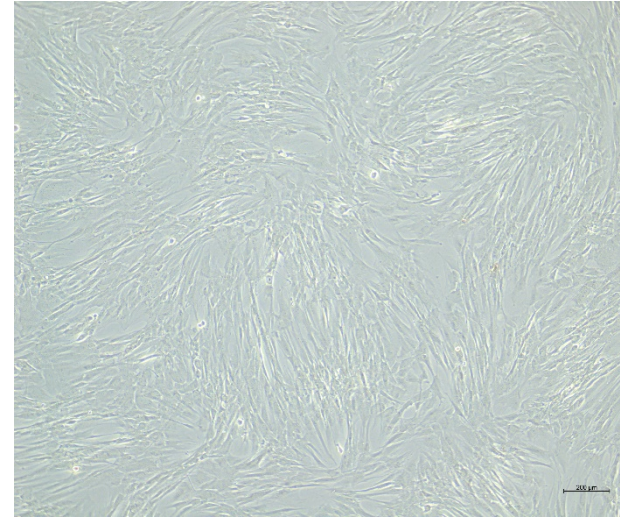
Figure 3.5. Morphology of adipose-derived stem/stromal cells isolated from 8 different donors.
MSCs isolated from different adipose tissue all showed a flattened fibroblastic morphology.

Cell viability and immunophenotyping was done before the start of experiments and will be described in Chapter 4.

3.5. Discussion

The isolation of ASCs from adipose tissue has been well documented by many research groups [54,63,194,214]. Two main methods of isolation, the enzymatic technique, or the explant method, are used. Currently there is no consensus regarding which method is the best. There is also a lack of standardisation of isolation protocols. These are important challenges that need to be addressed to ensure reproducible results in the clinical setting. The ISCAT and IFATS have attempted to create some standardisation when it comes to the characterization of ASCs, and have included guidelines regarding acceptable viability, minimum phenotypic criteria that the isolated cells should adhere to, morphology, and ability to differentiate into cells of mesodermal origin [34].

A total of 8 patients undergoing routine liposuction were consented and their lipoaspirate was collected. The SVF was obtained from the lipoaspirate samples through centrifugation and plated into culture flasks. The SVF is a highly heterogenous population consisting of pre-adipocytes, fibroblasts, endothelial cells, pericytes, smooth muscle cells, macrophages and erythrocytes [34]. One of the properties of ASCs is their ability to adhere to plastic. This property is used to isolate the ASCs from heterogenous SVF.

We adopted the enzymatic digestion and density centrifugation method of isolation from adipose tissue. However, this procedure can be expensive and thus more cost-effective alternatives (isolation procedures) should be explored. A study done by Markarian et al. [288] compared 3 alternative isolation methods. All three methods presented with smaller cell yields than the conventional collagenase method. Priya et al. [289] suggests an explant method that is more simple, efficient and economical. In this method, lipoaspirate samples were washed to remove excess blood. The fat was then minced in a tissue culture dish and spread out. Just enough culture medium was added to the dish to ensure that the fat pieces remained in contact with the culture dish and were not floating on top of the culture medium. The culture dishes were then maintained in a 37°C, 5% CO_2 incubator for 5 – 7 days. A higher cell yield was obtained from the explant method when compared to the enzymatic isolation method. However, Priya et al. [289] suggests that this technique is likely to select for cells with grater migratory potential.

The age and health of the donor are two demographic factors that can influence the quality of ASCs in terms of their differentiation capacity. Studies done by both Barboni et al. and Xin et al. [202,203] demonstrated that there was a positive correlation between the age of the donor and methylation status. The health of individual donors also has an effect on the quality, viability and consistency of ASCs isolated [290]. All our donors were of a relatively young age (between 33 and 45) and none of our donors smoked, had diabetes, cardiovascular disease or hypertension, making them suitable for this study. In conclusion, ASCs were successfully isolated from the 8 patients and produced adherent, fibroblast-like cells for downstream experiment

Chapter 4: Determining the Optimal Osteogenic Differentiation Medium

4.1. Introduction

As mentioned in the previous chapter, one of the characteristics of adipose-derived stem/stromal cells (ASCs) is that they are able to differentiate into many cells types of the mesodermal layer, one cell type being osteoblasts [1]. Osteogenic differentiation is induced by exposing a confluent monolayer of multipotent ASCs to an osteogenic differentiation cocktail consisting of β-glycerophosphate, ascorbate-2-phosphate and dexamethasone. β-glycerophosphate, ascorbate-2-phosphate and dexamethasone, which together orchestrate several regulatory mechanisms such as various transcription factors, stimulators and inhibitors to induce osteogenesis *in vitro* [177,178,180,291]. To achieve successful osteogenesis, ASCs need to be cultured/maintained in complete growth medium (CGM) supplemented with the three compounds, β-glycerophosphate, ascorbate-2-phosphate and dexamethasone, for a minimum period of three weeks [292].

Although these three compounds are consistently described as being used in osteogenic differentiation medium, there is currently no consensus regarding the most optimal concentrations for osteogenic differentiation of ASCs *in vitro* as the concentrations of the stimulating factors vary amongst published osteogenic induction media (Chapter 2, Table 3). The dexamethasone concentration used in osteogenic induction media used in studies varies the most. Dexamethasone is one of the key inducing factors of osteogenesis as it increases alkaline phosphatase (ALP) activity, an important enzyme which promotes extracellular matrix calcification [105,177]. Dexamethasone also promotes the proliferation of ASCs by preventing apoptosis [293,294]. Furthermore, dexamethasone is known to regulate the expression of runt-related transcription factor 2 (RUNX2), a master regulator of osteogenesis [180]. Together with dexamethasone, ascorbate-2-phosphate also increases the activity of ALP. In addition, ascorbate-2-phosphate plays an important role during the early stages of osteogenesis and induces the secretion of collagen type I into the extracellular matrix [291,295]. β-glycerophosphate plays a role in the later stages of osteogenesis by facilitating

the mineralization of the extracellular matrix [178]. β-glycerophosphate acts as source of phosphate to produce the mineral hydroxyapatite, the main compound found in mineralized bone extracellular matrix [296].

In this chapter, the differentiation of ASCs into osteoblasts *in vitro* using three previously published osteogenic differentiation formulations will be described. The three different osteogenic differentiation media all contain β-glycerophosphate, ascorbate-2-phosphate and dexamethasone, but in varying concentrations (Table 4.1). This study will evaluate the three osteogenic differentiation media based on their ability to differentiate ASCs into osteoblasts using two different osteogenic assays namely the ARS assay and the ALP assay.

Table 4.1. A summary of the different osteogenic differentiation media that will be tested in the study.

Differentiation medium	Dexamethasone	Ascorbate-2-phosphate	β-glycerophosphate	Reference
1	10 nM	50 mg/L (155269 nM)*	10 mM	[189]
2	0.1 µM (100 nM)	6000 nM	10 mM	[188]
3	50 nM	0.2 nM	10 mM	[177]

* Please see Supplementary information for calculations for each osteogenic differentiation.

4.2. Materials and reagents

Please refer to chapter 3 section 3.2 Materials and reagents.

New materials and reagents include Sigma Aldrich Chemie (Darmstadt, Germany) was the supplier of ascorbate-2-phosphate, B-glycerophosphate, dexamethasone, paraformaldehyde, and the ARS stain. Flow-Count™ fluorospheres, flow cytometry test tubes and 7-aminoactinomycin D (7-AAD) were purchased from Beckman Coulter (California, USA). Table 4.2 summarizes the monoclonal antibodies, fluorochromes and their respective manufacturers used in flow cytometric assays in this study. Parafilm, acetic acid and ammonium hydroxide were purchased from Thermo Scientific, Lasec, South Africa. The 96-well plates used for qPCR experiments were ordered from Roche (Basel, Switzerand).

Table 4.2. Monoclonal antibodies, function, fluorochromes, detector channels, lasers, filters and their respective manufacturers

Monoclonal antibodies	Function	Fluorochromes	Fluorescent detector channel (FL)	Laser and band pass filters	Manufacturer
Mouse anti-human CD90	MSC surface marker	Fluorescein Isothiocyanate (FITC)	FL1	488 nm (525/40)	Beckman Coulter, Miami, USA
Mouse anti-human CD105	Endothelial cell marker	Phycoerythrin (PE)	FL2	488 nm (585/42)	Beckman Coulter, Miami, USA
Mouse anti-human CD34	Primitive/Stem cells marker	Phycoerythrin-Cyanin 5 (PC5)	FL5	488 nm (690/50)	Beckman Coulter, Miami, USA
Mouse anti-human CD36	ASC surface marker	Allophycocyanine (APC)	FL6	635 nm (660/10)	Beckman Coulter, Miami, USA
Mouse anti-human CD44	Surface adhesion receptor present on MSCs	Allophycocyanin: Cy-7 tandem conjugate (APC Cy7)	FL8	635 nm (780/60)	BioLegend, San Diego, USA
Mouse anti-human CD73	MSC surface marker	Brilliant Violet 421 (BV)	FL9	405 nm (450/45)	BD Biosciences, Franklin Lakes, New Jersey, USA
Mouse anti-human CD45	Heamatological marker, to exclude hematological cells	Krome Orange (KO)	FL10	405nm (525/40)	Beckman Coulter, Miami, USA

4.3. Methods

Adipose-derived stromal/stem cells were used to determine the optimal osteogenic medium from three previously published protocols. In this chapter osteogenic differentiation medium was supplemented with Foetal Bovine Serum (FBS) as it is commonly used for cell culture and was also used in the original publication.

4.3.1. Isolation of ASCs

MSCs isolated from adipose tissue were collected from 7 female patients undergoing liposuction or abdominoplasty procedures after obtaining informed consent. The age of the patients ranged between 33 and 45. All samples in this study tested negative for HIV, Hepatitis B and C and mycoplasma. ASCs were isolated as described in in Chapter 3.

4.3.2. Thawing of ASCs

Cryovials containing ASCs were removed from the liquid nitrogen Dewar and allowed to thaw slightly on ice. For each sample, 10 mL pre-warmed CGM (CGM; DMEM, 10% FBS, 2% pen/strep, 25 μg/mL amphotericin) was added to a 15 mL centrifuge tube (one tube per sample). From the 15 mL centrifuge tube, 1 ml of the pre-warmed complete DMEM was added to the cyrovial and the contents of the vial were pipetted up down and transferred back to the 15 mL centrifuge tube. This was repeated until the sample was completely thawed.

After all the contents in the cryovial had been transferred to a 15 mL centrifuge tube, the cell suspension was centrifuged for 5 minutes (min) at 300 x g (SL 16R centrifuge from Thermo Fischer Scientific, Waltham, Massachusetts, USA). The supernatant was aspirated, leaving behind the cell pellet. Complete DMEM was added (1 ml per flask) to re-suspend the cells after which the cell suspension was seeded in T75 cm^2 culture flasks at 5000 cells/cm^2 and placed in a 37°C/5% carbon dioxide (CO$_2$) water-jacketed incubator (Thermo Scientific™) to allow for cell growth and expansion of culture.

4.3.3. Cell passaging and maintenance of ASCs

The thawed cells were maintained in a 37°C/5% CO$_2$ water-jacketed incubator and were assessed 2-3 times a week during which the culture medium was replaced with fresh CGM. Once the cells reached 80-90% confluency, they were either cryopreserved for later use or plated for an experiment. To passage cells, the cells in the culture flasks were first washed with 4 mL pre-warmed PBS (2% pen/strep), after which 2-3 mL 0.25% of Trypsin-EDTA was added and incubated for 7 min at 37°C. To neutralize the trypsin, 2-3 mL CGM was added to the cell suspension, and the contents were swirled gently to mix. The cell suspension was

transferred to a 15 mL or 50 mL centrifuged tube (each sample in a separate tube; tube size dependant on the number of culture flasks per culture) and centrifuged at 300 x *g* for 5 min. The supernatant was aspirated, and the cell pellet was re-suspended in CGM (1 mL per flask). To count the number of cells, 100 μl of cell suspension, 5 μl of 7-AAD, 100 μl of Flow-Count™ Fluorospheres and 400 μl of PBS was added to a flow tube and analysed on the CytoFLEX flow cytometer (Figure 4.1). To get to the ASC population, a 7-AAd vs. SSC plot was created to exclude any non-viable cells. Next a SSC vs. FSC plot was created gated on the viable cells from the previous plot. Cells were seeded at 5000 cells/cm^2 and the CGM was replaced every 3-4 days.
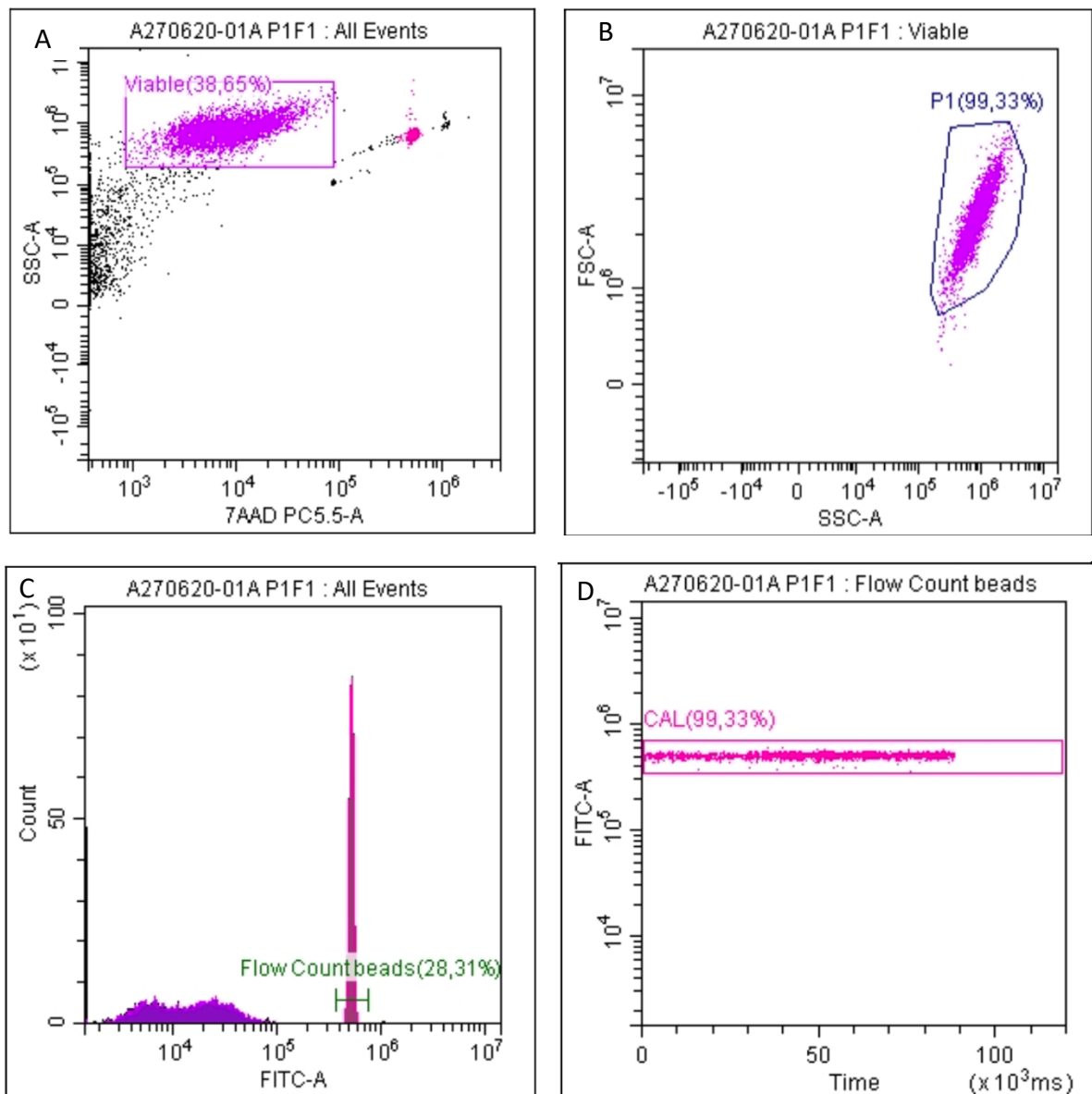
E Tube Name: A270620-01A P1F1
Sample ID:
Absolute Count: Beads Population=CAL, Beads Count=1007, Sample Volume=1µL

Population	Events	% Total	% Parent	Events/µL(B)
⚫All Events	10000	100,00%	100,00%	3581,08
🔵P1	3839	38,39%	99,33%	1374,78
🟣Viable	3865	38,65%	38,65%	1384,09
🟢Flow Count beads	2831	28,31%	28,31%	1013,80
🔴CAL	2812	28,12%	99,33%	####

Figure 4.1. Schematic representation of the gating strategies used to determine cell number and cell viability.
A. A Side-scatter versus 7-AAD plot was used to select for viable cells. B. A forward scatter versus side-scatter plot gated on viable cells was used to select (Region P1) and enumerate (cells/ul) intact, viable ASCs. C. A count versus FITC plot was used to identify the Flow-Count™ fluorospheres. D. A FITC versus time plot gated on the region "FlowCount beads" was used to identify and select intact fluorospheres. E. The cell concentration (Events/ul) was calculated by the CytoFLEX software and used to calculate the total cell count. Percentage total refers to the number of events in question divided by the total number of events analysed multiplied by 100 while the percentage parent refers to the number of events in question divided by the number of events that the cells are gated on multiplied by 100. E.g. Population P1; %Total = 3839/10000 x 100 and %Parent = 3839/3865 x100.

4.3.4. Immunophenotyping of ASCs

The ISCT guidelines recommended that ASCs should express certain pre-defined cell surface markers. The ASCs were immunophenotyped by staining them with a panel of monoclonal antibodies consisting of CD34, CD36, CD44, CD45, CD73, CD90 and CD105.

It is important to set up compensation experiments before doing a multi-colour immunophenotyping panel as fluorochromes have a wide fluorescence emission spectrum and the emitted fluorescence may spill-over in more than one channel which may lead to false positive results. In a compensation experiment, single fluorochrome tubes are run and the level of spectral spill over is measured. This spectral spill over is then removed from the respective channel. A colour compensation matrix is then calculated by the software to determine how much spill over should be removed from each channel (See figure 4.3I).

The following tubes were prepared to generate a colour compensation matrix for the combination of fluorochromes used for phenotyping of the ASCs: Tube 1, "unstained cells"; Tube 2, an unstained positive and negative VersaComp beads tube; Tubes 3-8 contained positive and negative VersaComp beads stained with the individual monoclonal antibodies; Tube 9 contained cells stained with CD90; and Tube 10 contained cells simultaneously stained with all 7 monoclonal antibodies (combination tube) - this tube was used to verify the

compensation matrix generated using the single colour staining tubes and to make final adjustment where need (Table 4.3). The VersaComp Kit consist of two vials, a vial with positive beads and a vial with negative beads. Positive beads are coated with IgG binding agent, whereas the negative beads are not. Antibodies will bind to the positive beads and cause a fluorescence. This will create a distinct positive population in the relevant channel (Figure 4.2A). The positive population will be gated and used to detect the spectral spill over in other channels (Figure 4.2B). This setup is repeated for each monoclonal antibody in the panel.
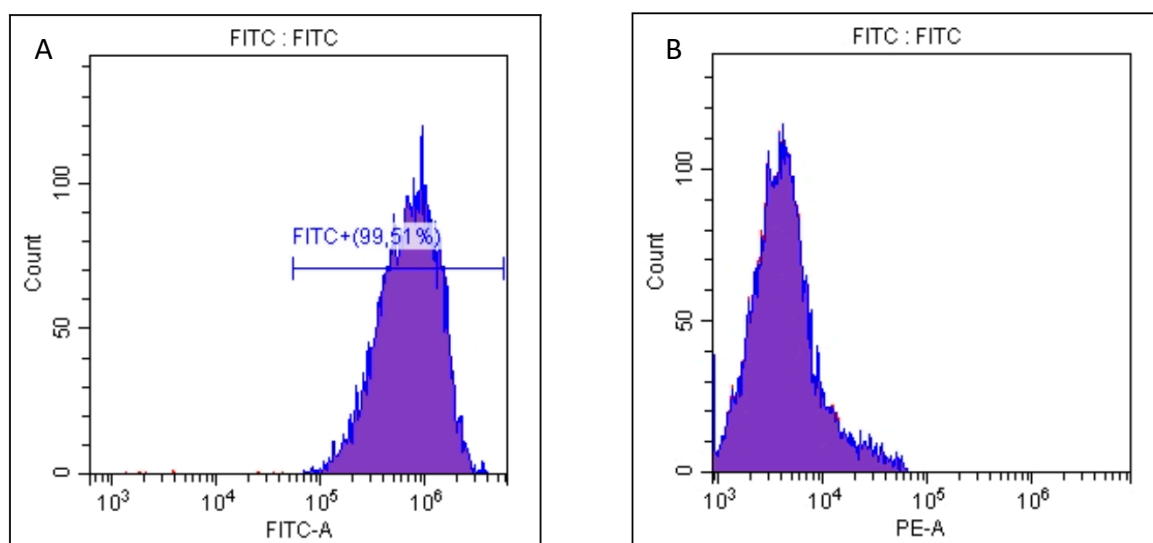
Figure 4.2. Example of compensation experiment of FITC monoclonal antibody.
A. Single stained FITC tube run on the DxFLEX produces a positive FITC population that is used to gate other channels on to determine the amount of spill over to be removed from respective channels. B. Spill over of FITC fluorescence into PE channel that needs to be removed.

Positive and negative VersaComp beads were vortexed before use and one drop of each bead type (negative and positive) was added to the respective tubes (Tube 2-8); Tube 9 contained a single stain of CD90, however CD90 does not have a high binding affinity to the beads and therefore cells were used instead. Once all the antibodies were added to the respective tubes; the flow cytometry tubes were then vortexed and incubated in the dark for 20 min. After incubation, the beads and cells were washed by adding 3 mL PBS (2% pen/strep) to the tubes followed by centrifugation 300 *x g* for 10 min. The supernatant was aspirated and the cells or beads were resuspended in 400 µl of PBS (2% pen/strep) before analysis on the CytoFLEX flow cytometer. Analyses were performed on a minimum of 5 000 viable beads or ASCs.

Table 4.3. Setup of experiment to calculate the ASC phenotype compensation matrix.

	Tube 1	Tube 2	Tube 3	Tube 4	Tube 5	Tube 6	Tube 7	Tube 8	Tube 9	Tube 10
Flow tubes										
Cells	x								*x	x
Beads (Positive and negative)		x	x	x	x	x	x	x		
Addition of monoclonal antibodies										
CD34			x							x
CD36				x						x
CD44					x					x
CD45						x				x
CD73							x			x
CD90								x		x
CD105									x	x

* CD90 does not bind tightly to the beads, therefore cells are used.

The ASC population was visualised using an FSC-A vs. SSC-A two-parameter dot plot (Figure 4.1- A). A gate was drawn around the intact ASC population to exclude any debris present in the samples. A histogram plot (Count vs. respective fluorescent channel) was created for each of the fluorochromes (Figure 4.4). All the histograms were gated on the intact ASC population. In the respective single colour positive tube (e.g Count vs FITC) a positive signal for that fluorochrome was observed. A region of interest was positioned over the positive population. If this fluoresce was picked up in any other channel it was subtracted from that channel and so a compensation matrix was set up to remove any spill-over that might occur during further immunophenotyping experiments (Figure 4.1-I). See Appendix B for full compensation experiment.

Autofl.	Channel	-FITC%	-PE%	-PC7%	-APC%	-APC-A750%	-PB450%	-KO525%
1,10	FITC		2,37	0,45	1,51	0,61	0,09	0,45
1,14	PE	26,37		4,62	1,69	0,85	0,08	0,39
0,20	PC7	0,15	0,76		0,89	2,07	0,02	0,01
0,21	APC	0,00	0,05	0,01		2,14	0,00	0,01
0,24	APC-A750	0,01	0,09	7,68	24,57		0,04	0,00
15,40	PB450	0,10	1,32	0,00	1,78	0,78		2,48
6,27	KO525	4,45	2,15	0,00	3,03	1,33	8,73	
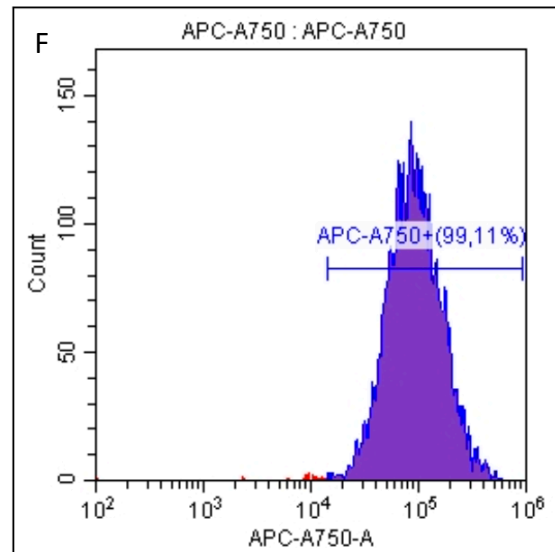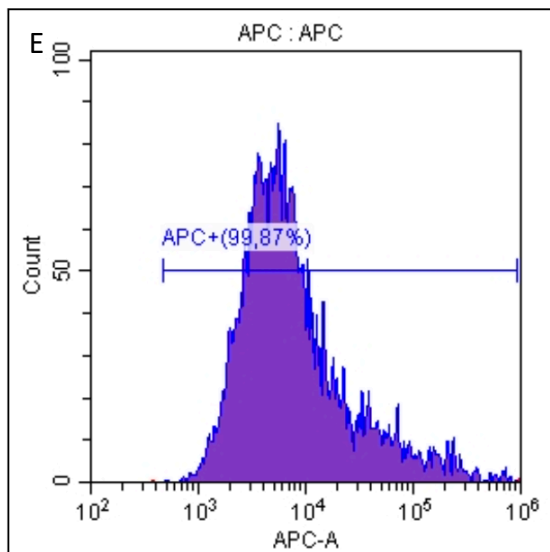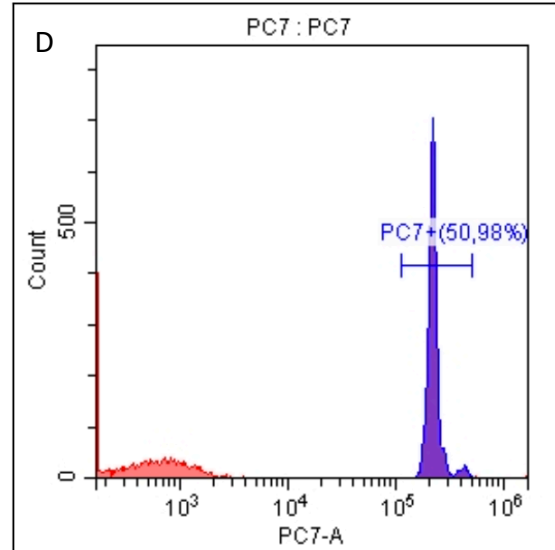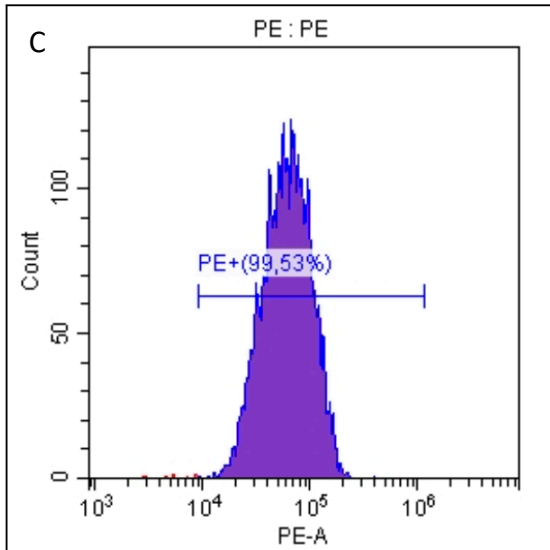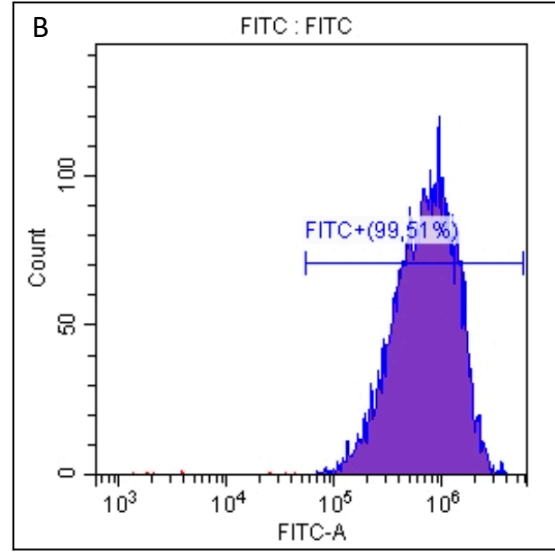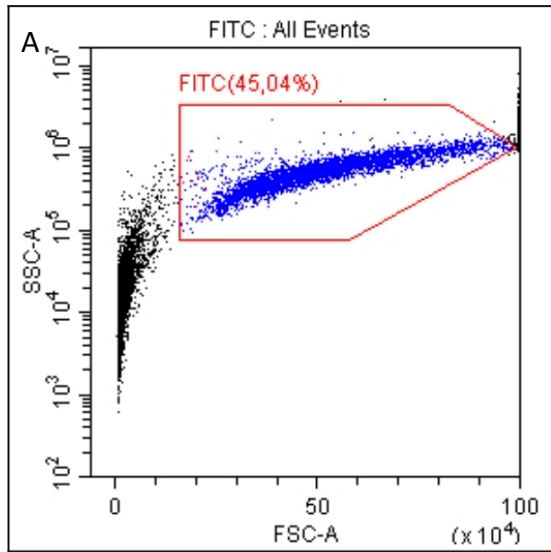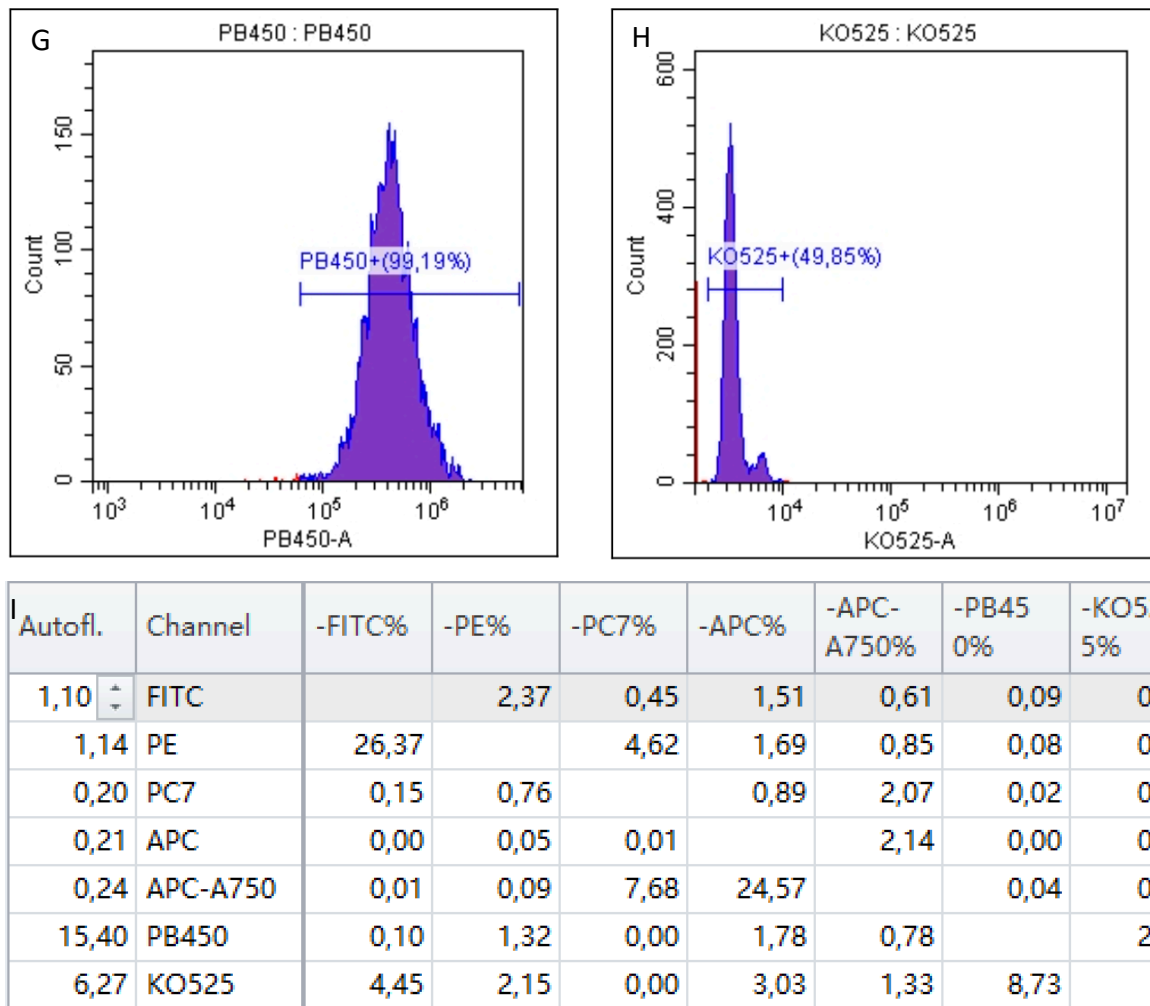
Figure 4.3. Colour compensation experiment set up for the use in downstream multi-colour immunophenotype panel. Positive single colour tubes (B-H) were stained and analysed on the CytoFLEX. Any spectral spill-over fluorescence was calculated, and a compensation matrix was generated (I).

The immunophenotype of the ASCs used in experiments was determined before cells were plated for an experiment. A multi-colour immunophenotype panel (CD31^{-} /CD34[variable]/CD45^{-} /CD44^{+}/CD73^{+}/CD90^{+}/CD105^{+}) was designed in-house at the ICMM based on previously published ASC cell surface marker expression data [31,34,297]. ASCs stained with the monoclonal antibody panel were analysed on the CytoFLEX flow cytometer (Figure 4.4) and the data was then analysed (post-acquisition) using the Kaluza® Flow Cytometry Data Analysis (Beckman Coulter, Miami, USA). Dominici *et al.* 2006 and Bourin *et al.* 2013 described the minimum immunophenotype criteria, as recommended by the International Federation for Adipose Therapeutics and Science (IFATS) and the ISCT, for MSCs, in which 95% of the ASC population must express CD105, CD73 and CD90 [31,34].
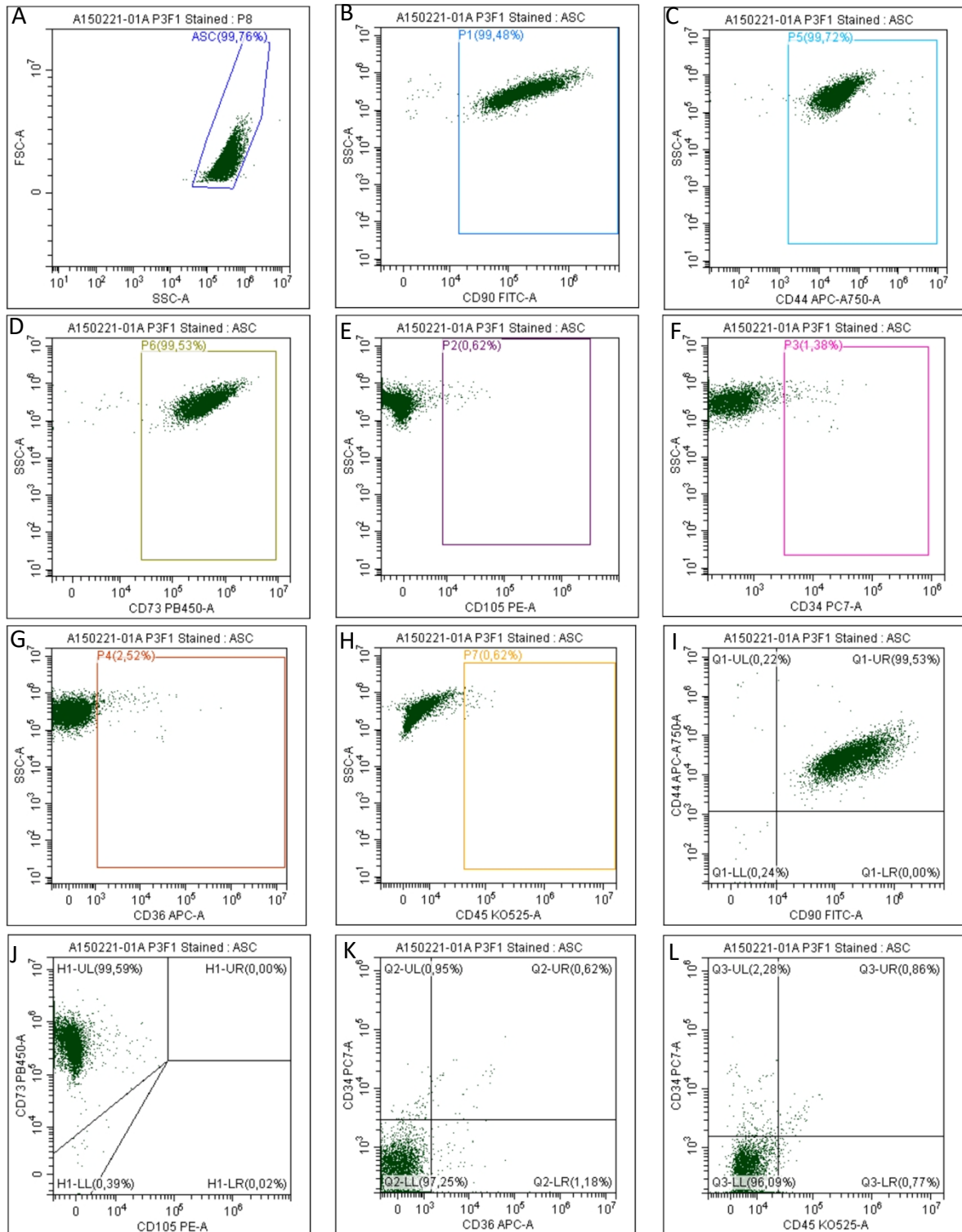
Figure 4.4. Schematic representation of the gating strategies used to determine the immunophenotype of the ASCs. A. Intact ASCs were identified using a forward versus side-scatter plot. Plots B-L were all gated on ASCs for subsequent analysis. Plots B-H were one parameter plots versus side-scatter to determine the expression profiles, the positive gates were set using unstained samples. Plots I-L are two-parameter plots to verify colour compensation.

58

4.3.5. Osteogenic differentiation

Once seeded in 6 well plates (5000 cells/cm^2), ASCs were grown to 70-80% confluence (Passage 2-4) after which the CGM was removed and replaced with osteogenic differentiation medium. ASCs not exposed to osteogenic differentiation medium were maintained in CGM and served as negative (undifferentiated) controls. The efficiency of the differentiation media was assessed through a range of osteogenic assays (described later in this chapter) on days 0 (day of induction) and 28 (day of termination). We opted for a 28-day differentiation period based on a study done by Mohamed-Ahmed et al. 2018 who reported that ASCs have a longer proliferation period and only switch to the differentiation phase on day 21 as well as preliminary experiments[213]. In preliminary experiments (n=2), we too did not observe bone formation at day 21 and consequently decided to extend the differentiation period to 28 days as suggested by Mohamed-Ahmed et al (2018) (Figure 4.5).
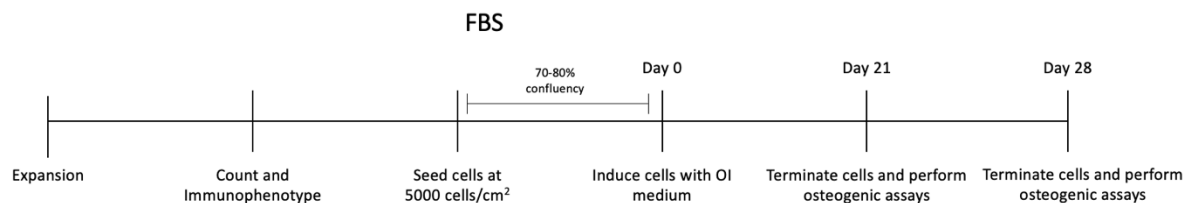
Figure 4.5. Timeline of osteogenic induction.
The illustration shows when the cells were induced and the differentiation timelines. Osteogenic differentiation of ASCs maintained in osteogenic differentiation medium supplemented with FBS was assessed at days 21 and 28. Media was changed twice a week.

Day 0
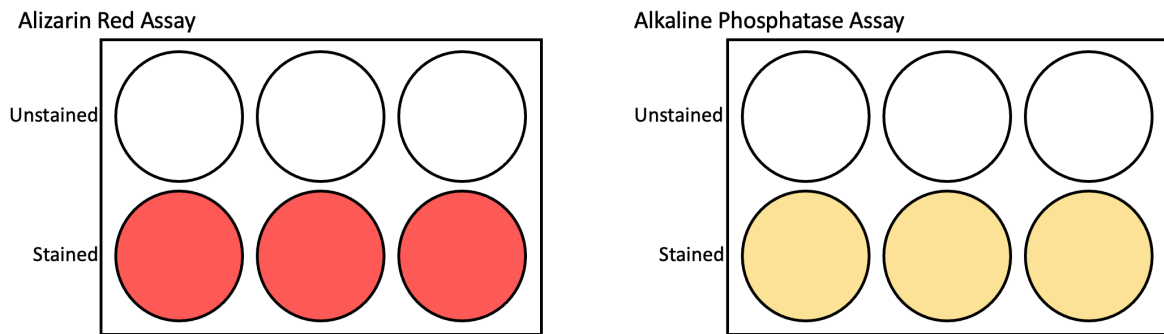
Day 21/28
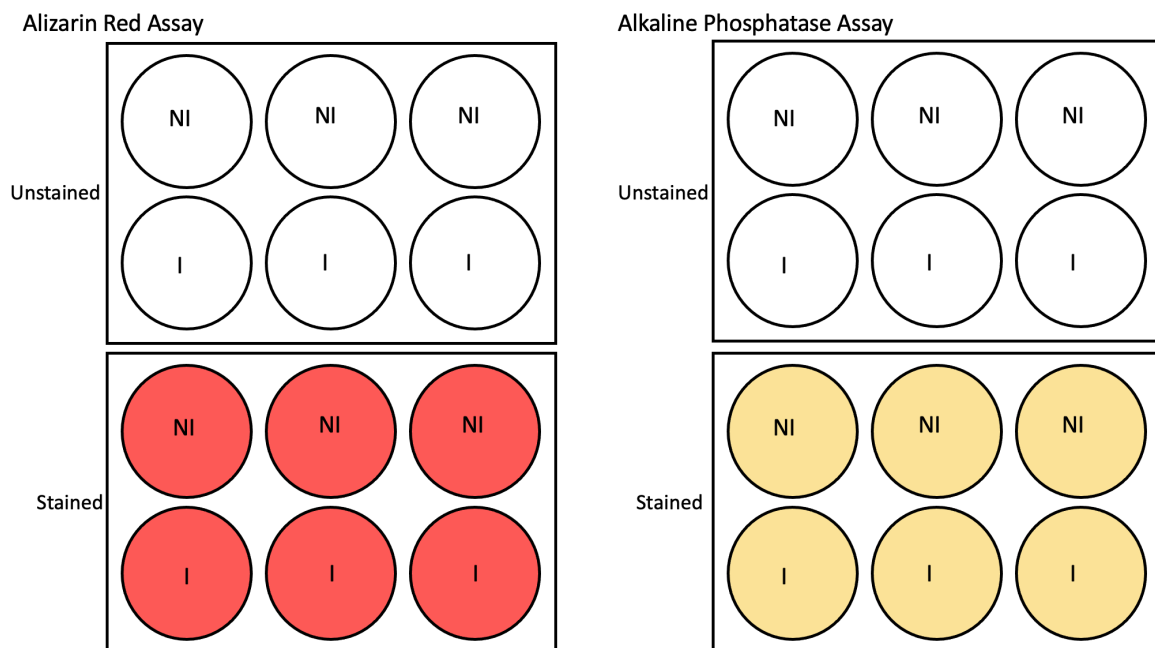
Figure 4.6. Experimental layout used for Alizarin Red (ARS) and Alkaline Phosphatase assays.
ASCs were seeded into 6 well plates at 5000 cells/cm². Day 0; not induced samples at day of osteogenic differentiation induction and unstained controls were assessed. On day 21/28 samples, not induced controls, induced samples as well as unstained controls were assessed. Unstained controls were processed as for the stained samples except for not adding ARS stain. ARS stain was replaced with PBS in the unstained controls.

4.3.6. Osteogenic differentiation assays

Alizarin Red (ARS) Staining Assay

On the day of termination, the ASC monolayer in 6 well plates (9.6 cm²/well) was washed with PBS (2% pen/strep) after which the cells were fixed by adding 2 mL paraformaldehyde (4%) per well followed by incubation for 15 min at room temperature. After 15 minutes, the

paraformaldehyde was removed, and the cells were washed with PBS. The PBS was removed completely before adding 2 mL of a 2% ARS staining solution to the wells followed by incubation at room temperature for 10 min. After aspirating the unincorporated staining solution, cells were washed four times with PBS (2% pen/strep). Excess PBS was removed by incubating the plates at an angle to drain and remove any excess PBS. Plates were air dried overnight, and the stained monolayer was visualized by light microscopy (Carl Zeiss Werke, Göttingen, Germany) and images were captured using a Zeiss Axiocam digital camera (Carl Zeiss Werke, Göttingen, Germany).

The level of osteogenic differentiation was quantified by determining the concentration of ARS in each well. To quantify the ARS concentration, 2 mL of acetic acid (10%) was added to each well followed by incubation for 30 min at room temperature. This was done to extract bound ARS from the cells. The reaction was stopped by adding 200 µl of ammonium hydroxide (10%) to each well. An aliquot (100 µl) from each well was then transferred into a 96-well plate (opaque-walled, transparent-bottomed plates) and the ARS concentration in milli mole mM from each well was determined using a spectrophotometer (PowerWave X, BioTek Instruments Inc, Winooski, USA) at 405nm and 650 nm (reference wavelength).

To determine the concentration (mM) of ARS, a standard curve was prepared. This was done by preparing a 4 mM ARS stock solution. A 1:1 serial dilution was performed to obtain concentrations ranging from 4 mM to 0.0625 mM. The optical density (OD) of each concentration was determined (in triplicate) by transferring the relevant staining solutions to the wells of a 96-well plate. The average OD_{405nm} readings of the ARS standards, blanks and sample readings were calculated and the average OD_{405nm} of the blanks was subtracted from the average OD_{405nm} from each concentration. Using the OD_{405nm} readings of the ARS standards, a standard curve was drawn up by plotting the absorbance (405 nm) OD_{405nm} readings against the ARS concentrations. The ARS concentration of the samples was extrapolated from the standard curve.

The acetic acid was aspirated, and the cells were washed with PBS (2% pen/strep). PBS (2% pen/strep) was added and 1 µl of DAPI (0.02 µg/ml in molecular grade H_2O), a fluorescent nuclear stain, was added to each well to stain the nuclei of the cells to perform a cell count

for normalization. The DAPI (0.02 μg/ml in molecular grade H_2O) was incubated for 5 min and images were taken on the Zeiss AxioVert A1 fluorescence microscope (Carl Zeiss Werke, Göttingen, Germany) using the Zeiss Axiocam digital camera (Carl Zeiss Werke, Göttingen, Germany). The ARS concentrations were adjusted (normalized) to the relative number of cells using the following formula:

$$Normalization = \frac{OD\ value\ or\ Concentration}{Cell\ number}\ x\ Value$$

Equation 4.1. Formula used to normalize the OD value i.e. the amount of stain, to the number of cells

Alkaline Phosphatase Assay

As described for the ARS assay, the cultures were washed to remove any free-floating cells and fixed using paraformaldehyde (4%). An ALP buffer (2 mL/well) was then added to the cells and incubated for 60 min at 37°C. The composition of the ALP buffer was 4-nitrophenylphosphate (5 mM), magnesium chloride ($MgCl_2$) hexahydrate (0.5 mM), Tris-HCl (50 mM) and Triton X-100 (0.01%). An aliquot (100 μl) of each reaction was transferred into a 96-well plate and the absorbance of each reaction was read at 405 nm and 650 nm (reference wavelength). Like with the ARS assay, the ALP assay solution was aspirated, and the cells were stained with DAPI (0.02 μg/ml in molecular grade H_2O) to determine the average number of cells/well.

As for the ARS assay, the ALP concentrations were adjusted for the (normalized relative number of cells/well using the same formula (Equation 4.1).

4.3.7. Microscopy

Light microscopy

Bright field microscopy images were captured on days 0 and day 21 or 28 using the Zeiss Primo Vert inverted light microscope (Carl Zeiss Werke, Göttingen, Germany) and Zeiss Axiocam digital camera. The ZEN software (version 2.6) was used to capture the images. Bright field images were used to compare the morphology of cells grown in different osteogenic differentiation media. Images were also taken after the cells had been stained

with ARS to visually assess the degree of osteogenic differentiation. 5x magnification was used.

Fluorescence microscopy

To normalize the levels of ARS and ALP to the relative number of cells (calculated as the average number of nuclei per well), cells were stained with DAPI (0.02 µg/ml in molecular grade H_2O) and imaged using the Zeiss AxioVert A1 fluorescence microscope (blue filter-531/40) and Zeiss Axiocam digital camera. A 5x/10x/20x/40x objective lens magnification was used depending on the number of cells present in each well. The more cells there were the more difficult it was to accurately determine the relative number of cells. For this reason, a higher magnification was used to decrease the number of cells per field of vision making the identification of single cells easier for downstream counting analysis. The scale bar was used to calculate the area of the field of vision. The average of five fields of vision were used as a representative count per well (Figure 4.7). The following equation was used to calculate an approximate cell count per well (9.6 cm^2) thus allowing for the comparison of counts even if different magnifications were used:

$$Approximate\ cell\ count$$
$$= \frac{Average\ cells\ from\ the\ 5\ representative\ images\ x\ 9.6\ cm^2}{Area\ of\ field\ of\ vision}$$

Equation 4.2. Formula used to calculate the approximate number of cells in each well of a 6-well plate.
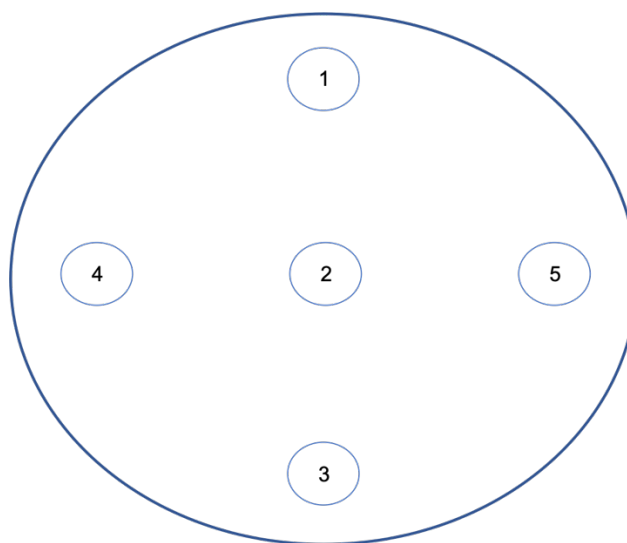
Figure 4.7. Schematic illustration of the fields of visions used to calculate a representative cell count per well.

Protocol for obtaining cell numbers within a well using ImageJ

Images captured on the fluorescent microscope were saved as a .tiff files and were opened and processed in ImageJ (Version 2.1.0/1.53c; Laboratory for Optical and Computational Instrumentation, University of Wisconsin, Wisconson, USA). The brightness and contrast of the images was adjusted, but the images were not manipulated. The image was converted into an 8-bit image and the threshold was adjusted to Black and White ("B&W"). The image was converted into a mask using the binary option in ImageJ (Menu: Process > Binary > Convert to Mask). Watershed was then applied to the image (Menu: Process > Binary > Watershed) to separate out connected particles. The particles (individual nuclei) were then analysed using the count function under the Analyse menu (Menu: Analyse > Analyse particles). Everything less than 200-pixel units was excluded as this was seen as debris and not cells. The number of cells were displayed. Cells close to each other were sometimes identified (called) as a single cell. Therefore, images were also manually assessed to ensure that the correct calls were made by the software and the necessary adjustments were made when needed. The scale was calibrated by measuring the scale bar to determine the number of pixels (indicated as the yellow line) and setting the known distance given on the scale bar (e.g., 50μm) and entering the correct units (μm). The pixel aspect ratio is by default 1, meaning that the height and width of individual pixels are equal. The area of the field of vision is calculated using the formula A = length x breadth. The length and breadth of the field of vison is given by the software once the distance in pixels, known distance and the correct units are entered e.g., 642.59 x 480.56 μm (Figure 4.8B).
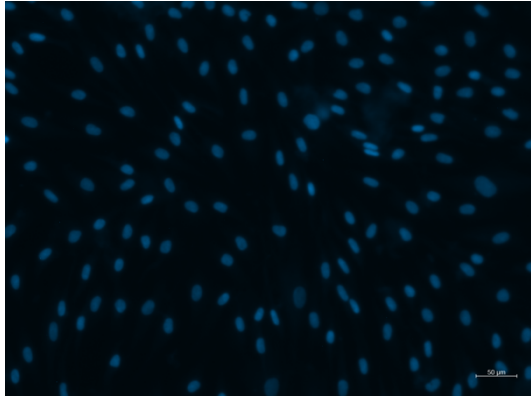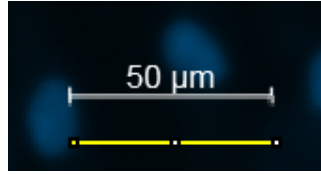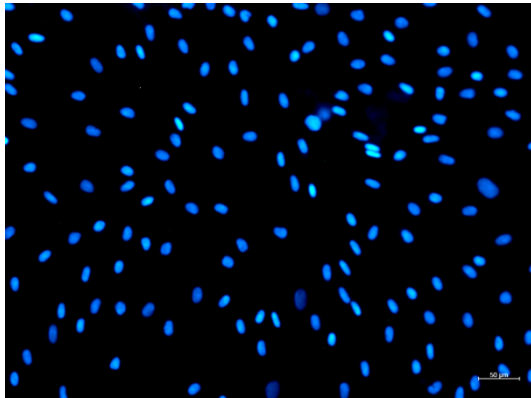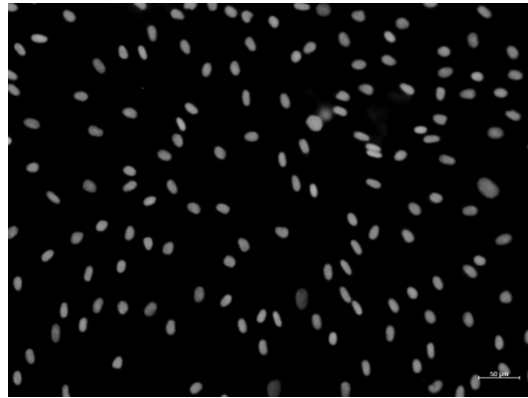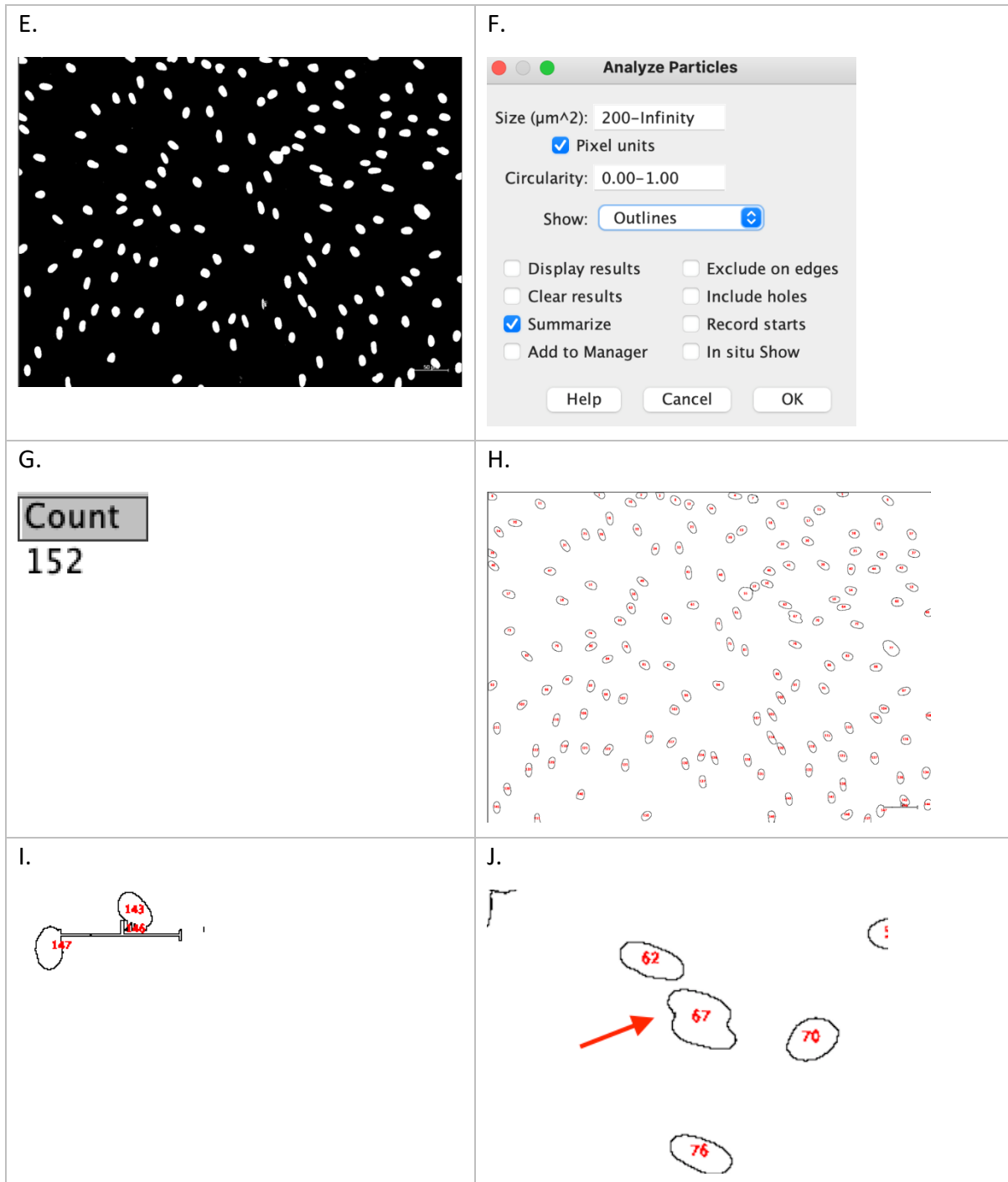
Figure 4.8. A summary of the steps followed to obtain an approximate cell count per well using ImageJ software.
A. The original image captured. B. The scale was calibrated by measuring the scale bar to determine the number of pixels, setting the known distance and entering the correct units. These parameters were all used to calculate the area of the field of vision displayed by the software in the top left-hand corner e.g., 642.59 x 480.56 μm. C. The brightness of the images was adjusted to improve the resolution of the nuclei. D. The image was converted to an 8-bit image. E. Threshold was adjusted to "B&N". F. The image was analysed to determine the number of nuclei per field of vision. G. The nuclei count as determined by the ImageJ software. I & J. Images were manually assessed and incorrect calling of events (nuclei), such as the scale bar counted as a nucleus (I) or nuclei in close proximity counted as a single event were corrected.

4.3.8. Statistical analysis

Statistical analysis of data was performed in R (Version 4.0.1) and RStudio (Version 1.3.959). Data is reported as mean ± Standard Deviation (SD). To test statistical significance, a one-way ANOVA was performed. This test was followed by a Tukey's test to determine the individual significance between each treatment group. A p-value $\leq$ 0.05 was considered statistically significant.

4.4. Results

4.4.1. ASC Isolation and Characterisation

Prior to plating for each experiment ASC morphology was checked, cells were counted, their viability was checked, and their phenotypic profiles were assessed. Plastic adherent ASCs had a typical fibroblastic morphology. Cells grown in CGM supplemented with FBS revealed a more flattened, broader spindle morphology (Figure 4.9). Cell numbers were determined using Flow-Count™ fluorospheres. The average cell viability was 38.17% $\pm$ 6.72. The low cell viability in FBS supplemented CGM can be due to long expansion periods. FBS cells took longer to proliferate to reach the desired cell numbers and were kept in culture for extended periods. The immunophenotype of the ASCs was determined by analysing individual cell surface markers. The expression profile was as follows: CD90 on 97.02% $\pm$ 3.38 of ASCs, CD105 on 0.43% $\pm$ 0.38 and CD34 on 3.51% $\pm$ 3.4 ASCs. CD36 was present on 31.5% $\pm$ 25.61 of cells, CD44 on 99.66% $\pm$ 0.2, CD73 on 81.69% $\pm$ 19.67 and CD45 on 0.3% $\pm$ 0.31 (Figure 4.10). The immunophenotype of the individual cultures were as follows; A150221-01A was $CD90^{+}/CD44^{+}/CD73^{+}/CD105^{-}/CD34^{-}/CD36^{-}/CD45^{-}$, A231019 was $CD90^{+}/CD44^{+}/CD73^{+}/CD105^{-}/CD34^{variable}/CD36^{variable}/CD45^{-}$, A311019-01A was $CD90^{+}/CD44^{+}/CD73^{+}/CD105^{-}/CD34^{-}/CD36^{variable}/CD45^{-}$, and A311019-02T was $CD90^{+}/CD44^{+}/CD73^{+}/CD105^{-}/CD34^{-}/CD36^{variable}/CD45^{-}$.

Cultures

A311019-01A

A311019-02T
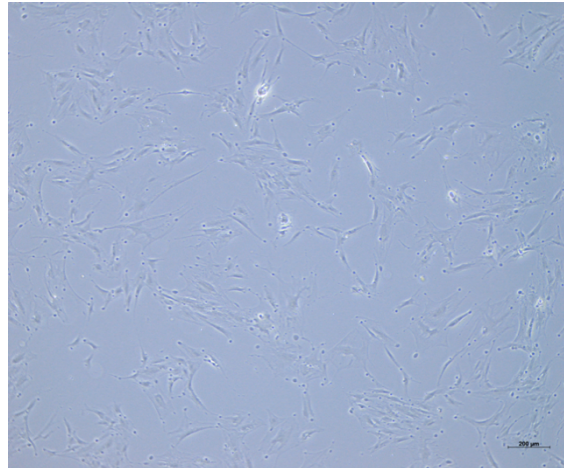
A231019
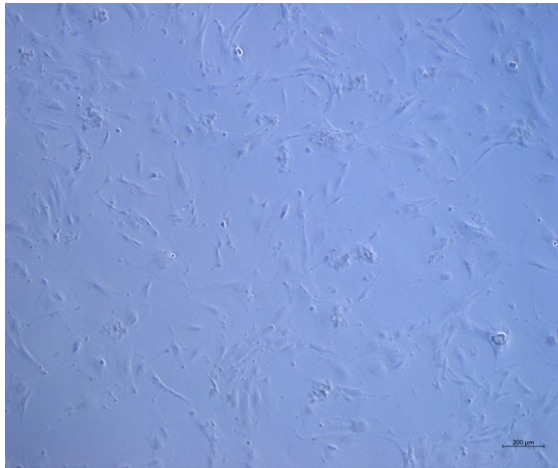
A150221-01A
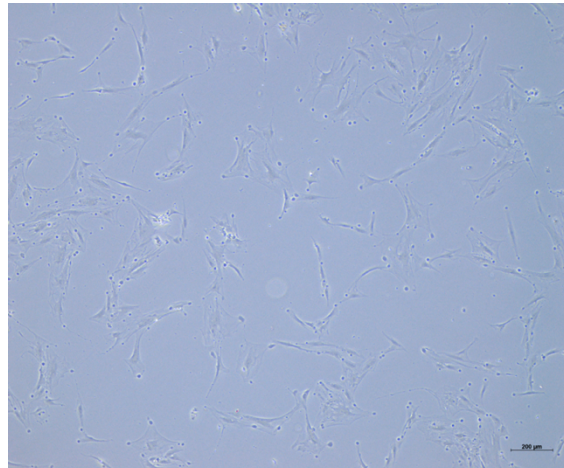
Figure 4.9. Morphology of different adipose-derived MSC cultures expanded in FBS supplemented growth.
Cells grown in CGM supplemented with FBS have a flattened appearance. No apparent differences are seen in the morphology between different osteogenic differentiation media.
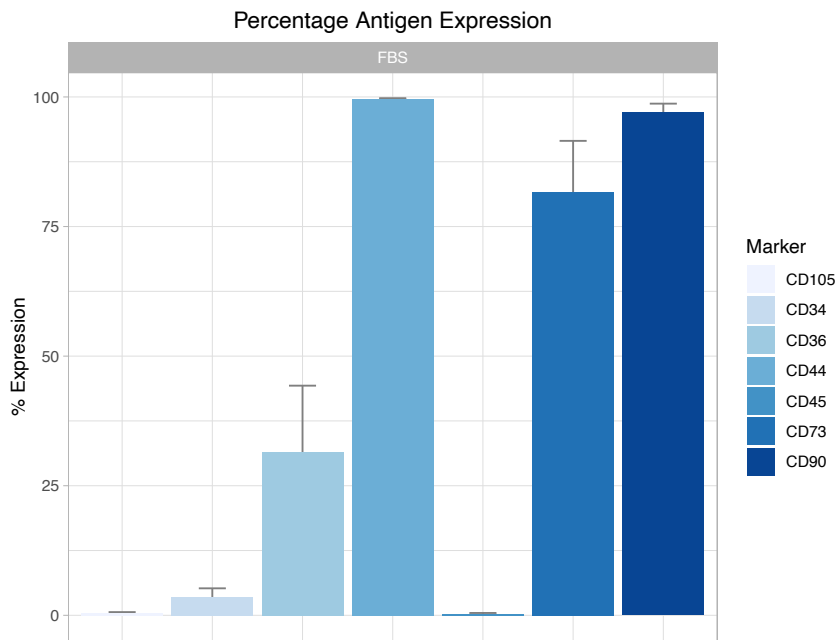
Figure 4.10. Percentage expression of the respective surface antigens on ASCs before plating for experiments.
The graph shows the average proportion (%) of ASCs expressing the respective markers. The ASCs were cultured/maintained in CGM FBS-supplemented medium before plating for experiments. Results are expressed as mean ± standard deviation (SD). Only a very small proportion of ASCs expressed CD45 and CD105. More than 75% of the ASCs expressed CD44, CD73 and CD90.

4.4.2. Osteogenic differentiation

Osteogenic differentiation was assessed in a semi-quantitative manner using either ARS staining or an ALP assay. The results of both assays were measured on a spectrophotometer. Results of both assays were normalised against the average cell number per well. In addition, brightfield images were captured of the ARS assays.

Alizarin Red S Assay

At the day of termination (day 21/28), the cells were fixed and stained with ARS as described earlier. Unstained samples were included as non-specific staining controls (Figure 4.11A, C, E, F). Non-induced samples that were maintained in CGM were included an undifferentiated control (Figure 4.11B, D, F, G). On day 0, both the stained and unstained samples did not show any presence of ARS stain (Figure 4.11 A, B). On day 21, both non-induced controls and induced samples showed very low levels of ARS staining if any (Figure 4.11 D, F). Due to little osteogenic differentiation, samples were differentiated for an additional 7 days to day 28.

On day 28, the induced samples showed increased amounts of calcium deposition compared to day 21 induced samples (Figure 4.12).

A. Day 0 Unstained
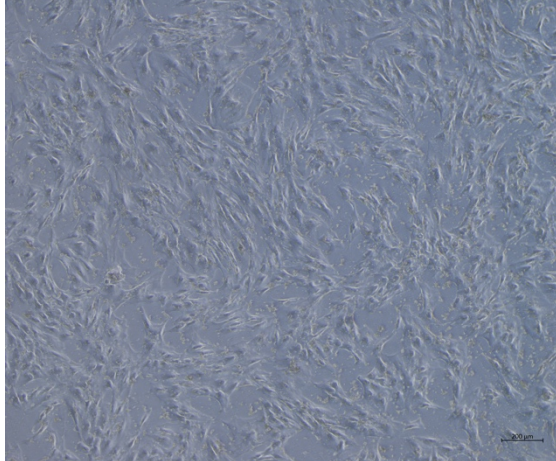
B. Day 0 Stained
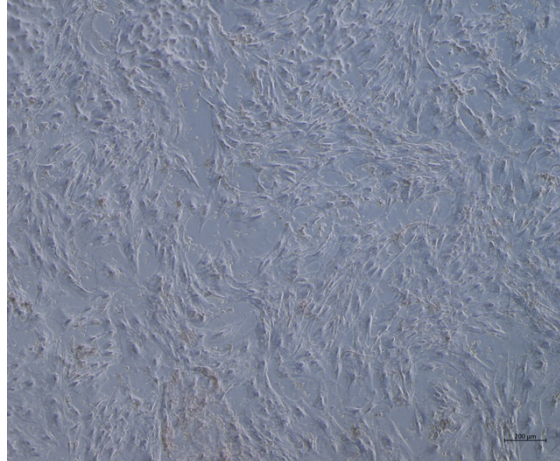
C. Day 21 Non-induced Unstained
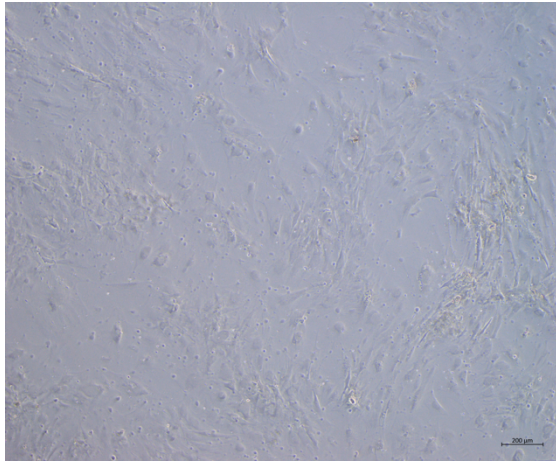
D. Day 21 Non-induced Stained
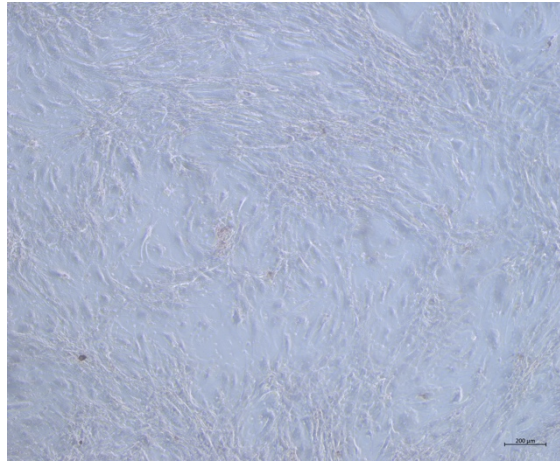
E. Day 21 Induced Unstained
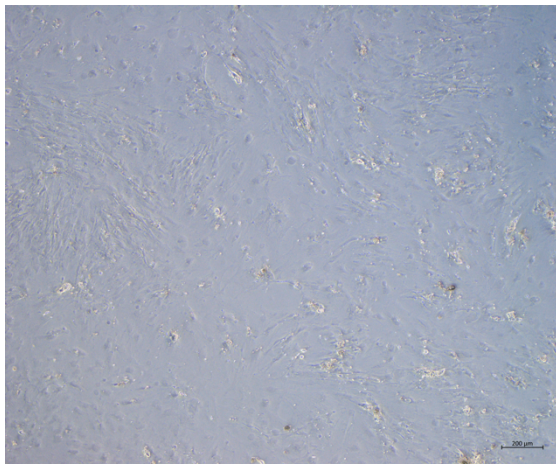
F. Day 21 Induced Stained
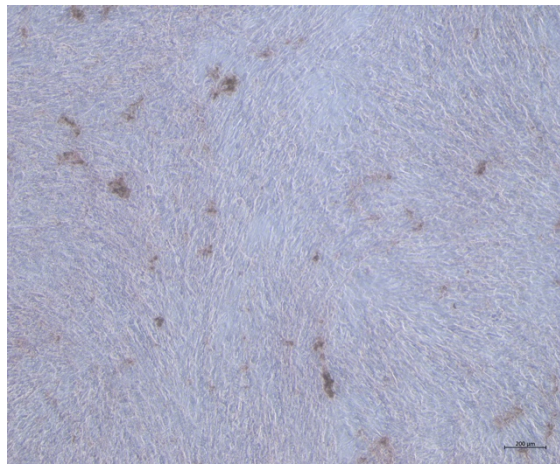
G. Day 28 Not Induced Unstained
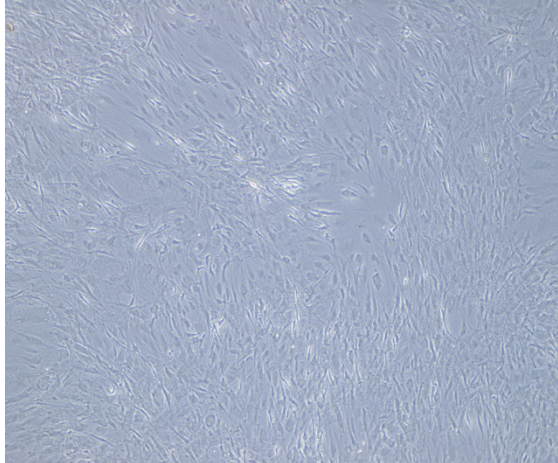
H. Day 28 Not Induced Stained
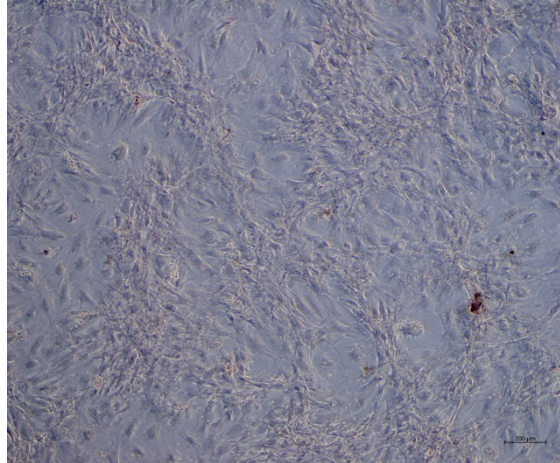
I. Day 28 Induced Unstained
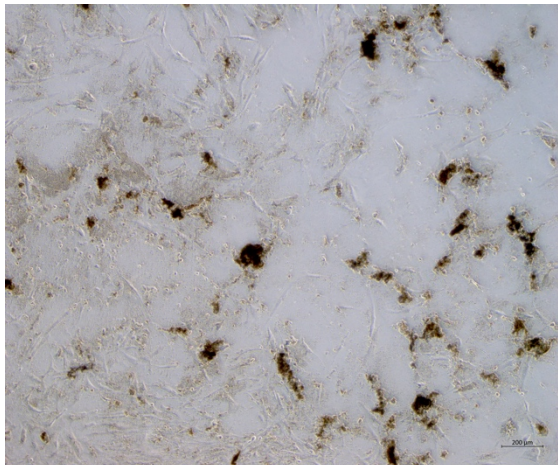
J. Day 28 Induced Stained
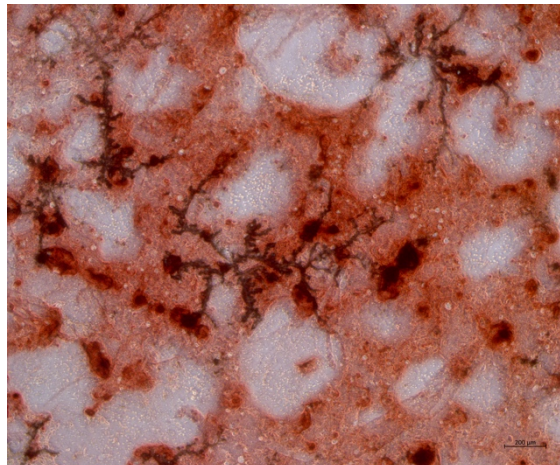
Figure 4.11. Examples of the different control and experimental groups.
Once cultures reached 70–80% confluency, they were induced to undergo osteogenic differentiation. On day 0, both unstained and stained samples were included (A and B). On day 21 and 28, samples were divided into 4 groups namely non-induced unstained (C and G), non induced stained (D and H), induced unstained (E and I) and induced stained (F and J).

A. Day 21 Induced Stained
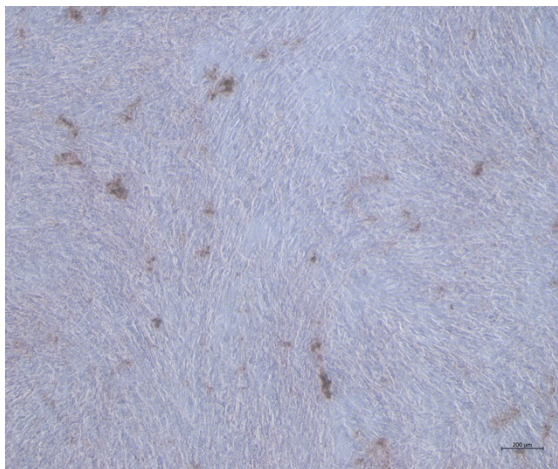
B. Day 28 Induced Stained
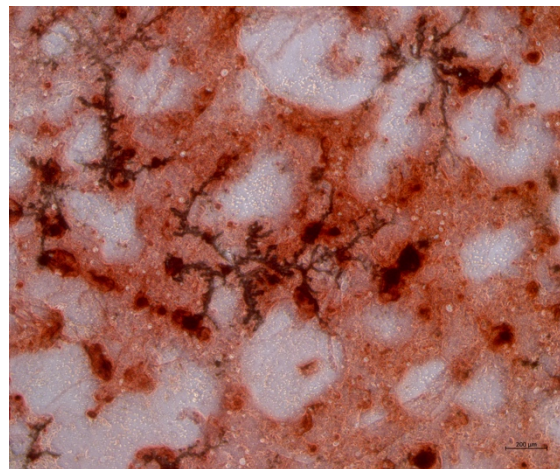
Figure 4.12. Comparison between amount of calcified bone product on day 21 and day 28.
Very little calcium deposition was seen on day 21 (A). The differentiation period was extended to 28 days based on observations reported by Mohamed-Ahmed et al. 2018 and an increase of stain i.e differentiation was seen (B).

An ARS standard curve was used to convert OD readings into ARS concentrations (mM). The serial dilution ranged from 4 mM to 0.0625 mM ARS. The OD readings were read at 405 nm and 650nm (Reference wavelength used as an internal reference where no signal should be picked up). The average blank reading (reading of distilled water) was subtracted from all the other readings. The adjusted OD results were converted into a concentration using the formula $y = 1.05119977x - 0.03407551$; where y is equal to the OD reading and x is the concentration of ARS Stain in mM. The linear correlation (R^2) of the standard curve was 0.9997746 (Figure 4.13).

ARS Standard Curve (n=3)

$$y = 1.05119977x - 0.03407551$$
$$R^2 = 0.9997746$$
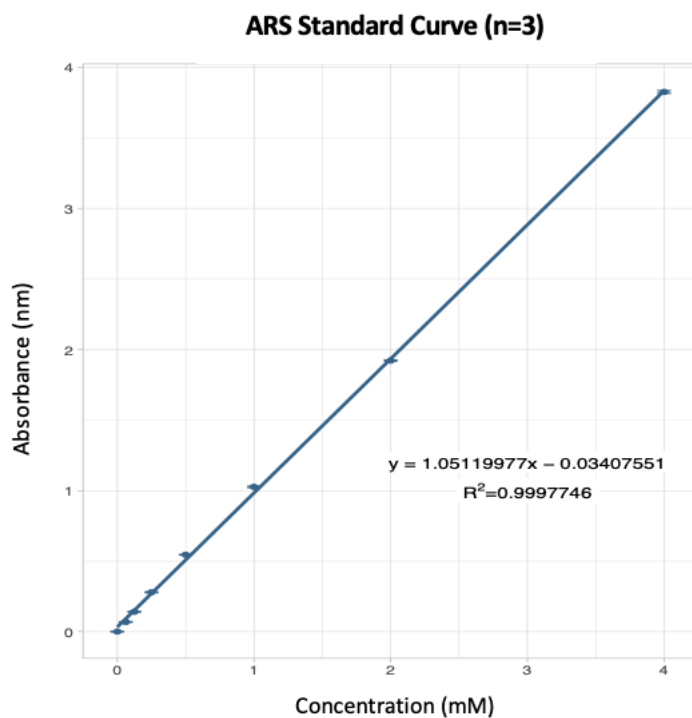
Figure 4.13. ARS Standard Curve
Standard curve displaying the equation $y = 1.05119977x - 0.03407551$ used to calculate the concentration of ARS

Differentiation medium 1 resulted in a gradual increase in calcium deposition from day 0 to day 21 to day 28 (Figure 4.14), which was significantly greater ($p = 0.0058302$) at day 28 when compared to day 0. Differentiation medium 2 resulted in only low levels of calcium deposition at day 21, which were not significant when compared to the levels measured at day 0; however, there was a significant increase in ARS staining, i.e., calcium deposition, on day 28 ($p = 0.0003160$). Differentiation medium 3 showed a noticeable increase of ARS staining on both day 21 and day 28 compared to day 0. However, the day 21 results should be interpreted

with caution as only one of the two cultures showed unusually high levels of calcium deposition on day 21.

The level of ARS stain was the highest on day 28 for differentiation medium, although the variability was relatively high between the four biological repeats. There was also no significant difference in the ARS concentration on day 28 between the three differentiation media. However, based on the more gradual increase observed in calcium deposition and the more consistent results observed at day 21 for differentiation medium 1, we opted for this medium (differentiation medium 1) for further experiments described in the chapters to follow (Figure 4.14).
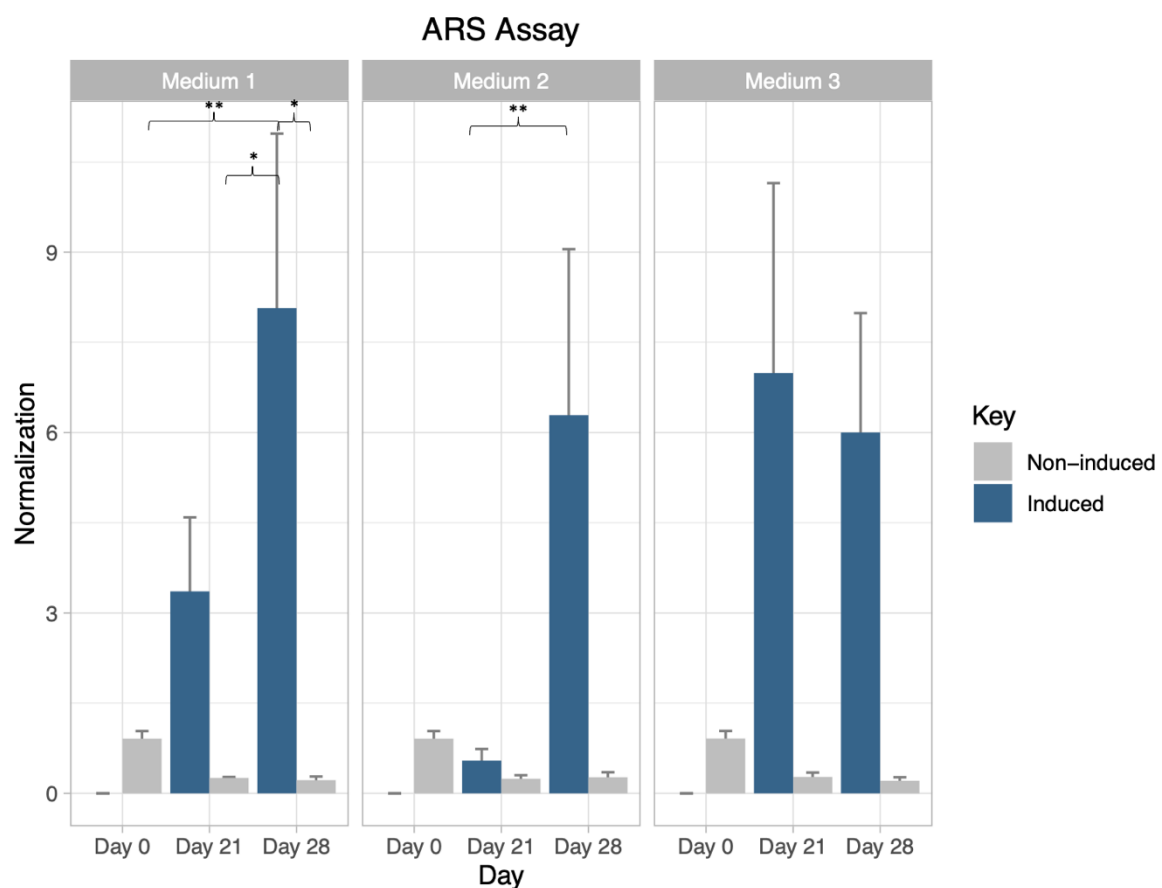
Figure 4.14. ARS stain concentration eluted from various samples.
Differentiation medium 1 had more consistent osteogenic differentiation at day 28 and had a significant increase in ARS present from day 0 and day 21. For differentiation medium 2 very little ARS staining was present at day 21. A large degree of variation was observed between different biological repeats which resulted in large error bars. Results are displayed and mean ± SD.. Significance: p <0.00001 "***", p<0.01 "**", p<0.05 "*".
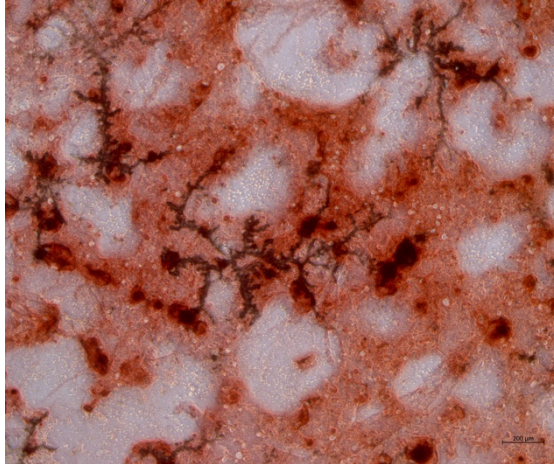
Culture	Condition		
	Medium 1	Medium 2	Medium 3
A311019-01A			
A311019-02T			
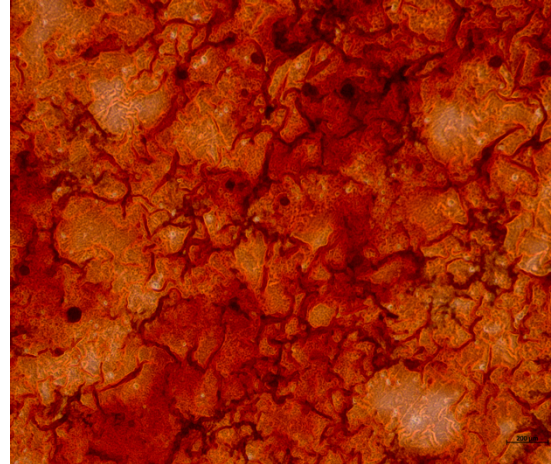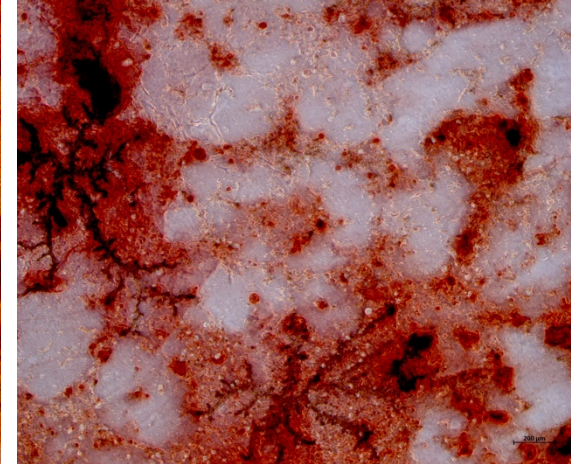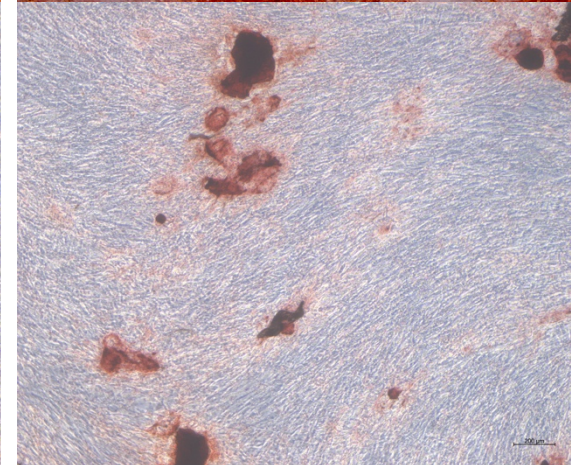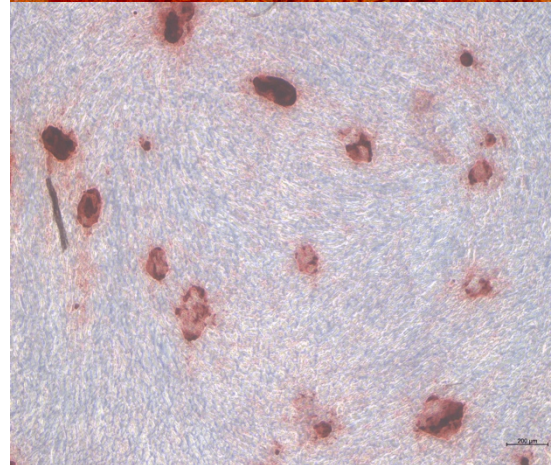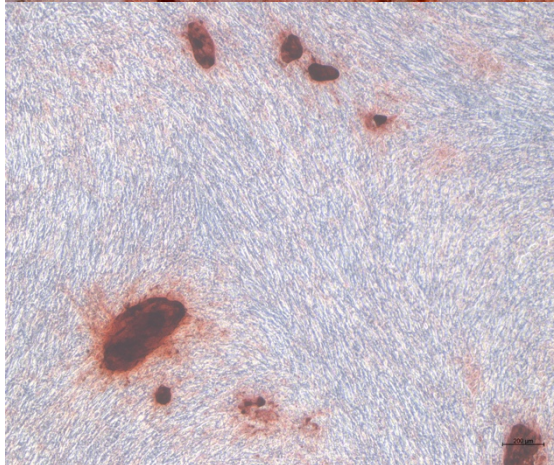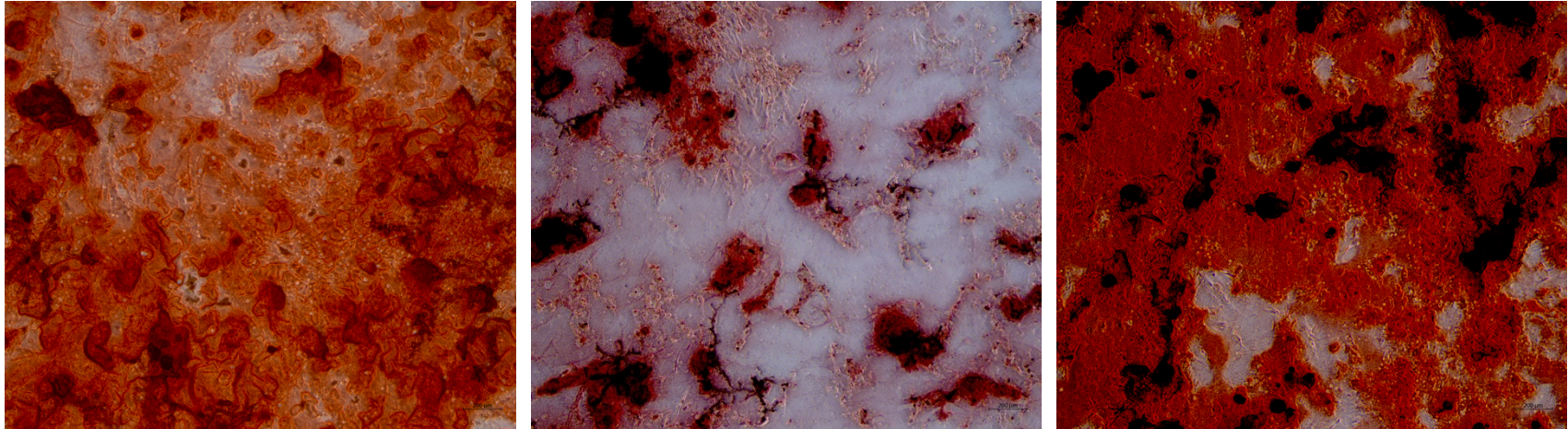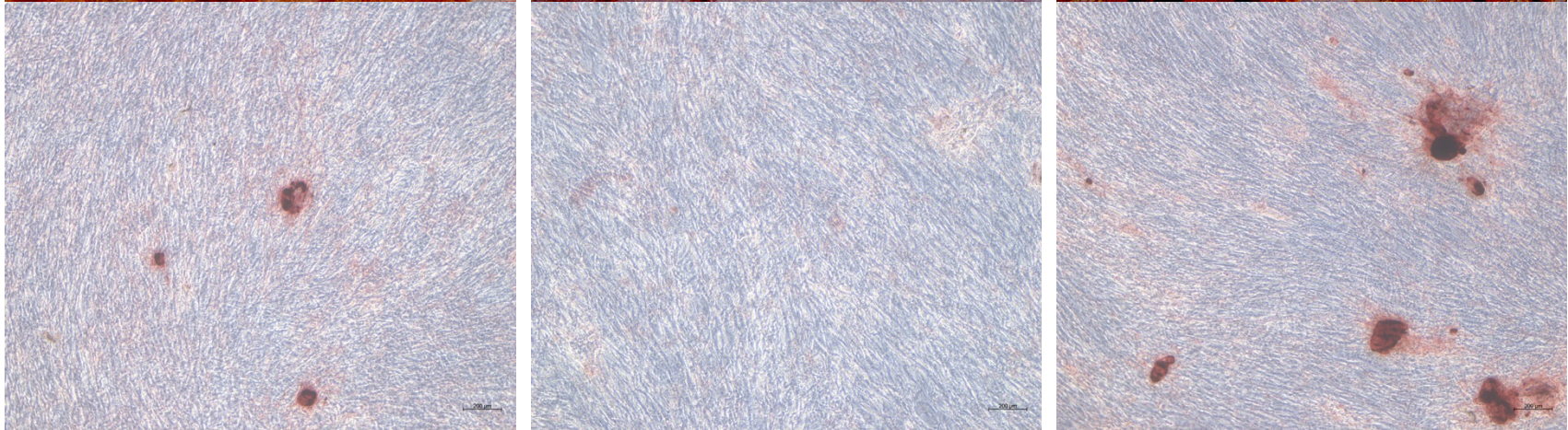
Figure 4.15. Representative brightfield images of differentiated ASCs stained with Alizarin Red S on day 28.
When ASCs reached 70 – 80% confluency, they were induced to undergo osteogenic differentiation. Osteogenic differentiation was assessed on days 21 and 28. Images were captured at two different magnifications, 5x (scale bar 200 μm) and 20x (scale bar of 50 μm). Four biological repeats were included as 2 out of the 4 repeats did not show osteogenic differentiation.

Alkaline Phosphatase Assay

ALP activity was measured at Day 0 and on the day of termination in non-induced and induced samples. On day 0, ASCs showed relatively high ALP activity. As expected, the level of ALP activity significantly decreased during the differentiation period. There was a significant increase in ALP activity on day 21 in ASCs induced with osteogenic medium 2 before the levels diminished as expected. This observation is aligned with the ARS results observed using medium 2 and explains why ARS stain was only seen to increase at day 28 in cultures induced with medium 2. When looking at the ALP activity in ASCs differentiated in osteogenic medium 3, the activity is also seen to decrease significantly when comparing day 0 and day 28 samples (Figure 4.16). Results from osteogenic medium 1 support the ARS data that osteogenic differentiation medium 1 is the most optimal for ASCs osteogenic differentiation as the level of ALP activity on day 21 is less than the level of ALP activity of both osteogenic differentiation medium 2 ($p<0.01$) and 3 (Not significant).
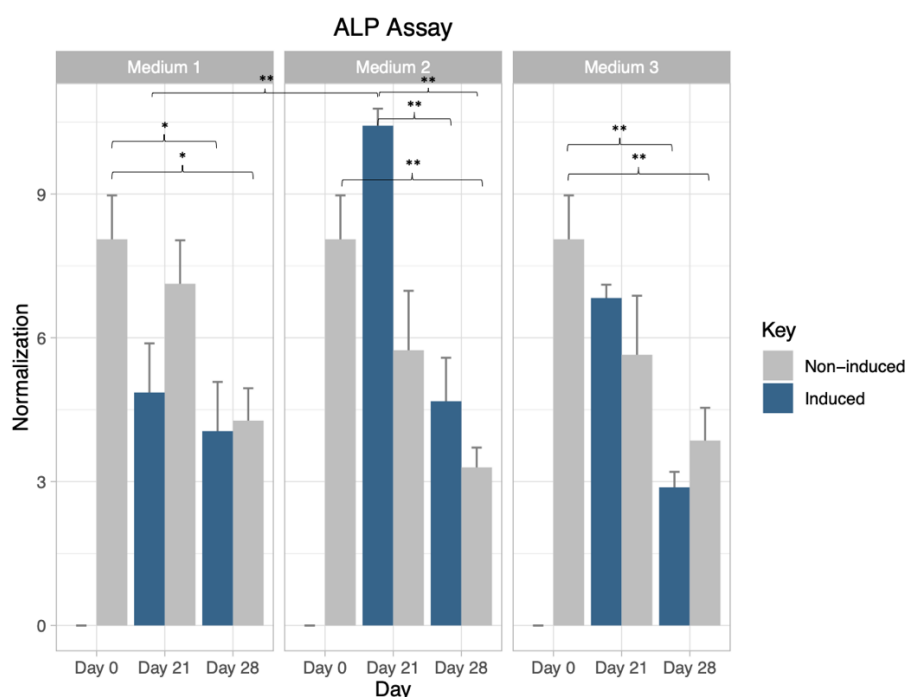
Figure 4.16. Level of alkaline phosphatase activity in the various samples.
The amount of ALP activity present in differentiation medium 1 decreased gradually but significantly during the differentiation period. For differentiation medium 2, ALP activity increased initially (day 21) before decreasing, indicating that ASCs were still in the early stages of osteogenesis at day 21. As for differentiation medium 3, the amount of ALP activity decreased gradually but significantly over the differentiation period. Significance: $p <0.00001$ "***", $p<0.01$ "**", $p<0.05$ "*".

4.5. Discussion

In this chapter we evaluated three previously published osteogenic differentiation media to determine which is the optimal for ASC osteogenic differentiation. We used two different osteogenic assays to evaluate the degree of osteogenesis, namely an ARS assay and an ALP assay.

It is commonly known that ASCs possess the ability to differentiate into osteoblasts. *In vitro* this is achieved by the addition of osteogenic inducing compounds, such as β-glycerophosphate, dexamethasone and ascorbate-2-phosphate, to complete growth medium. In the early stages of osteogenesis, the level of ALP will first increase to form the extra-cellular matrix which is later calcified to form the final bone product. Both dexamethasone and ascorbic acid are responsible for the upregulation of ALP that initiates the osteogenic differentiation process [177]. Ascorbic acid promotes collagen synthesis during early stages of osteogenic differentiation process [178,291]. Dexamethasone, in addition, upregulates RUNX2, the master regulator of the osteogenic differentiation process osteogenic regulator, at the early stages of osteogenesis [180]. In the later stages of osteogenesis, β-glycerophosphate helps with mineralisation of the extra cellular matrix. Although there is agreement regarding the essential components of osteogenic medium, there is a lack of consensus regarding the optimal concentration of the different compounds.

Osteogenesis consists of four sequential phases namely lineage commitment, proliferation, matrix synthesis and lastly matrix mineralization [298]. Most studies assess osteogenic differentiation over a 21-day period [16,184,188,191]. Initially we adopted the suggested 21-day induction period and differentiated two independent primary ASC cultures for 21 days but observed almost no calcification after this time. Mohamed-Ahmed et al. [213] compared the osteogenic differentiation of MSCs isolated from bone marrow (BM-MSCs) and MSCs isolated from adipose tissue (ASCs). They found that BM-MSCs have a shorter proliferation period than ASCs and that BM-MSCs start the formation and calcification of the collagenous matrix as early as day 14 whereas ASCs have an extended proliferation period and only start the mineralization phase on day 21. Based on these observations, we decided to extend our

osteogenic differentiation a further 7 days and to terminate the differentiation process at day 28. Two out of the three osteogenic differentiation media showed an increase in ARS staining i.e. amount of calcium deposition, from day 21 to day 28, while all three osteogenic differentiation media resulted in noticeable calcium deposition at day 28. Our data therefore suggest that osteogenic differentiation supplemented with FBS should be assessed 28 days post induction and not on day 21 as the majority of current research studies suggest.

Looking at the ARS data, medium 1 is the only medium out of the three osteogenic differentiation media that showed a significant increase in the amount of ARS stain present from day 0 to day 28, however there was not statistical difference between the different osteogenic media. Although medium 1 and 3 had similar levels of ARS concentrations at day 28, the results were not significant for medium 3. Medium 3 had large biological variance due to 1 biological repeat showing increased osteogenic differentiation. Medium 1 has the lowest concentration of dexamethasone out of the three osteogenic differentiation media. Medium 2 and 3 have relatively the same amount of ARS stain present at day 28 although medium 2 has double the amount of dexamethasone present when compared to medium 3. Langenbach et al. [296] found that the physiological level of dexamethasone from 30 healthy bone marrow donors was 10 nM and that this is the optimal concentration for osteogenesis. Interestingly, this is the same dexamethasone concentration present in medium 1. Sordi et al. [299] reported that a dexamethasone concentration of 100 nM favoured the proliferation phase of MSCs. This may explain why delayed terminal differentiation was observed when medium 2, which contains 100 nM, was used as in the differentiation medium. Medium 2 resulted in low levels of calcium deposition on day 21 and variable amounts of calcium deposition on day 28. This observation is supported by the ALP assay data, where an increase in ALP activity on day 21 was observed in ASCs that were differentiated using medium 2, suggesting that ASCs are still in the early stages on osteogenic differentiation at day 21 when medium 2 was used.

As mentioned previously, ascorbate-2-phosphate plays a role in collagen synthesis by promoting the secretion of collagen type 1 into the extracellular matrix. The concentration of ascorbate-2-phosphate also varies in osteogenic differentiation medium used to differentiate ASCs; however Jaiswal et al. [300] determined the optimal concentration of

ascorbate-2-phosphate to be 50 μM. Of the three differentiation media tested in this study, medium 2 contains 60 μM of ascorbate-2-phosphate, which was the closest to the optimal ascorbate-2-phosphate concentration suggested by Jaiswal et al. [300]. However, the observations made in this study suggest that optimizing the concentrations of differentiating agents that play a role in the early stages of osteogenic differentiation is more important as medium 2 produced noticeably less bone product compared to the bone formation observed when the other two media was used. In support of this hypothesis, medium 1 contained the highest concentration of ascorbate-2-phosphate and produced the greatest amount of calcified bone product.

There is consensus in the literature regarding the concentration of β-glycerophosphate, as many studies have tested and agreed that the optimal concentration of β-glycerophosphate in osteogenic medium is 10 mM [16,54,177,186,188–193]. Aligned with this observation, all three the differentiation media tested in this study contained 10 mM of β-glycerophosphate. β-glycerophosphate acts as a source of phosphate needed for the production of hydroxyapatite mineral and regulates important osteogenic genes in the later stages of osteogenesis [299].

In conclusion, ASCs differentiated in the presence of FBS showed minimal differentiation on day 21 but acceptable levels of osteogenic differentiation on day 28. Based on these findings we suggest that a differentiation period of 28 days should be used when assessing osteogenic differentiation of ASCs supplemented with FBS. Differentiation medium 1 showed a significant increase in the amount of ARS stain present (i.e., the amount of calcified bone product) from day 0 to day 28. Differentiation medium 1 also showed a greater decrease in ALP activity on day 21. It is for both these reasons that medium 1 was deemed the most optimal differentiation medium out of the three published differentiation media. Both ARS and ALP assays indicate that medium 1 was promoting differentiation into the later stages of osteogenesis faster than media 2 and 3. Medium 1 was thus retained for downstream testing.

Chapter 5: Optimal Human Alternative for Osteogenic Differentiation

5.1. Introduction

Over the years, the use of adipose-derived stem/stromal cells (ASCs) in clinical applications have increased, especially in the field of regenerative medicine. As mentioned before, one of the main reasons why ASCs are preferred over bone marrow mesenchymal stem/stromal cells (BM-MSCs), is the fact that isolation from adipose tissue yields more stem/stromal cells when compared to isolation from bone marrow. The ability of ASCs to differentiate into various cells types, including adipocytes, osteoblasts, chondrocytes and myocytes, makes them attractive for use in regenerative medicine [277]. However, the clinical use of ASCs requires more research, optimization, and standardization of isolations and differentiation methods before they can be considered as a therapeutic product.

The attachment, growth, maintenance and proliferation of ASCs is dependent on components present in FBS such as amino acids, hormones, various growth factors, vitamins, attachment factors like fibronectin, collagen and other trace elements like copper, zinc, tin and lead to name a few [301,302]. FBS has commonly been used in medium supplementation for cell culture despite all the associated disadvantages. Some of these disadvantages include batch-to-batch variation, possibility of mycoplasma infection, prions and viral contamination, introduction of xenogeneic antigens causing immune activation during cell expansion, ethical concerns about animal welfare, and prolonged proliferation rates of ASCs [74,302–305]. These factors make the use of FBS in a cell culture setting non-compliant with Good Manufacturing Principles (GMP). One of the greatest disadvantages of FBS is the fact that it does not mimic the human environment which can lead to inaccurate results when measuring any cellular response [59]. Researchers therefore are continuously seeking alternatives to FBS that will result in cell therapy products that are GMP compliant and are more physiologically compatible with the human body. Alternatives to FBS include chemically defined medium, or supplementing culture medium with additional growth factors, human serum albumin, human serum, platelet poor plasma (PPP), platelet rich plasma (PRP), fresh frozen plasma

(FFP) or pooled human platelet lysate (pHPL). Using these human alternatives to FBS, the culture environment is more physiologically compatible with the human body and will likely result in a more accurate and reliable translation to the clinic [306]. The use of human blood products also reduces the risk of immune activation due to the absence of xenogeneic proteins [304].

In this study we investigated the effect of two of the human alternatives, PRP and pHPL, on osteogenic differentiation of ASCs. PRP is produced through the centrifugation of whole blood at reduced speeds to prevent platelets clumping. However, the platelets remain in the plasma, resulting in plasma that is enriched in platelets [64]. Platelets can release growth factors upon activation that promote cell proliferation. This activation can occur in three ways, namely through a single freeze thaw cycle, addition of thrombin or addition of Ca^{+2} *in vitro* [304]. The classic spindle-shape morphology of ASCs and phenotype is maintained when these cells are exposed to PRP-supplemented media. However, the proliferation rate of ASCs is significantly increased in PRP-supplemented media when compared to FBS-supplemented media [307]. Several studies have shown improved osteogenic differentiation of ASCs when PRP was used as a supplement in the culture medium [71,308–311]. Some of the disadvantages associated with PRP include batch-to-batch variation due to biological differences between donors and the absence of a standardised protocol in the production of PRP, which may lead to inconsistency and variability in results [312].

Another promising human alternative to FBS is pHPL, as it is associated with lower biological variability and higher yield quantities per batch for clinical applications [71]. pHPL is produced by pooling various donor platelet concentrates, routinely manufactured by blood banks, and subjecting these pooled concentrates to multiple freeze thaw cycles. The multiple freeze thaw cycles lyse the platelets which results in the release of growth factors [302]. Consequently, growth factor concentrations are much higher in pHPL compared to PRP [313]. pHPL is readily available as it is manufactured worldwide by blood banks for the treatment of various disorders [303]. Like PRP, pHPL supplementation seems to influence the morphology and phenotype of ASCs. As reported for PRP, the proliferation rate of ASCs expanded in pHPL is also significantly higher than ASCs expanded in FBS [59,69,303]. Studies have shown that ASCs are capable of successful osteogenic differentiation in the presences of pHPL and that

osteogenesis is enhanced when compared to ASCs differentiated in FBS [314–318]. There may also be variability in the production of pHPL, especially regarding the concentration of cytokines and growth factors present in the various batches produced.

ASC can be differentiated into osteoblasts through the addition of dexamethasone, β-glycerophosphate and ascorbate-2-phosphate to the complete growth/culture medium. Ascorbic acid and dexamethasone upregulate the activity of alkaline phosphatase (ALP), and therefore increase the rate at which osteogenesis occurs [177]. In the early stages of osteogenesis, ascorbic acid is responsible for the synthesis of the collagen matrix, which is later mineralized to form bone [291]. β-glycerophosphate plays a role in this mineralization process [178]. Dexamethasone, β-glycerophosphate and ascorbate-2-phosphate act on genes that play an important role during osteogenic differentiation [177,178,180,291]. In this study, osteogenic differentiation of ASCs maintained in CGM supplemented with FBS was compared to the osteogenic differentiation of ASCs maintained in CGM supplemented with pHPL or PRP.

5.2. Methods

5.2.1. Isolation of ASCs

The isolation of ASCs used for these experiments is described in Chapter 3: Isolation of primary MSCs from lipoaspirate.

5.2.2. Characterisation of ASCs

In chapter 3, we showed that the ASCs used in this study adhered to the surface of the culture vessels. As mentioned before, the ISCT guidelines recommended that ASCs should express certain pre-defined cell surface markers. Cells were thawed and plated. The respective human alternatives were added to the cells as to allow the cells to adjust to the human alternatives. These cells were maintained in the respective human alternative for a minimum of 2 weeks. Only after weaning the cells off of FBS, did we immunophenotyped the ASCs by staining them with the same panel of monoclonal antibodies consisting of CD34, CD36, CD44, CD45, CD73, CD90 and CD105.

New compensation experiments were set up for pHPL and PRP. Compensation experiments and immunophenotyping experiments are described in Chapter 4: Optimal differentiation medium for osteogenesis.

5.2.3. Production of Human Alternatives

Pooled Human Platelet Lysate (pHPL)

Platelet concentrates (4 bags; independent donors) and one bag of plasma were donated by the South African National Blood Service (SANBS). On receipt, the bags were frozen for 24 hours at -20°C, after which pHPL was manufactured according to the protocol described by Schallmoser & Strunk protocol [319] with minor modifications. In summary, platelet concentrates were thawed after 24 hours in a 37°C water bath and the platelet concentrates from the four independent donors were pooled. The pooled platelet concentrates were again frozen for 24 hours at -20°C. After 24 hours, the frozen pooled platelet lysate was thawed in a 37°C water bath. At this point the product is known as pHPL. The pHPL was aliquoted into 50 mL conical tubes and centrifuged at 4 000 x *g* at 4°C for 15 min. The supernatant was transferred into new 50 mL conical tubes and stored at -20°C for future use.

Platelet Rich Plasma (PRP)

Platelet rich plasma was collected by SANBS via the Spectra Optia® Apheresis system. As per the SANBS protocol, the calcium, magnesium, and potassium levels in the donor's blood was assessed before donation. Some patients might experience hypocalcaemia during PRP donation and therefore it is important to know whether patients have normal calcium, magnesium, and potassium levels before collection starts [320]. A report of donor PRP070721's calcium, magnesium, and potassium levels were not available. This donor is a regular platelet donor for SANBS and thus it was not necessary for pre-screening. Sterility tests and pH levels were also determined as per the SANBS protocol. All results are in Appendix D.

On receipt of the PRP bags from SANBS, samples were aliquoted into 15 ml tubes and frozen at -20°C. One freeze-thaw cycle was allowed to activate the platelets before use. Before freezing the products, an aliquot was taken to determine the number of platelets/μl

(CD42a -positive), if the platelets were active (CD61-positive) and the percentage of white blood cells (WBC; CD45-positive) present in the sample. Briefly, a 100x dilution was made of the product using PBS and stained with CD42a, CD61 and CD45 (5 μl of each antibody). Stained samples were incubated for 20min in the dark. After incubation, 400 μl PBS was added, and the results were analysed on the CytoFLEX. Unstained samples were also run to determine where positive gates should start.

When aliquots were thawed for use, the samples were again stained with CD42a and CD61 to determine if the platelets were activated by the freeze-thaw cycle.

5.2.4. Thawing of ASCs, Call Passaging and Maintenance

The thawing, cell passaging and maintenance of ASCs in cell culture is described in Chapter 4: Optimal differentiation medium for osteogenesis.

In this chapter complete growth medium (CGM) refers to 10% nutritional supplement, either FBS, pHPL or PRP; 2% penicillin/streptomycin (pen/strep); 25 μg/mL Amphotericin; and when human alternatives were used, 2U/mL of heparin was added. To passage the cells, the attached cells were first washed with 4 mL pre-warmed PBS (2% pen/strep), and 2-3 mL 0.25% of Trypsin-EDTA was added for 7-15 min to cultures maintained in FBS-supplemented medium or Tryple was added for 7-15 min to cultures maintained in medium supplemented with human alternatives. To neutralize the trypsin/, 2-3 mL of CGM/PBS was added, and the contents swirled gently.

5.2.5. Osteogenic differentiation

Cells were seeded in 6-well (9.6cm^2/well) plates at 5000 cells/cm^2 and grown to 70-80% confluence (Passage 2-4) after which the CGM was removed and replaced with osteogenic induction medium (10nM Dexamethasone, 50mg/mL ascorbate-2-phosphate, 10mM β-glycerophosphate). ASCs that were not exposed to osteogenic induction medium were maintained in CGM and served as negative (undifferentiated) controls. The experimental layout is depicted in Figure 5.1. Osteogenic differentiation was assessed using two osteogenic assays (described later in this chapter) and gene expression studies. Osteogenic differentiation was assessed on day 0 (baseline measurements) and on day 21 (PRP and pHPL

samples)/28 (FBS samples). The reason for using different termination days for FBS and the two human alternatives is based on initial observations in which we found no/poor osteogenic differentiation at day 21 for the cultures maintained in CGM (FBS). Our findings were aligned with the findings described by Mohamed-Ahmed et al. 2018 in which these investigators showed that ASCs have a longer proliferation period and only stop proliferating and start differentiating on day 21 [213]. Based on these findings we decided to extend the differentiation period for cultures maintained in CGM (FBS) to 28 days. On the other hand, some studies have reported that pHPL and PRP increased the rate at which osteogenesis occurs and therefore we kept the differentiation period of the two human alternatives to 21 days (Figure 5.2). RNA was isolated at four different time points (day 0, 7, 14 and 21) to determine the kinetic expression of osteogenic genes during the differentiation process (Figure 5.3).

Day 0
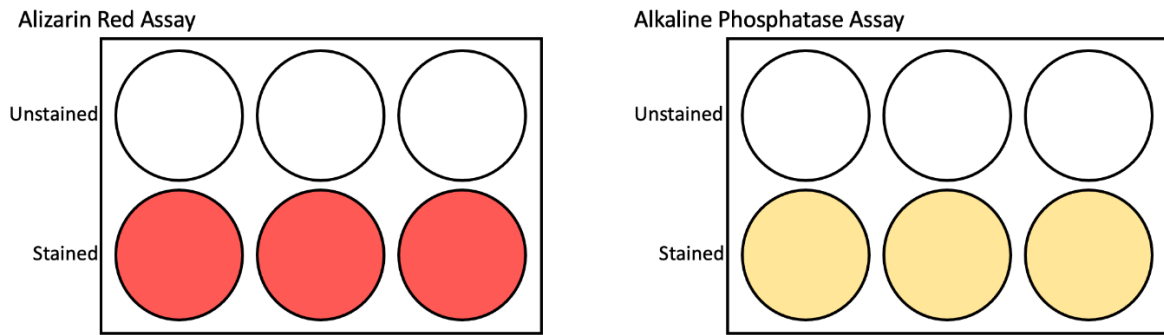
Day 21/28
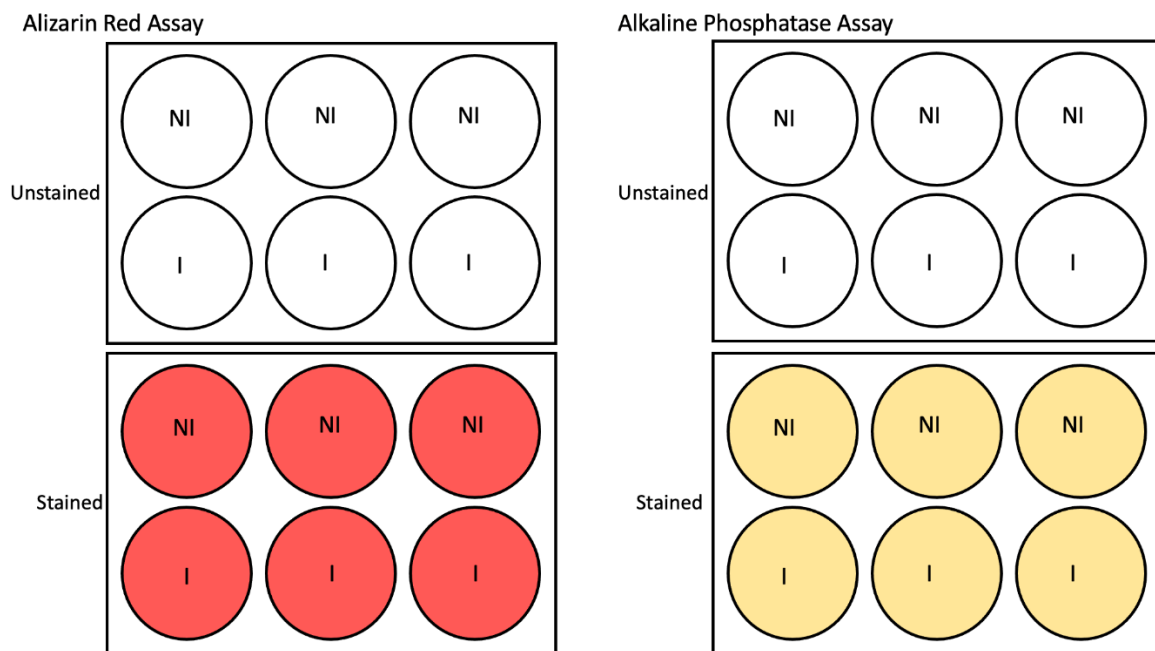
Figure 5.1. Experimental culture plate setup for experimental days.

ASCs were seeded into 6 well plates at 5000 cells/cm^2. Day 0 represents non-induced samples on the day of osteogenic induction (rest of induced wells). An unstained control was included in each assay to determine the amount of background staining. For day 21/28 samples, a non-induced control as well as unstained controls were included for each of the assays. The same experimental procedure was followed to process both the unstained and stained wells, with the only exception being the exclusion of addition of Alizarin Red S or Alkaline phosphatase assay buffer in the respective unstained wells. PBS instead of the staining/buffer solution was added to the unstained controls wells.
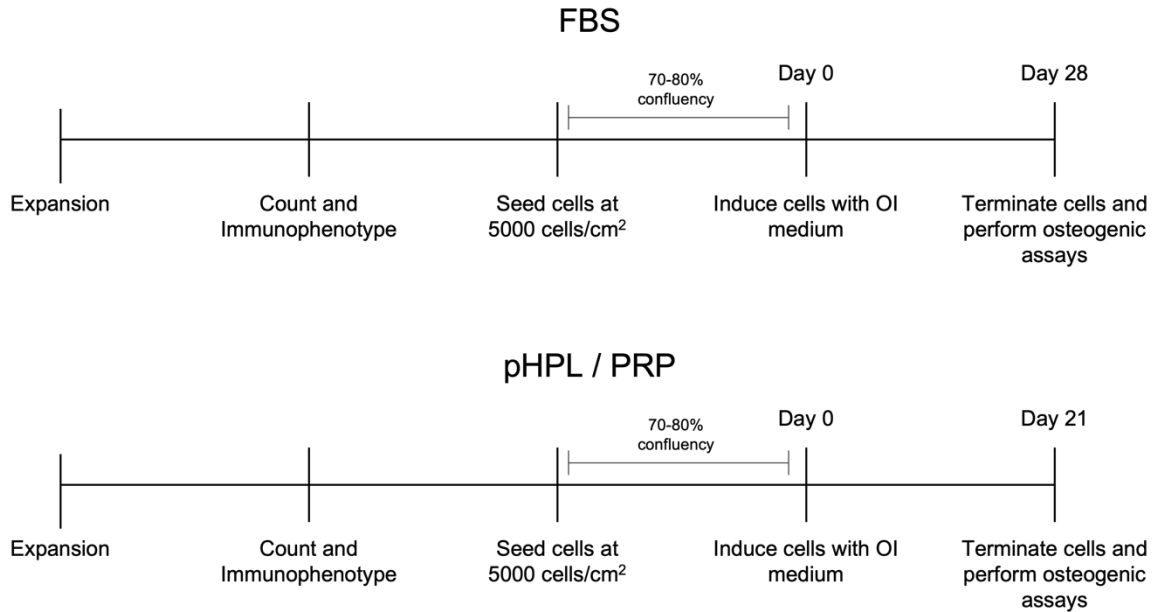
Figure 5.2. Timeline of osteogenic induction.

A basic illustration of the steps followed during osteogenic differentiation of the primary ASC cultures. Cells supplemented with FBS were investigated over a 28-day period while the pHPL and PRP supplemented cells were investigated over a 21-day period. CGM and osteogenic differentiating media was replaced twice a week. OI; Osteogenic induction medium
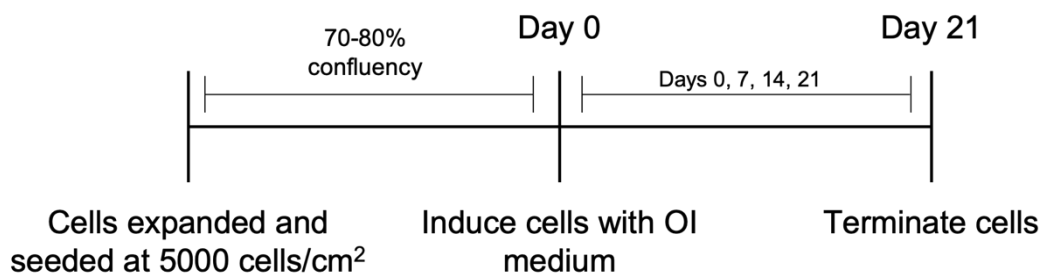
Figure 5.3. RNA isolation strategy.

Cells were expanded and seeded at 5000 cells/cm². Once cells reached between 70 – 80% confluency they were induced with an osteogenic induction medium. Cells were terminated on days 0, 7, 14 and 21 for RNA extraction. CGM and osteogenic differentiating media was replaced twice a week.

5.2.6. Osteogenic differentiation assays

Alizarin Red S (ARS) Staining Assay

The ARS assay is described in Chapter 4: Optimal differentiation medium for osteogenesis.

Alkaline Phosphatase Assay

The ALP assay is described in Chapter 4: Optimal differentiation medium for osteogenesis.

5.2.7. Microscopy

Light microscopy

As described in Chapter 4: Optimal differentiation medium for osteogenesis.

Fluorescence microscopy

As described in Chapter 4: Optimal differentiation medium for osteogenesis.

Protocol for obtaining cell numbers within a well using ImageJ

As described in Chapter 4: Optimal differentiation medium for osteogenesis.

5.2.8. RNA isolation

Cells were washed with ice cold PBS (2% pen-strep) and lysed using TriZol (1 mL for every 10cm^2). After 3 min incubation, the lysate was transferred into Eppendorf tubes and placed on ice for a further 5 min to permit complete dissociation of the nucleoprotein complex. Chloroform was added to the lysate (0.2mL for 1 mL of Trizol), vortexed and incubated at room temperature for 2-3 min after which samples were centrifuged at 12 000 x g for 15 min. The mixture separated into 3 layers; a lower red phenol-chloroform layer, an interphase layer, and an upper aqueous layer. The aqueous layer was transferred into a new Eppendorf tube and ice-cold isopropyl alcohol was added (0.5 mL for every 1 mL of TriZol). Tubes were inverted several times and incubated at room temperature for 10 min. Samples were then centrifuged for 20 min at max speed. The supernatant was removed, and the RNA precipitate was re-suspended in 75% ice cold ethanol. The RNA was further purified using the PureLink$^®$ RNA Mini Kit from Thermo Fischer. The concentration, A260/280 and A260/230 values were measured on a NanoDrop® ND 1000 spectrophotometer (Thermo Fisher Scientific; Waltham, MA, USA).

5.2.9. RNA integrity

The RNA integrity was tested using the 2200 Tape Station (Agilent Technologies, California, United States). Representative samples from each time point were selected at random to test

the RIN values. In summary, samples were diluted to achieve a concentration between 25 and 500 ng/μL. Sample buffer (5μL) was added to 1μL RNA sample and vortexed. The samples were denatured for 3 min at 72°C and placed on ice for 2 min. The samples were loaded into strips and analysed on the instrument.

5.2.10. cDNA synthesis

Any sample with a RIN^e value lower than 6.5 was excluded from downstream experiments. The RNA with RIN^e values above 6 were converted into cDNA using the Sensifast™ cDNA conversion kit from Celtic (Bioline, London, England). For every different expansion condition, 3 random samples were selected for no reverse transcriptase (NRT) controls, to determine if the samples or the buffers contained any genomic DNA contamination.

Table 5.1. Composition and volume of reaction mixture for cDNA synthesis

Reagent	Sample	NRT Control
5x TransAmp buffer	4 μL	4 μL
Reverse Transcriptase	1 unit	None
Molecular grade water	Variable	Variable
RNA	Variable	Variable
Total reaction volume	20 μL	20 μL

Sample mixes were placed in a thermal cycler (Gene Amp® PCR system 9700 from Applied Biosystems, Life Technologies®/Thermo Fisher Scientific, Carlsbad, California, USA) and processed according to the following cycling conditions; 10min at 25°C, 15 min at 42°C for reverse transcription, 5 min at 85°C to inactivate the reverse transcriptase enzyme, followed by cooling of the reaction for 5 min at 4°C. The cDNA was stored at -20°C until it was used.

5.2.11. Quantitative Polymerase Chain Reaction (qPCR)

Appropriate reference genes should show stable expression regardless of the experimental conditions. Four reference genes were tested for use in the study. Representative samples from each experimental group were selected to test for appropriate reference genes.

To test the efficiency of the primers, standard curve experiments were setup. In short, DNA samples were subjected to at least 5, 10-fold dilutions and run on a SYBR green protocol in triplicate. The Ct value was recorded and plotted on the y-axis while the concentration of cDNA was plotted on the x-axis. The primer efficiency could then be determined using the LightCycler 480 II software.

All samples were prepared in triplicate and 10 μL reaction volumes were used. The LightCycler 480 II instrument (Roche, Basel, Switzerland) was used for qPCR amplification and detection. Each plate also included no template control (NTC) samples (in triplicate), 3 reference genes (*TBP*, *GUSB* and *YWHAZ*), representative samples from the two time timepoints (Day 0 and Day 21 or Day 28) and standards from standard curve experiments. By including standards on each plate, we can use the primer efficiency calculated in the standard curve experiments to calculate relative gene expression values using the comparative Ct method.

Primers were made up to a stock concentration of 100 μM using TE Buffer, according to manufacturer's instructions. Stock solutions were then diluted with molecular grade water into working solutions of 10 μM and stored at -20°C. The osteogenic primers RUNX2, ALP and Osteocalcin were used to determine at which stage of osteogenesis the samples were at termination. Two adipogenic genes (PPARγ and FABP4) were included as the osteogenic differentiation process and the adipogenic differentiation process are mutually exclusive. Reference genes included in the study were TBP, GUSB and YWHAZ. All primers were purchased from Integrated DNA Technologies (IDT, Coralville, Iowa USA) and are listed in Table 5.2.

Table 5.2. Primer sequences used in the study.

Abbreviation	Description	Forward primer sequence	Reverse primer sequence
RUNX2	Runt-related transcription factor 2	ACCCATATCAGAGTTCCAG	GACCGTCTAAAGAGCAAAC
ALP	Alkaline phosphatase	GCAACTCTATCTTTGGTCTG	GGTAGTTGTTGTGAGCATAG
OCN	Osteocalcin	ACCCTTCTTTCCTCTTCC	CCCACAGATTCCTCTTCT
PPARγ	Peroxisome proliferator-activated receptor gamma	CGTGGATCTCTCCGTAAT	TGGATCTGTTCTTGTGAATG
FABP4	Fatty acid binding protein 4	ATCAACCACCATAAAGAGAAA	ACCTTCAGTCCAGGTCAA
TBP	TATA binding protein	CCGAAACGCCGAATATAA	GGACTGTTCTTCACTCTTG
GUSB	Glucuronidase, beta	GATCGCTCACACCAAATC	TCGTGATACCAAGAGTAGTAG
YWHAZ	Tyrosine 3-Monooxygenase/Tryptophan 5-Monooxygenase Activation Protein, Zeta	TGACATTGGGTAGCATTAAC	GCACCTGACAAATAGAAAGA

Primers were designed and assessed on the IDT website (*see MIQE guidelines, Appendix F*)

A previously optimized SYBR Green protocol was carried out in 10 μL reactions, containing between 25 – 50 ng of template cDNA, 400 nM of forward and reverse primer respectively, 5 μL of 1x SYBR Green Master Mix. The following cycling conditions were used; a one-step denaturation at 95°C for 5 min, an amplification series of 45 cycles consisting of the following 3 steps; 95°C for 30s, 62°C for 30s and 72°C for 30s. Following the amplification step, a two-step melt curve was performed; 95°C for 30s and 40°C for 30s. The average ramp rate for the qPCR reaction was 0.1°C/s.

Melt curves were analysed after each run to determine the specificity of each primer and that the product amplified is homogenous.

5.2.12. Statistical Analysis

Statistical analysis of data was performed in R (Version 4.0.1) and RStudio (Version 1.3.959). Data is reported as mean ± standard deviation (SD). Gene expression data is reported as standard error of mean (SEM). To test statistical significance, a one-way ANOVA was performed. This test was followed by a Tukey's test to determine the individual significance between each treatment group. A p-value $\leq$ 0.05 was considered statistically significant.

5.3. Results

5.3.1. Platelet rich plasma characterization

Platelet rich plasma (PRP) was collected from 3 male donors and was labelled as PRP070821, PRP240821 and PRP260821. On the day of collection, the PRP was characterized as follows: cells were stained with CD42a to identify and enumerate the platelets, CD61 to determine the percentage of activated platelets and CD45 to check for WBC contamination. After assessing the above-mentioned parameters, the PRP was stored at -20^{0}C until needed. Once the PRP was thawed, the level of platelet activation was determined by performing another immunophenotype. PRP070821 had a platelet count of 22 482.3 platelets/μl and a WBC count of 30.11 cells/μl. Almost all the platelets were resting (not activated) as only 0.01% of the platelets expressed CD61. PRP240821 had a platelet count of 16 939.99 platelets/μl and WBC count of 7.87 cells/μl. Again, the majority of the platelets were not active with only 0.43% of platelets expressing CD61. PRP260821 had a platelet count of 35 918.37 platelets/μl and a WBC count of 141.6 cells/μl. As with the two previous collections, the majority of the platelets were not active with only 0.11% of the platelets expressing CD61. After thawing, 0.21% (PRP070821), 3.33% (PRP240821) and 48.29% (PRP260821) of the platelets expressed the activation marker CD61 (Figure 5.4).
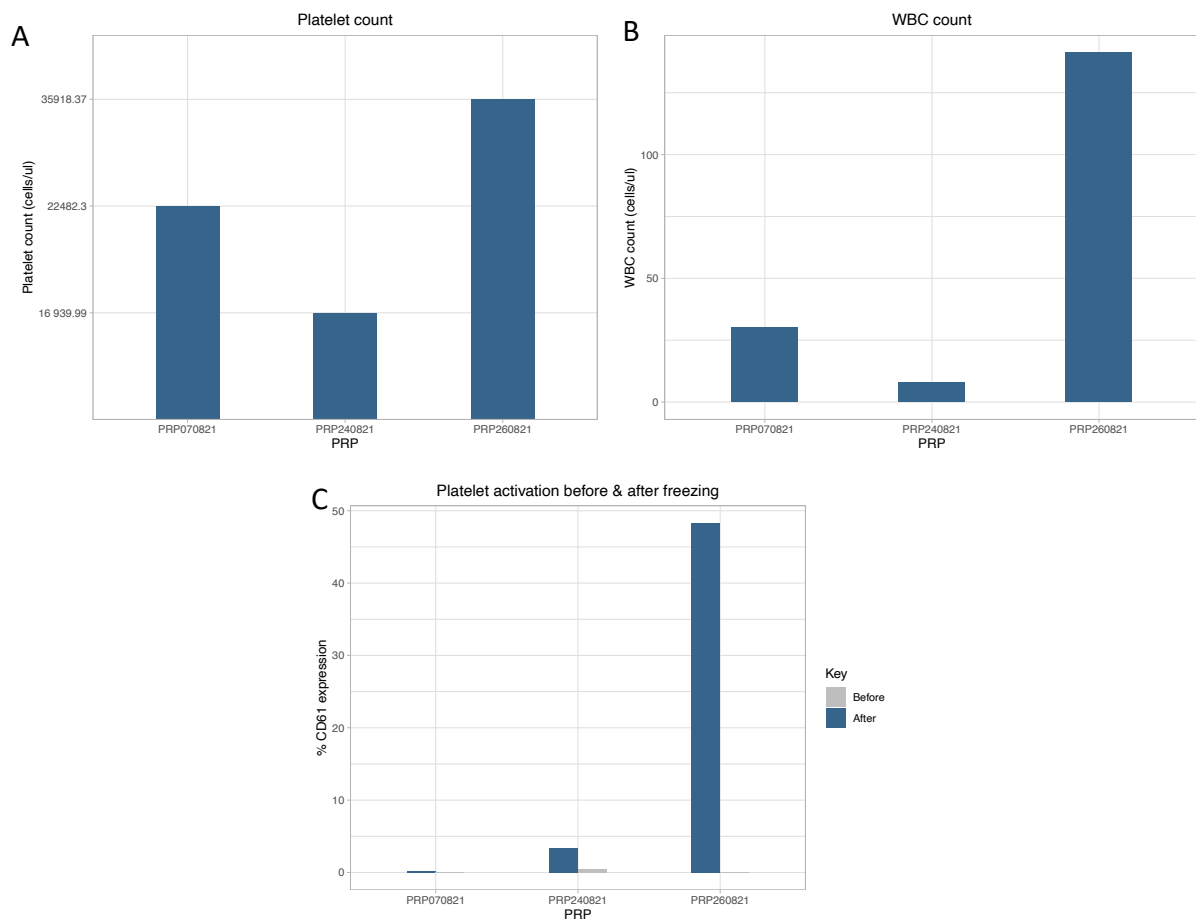
Figure 5.4. Summary of platelet data.
A. Platelet count after collection of platelet-rich plasma. B. White cell contamination in platelet product. C. Percentage activation of platelets, expressed as a percentage of CD61-positive platelets, before and after one freeze-thaw cycle.

5.3.2. ASC Isolation and Characterisation

Representative micrographs of ASCs cultured in media supplemented with either FBS, pHPL or PRP are displayed in Figure 5.5. Plastic adherent ASCs had a typical fibroblastic morphology. Cells grown in medium supplemented with FBS revealed a more flattened, broader spindle morphology when compared to the morphology of ASCs grown in a medium supplemented with a human alternative (both pHPL and PRP), which were smaller in size, more elongated and had a tighter spindle shape. The size difference between ASCs grown in FBS vs ASCs grown in pHPL or PRP correlated to flow cytometry forward scatter measurements, which measures relative cell size. The forward scatter of ASCs grown in FBS was slightly larger than ASCs grown in pHPL or PRP (Figure 5.6).

Culture	Condition		
	FBS	pHPL	PRP
A31101 9-01A			
A31101 9-02T			

94
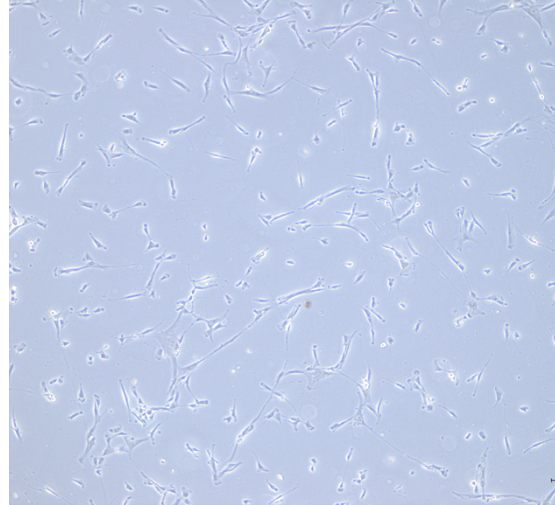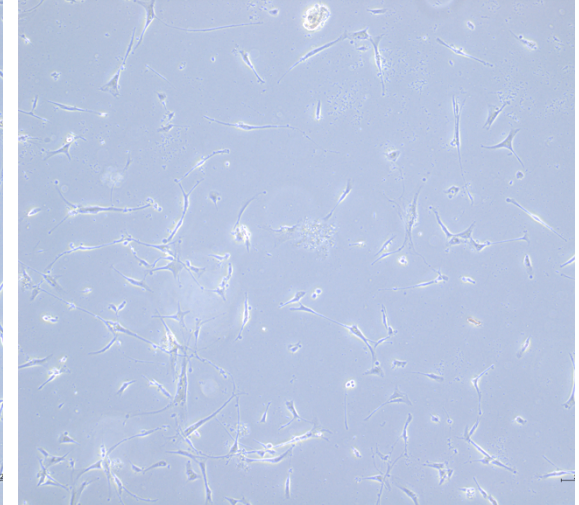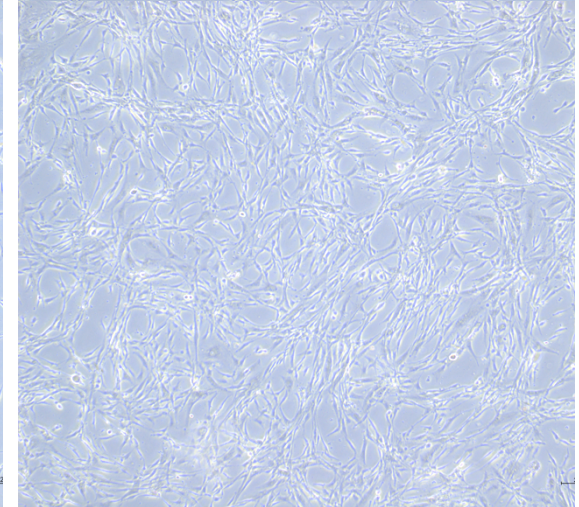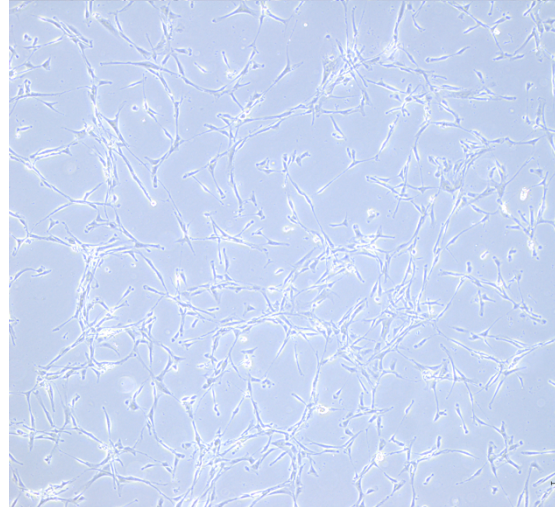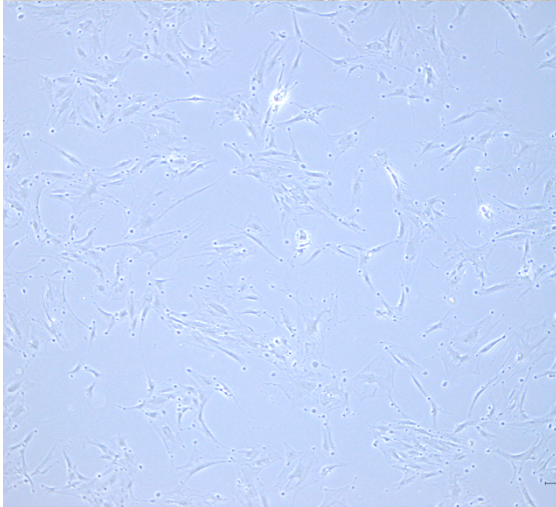
A28062 1-01R
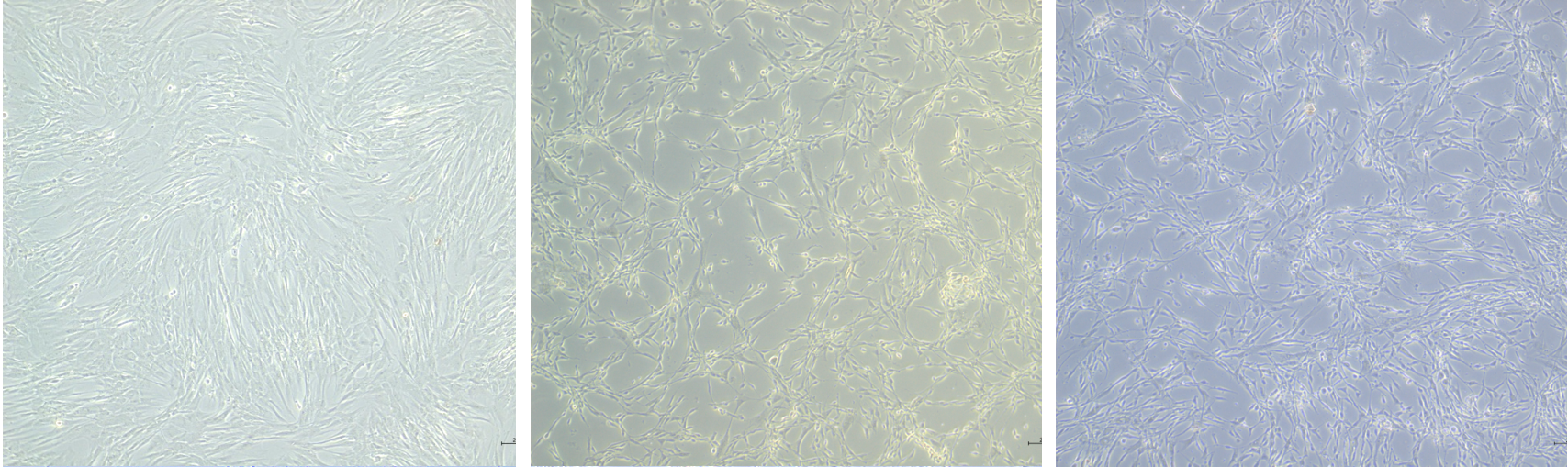
A15022 1-01A
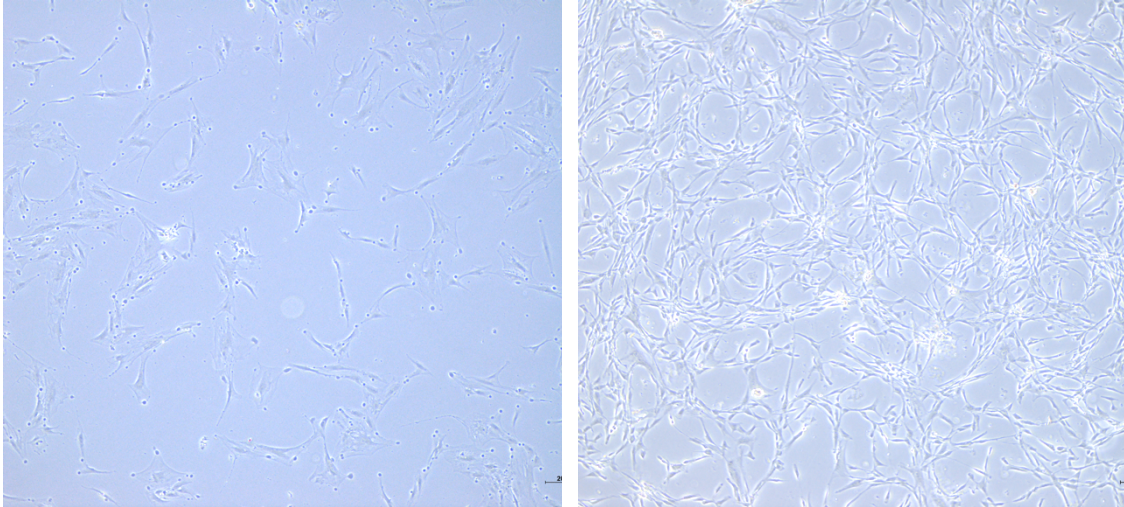
Figure 5.5. Morphology of ASCs cultured in the three different media formulations.
Slight differences can be seen in the morphology of ASCs cultured using FBS versus ASCs cultured using either pHPL or PRP. Cells grown in medium supplemented with FBS has a more flattened appearance while ASCs cultured in either pHPL or PRP displayed a more elongated and smaller cell size.

95
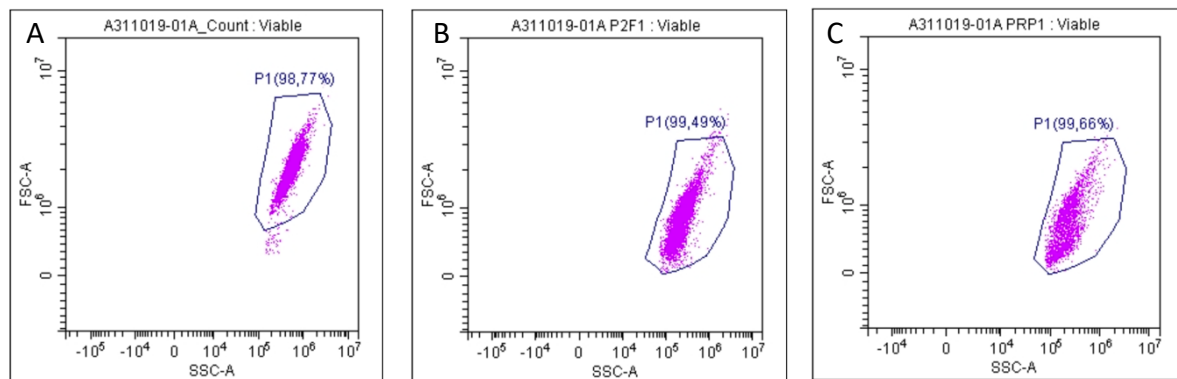
Figure 5.6. Differences in forward scatter of ASCs cultured in FBS, pHPL and PRP.
ASCs cultured using FBS (A) show a slightly higher forward scatter compared to cultured using pHPL and PRP (respectively B & C). Forward scatter is representative of cell size. An increase in forward scatter (upwards shift on y-axis) suggests an increase in cell size

Prior to plating for each experiment, ASCs were counted, and cell viability and phenotypic profiles were assessed. Absolute cell numbers were determined on the CytoFlex flow cytometer using Flow-Count™ Fluorospheres. The average cell viability was 38.17% $\pm$ 6.72% in FBS, 54.6% $\pm$ 11.12% in pHPL, and 19.22% $\pm$ 1.21% in PRP (Figure 5.7). The low cell viability in the human alternative supplemented expansion medium could be attributed to the fact the cells proliferated at a faster rate and that the cells started lifting off the culture dish. The low cell viability in cells supplemented with FBS expansion medium can be due to long expansion periods. FBS cells took longer to proliferate to reach the desired cell numbers and were kept in culture for extended periods. The ASCs were stained with a panel of monoclonal antibodies (CD34, CD36, CD44, CD45, CD73, CD90 and CD105). Using single-parameter plots, the expression of the individual markers was determined. In FBS, CD90 was expressed on 97.02% $\pm$ 3.38%, CD44 was expressed on 99.66% $\pm$ 0.2% an CD73 was expressed 81.69% $\pm$ 19.67% of ASCs. CD36 was present on 31.5% $\pm$ 25.61% of the cells and 3.51% $\pm$ 3.4% of the ASCs expressed detectable levels of CD105. CD34 and CD45 were only expressed on 0.43% $\pm$ 0.38% and 0.3% $\pm$ 0.31% of the cells respectively. In pHPL, CD44 was expressed on 99.23% $\pm$ 0.57% and CD73 was expressed on 98.61% $\pm$ 0.88% of ASCs. Interestingly the percentage of cells that expressed CD90 on ASCs cultured and maintained in medium supplemented with pHPL was lower (43.78% $\pm$ 33.35%) compared to the expression levels of the same marker on ASCs cultured in medium supplemented with FBS (As CD90 is a common marker for MSCs). In contrast to CD90, a higher percentage of the ASCs expressed

CD105 (23.65% $\pm$ 44.55%) and CD34 (18.83% $\pm$ 32.23%). CD36 was present on 47.42% $\pm$ 38.32% of the cells, while an almost negligible percentage (0.38% $\pm$ 0.88%) of ASCs expressed CD45. In PRP, CD44 was expressed on 85.99% $\pm$ 8.49% and CD73 80.01% $\pm$ 6.1% of the ASCs. The percentage of ASCs expressing CD90, CD105 and CD34 were 16.47% $\pm$ 11.56%, 28.4% $\pm$ 23.41% and 5.22% $\pm$ 1.57% respectively. CD36 was present on 66.6% $\pm$ 10.7% of cells, and CD45 on 0.35% $\pm$ 0.35% (Figure 5.8). In both human alternative supplemented media, CD90, CD105 and CD36 expression had a very high standard deviation, and this was due to half of the biological repeats expressing the relative cell surface marker and the other half of the biological replicates not expressing the relative cell surface marker. The immunophenotype of the individual cultures for pHPL were as follows; A150221-01A was CD90^{variable}/CD44$^+$/CD73$^+$/CD105$^-$/CD34$^-$/CD36$^-$/CD45$^-$, A280621-01R was CD90^{variable}/CD44$^+$/CD73$^+$/CD105$^-$/CD34^{variable}/CD36$^+$/CD45$^-$, A311019-01A was CD90^{variable}/CD44$^+$/CD73$^+$/CD105$^+$/CD34$^-$/CD36$^-$/CD45$^-$, and A311019-02T was CD90$^+$/CD44$^+$/CD73$^+$/CD105$^-$/CD34$^-$/CD36^{variable}/CD45$^-$. The immunophenotype of the individual cultures for PRP were as follows; A280621-01R was CD90$^-$/CD44$^+$/CD73$^+$/CD105$^-$/CD34$^-$/CD36$^+$/CD45$^-$, A311019-01A was CD90^{variable}/CD44$^+$/CD73$^+$/CD105$^+$/CD34$^-$/CD36^{variable}/CD45$^-$, and A311019-02T was CD90^{variable}/CD44$^+$/CD73$^+$/CD105$^+$/CD34$^-$/CD36^{variable}/CD45$^-$.

In summary, in all three cultures ASCs expressed CD44, CD73 and CD90 and were negative for CD45. Interestingly, only a small percentage of ASCs cultured/maintained in FBS-supplemented medium did not express detectable levels of CD105 while CD105 expression was observed in a larger percentage of ASCs cultured/maintained in human alternative-supplemented medium (Not significant). CD34 and CD36 expression was variable in all three culture conditions. FBS cultured cells showed the highest percentage expression of CD90, followed by pHPL and PRP (FBS vs, PRP; p=0.0000158).
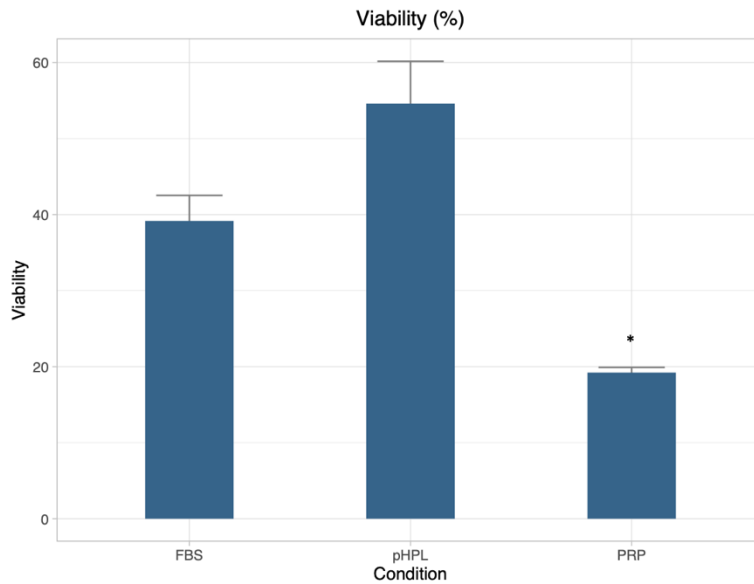
Figure 5.7. Cell viability in the different culture condition.
pHPL samples showed the highest cell viability percentage followed by FBS and then PRP ($p < 0.05$). Significant codes *: $p < 0.05$.
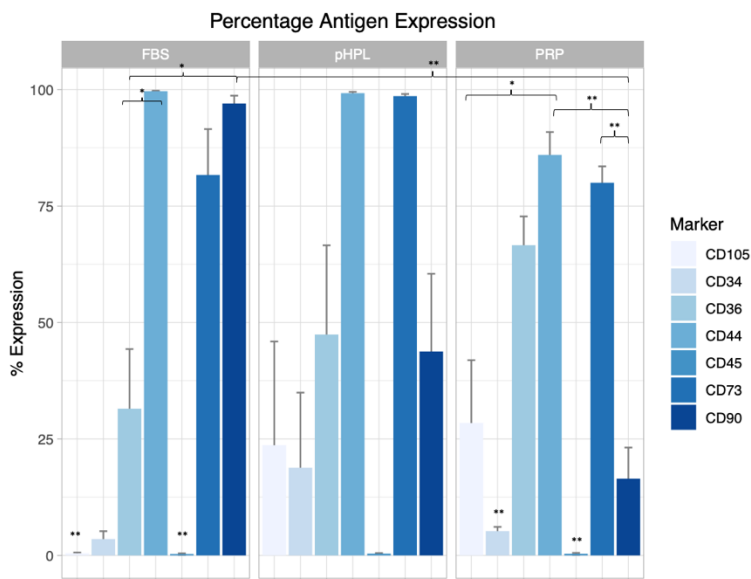
Figure 5.8. Percentage expression of surface antigens on ASCs in the different culture condition.
The data represent the average percentage of ASCs expressing the different cell surface markers ± standard deviation (SD) in different the different culture conditions before plating for experiments. ASCs did not express CD45 in all three the culture conditions. CD44, CD73 and CD90 expression was seen in all three culture conditions. Higher percentages of ASCs expressed CD105 when cultured/maintained in human alternative-supplemented media. The percentage of ASC expressing CD90 decreased when cultured in the presence of pHPL and PRP compared to FBS. Significant codes: ***: $p = < 0.001$; **: $p < 0.01$, *: $p < 0.05$.

5.3.3. Osteogenic differentiation

Osteogenic differentiation was assessed using two semi-quantitative assays namely, an ARS stain, that was quantified on a spectrophotometer and secondly an ALP assay that was also

measured on a spectrophotometer. Brightfield images were taken of the ARS assays to visually confirm the success of osteogenic differentiation. Fluorescent images were taken of both the ARS and ALP assays where cells were stained with DAPI (0.02 μg/ml in molecular grade H_2O) to quantify the number of cells by staining the nuclei. These images were used to quantify the number of cells per well as explained in the methodology section for normalization. Lastly, RNA was extracted from ASCs expanded in growth medium and ASCs undergoing osteogenic differentiation in T_{24} flasks at 4 different timepoints. The relative gene expression of 3 osteogenic genes and 2 adipogenic genes was assessed.

Alizarin Red S Assay

At day 21/28 post induction of osteogenesis, cells were fixed with 2% and stained with ARS. Two different controls were included (in triplicate): (1) samples not stained with ARS (Figure 5.9A, C & E) and (2) non-induced samples that were maintained in CGM (Figure 5.9D). No ARS staining was observed on day 0 (Figure 5.9A & B). On day 21, the non-induced controls showed little to no ARS staining in both pHPL and PRP supplemented media (Figure 5.9D), whereas clear ARS staining was observed in the induced samples indicating the presence of calcium deposition (Figure 5.9F). Induced samples supplemented with FBS showed noticeably less ARS staining when compared to ARS staining present in induced samples supplemented with either pHPL or PRP medium (Figure 5.10).

A. Day 0 Unstained
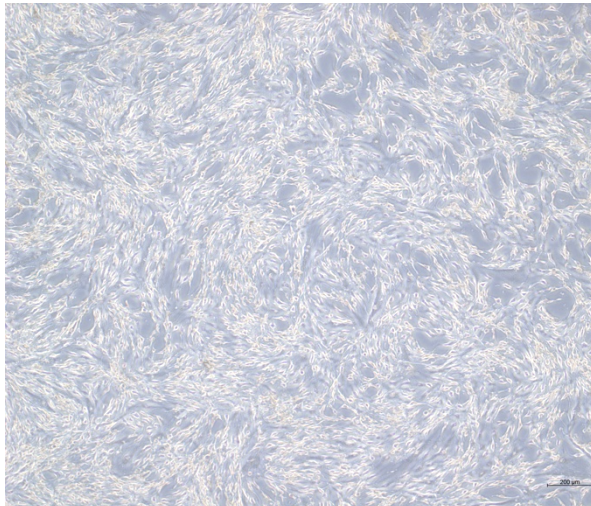
B. Day 0 Stained
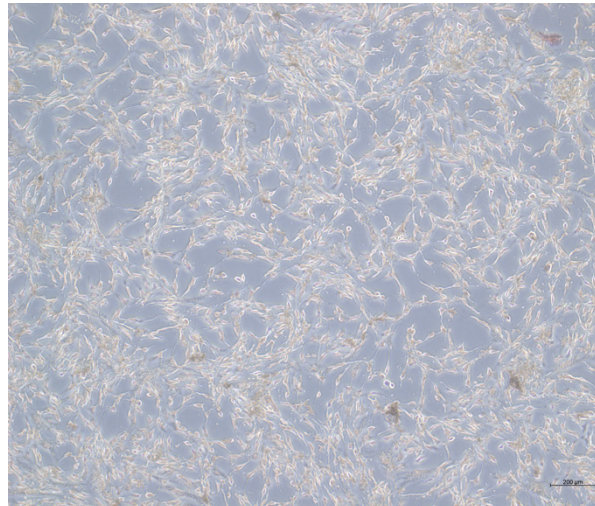
C. Day 21/28 Non-Induced Unstained
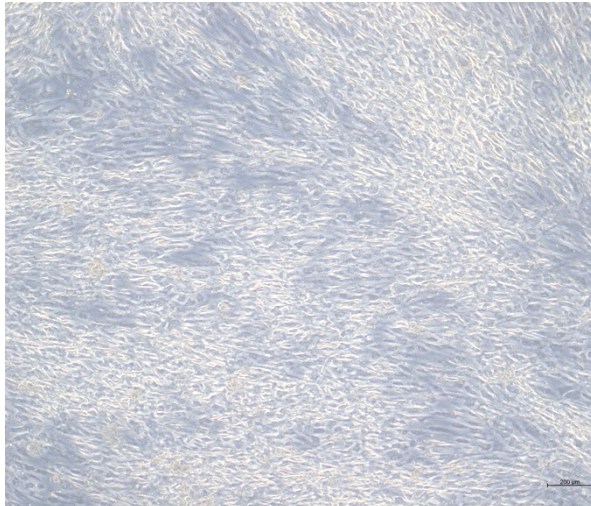
D. Day 21/28 Non-Induced Stained
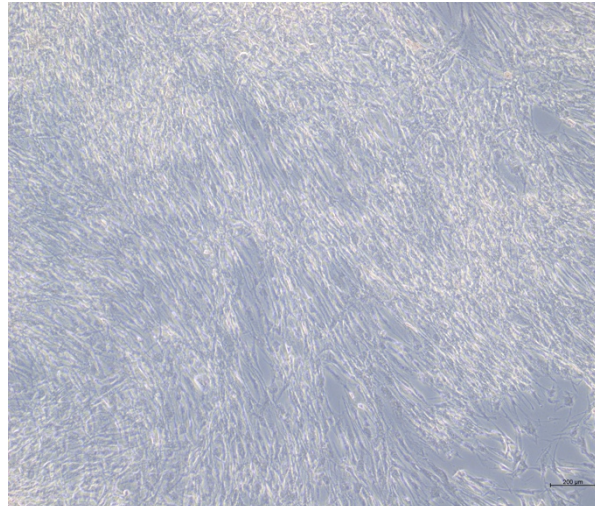
E. Day 21/28 Induced Unstained
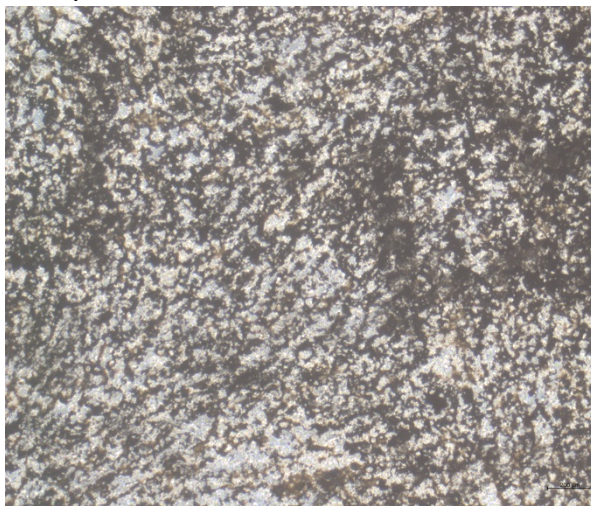
F. Day 21/28 Induced Stained
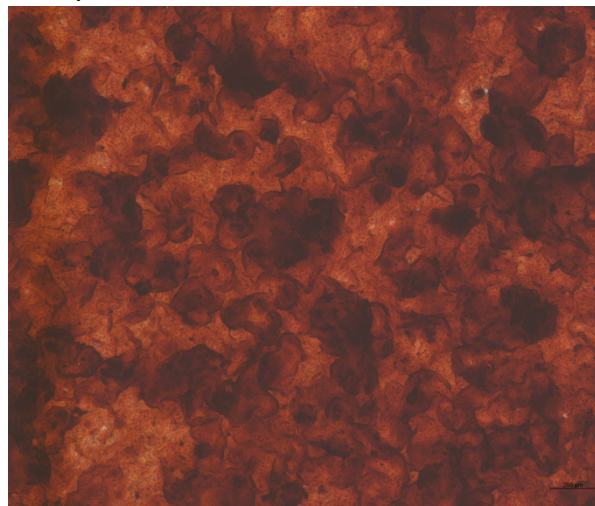
Figure 5.9. Representative images of the different controls used in the Alizarin Red assay.
A & B: Day 0 samples refer to samples on the day of osteogenic induction and were divided into unstained control samples (A) and stained samples (B). C-F: On day 21/28 samples were divided into non-induced (C & D) and induced samples (E & F). Non-induced and induced samples (day 21/28) were further divided into unstained controls (C & E) and stained samples (D & F).

Culture	Condition		
	FBS (Day 28)	**pHPL (Day 21)**	**PRP (Day 21)**

A311019 -01A

A311019 -02T

101
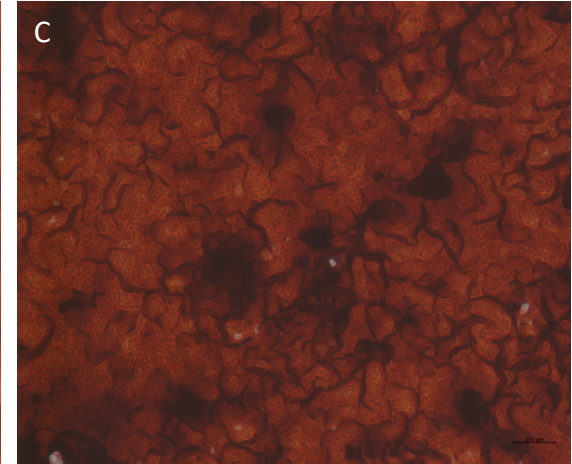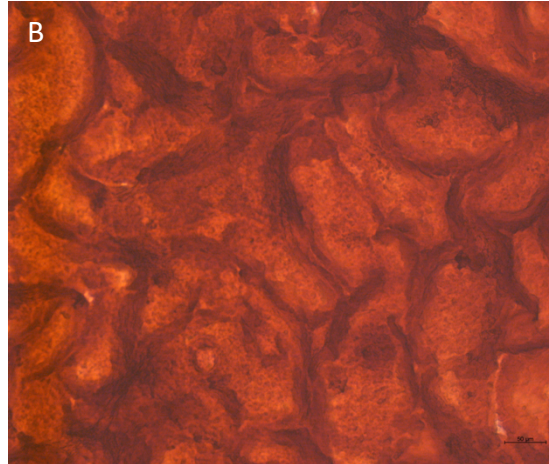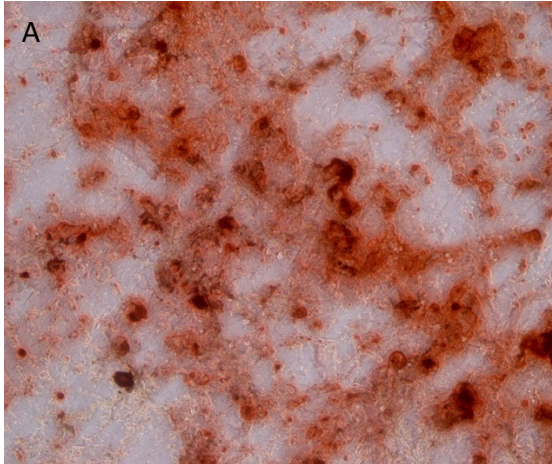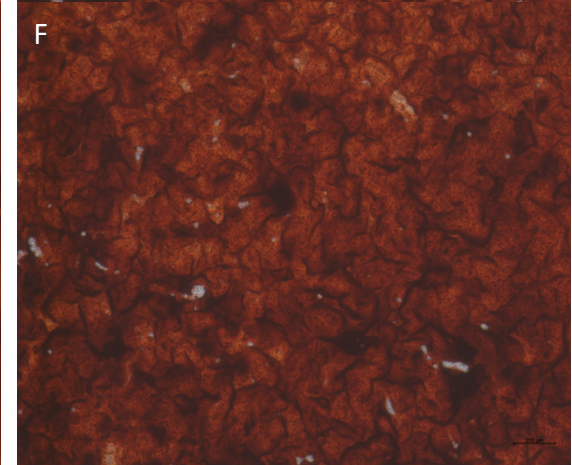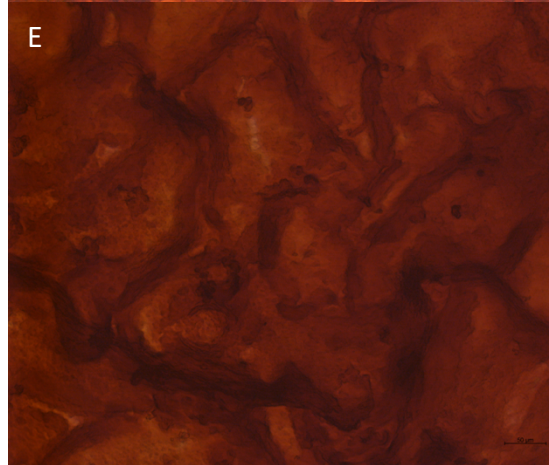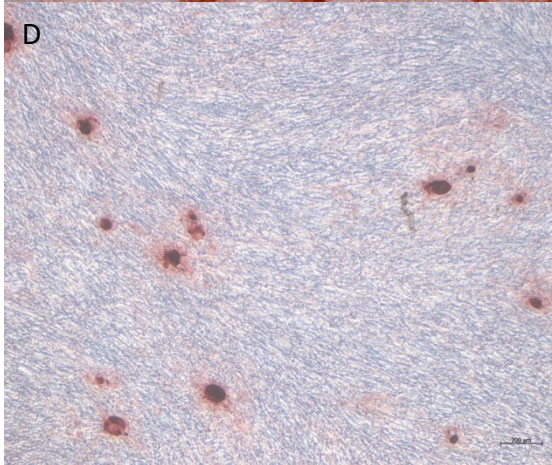
A280621 -01R
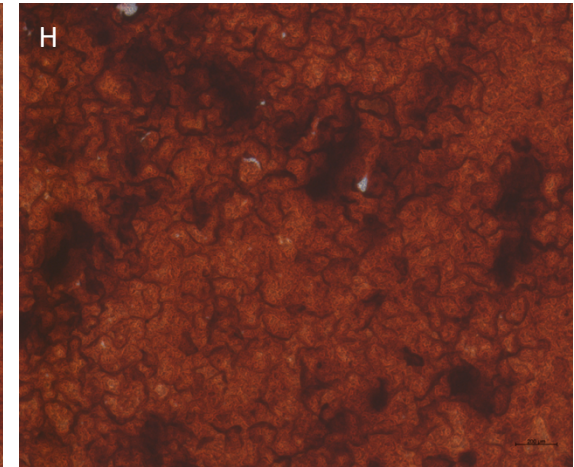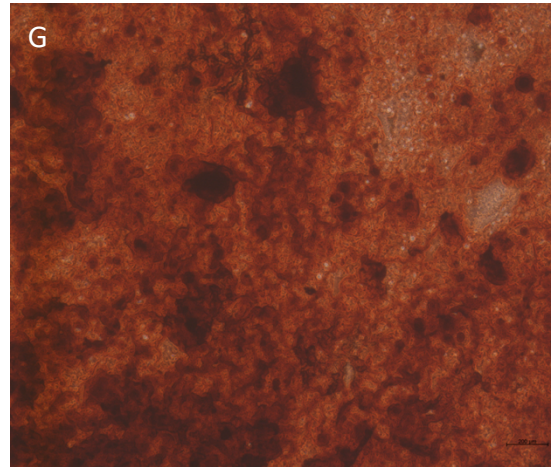
A150221 -01A
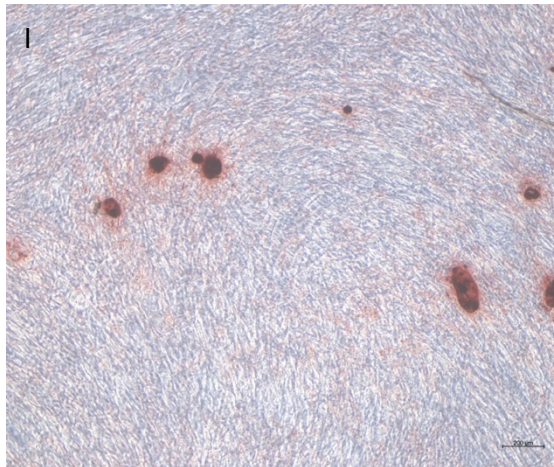
A230221 -01A
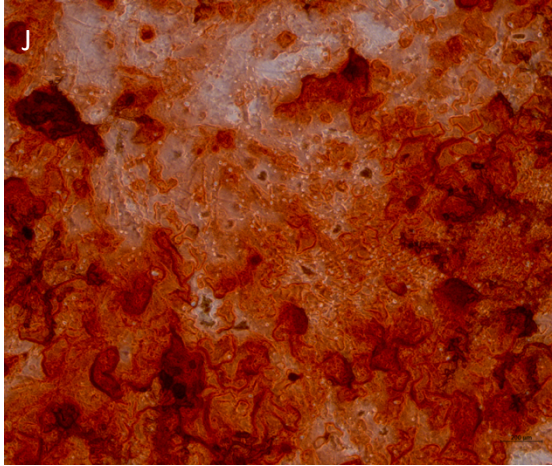
Figure 5.10. Representative brightfield images of differentiated (induced) ASCs stained with Alizarin Red S.

ASCs were induced to undergo osteogenic differentiation for 21 days (pHPL and PRP) or 28 days (FBS). After the differentiation period cells were fixed with paraformaldehyde and stained with ARS. Images taken at 5x magnification show a scale bar of 200 μm and images taken at 20x magnification show a scale bar of 50 μm. For FBS samples 4 biological repeats were used and for pHPL and PRP samples 3 biological repeats were used. Where possible the same ASC culture was used but was not possible for all cultures thus the reason for open spaces.

ARS standard curve results are described in Chapter 4: Optimal differentiation medium for osteogenesis and yielded a formula y = 1.05119977x – 0.03407551; where y is equal to the OD reading and x is the concentration of ARS Stain in mM..

The ARS was eluted with a solution of acetic acid (10% v/v) and the amount of stain was quantified on a spectrophotometer and results are displayed in Figure 5.11. Differentiated ASCs cultured in pHPL-supplemented osteogenic differentiation medium showed significantly more (p < 0.05) osteogenic differentiation (significantly higher levels of ARS per well) on the day of termination when compared to the levels of osteogenic differentiation achieved in PRP- and FBS-supplemented media. The level of osteogenic differentiation achieved in osteogenic differentiation medium, supplemented with PRP samples was lower than the differentiation levels achieved using pHPL supplementation (p < 0.05), but significantly higher than the osteogenic differentiation achieved when ASCs were cultured in supplemented with FBS (p < 0.001). In summary, more ARS staining was present in both human alternative samples compared to FBS, suggesting more calcium deposition and thus higher levels of osteogenic differentiation was achieved using human alternative supplementation.
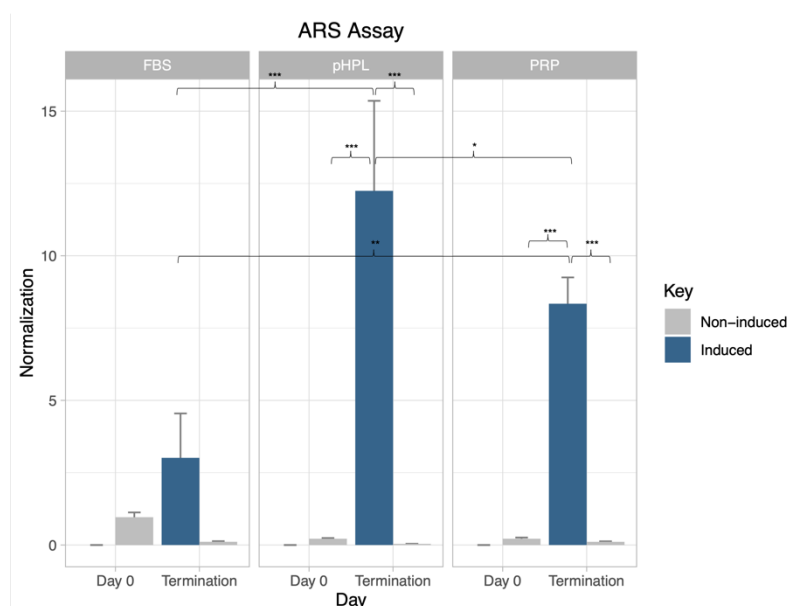
Figure 5.11. ARS concentrations eluted from various samples normalized to cell number and to unstained controls.
ASCs cultured in the presence of pHPL had the most amount of calcium deposition present followed by PRP. Samples cultured in FBS supplementation had the least amount of ARS stain present indicating lower levels of calcium deposition in ASCs cultured in FBS-supplementation. Results from the unstained controls were also included and showed little to no stain present and were also used to normalize the stained results. Significant codes: ***: p < 0.001; **: p<0.01, *: p<0.05. Day of

Termination refers to day 28 post induction in FBS supplemented medium and day 21 post induction in pHPL/PRP supplemented media.

Alkaline Phosphatase Assay

The activity of ALP was measured at day 0 and on the day of termination in non-induced and induced samples. ASCs cultured/maintained in FBS-supplemented osteogenic medium showed the highest activity of ALP on day 0 compared to ALP activity levels measured for ASCs differentiated in pHPL- and PRP-supplemented medium (Figure 5.12). At termination (day 21/28) the level of ALP activity was higher in the non-induced samples compared to the induced samples for all three the culture conditions (Figure 5.12). For ASCs cultured in FBS-supplemented CGM, the level of ALP activity decreased in both non-induced and induced at day 28 when compared to day 0 ALP levels (Not significant). For ASCs cultured/maintained in either pHPL or PRP samples the level of ALP activity, increased significantly (pHPL: $p < 0.0001$; PRP: $p < 0.0001$) in the non-induced samples when compared to the on day 0 (Figure 12). In contrast, the ALP levels were significantly decreased (pHPL: $p < 0.001$; PRP: $p < 0.001$) in the induced samples of pHPL and PRP supplemented media compared to the ALP levels recorded at day 0 (Figure 5.12). For the induced samples, the level of ALP activity was significantly higher ($p < 0.01$) in ASCs cultured in FBS-supplemented CGM than the ALP activity of both pHPL and PRP samples. In both pHPL and PRP samples there is a significant increase between the level of ALP activity in the non-induced and induced samples on the day of termination (pHPL: $p < 0.001$; PRP: $p < 0.001$) (Figure 5.12).
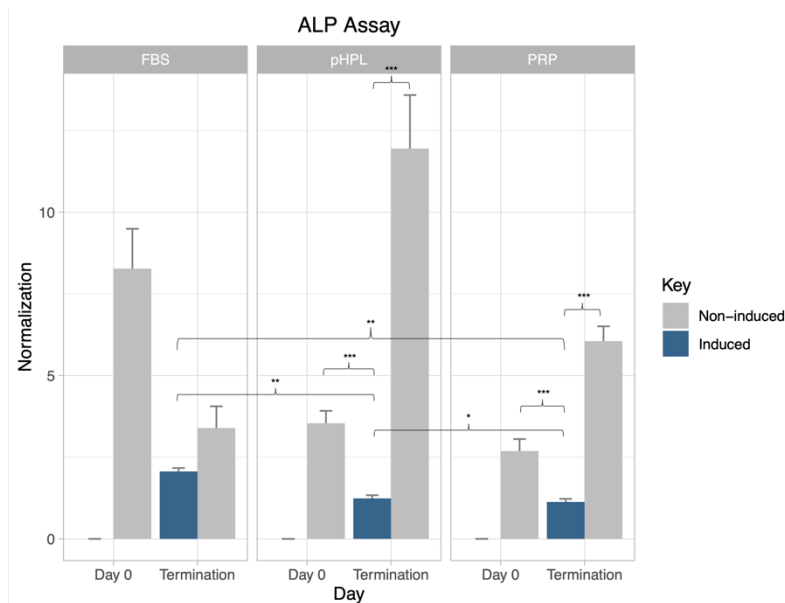
Figure 5.12. Level of alkaline phosphatase activity in various samples.
When looking at FBS samples, the level of ALP activity decreased from day 0 to the day of termination in both non-induced and induced samples. In both pHPL and PRP samples, the level of ALP activity decreased from day 0 to the day of termination in induced samples and increased in the non-induced samples. The level of ALP activity in FBS samples on the day of termination was significantly higher in FBS samples when compared to pHPL and PRP samples. Significant codes: ***: $p < 0.001$; **: $p<0.01$, *: $p<0.05$.

5.3.4. Relative gene expression

We also investigated the kinetics of osteogenic gene expression at various time points during the differentiation process. RNA was isolated at 4 timepoints throughout the differentiation process namely day 0, 7, 14 and 21. Once the RNA was isolated, RIN values were obtained to ensure that only RNA samples of acceptable quality were used in downstream applications. For this reason, samples with RIN values below 5 were excluded from downstream testing. Samples excluded were the A311019-01A pHPL Day 14 induced sample as well as A311019-01A pHPL Day 21 induced sample as their RIN values were 3.7 and 2.7 respectively. Their corresponding non-induced samples were also not used in downstream experiments. The expression of three osteogenic genes (RUNX2, ALP and OCN) were monitored in both non-induced and induced samples. The relative expression of target genes normalized to the three reference genes over the 21-day differentiation period is summarized in Figure 5.13.

The stability of the reference genes was tested over the 21-day culture period in both non-induced and induced samples. ΔCt values comparing three potential reference genes

were calculated and the total standard deviation in comparison was as follows: TBP vs GUSB = 1.18; TBP vs YWHAZ = 1.19 and GUSB vs YWHAZ = 1.02, all below a standard deviation of 2, which indicates that all three reference genes are acceptable to use in the study (Table 3) [321]. When testing the stability of the reference genes, a slight up-regulation of all three reference genes were observed on day 21. For this reason, two sets of samples for each reference gene were included on each experimental plate: one sample from day 7 and one sample from day 21. The average Ct value between these two-time points was used as reference samples.

Standard curves were generated for all target genes as well as the three references genes. Standard curves generated using samples from two time points, reason described above, for the three references genes. Table 4 summarizes the efficiency of each pair calculated from individual standard curves using the slope and y-intercept values. An efficiency of 100% is equal to 2 and the optimal efficiency ranges from 90% - 100% (1.8 – 2). ALP standard curve had an efficiency of 1.72 (86%) and might be indicative of the presence of PCR inhibitors or that the primer sequence might not be optimal. OCN, TBP and YWHAZ had and efficiency of 2.144 (107.2%), 2.090 (104.5%) and 2.111 (105.55%) which might indicate the presence of PCR inhibitor or non-specific binding of the primers. Although these values are outside the optimal ranges they are still acceptable [322].

Table 5.3. Summary of the Cp values obtained for the 3 reference genes across multiple time points

Sample number	Sample name	Condition	Day	NI	TBP (A)		GUSB (B)		YWAZ (C)		ΔCt (A vs. B)	ΔCt (A vs. C)	ΔCt (B vs. C)
					MeanCp	STD Cp	MeanCp	STD Cp	MeanCp	STD Cp			
1	A150221-01A	FBS	0		25.7301935	0.13321461	22.9911711	0.03694415	19.5133999	0.04046452	2.73902246	6.21679362	3.47777116
8	A311019-02T	FBS	7	NI	26.1618342	0.20496412	22.7886815	0.14940181	20.6394519	0.8334067	3.37315264	5.5223823	2.14922966
9	A311019-02T	FBS	7	I	24.7524797	0.52026347	21.2989017	0.28546395	19.5298356	0.87795414	3.45357796	5.22264403	1.76906606
14	A311019-02T	FBS	14	NI	25.5428227	0.08383871	22.4163528	0.15774879	19.8025726	0.04947389	3.12646985	5.74025007	2.61378023
15	A311019-02T	FBS	14	I	25.2457346	0.5989449	22.5129817	0.0804652	19.1407104	0.41671256	2.73275289	6.10502411	3.37227122
16	A150221-01A	FBS	21	NI	25.4762427	0.25043689	23.6214432	0.06633348	19.2677901	0.35056378	1.85479948	6.20845255	4.35365307
17	A150221-01A	FBS	21	I	24.647768	0.26050731	22.7503425	0.13683559	19.0669968	0.11305974	1.89742553	5.5807712	3.68334568
66	A280621-01R	pHPL	0		24.9433464	0.7625542	21.8093377	0.06557392	18.6159384	0.18297832	3.13400869	6.32740795	3.19339927
67	A311019-01A	pHPL	7	NI	27.3693712	0.70211425	25.7907888	0.06182261	22.0165805	0.67089676	1.57858245	5.35279074	3.77420828
72	A280621-01R	pHPL	7	I	24.6398627	0.36116926	22.5519129	0.14659278	19.6811131	0.41730581	2.08794976	4.9587496	2.87079985
77	A280621-01R	pHPL	14	NI	25.7202892	0.2364826	22.2404961	0.27713398	20.3478067	0.33956075	3.47979305	5.3724825	1.89268945
78	A280621-01R	pHPL	14	I	28.2892619	0.47598923	24.5349091	0.02187088	22.2080893	0.83146506	3.75435286	6.08117258	2.32681971
83	A280621-01R	pHPL	21	NI	25.8679535	0.59156378	22.0761217	0.03985987	20.0914738	0.31824935	3.79183179	5.7764797	1.98464791
84	A280621-01R	pHPL	21	I	29.2341469	0.8339322	26.5818049	0.26923433	24.4489757	0.23185172	2.65234205	4.78517121	2.13282917
22	A280621-01R	PRP1	0		25.0646633	0.58924321	22.3978087	0.10779837	20.9716363	0.86081448	2.66685465	4.093027	1.42617234
25	A280621-01R	PRP1	7	NI	24.925458	0.25081028	21.990602	0.07668699	19.7252812	0.09146504	2.934856	5.20017683	2.26532083
26	A280621-01R	PRP1	7	I	25.0183464	0.2206534	23.9150775	0.08871236	19.7149191	0.54995028	1.10326889	5.30342726	4.20015836
33	A311019-01A	PRP1	14	NI	25.652697	0.28837344	22.5954613	0.1497299	19.9319249	0.28025968	3.05723564	5.72077209	2.66353646
34	A311019-01A	PRP1	14	I	31.8194397	0.93762176	27.5801104	0.03933793	25.0572069	0.81758299	4.23932923	6.76223271	2.52290347
39	A311019-01A	PRP1	21	NI	25.1595763	0.04432224	22.5512237	0.09980989	19.9637209	0.09027012	2.60835251	5.19585537	2.58750286
38	A280621-01R	PRP1	21	I	29.9914351	0.25787105	28.0957536	0.21261168	24.6209301	0.20812838	1.89568147	5.37050503	3.47482356
43	A280621-01R	PRP2	0		25.1896418	0.07030338	22.5794604	0.03036281	18.9461375	0.44245394	2.6101814	6.24350429	3.63332289
47	A280621-01R	PRP2	7	I	25.7855549	0.39615927	25.8738085	0.0527923	23.3976151	0.39607713	0.08825361	2.38793983	2.47619343

48	A311019-01A	PRP2	7	NI	24.5323074	0.81176826	22.0515089	0.09615275	21.4468802	1.70360059	2.48079852	3.08542719	0.60462868
52	A280621-01R	PRP2	14	NI	25.0296279	0.80968614	21.4302131	0.18175516	19.2450481	0.65114304	3.59941483	5.78457985	2.18516502
57	A311019-02T	PRP2	14	I	24.3529326	0.36207756	22.2966009	0.16768589	19.574852	0.13960382	2.05633173	4.77808057	2.72174885
58	A280621-01R	PRP2	21	NI	24.7573118	0.16964675	21.0730821	0.16583025	20.9221226	0.22556542	3.68422969	3.83518914	0.15095945
59	A280621-01R	PRP2	21	I	29.8169388	1.60456121	26.8032073	0.07515569	24.1829408	0.06210276	3.01373149	5.633998	2.62026651
85	A280621-01R	PRP3	0		28.4344303	0.2018182	24.7347779	0.003018	22.095978	0.36642374	3.69965236	6.3384523	2.63879994
90	A311019-01A	PRP3	7	NI	27.7735829	0.61430609	24.2482344	0.05801526	22.4569116	0.39787163	3.52534849	5.31667128	1.79132278
89	A280621-01R	PRP3	7	I	26.0785008	0.16268396	24.0131933	0.16092657	21.6378247	0.85908451	2.06530754	4.44067611	2.37536857
94	A280621-01R	PRP3	14	NI	29.8370575	4.45850831	32.8353864	0.18317373	28.8765006	0.55283858	2.99832887	0.96055685	3.95888572
99	A311019-02T	PRP3	14	I	26.6371015	0.14023516	23.0765297	0.07634653	22.6938426	0.2068151	3.56057183	3.94325889	0.38268706
100	A280621-01R	PRP3	21	NI	26.3938383	0.46115834	22.2266667	0.06506407	20.8610107	0.0530632	4.16717168	5.53282769	1.36565601
101	A280621-01R	PRP3	21	I	35.3203699	2.07358424	27.8995102	0.04315052	29.3891953	2.10454755	7.42085969	5.93117459	1.4896851
										Mean	2.94662347	5.17454014	2.48941767
										SD	1.18132357	1.19004992	1.01978418

Table 5.4. Amplification efficiency of the primers used in the study. Efficiency was determined using standard curves.

Target Gene	Efficiency	Error	Slope	Y Intercept
ALP	1.72	0.0784	-4.245	39.32
RUNX2	1.988	0.0180	-3.350	33.27
OCN	2.144	0.149	-3.020	39.19
PPARγ	1.850	0.0205	-3.743	35.95
FABP4	1.974	0.0232	-3.386	29.16
Reference Genes				
TBP	2.090	0.0450	-3.124	33.71
GUSB	1.9	0.00801	-3.856	33.28
YWHAZ	2.111	0.0448	-3.083	29.52

109

The comparative Ct method was used to represent gene expression as relative fold changes. When analysing the mRNA expression level, three different strategies was used. Firstly, the relative gene expression of target genes was normalized to reference genes (the average Ct value of 3 reference gene which each had 2 time point), next the relative gene expression was normalized to day 0 (Figure 5.13). Lastly, the relative gene expression of target genes was double normalized, first to day 0 samples then to NI samples (Figure 5.14).

The non-induced ASCs grown in FBS, pHPL and PRP did not show significant changes in any genes of interest over the 21-induction period (Figure 5.13 A-E). For induced ASCs grown in FBS supplemented osteogenic differentiation medium; a gradual increase in *RUNX2* expression levels were observed over the 21-day induction period, there was a gradual decrease in *ALP* expression and, *OCN* expression levels decreased over the 21-day culture period with the highest expression levels observed on day 7 (NS). In induced ASCs culture in FBS-supplemented ODM, *PPARγ* gradually decreased, while the *FABP4* expression levels (Figure 5.13 E) increased over the 21-day culture period (Figure 5.13D). The expression levels of both *PPARγ* (days 7, p=0.0000005; day 14, p=0.0006142) and *FABP4* (day 14, p = 0.0000303; day 21, p = 0.00000001) were significantly higher in the induced ASCs cultured in FBS-supplemented ODM compared to the non-induced ASCs grown in FBS on (significance was seen). ASCs grown in pHPL did not show significant differences between the non-induced and the induced samples when looking at *RUNX2, OCN, PPARγ* and *FABP4*. The expression of *ALP* in ASCs grown in pHPL did decrease after day 7 in the induced samples compared to the non-induced samples. For the ASCs grown in PRP; *RUNX2* was significantly higher in the induced samples than the non-induced samples (Day 21, p = 0.0001499). ASCs grown in PRP-supplemented osteogenic differentiation medium did show a higher expression of *ALP* over the 21-day induction period, this difference was not significant due to the high standard deviation from one biological repeat expressing high levels of *ALP* and the other two biological repeats not expressing *ALP* (Figure 5.13B). The expression of *OCN* and *PPARγ* in ASC grown in PRP-supplemented ODM was not significantly different when comparing non-induced and induced samples. Lastly, *FABP4* had a higher level of

110

expression in the induced ASCs grown in PRP but gradually decreased over the 21-day induction period.
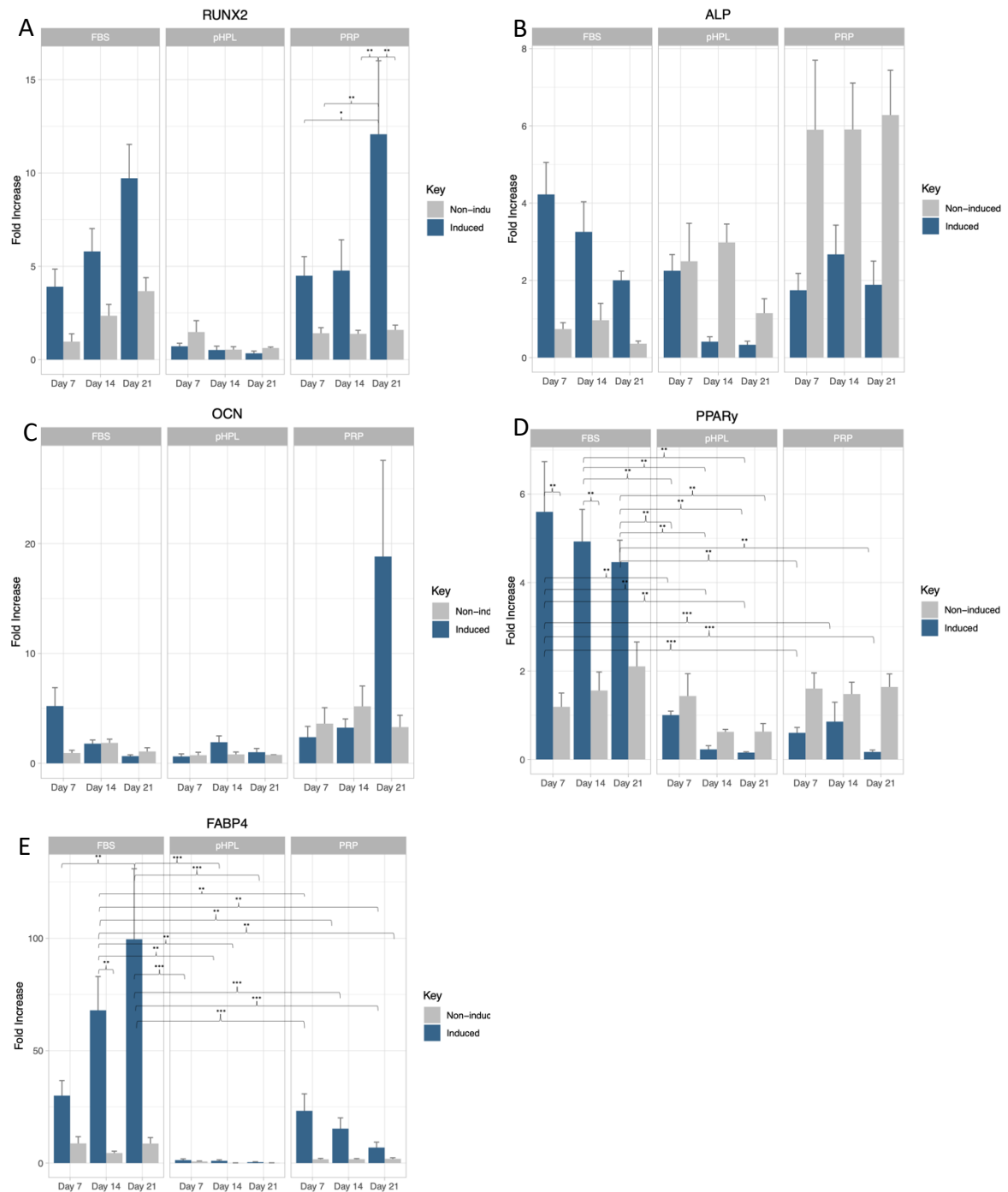
Figure 5.13. Relative fold increase of gene expression normalized to day 0.
RUNX2, ALP, OCN, PPARγ and FABP4 expression kinetics over a 21-day differentiation period in samples supplemented with either FBS, pHPL or PRP. Significant codes: ***: p < 0.001; **: p<0.01, *: p<0.05.

When the results were normalized to day 0 then to the non-induced samples for the respective experimental groups, the differences were highlighted more (Figure 5.14). There were no significant findings when looking at *RUNX2* expression in all three experimental group, but it is worthy to note that in ASCs grown in FBS and PRP showed a gradual increase in *RUNX2* expression over the 21- day differentiation period. *RUNX2* is down regulated in pHPL samples from as early as day 7. ASCs grown in FBS show a significantly higher *ALP* expression when compared to PRP (p = 0.0058226). Both ASCs grown in pHPL and PRP show a down regulation of *ALP* from as early as day 7. When looking at *OCN* expression, there was no significant differences however it can be seen that there is an upregulation of *OCN* on day 21 of ASCs grown in PRP. When looking at the two adipogenic genes, FBS samples showed significant expression of both these genes in induced samples when compared to pHPL and PRP samples (p<0.01). *PPARγ* and *FABP4* were both down regulated in pHPL and PRP samples whereas these two genes were upregulated in ASCs grown in FBS. These findings are of interest as adipogenic genes need to be down regulated for osteogenesis to occur which is the case in pHPL and PRP samples but not the case in FBS samples.
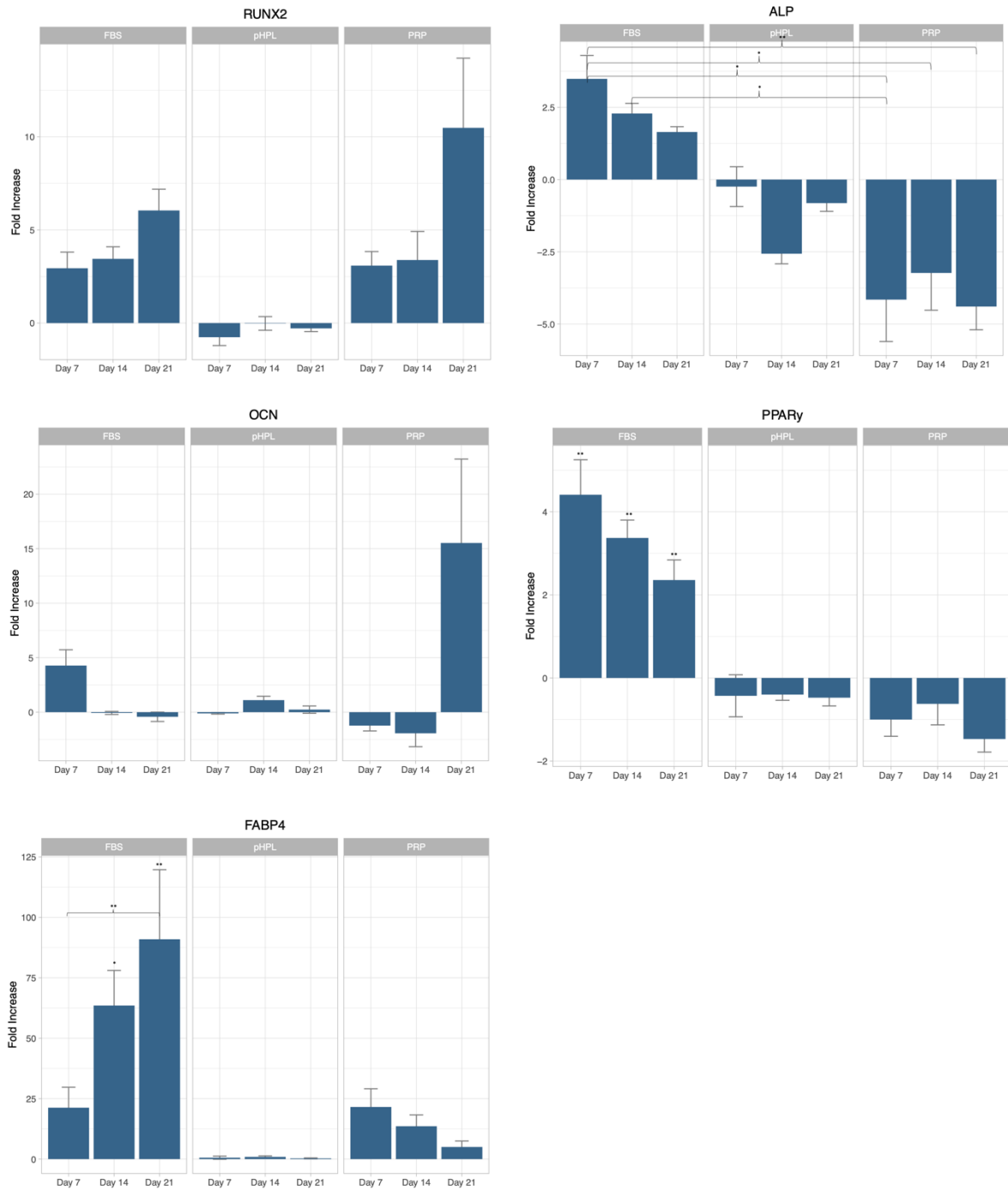
Figure 5.14. Relative fold increase of gene expression normalized to day 0 then non-induced samples.

RUNX2, ALP, OCN, PPARγ and FABP4 expression kinetics over a 21 day differentiation period in samples supplemented with either FBS, pHPL or PRP. Significant codes: ***: p < 0.001; **: p<0.01, *: p<0.05.

5.4. Discussion

The use of ASCs in regenerative medicine holds the potential for many applications. Expanding and differentiating ASCs in FBS, which is currently the gold standard, does not comply with GMP regulations [323]. Not only does FBS not comply with GMP guideline, FBS also has many disadvantages such as batch-to-batch variations, possibility of transmitting zoonotic agents and complications with animal welfare [56–59]. To date there has been a lot of research done in finding the best suited alternative to FBS that does indeed comply to GMP regulations [58,59,66,304,324]. Two attractive alternatives to FBS that stand-out are pHPL and PRP. Although PRP may be superior to FBS, large biological variance can be seen between different PRP samples, making pHPL more advantageous over PRP because pHPL reduces biological variance through pooling multiple donors [64,325]. There are clinical trials underway that have started expanding ASCs in pHPL [326,327]. In this study we investigated the osteogenic potential of ASCs supplemented with either FBS, pHPL or PRP. The composition of the osteogenic differentiation media remained the same except for the serum/plasma/growth factor supplementation (FBS, pHPL or PRP). Previously collected pHPL met the quality controlled criteria set out by Schallmoser & Strunk [319].

Both pHPL and PRP use platelet concentrates to get to the final product. Blood donation centres worldwide collect and manufacture these platelet concentrates for the treatment of multiple disorders. [328–331]. Not only is the collection of platelet concentrates routinely done but platelet concentrates are also discarded after 5 days and thus an attractive alternative to FBS [332]. Platelets are found in circulating human blood and their primary functions involve coagulation and haemostasis. Platelets play an important role in cell culture because they have the ability to release growth factors and cytokines. These growth factors and cytokines can stimulate multiple biological processes, differentiation, cell recruitment and cellular communication [333].

ASCs grown in either FBS, pHPL or PRP maintained the classic fibroblast morphology [334,335]. It was noted that ASCs grown in pHPL and PRP were not only smaller in size but also thinner and more elongated. ASCs grown in FBS on the other hand were larger in size

114

and flatter in their morphology. Bieback et al. [66] suggests this may be due to pHPL or PRP selecting for a more primitive/less differentiated ASC.

Other studies have found that there were no major differences when it came to the viability of cells grown in different supplemented media and that cells grown in media supplemented with a human alternative to FBS actually enhanced proliferation rates and cell viabilities [69,303,307,336]. In this study, cells grown in pHPL had the highest viability followed by FBS and then PRP. The low cell viability in PRP can be attributed to rapid cell proliferation, leading to cells reaching confluency much quicker (This has also been previously described, [337]). ASCs have contact inhibition property that causes ASCs to lift off culture dishes leading to the decrease in viability that was noticed [338,339].

ASCs were immunophenotyped based on the recommendations of Bourin et al. 2013 [34]. The ASCs displayed a highly variable immunophenotype, especially when it came to CD105, CD36 and CD34. This variability has been reported by multiple research groups and is due to the heterogenous population of cells that make up the SVF. The immunophenotype of ASCs can also vary between different donors and different tissue sites [297,340]. No consensus has been reached to what panel of cell surface markers is ideal for the classification of ASCs. Positive markers included were CD 90, CD73 and CD44. The most common negative marker that was included was CD45, as CD45 is a common haemopoietic marker and was observed in less than 2% of ASCs across all the different media [341]. It is recommended by the ISCT that additional markers should be added to better characterize ASCs [34]. In this study we included CD105, CD34 and CD36. CD44 and CD73 were expressed in more than 80% of ASCs across all the different media. CD90 expression was positive in more than 80% of ASCs grown in FBS but there was a decrease in CD90 expression in ASCs grown in the human alternative that has not been documented before. A study done by Park et al. described a population of pericytes that were found to have decreased CD90 expression and could explain the decrease we saw as pericytes are in the SVF and have similar plastic adherent properties like ASCs [342–344]. CD34 expression is variable and unstable in ASC cultures and there is contradictory research available that both supports the argument that ASCs should be CD34 positive and arguments that support ASCs being CD34 negative [34,297,345,346]. Bourin et al. describe the differences between a CD36 positive and CD36 negative population

[34], namely that MSCs isolated from adipose tissue are CD36 positive, while MSCs isolated from bone marrow are CD36 negative. We saw variable CD36 expression across the various supplemented media. CD105 was another variable marker seen in this study, with an increase in CD105 expression seen in media supplemented with human alternative. Again, Bourin et al. characterize ASCs as either CD105 positive or CD105 negative [34]. The use of anti-fungal treatment, especially the use of Amphotericin, has been seen to negatively impact the expression of CD105 [347]. The use of trypsin has also been associated with the loss of CD105 expression as trypsin damages cell surface proteins like CD105 [201]. This can explain the difference we see between FBS cultures and human alternative cultures as we used tryple and not trypsin in human alternative cultures.

ASCs possess the ability to differentiate into osteoblasts which are bone forming cells. We observed that both pHPL and PRP supplemented osteogenic media promoted osteogenesis when compared to FBS. This was assessed using microscopy, spectrophotometry, and gene expression analysis. Our results were in line with what others have found [348–350]. Chignon-Sicard and colleagues showed that PRP inhibits adipogenesis by down regulation of adipogenic genes PPARγ and FABP4 [351]. EGF and PDGF are growth factors that are abundant in PRP. It is these growth factors that specifically inhibit the transcription of PPARγ and FABP4 via the MAP kinase cascade [351]. Adipogenesis and osteogenesis are two mutually exclusive processes. For osteogenesis to take place, adipogenesis needs to be inhibited. This is mainly achieved through the inhibition of PPARγ [104]. Therefore, the use of PRP in osteogenesis proves to be superior to the use of FBS as growth factors found in PRP inhibit adipogenesis.

Osteogenesis is comprised of four sequential phases namely lineage commitment, proliferation, synthesis of the matrix and lastly mineralization of the matrix [298]. Successful mineralization was measured using ARS assays, where ARS stains calcium deposits [182]. Some mineralization was seen in FBS samples but was very variable. ASCs differentiated in both pHPL and PRP showed greater and more consistent mineralization. ALP is an early-stage osteogenic marker and is expressed during the proliferation period of osteogenesis. On the day of termination, the level of ALP activity in the induced samples was significantly higher in FBS samples when compared to pHPL or PRP samples and can thus explain why

mineralization has not occurred in FBS samples because FBS samples were still in the proliferation phase of osteogenesis and not the mineralization phase [213].

To examine the kinetics of the osteogenic process, expression of 3 osteogenic genes was monitored namely *RUNX2*, *ALP* and *OCN*. *RUNX2* is the master regulator when it comes to osteogenesis and is mainly responsible for the differentiation of ASCs into preosteoblasts [84]. *RUNX2* is down-regulated in the later stages of osteogenesis [84]. FBS and PRP induce an increase in *RUNX2* expression over the differentiation period, while pHPL induces a down regulation of *RUNX2* as early as day 7, indicating that ASC differentiation to preosteoblasts had to have happened before day 7 already. Both FBS and PRP samples had less calcium deposition than pHPL, suggesting that because pHPL samples differentiated into preosteoblasts earlier, they had more time to calcify the extra cellular matrix. *ALP*, like *RUNX2*, is an early osteogenic gene that plays an important role in matrix formation through the hydrolysation of inorganic phosphate [105]. *ALP* expression slowly decreased in FBS samples indicating that matrix formation was still taking place at the day of termination. The level *ALP* expression in both pHPL and PRP samples was downregulated indicating that matrix formation had already occurred as early as day 7. *OCN* is used as a biochemical marker for bone formation, as it is the most abundant non-collagenous protein in bone tissue [126]. FBS samples showed almost no expression of *OCN* on the day of termination which correlates with ARS assay results. pHPL samples also showed no expression of *OCN* on the day of termination; however, ARS assay results showed that pHPL samples had the highest amount of calcified bone product. PRP samples showed an increased expression of *OCN* on the day of termination which coincides with ARS assay results as PRP samples did show calcified bone product on the day of termination. Two adipogenic genes were included as controls. As mentioned previously, *PPARγ* is the main transcription factor in adipogenesis and needs to be inhibited for osteogenesis to occur [104]. In both pHPL and PRP samples, *PPARγ* is down-regulated as early as day 7. This however is not true for FBS samples. *PPARγ* gradually decreases over the differentiation period but is never fully downregulated. *FABP4* is a late adipogenic marker and plays a role in lipid formation [352]. FBS samples show a gradual increase in *FABP4*, with the highest expression of *FABP4* on the day of termination. In pHPL samples, *FABP4* is downregulated across the entire differentiation period. PRP samples show little *FABP4* expression, and the expression decreases until the day of termination. Results from both

adipogenic genes explains why there is little to no osteogenesis taking place in FBS samples as adipogenic genes are being expressed. In both pHPL and PRP samples both the adipogenic genes are downregulated allowing for osteogenesis to take place.

In conclusion, for ASCs to be a GMP compliant therapeutic product, the standardization of isolation, expansion and differentiation protocols needs to be done as well as the replacement of FBS as a supplementation factor. FBS is seen as a xenogeneic contaminant and therefore the use of FBS in culture medium does not meet GMP standards. In the current study, we looked at two possible alternatives to FBS namely pHPL and PRP. Our results show that not only were the two human alternatives able to sustain and differentiate ASCs into osteoblasts, they also out-performed ASCs differentiated in FBS. According to the gene expression kinetics of the osteogenic genes, ASCs also differentiated at a higher rate in pHPL and PRP supplemented media when compared to FBS. This fact is especially important when it comes to clinical applications as it shortens the time required for differentiation. ASC's osteogenic differentiating capacity make them attractive in treating bone defects/disorders. It is important to keep in mind that multiple *in vitro* discrepancies exist, and it is therefore important to further test this work *in vivo.*

Chapter 6: Concluding Discussion and Future Perspectives

The use of ASCs in regenerative medicine and cell-based therapies has elicited a great deal of interest due to their multipotent properties. ASCs meet the minimum criteria set out by the ISCAT on immunophenotype and morphology level, and they have the ability to differentiate into cells of mesodermal origin namely adipocytes, osteocytes, chondrocytes and myocytes [34]. This differentiation is achieved by exposing ASCs to various chemical compounds depending on what type of differentiation is desired. Osteogenic differentiation is achieved with a differentiation cocktail that is composed of dexamethasone, β-glycerophosphate and ascorbate-2-phosphate (Chapter 2, Table 2.3). The aim of this study was to optimize and standardize protocols to differentiate MSCs into osteoblasts. Firstly, ASCs were isolated from lipoaspirate samples, immunophenotyped, expanded and then differentiated into osteoblasts. The first half of this study aimed at finding the optimal differentiation medium while the second half of the study aimed at finding the optimal human alternative to FBS specifically for osteogenic differentiation. The differentiation period took place over 21/28 days and the success of the osteogenic differentiation was assessed using two osteogenic assays namely the Alizarin Red S assay and the alkaline phosphatase assay.

Cells isolated from adipose tissue were characterized using flow cytometry to determine whether the cell surface markers were classic ASC markers. Literature previously described ASCs to have the following cell surface marker phenotype: $CD90^+CD73^+CD44^+CD36^+CD34^{variable}CD105^+CD45^-$. In this study, ASCs displayed a highly variable immunophenotype, especially when it came to CD105, CD36 and CD34 (Described in Chapter 4 & 5).

To date there is no consensus regarding the optimal concentrations of osteogenic induction compounds in osteogenic differentiation medium. In the current study, we took three previously published media containing varying concentrations of osteogenic induction compounds and determined which is the most optimal for the osteogenic differentiation of ASCs. Out of the three media, the medium with the lowest concentration of dexamethasone showed the most successful osteogenic differentiation. A study done by Langenbach et al. [353] also found that the optimal concentration of dexamethasone in osteogenic

differentiation medium is 10nM, which is the same concentration of dexamethasone present in our most optimal media.

The most common osteogenic differentiation period is over 21-days. Two biological repeats were differentiated for 21 days and little to no osteogenic differentiation was seen. A study done by Mohamed et al. [213] compared the osteogenic differentiation of MSCs isolated from bone marrow (BM-MSCs) and MSCs isolated from adipose tissue (ASCs). They found that BM-MSCs have a shorter proliferation period than ASCs and that BM-MSCs start the formation and calcification of the collagenous matrix as early as day 14 whereas ASCs have an extended proliferation period and only start the mineralization phase on day 21. We thus decided to extend our differentiation period to 28 days and saw an increase in the amount of calcified bone product.

Out of the three osteogenic media tested, Osteogenic Differentiation Medium 1 showed optimal osteogenic differentiation in FBS. A study found that the physiological level of dexamethasone from 30 healthy bone marrow donors was 10nM and that this is the optimal concentration for osteogenesis [296], the same dexamethasone concentration found in Medium 1. Medium 1 had the highest concentration of ascorbate-2-phosphate and produced the highest amount of calcified bone product. There is a lot of consensuses in literature regarding the concentration of β-glycerophosphate. Many studies have tested a 10 mM [16,54,177,186,188–193]. Out of the three previously published osteogenic media, Medium 1 (Osteogenic media published by Li et al. 2015 [189]) produced the optimal osteogenic differentiation and thus was used for further testing of human alternatives to FBS experiments.

We next investigated the osteogenic potential of ASCs supplemented with either pHPL or PRP as alternatives to FBS. The composition of the osteogenic differentiation medium remained the same except for the supplementation (FBS, pHPL or PRP). ASCs grown in either FBS, pHPL or PRP maintained the classic fibroblast morphology [334,335]. It was noted that ASCs grown in pHPL and PRP were not only smaller in size but also thinner and more elongated. ASCs grown in FBS on the other hand were larger in size and flatter in their morphology. The ASCs displayed a highly variable immunophenotype, especially when it

came to CD105, CD36 and CD34. This variability has been reported by multiple research groups and is due to the heterogenous population of cells that make up SVF. The immunophenotype of ASCs can also vary between different donors and different tissue sites [297,340]. No consensus has been reached as to what panel of cell surface markers is ideal for the classification of ASCs.

We observed that both pHPL and PRP supplemented osteogenic media promoted osteogenesis when compared to FBS. The use of PRP in osteogenesis proved to be superior to the use of FBS, as factors found in PRP inhibit adipogenesis, thus in turn enhancing osteogenesis. Some mineralization was seen in FBS samples but was very variable. ASCs differentiated in both pHPL and PRP showed greater and more consistent mineralization. On the day of termination, the level of ALP activity in the induced samples was significantly higher in FBS samples when compared to pHPL or PRP samples and can thus explain why mineralization has not occurred in FBS samples because FBS samples were still in the proliferation phase of osteogenesis and not the mineralization phase.

When looking at the kinetics of osteogenic differentiation, FBS and PRP induced an increase in RUNX2 expression over the differentiation period, while pHPL induced a down regulation of RUNX2 as early as day 7, indicating that MSC differentiation into preosteoblasts had to have happened before day 7. Both FBS and PRP samples had less calcium deposition than pHPL, suggesting that because pHPL samples differentiated into preosteoblasts earlier, they had more time to calcify the extracellular matrix. ALP expression slowly decreased in FBS samples indicating that matrix formation was still taking place at the day of termination. The level ALP expression in both pHPL and PRP samples was downregulated indicating that matrix formation had already occurred as early as day 7. FBS samples showed almost no expression of OCN on the day of termination which correlates with the ARS assay results. pHPL samples also showed no expression of OCN on the day of termination; however, ARS assay results showed that pHPL samples had the most amount on calcified bone product. PRP samples showed increased expression of OCN on the day of termination which coincides with ARS assay results as PRP samples did show calcified bone product on the day of termination.

By studying the various human alternative supplements as alternatives to FBS in cell culture, we are moving closer to a GMP compliant cell therapeutic product. Our results have showed that both human alternatives, pHPL and PRP were able to not only differentiate ASCs into osteoblasts *in vitro*, but also enhance osteogenic differentiation and thus should be considered in future studies. Future studies should include (1) the standardization an optimization of protocols regarding the manufacturing of human alternative blood products; (2) investigations of what concentrations of human alternative are optimal for osteogenic differentiation of ASCs; (3) testing optimal concentrations of the various components of osteogenic differentiation medium; (4) testing earlier timepoints for human alternatives (pHPL and PRP) to determine where exactly the cells switch from the proliferative phase to the differentiation phase; and (5) testing the kinetics of more osteogenic genes throughout the differentiation process.

Chapter 7: References

1. Wei, X.; Yang, X.; Han, Z.; Qu, F.; Shao, L.; Shi, Y. Mesenchymal stem cells : a new trend for cell therapy. *Nat. Publ. Gr.* **2013**, *34*, 747–754, doi:10.1038/aps.2013.50.

2. Granero-molto, F.; Weis, J.A.; Longobardi, L.; Spagnoli, A.; Granero-molto, F.; Weis, J.A.; Longobardi, L.; Spagnoli, A. Role of mesenchymal stem cells in regenerative medicine : application to bone and cartilage repair. *Expert Opin. Biol. Ther.* **2017**, *8*, 255–268, doi:10.1517/14712598.8.3.255.

3. Champlin, R.E.; Schmitz, N.; Horowitz, M.M.; Chapuis, B.; Chopra, R.; Cornelissen, J.J.; Gale, R.P.; Goldman, J.M.; Jr, F.R.L.; Hertenstein, B.; et al. Blood stem cells compared with bone marrow as a source of hematopoietic cells for allogeneic transplantation. **2000**, *95*, 3702–3709.

4. Stamm, C.; Westphal, B.; Kleine, H.; Petzsch, M.; Kittner, C.; Klinge, H.; Schümichen, C.; Nienaber, C.A.; Freund, M.; Steinhoff, G. Autologous bone-marrow stem-cell transplantation for myocardial regeneration. **2003**, *361*, 45–46.

5. Kelly, S.J. Studies of the Developmental Potential of 4- and 8-Cell Stage Mouse Blastomeres. *J. Exp Zool* **1997**, 365–376.

6. Hanna, J.H.; Saha, K.; Jaenisch, R. Somatic cell reprogramming and transitions between pluripotent states: facts, hypotheses, unresolved issues. *Cell* **2010**, *143*, 508–525, doi:10.1016/j.cell.2010.10.008.Somatic.

7. Velten, L.; Haas, S.F.; Raffel, S.; Blaszkiewicz, S.; Hennig, B.P.; Hirche, C.; Lutz, C.; Buss, E.C.; Boch, T.; Hofmann, W.; et al. Human haematopoietic stem cell lineage commitment is a continuous process. *Nat Cell Biol.* **2017**, *19*, 271–281, doi:10.1038/ncb3493.Human.

8. Reyes, M.; Verfaillie, C.M. Characterization of Multipotent Adult Progenitor Cells , a Subpopulation of Mesenchymal Stem Cells. *Ann. New York Acad. Sci.* **2001**, *938*, 231–235.

9. Kaufmant, M.H. Establishment in culture of pluripotential cells from mouse embryos. *Nature* **1981**, *292*, 154–156.

10. Junying, Y.; A., V.M.; Kim, S.-O.; Jessica, A.-B.; L., F.J.; Shulan, T.; Jeff, N.; A., J.G.; Victor, R.; Ron, S.; et al. Induced Pluripotent Stem Cell Lines Derived from Human Somatic Cells. *Science (80-.).* **2007**, *318*, 1917–1920, doi:10.1126/science.1151526.

11. Takahashi, K.; Tanabe, K.; Ohnuki, M.; Narita, M.; Ichisaka, T.; Tomoda, K. Induction of Pluripotent Stem Cells from Adult Human Fibroblasts by Defined Factors. *Cell* **2007**, *131*, 861–872, doi:10.1016/j.cell.2007.11.019.

12. Clevers, H.; Watt, F.M. Defining Adult Stem Cells by Function, not by Phenotype. *Annu. Rev. Biochem.* **2018**, *87*, 1–13.

13. Seita, J.; Weissman, I.L. Hematopoietic Stem Cell: Self-renewal versus Differentiation. *WILEY Interdiscip. Rev. Biol. Med.* **2010**, *2*, 640–653, doi:10.1002/wsbm.86.Hematopoietic.

14. Horwitz, E.M.; Blanc, K. Le; Dominici, M.; Mueller, I.; Marini, F.C.; Deans, R.J.; Krause, D.S.; Keating, A. Clarification of the nomenclature for MSC : The International Society for Cellular Therapy position statement. **2005**, *7*, 393–395, doi:10.1080/14653240500319234.

15. Pittenger, M.F.; Mackay, A.M.; Beck, S.C.; Jaiswal, R.K.; Douglas, R.; Mosca, J.D.; Moorman, M.A.; Simonetti, D.W.; Craig, S.; Marshak, D.R. Multilineage Potential of Adult Human Mesenchymal Stem Cells. *Science (80-.).* **1999**, *284*, 143–148.

16. Wagner, W.; Wein, F.; Seckinger, A.; Frankhauser, M.; Wirkner, U.; Krause, U.; Blake, J.; Schwager, C.; Eckstein, V.; Ansorge, W.; et al. Comparative characteristics of mesenchymal stem cells from human bone marrow , adipose tissue , and umbilical cord blood. *Elsevier* **2005**, *33*, 1402–1416, doi:10.1016/j.exphem.2005.07.003.

17. Cai, J.; Li, W.; Su, H.; Qin, D.; Yang, J.; Zhu, F.; Xu, J.; He, W.; Guo, X.; Labuda, K.; et al. Generation of Human Induced Pluripotent Stem Cells from Umbilical Cord Matrix and Amniotic Membrane Mesenchymal Cells *. *J. Biol. Chem.* **2010**, *285*, 11227–11234, doi:10.1074/jbc.M109.086389.

18. Anker, P.S. in 't; Scherjon, S.A.; Keur, C.K. der; Noort, W.A.; Claas, F.H.J.; Willemze, R.; Fibbe, W.E.; Kanhai, H.H.H. Amniotic fluid as a novel source of mesenchymal stem cells for therapeutic transplantation. *Blood* **2003**, *102*, 1548–1549.

19. Raynaud, C.M.; Maleki, M.; Lis, R.; Ahmed, B.; Malek, J.; Safadi, F.F.; Rafii, A. Comprehensive Characterization of Mesenchymal Stem Cells from Human Placenta and Fetal Membrane and Their Response to Osteoactivin Stimulation. *Stem Cells Int.* **2012**, *2012*, doi:10.1155/2012/658356.

20. Kita, K.; Gauglitz, G.G.; Phan, T.T.; Herndon, D.N.; Jeschke, M.G. Isolation and Characterization of

Mesenchymal Stem Cells From the Sub-Amniotic Human Umbilical Cord Lining Membrane. *Stem Cells Dev.* **2010**, *19*, 491–501, doi:10.1089/scd.2009.0192.

21. Andreas N. Schuring; Schulte, N.; Kelsch, R.; Ropke, A.; Kiesel, L.; Gotte, M. Characterization of endometrial mesenchymal stem-like cells obtained by endometrial biopsy during routine diagnostics. *Fertil. Steril.* **2011**, *95*, 423–426, doi:10.1016/j.fertnstert.2010.08.035.

22. Huang, G.T.J.; Gronthos, S.; Shi, S. Mesenchymal Stem Cells Derived from Dental Tissues vs . Those from Other Sources : Their Biology and Role in Regenerative Medicine. *J Dent Res* **2009**, *88*, 792–806, doi:10.1177/0022034509340867.

23. Allickson, J.G.; Sanchez, A.; Yefimenko, N.; Borlongan, C. V; Sanberg, P.R. Recent Studies Assessing the Proliferative Capability of a Novel Adult Stem Cell Identified in Menstrual Blood. *Open Stem Cell J.* **2011**, *3*, 4–10, doi:10.2174/1876893801103010004.Recent.

24. Kadir, R.A.; Hisham, S.; Ariffin, Z.; Megat, R.; Wahab, A.; Kermani, S.; Senafi, S. Characterization of Mononucleated Human Peripheral Blood Cells. *Sci. World J.* **2012**, *2012*, doi:10.1100/2012/843843.

25. Bartsch, G.; Yoo, J.J.; Coppi, P.D.E.; Siddiqui, M.M.; Schuch, G.; Pohl, H.G.; Fuhr, J.; Perin, L.; Soker, S.; Atala, A. Propagation, Expansion, and Multilineage Differentiation of Human Somatic Stem Cells from Dermal Progenitors. *Stem Cells Dev.* **2005**, *348*, 337–348.

26. Morito, T.; Muneta, T.; Hara, K.; Ju, Y.; Mochizuki, T.; Makino, H.; Umezawa, A.; Sekiya, I. Synovial fluid-derived mesenchymal stem cells increase after intra-articular ligament injury in humans. *Rheumatology* **2008**, *47*, 1137–1143, doi:10.1093/rheumatology/ken114.

27. Wang, H.; Hung, S.; Peng, S.; Huang, C.; Wei, H.; Guo, Y.; Fu, Y.; Lai, M.; Chen, C.; Biology, C.; et al. Mesenchymal Stem Cells in the Wharton's Jelly of the Human Umbilical Cord. *Stem Cells* **2004**, *22*, 1330–1337, doi:10.1634/stemcells.2004-0013.

28. Blanc, K. Le; Mougiakakos, D. Multipotent mesenchymal stromal cells and the innate immune system. *Nat. Rev. Immunol.* **2012**, *12*, 383–396, doi:10.1038/nri3209.

29. Sacchetti, B.; Funari, A.; Michienzi, S.; Cesare, S. Di; Piersanti, S.; Saggio, I.; Tagliafico, E.; Ferrari, S.; Robey, P.G.; Riminucci, M. Self-Renewing Osteoprogenitors in Bone Marrow Sinusoids Can Organize a Hematopoietic Microenvironment. **2007**, 324–336, doi:10.1016/j.cell.2007.08.025.

30. Schraufstatter, I.U.; Discipio, R.G.; Khaldoyanidi, S. Mesenchymal stem cells and their microenvironment. *Front. Biosci.* **2011**, *16*, 2271–2288, doi:10.2741/3853.

31. Dominici, M.; Blanc, K. Le; Mueller, I.; Marini, F.C.; Krause, D.S.; Deans, R.J.; Keating, A.; Prockop, D.J.; Horwitz, E.M. Minimal criteria for defining multipotent mesenchymal stromal cells . The International Society for Cellular Therapy position statement. *Cytotherapy* **2006**, *8*, 315–317, doi:10.1080/14653240600855905.

32. Witwer, K.W.; Van Balkom, B.W.M.; Bruno, S.; Choo, A.; Dominici, M.; Gimona, M.; Hill, A.F.; De Kleijn, D.; Koh, M.; Lai, R.C.; et al. Defining mesenchymal stromal cell (MSC)-derived small extracellular vesicles for therapeutic applications. *J. Extracell. Vesicles* **2019**, *8*, 1609206, doi:10.1080/20013078.2019.1609206.

33. Ghaneialvar, H.; Soltani, L.; Rahmani, H.R.; Lotfi, A.S.; Soleimani, M. Characterization and Classification of Mesenchymal Stem Cells in Several Species Using Surface Markers for Cell Therapy Purposes. *Indian J. Clin. Biochem.* **2018**, *33*, 46–52, doi:10.1007/s12291-017-0641-x.

34. Bourin, P.; Bunnell, B.A.; Casteilla, L.; Dominici, M.; Katz, A.J.; March, K.L.; Redl, H.; Rubin, J.P. Stromal cells from the adipose tissue-derived stromal vascular fraction and culture expanded adipose tissue-derived stromal/ stem cells: a joint statement of the International Federation for Adipose Therapeutics (IFATS) and Science and the International S. *Cytotherapy* **2013**, *15*, 641–648, doi:10.1016/j.jcyt.2013.02.006.Stromal.

35. Gronthos, S.; Graves, S.E.; Ohta, S.; Simmons, P.J. The STRO-l+ Fraction of Adult Human Bone Marrow Contains the Osteogenic Precursors. *Blood* **2017**, *84*, 4164–4173.

36. Mildmay-White, A.; Khan, W. Cell Surface Markers on Adipose-Derived Stem Cells: A Systematic Review. *Curr. Stem Cell Res. Ther.* **2017**, *12*, 484–492, doi:10.2174/1574888X11666160429122133.

37. Pendleton, C.; Li, Q.; Chesler, D.A.; Yuan, K.; Guerrero-cazares, H.; Quinones-hinojosa, A. Mesenchymal Stem Cells Derived from Adipose Tissue vs Bone Marrow : In Vitro Comparison of Their Tropism towards Gliomas. *PLoS One* **2013**, *8*, doi:10.1371/journal.pone.0058198.

38. Ma, J.; Wu, J.; Han, L.; Jiang, X.; Yan, L.; Hao, J.; Wang, H. Comparative analysis of mesenchymal stem cells derived from amniotic membrane , umbilical cord , and chorionic plate under serum-free condition. *Stem Cell Res. Ther.* **2019**, *10*, 1–13.

39. Spitzhorn, L.-S.; Rahman, M.S.; Schwindt, L.; Ho, H.-T.; Wruck, W.; Bohndorf, M.; Wehrmeyer, S.; Ncube, A.; Beyer, I.; Hagenbeck, C.; et al. Isolation and Molecular Characterization of Amniotic Fluid-

Derived Mesenchymal Stem Cells Obtained from Caesarean Sections. *Stem Cells Int.* **2017**, *2017*, 5932706, doi:10.1155/2017/5932706.

40. Tsai, M.; Lee, J.; Chang, Y.; Hwang, S. Isolation of human multipotent mesenchymal stem cells from second-trimester amniotic fluid using a novel two-stage culture protocol. *Hum. Reprod.* **2004**, *19*, 1450–1456, doi:10.1093/humrep/deh279.

41. BUHRING, H.-J.; VENKATA, L.B.; TREML, S.; BERNHARD, S.; KANZ, L.; VOGEL, W. Novel Markers for the Prospective Isolation of Human MSC. *Ann. New York Acad. Sci.* **2007**, *271*, 262–271, doi:10.1196/annals.1392.000.

42. Liu, Y.; Du, H.; Wang, Y.; Liu, M.; Deng, S.; Fan, L.; Zhang, L.; Sun, Y.; Zhang, Q. Osteoprotegerin-Knockout Mice Developed Early Onset Root Resorption. *J. Endod.* **2016**, *42*, 1516–1522, doi:10.1016/j.joen.2016.07.008.

43. Kadar, K.; Kiraly, M.; Porcsalmy, B.; Molnar, B.; Racz, G.Z.; Blazsek, J.; Kallo, K.; Szabo, E.L.; Gera, I.; Gerber, G.; et al. DIFFERENTIATION POTENTIAL OF STEM CELLS FROM HUMAN DENTAL ORIGIN - PROMISE FOR TISSUE ENGINEERING. *J. Physiol. Pharmacol.* **2009**, *60*, 167–175.

44. Ledesma-Martínez, E.; Mendoza-Núñez, V.M.; Santiago-Osorio, E. Mesenchymal Stem Cells Derived from Dental Pulp: A Review. *Stem Cells Int.* **2016**, *2016*, 4709572, doi:10.1155/2016/4709572.

45. Khatun, M.; Sorjamaa, A.; Kangasniemi, M.; Sutinen, M.; Salo, T.; Liakka, A.; Lehenkari, P.; Tapanainen, J.S.; Vuolteenaho, O.; Chen, C.; et al. Niche matters : The comparison between bone marrow stem cells and endometrial stem cells and stromal fibroblasts reveal distinct migration and cytokine profiles in response to inflammatory stimulus. *PLoS One* **2017**, *12*, 1–21.

46. Wiegner, R.; Rudhart, N.-E.; Barth, E.; Gebhard, F.; Lampl, L.; Huber-Lang, M.S.; Brenner, R.E. Mesenchymal stem cells in peripheral blood of severely injured patients. *Eur. J. Trauma Emerg. Surg.* **2018**, *44*, 627–636, doi:10.1007/s00068-017-0849-8.

47. Lin, W.; Xu, L.; Lin, S.; Shi, L.; Wang, B.; Pan, Q.; Lee, W.Y.W.; Li, G. Characterisation of multipotent stem cells from human peripheral blood using an improved protocol. *J. Orthop. Transl.* **2019**, *19*, 18–28, doi:10.1016/j.jot.2019.02.003.

48. Kim, S.; Lee, S.K.; Kim, H.; Kim, T.M. Exosomes secreted from induced pluripotent stem cell-derived mesenchymal stem cells accelerate skin cell proliferation. *Int. J. Mol. Sci.* **2018**, *19*.

49. Coccini, T.; De Simone, U.; Roccio, M.; Croce, S.; Lenta, E.; Zecca, M.; Spinillo, A.; Avanzini, M.A. In vitro toxicity screening of magnetite nanoparticles by applying mesenchymal stem cells derived from human umbilical cord lining. *J. Appl. Toxicol.* **2019**, *39*, 1320–1336, doi:10.1002/jat.3819.

50. Bharti, D.; Shivakumar, S.B.; Park, J.; Ullah, I.; Park, B.; Rho, G. Comparative analysis of human Wharton's jelly mesenchymal stem cells derived from different parts of the same umbilical cord. *Cell Tissue Res* **2018**, *372*, 51–65, doi:10.1007/s00441-017-2699-4.

51. Lazarus, H.M.; Haynesworth, S.E.; Gerson, S.L.; Rosenthal, N.S.; Caplan, A.I. Ex vivo expansion and subsequent infusion of human bone marrow-derived stromal progenitor cells (mesenchymal progenitor cells): implications for therapeutic use. *Bone Marrow Transplant.* **1995**, *16*, 557–564.

52. Caplan, A.I. Mesenchymal stem cells. *J. Orthop. Res. Off. Publ. Orthop. Res. Soc.* **1991**, *9*, 641–650, doi:10.1002/jor.1100090504.

53. Gimble, J.M.; Katz, A.J.; Bunnell, B.A. Adipose-Derived Stem Cells for Regenerative Medicine. *Circ. Res.* **2017**, *100*, 1249–1260, doi:10.1161/01.RES.0000265074.83288.09.Adipose-Derived.

54. Zuk, P.A.; Ph, D.; Zhu, M.I.N.; Mizuno, H.; Benhaim, P.; Lorenz, H.P. Multilineage Cells from Human Adipose Tissue : Implications for Cell-Based Therapies. *Tissue Eng.* **2001**, *7*, 211–228.

55. Friedenstein, B.A.J. Osteogenesis in transplants of bone marrow cells. *J. Embryol.* **1966**, *16*.

56. Gottipamula, S.; Muttigi, M.S.; Kolkundkar, U.; Seetharam, R.N. Serum-free media for the production of human mesenchymal stromal cells : a review. *Cell Prolif.* **2013**, *46*, 608–627, doi:10.1111/cpr.12063.

57. Jayme, D.W.; Smith, S.R. Media formulation options and manufacturing process controls to safeguard against introduction of animal origin contaminants in animal cell culture. *Cytotechnology* **2000**, *36*, 27–36.

58. Burnouf, T.; Strunk, D.; Koh, M.B.C.; Schallmoser, K. Human platelet lysate: Replacing fetal bovine serum as a gold standard for human cell propagation? *Biomaterials* **2016**, *76*, 371–387, doi:10.1016/j.biomaterials.2015.10.065.

59. Bieback, K. Platelet lysate as replacement for fetal bovine serum in mesenchymal stromal cell cultures. *Transfus. Med. Hemotherapy* **2013**, *40*, 326–335, doi:10.1159/000354061.

60. Etulain, J. Platelets in wound healing and regenerative medicine. *Platelets* **2018**, *29*, 556–568, doi:10.1080/09537104.2018.1430357.

61. De Pascale, M.R.; Sommese, L.; Casamassimi, A.; Napoli, C. Platelet Derivatives in Regenerative

Medicine: An Update. *Transfus. Med. Rev.* **2015**, *29*, 52–61, doi:https://doi.org/10.1016/j.tmrv.2014.11.001.

62. Dohan Ehrenfest, D.M.; Andia, I.; Zumstein, M.A.; Zhang, C.-Q.; Pinto, N.R.; Bielecki, T. Classification of platelet concentrates (Platelet-Rich Plasma-PRP, Platelet-Rich Fibrin-PRF) for topical and infiltrative use in orthopedic and sports medicine: current consensus, clinical implications and perspectives. *Muscles. Ligaments Tendons J.* **2014**, *4*, 3–9.

63. Dessels, C. Expansion of human adipose-derived stem cells: Human alternatives to foetal bovine serum. **2016**.

64. Dessels, C.; Potgieter, M.; Pepper, M.S. Making the switch: Alternatives to fetal bovine serum for adipose-derived stromal cell expansion. *Front. Cell Dev. Biol.* **2016**, *4*, 1–10, doi:10.3389/fcell.2016.00115.

65. Bieback, K.; Hecker, A.; Schlechter, T.; Hofmann, I.; Brousos, N.; Redmer, T.; Besser, D.; Klter, H.; Mller, A.M.; Becker, M. Replicative aging and differentiation potential of human adipose tissue-derived mesenchymal stromal cells expanded in pooled human or fetal bovine serum. *Cytotherapy* **2012**, *14*, 570–583, doi:10.3109/14653249.2011.652809.

66. Bieback, K.; Hecker, A.; Kocaömer, A.; Lannert, H.; Schallmoser, K.; Strunk, D.; Klüter, H. Human alternatives to fetal bovine serum for the expansion of mesenchymal stromal cells from bone marrow. *Stem Cells* **2009**, *27*, 2331–2341, doi:10.1002/stem.139.

67. Atashi, F.; Jaconi, M.E.E.; Pittet-Cuénod, B.; Modarressi, A. Autologous platelet-rich plasma: a biological supplement to enhance adipose-derived mesenchymal stem cell expansion. *Tissue Eng. Part C. Methods* **2015**, *21*, 253–262, doi:10.1089/ten.TEC.2014.0206.

68. Marques, L.F.; Stessuk, T.; Camargo, I.C.C.; Sabeh Junior, N.; Santos, L. Dos; Ribeiro-Paes, J.T. Platelet-rich plasma (PRP): Methodological aspects and clinical applications. *Platelets* **2015**, *26*, 101–113, doi:10.3109/09537104.2014.881991.

69. Oikonomopoulos, A.; van Deen, W.K.; Manansala, A.-R.; Lacey, P.N.; Tomakili, T.A.; Ziman, A.; Hommes, D.W. Optimization of human mesenchymal stem cell manufacturing: the effects of animal/xeno-free media. *Sci. Rep.* **2015**, *5*, 16570, doi:10.1038/srep16570.

70. KOELLENSPERGER, E.; VON HEIMBURG, D.; MARKOWICZ, M.; PALLUA, N. Human Serum from Platelet-Poor Plasma for the Culture of Primary Human Preadipocytes. *Stem Cells* **2006**, *24*, 1218–1225, doi:10.1634/stemcells.2005-0020.

71. Chieregato, K.; Castegnaro, S.; Madeo, D.; Astori, G.; Pegoraro, M.; Rodeghiero, F. Epidermal growth factor, basic fibroblast growth factor and platelet-derived growth factor-bb can substitute for fetal bovine serum and compete with human platelet-rich plasma in the ex vivo expansion of mesenchymal stromal cells derived from adipose tis. *Cytotherapy* **2011**, *13*, 933–943, doi:10.3109/14653249.2011.583232.

72. Müller, I.; Kordowich, S.; Holzwarth, C.; Spano, C.; Isensee, G.; Staiber, A.; Viebahn, S.; Gieseke, F.; Langer, H.; Gawaz, M.P.; et al. Animal serum-free culture conditions for isolation and expansion of multipotent mesenchymal stromal cells from human BM. *Cytotherapy* **2006**, *8*, 437–444, doi:10.1080/14653240600920782.

73. Oikonomopoulos, A.; Deen, W.K. Van; Manansala, A. Optimization of human mesenchymal stem cell manufacturing : the effects of animal / xeno-free media. *Nat. Publ. Gr.* **2015**, *5*, 1–11, doi:10.1038/srep16570.

74. Trojahn Kølle, S.-F.; Oliveri, R.S.; Glovinski, P. V; Kirchhoff, M.; Mathiasen, A.B.; Elberg, J.J.; Andersen, P.S.; Drzewiecki, K.T.; Fischer-Nielsen, A. Pooled human platelet lysate versus fetal bovine serum-investigating the proliferation rate, chromosome stability and angiogenic potential of human adipose tissue-derived stem cells intended for clinical use. *Cytotherapy* **2013**, *15*, 1086–1097, doi:10.1016/j.jcyt.2013.01.217.

75. Karsenty, G.; Wagner, E.F. Reaching a Genetic and Molecular Understanding of Skeletal Development. *Dev. Cell* **2002**, *2*, 389–406.

76. Caetano-Lopes, J.; Canhão, H.; Fonseca, J. Osteoblasts and Bone Formation. *Acta Reum. Port.* **2007**, *32*, 103–110, doi:10.1016/S1569-2590(08)60130-5.

77. Marie, P.J.; Fromigué, O.; Modrowski, D. *Deregulation of osteoblast differentiation in primary bone cancers*; Second Edi.; Elsevier Inc., 2015; Vol. 15; ISBN 9780124167216.

78. Han, Y.; You, X.; Xing, W.; Zhang, Z.; Zou, W. Paracrine and endocrine actions of bone—the functions of secretory proteins from osteoblasts, osteocytes, and osteoclasts. *Bone Res.* **2018**, *6*, 16, doi:10.1038/s41413-018-0019-6.

79. Kenkre, J.S.; Bassett, J.H.D. The bone remodelling cycle. *Ann. Clin. Biochem.* **2018**, *55*, 308–327,

doi:10.1177/0004563218759371.

80. Yang, D.-H.; Yang, M.-Y. The Role of Macrophage in the Pathogenesis of Osteoporosis. *Int. J. Mol. Sci.* **2019**, *20*, 2093, doi:10.3390/ijms20092093.

81. Wittkowske, C.; Reilly, G.C.; Lacroix, D.; Perrault, C.M. In Vitro Bone Cell Models: Impact of Fluid Shear Stress on Bone Formation. *Front. Bioeng. Biotechnol.* **2016**, *4*, doi:10.3389/fbioe.2016.00087.

82. Teitelbaum, S.L. Bone Resorption by Osteoclasts. *Science (80-.).* **2000**, *289*, 1504–1509.

83. Zheng, L.; Tu, Q.; Meng, S.; Zhang, L.; Yu, L.; Song, J.; Hu, Y.; Sui, L.; Zhang, J.; Dard, M.; et al. Runx2/DICER/miRNA Pathway in Regulating Osteogenesis. *J. Cell. Physiol.* **2017**, *232*, 182–191, doi:10.1002/jcp.25406.

84. Bruderer, M.; Richards, R.G.; Alini, M.; Stoddart, M.J. Role and regulation of RUNX2 in osteogenesis. *Eur. Cell. Mater.* **2014**, *28*, 269–286, doi:10.22203/ecm.v028a19.

85. Zhang, X.; Yang, M.; Lin, L.; Chen, P.; Ma, K.T.; Zhou, C.Y.; Ao, Y.F. Runx2 overexpression enhances osteoblastic differentiation and mineralization in adipose - Derived stem cells in vitro and in vivo. *Calcif. Tissue Int.* **2006**, *79*, 169–178, doi:10.1007/s00223-006-0083-6.

86. Haxaire, C.; Haÿ, E.; Geoffroy, V. Runx2 Controls Bone Resorption through the Down-Regulation of the Wnt Pathway in Osteoblasts. *Am. J. Pathol.* **2016**, *186*, 1598–1609, doi:10.1016/j.ajpath.2016.01.016.

87. Thirunavukkarasu, K.; Halladay, D.L.; Miles, R.R.; Yang, X.; Galvin, R.J.S.; Chandrasekhar, S.; Martin, T.J.; Onyia, J.E. The osteoblast-specific transcription factor Cbfa1 contributes to the expression of osteoprotegerin, a potent inhibitor of osteoclast differentiation and function. *J. Biol. Chem.* **2000**, *275*, 25163–25172, doi:10.1074/jbc.M000322200.

88. Otto, F.; Thornell, A.P.; Crompton, T.; Denzel, A.; Gilmour, K.C.; Rosewell, I.R.; Stamp, G.W.H.; Beddington, R.S.P.; Mundlos, S.; Olsen, B.R.; et al. Cbfa1 , a Candidate Gene for Cleidocranial Dysplasia Syndrome, Is Essential for Osteoblast Differentiation and Bone Development. *Cell* **1997**, *89*, 765–771.

89. Mitra D. Adhami; Rashid, H.; Chen, H.; Javed, A. Runx2 activity in committed osteoblasts is not essential for embryonic skeletogenesis. *Connect Tissue Res.* **2014**, *55*, 1–7, doi:10.3109/03008207.2014.923873.Runx2.

90. Cheng, S.L.; Shao, J.S.; Charlton-Kachigian, N.; Loewy, A.P.; Towler, D.A. Msx2 Promotes Osteogenesis and Suppresses Adipogenic Differentiation of Multipotent Mesenchymal Progenitors. *J. Biol. Chem.* **2003**, *278*, 45969–45977, doi:10.1074/jbc.M306972200.

91. Willis, D.M.; Loewy, A.P.; Charlton-Kachigian, N.; Shao, J.S.; Ornitz, D.M.; Towler, D.A.; Bone, D.O.; Diseases, M. Regulation of osteocalcin gene expression by a novel Ku antigen transcription factor complex. *J. Biol. Chem.* **2002**, *277*, 37280–37291, doi:10.1074/jbc.M206482200.

92. Satokata, I.; Ma, L.; Ohshima, H.; Bei, M.; Ian, W.; Nishizawa, K.; Maeda, T.; Takano, Y.; Uchiyama, M.; Heaney, S.; et al. Msx2 deficiency in mice causes pleiotropic defects in bone growth and ectodermal organ formation. *Nat. Genet.* **2000**, *24*, 391–395, doi:10.1038/74231.

93. Rosen, C.J.; Donahue, L.R.; Hunter, S.J. Insulin-like Growth Factors and Bone: The Osteoporosis Connection. *Exp. Biol. Med.* **1994**, *206*, 83–102.

94. Lean, J.M.; Mackay, A.G.; Chow, J.W.M.; Jenny, M.; Mackay, A.G.; Chow, J.W.M.; Chambers, J.; Lilly, E. Osteocytic immediate expression of mRNA for c-fos and IGF-I : an early gene response to an osteogenic stimulus. *Am. J. Physiol. Metab.* **2018**, *270*, 937–945.

95. Sheng, M.H.C.; Zhou, X.D.; Bonewald, L.F.; Baylink, D.J.; Lau, K.H.W. Disruption of the insulin-like growth factor-1 gene in osteocytes impairs developmental bone growth in mice. *Bone* **2013**, *52*, 133–144, doi:10.1016/j.bone.2012.09.027.

96. Zhang, M.; Xuan, S.; Bouxsein, M.L.; Von Stechow, D.; Akeno, N.; Faugere, M.C.; Malluche, H.; Zhao, G.; Rosen, C.J.; Efstratiadis, A.; et al. Osteoblast-specific knockout of the insulin-like growth factor (IGF) receptor gene reveals an essential role of IGF signaling in bone matrix mineralization. *J. Biol. Chem.* **2002**, *277*, 44005–44012, doi:10.1074/jbc.M208265200.

97. Mohan, S.; Richman, C.; Guo, R.; Amaar, Y.; Donahue, L.R.; Wergedal, J.; Baylink, D.J. Insulin-Like Growth Factor Regulates Peak Bone Mineral Density in Mice by Both Growth Hormone-Dependent and -Independent Mechanisms. *Endocrinology* **2003**, *144*, 929–936.

98. Wang, W.; Lian, N.; Ma, Y.; Li, L.; Gallant, R.C.; Elefteriou, F.; Yang, X. Chondrocytic Atf4 regulates osteoblast differentiation and function via Ihh. *Development* **2012**, *139*, 601–611, doi:10.1242/dev.069575.

99. Wang, W.; Lian, N.; Li, L.; Moss, H.E.; Wang, W.; Perrien, D.S.; Elefteriou, F.; Yang, X. Atf4 regulates chondrocyte proliferation and differentiation during endochondral ossification by activating Ihh transcription. *Development* **2009**, *136*, 4143–4153, doi:10.1242/dev.043281.

100. Matsubara, T.; Kida, K.; Yamaguchi, A.; Hata, K.; Ichida, F.; Meguro, H.; Aburatani, H.; Nishimura, R.;

Yoneda, T. BMP2 regulates osterix through Msx2 and Runx2 during osteoblast differentiation. *J. Biol. Chem.* **2008**, *283*, 29119–29125, doi:10.1074/jbc.M801774200.

101. Han, Y.; Kim, C.Y.; Cheong, H.; Lee, K.Y. Osterix represses adipogenesis by negatively regulating PPAR γ transcriptional activity. *Nat. Publ. Gr.* **2016**, 1–11, doi:10.1038/srep35655.

102. Hilton, M.J.; Tu, X.; Wu, X.; Bai, S.; Zhao, H.; Kronenberg, H.M.; Teitelbaum, S.L.; Ross, F.P.; Long, F. Notch signaling maintains bone marrow mesenchymal progenitors by suppressing osteoblast differentiation. *Nat. Med.* **2009**, *14*, 306–314, doi:10.1038/nm1716.Notch.

103. Celil, A.B.; Campbell, P.G. BMP-2 and insulin-like growth factor-I mediate osterix (Osx) expression in human mesenchymal stem cells via the MAPK and protein kinase D signaling pathways. *J. Biol. Chem.* **2005**, *280*, 31353–31359, doi:10.1074/jbc.M503845200.

104. Kang, S.; Bennett, C.N.; Gerin, I.; Rapp, L.A.; Hankenson, K.D.; Macdougald, O.A. Wnt Signaling Stimulates Osteoblastogenesis of Mesenchymal Precursors by Suppressing CCAAT / Enhancer-binding Protein ⌣ and Peroxisome Proliferator-activated Receptor ∥ *. *J. Biol. Chem.* **2007**, *282*, 14515–14524, doi:10.1074/jbc.M700030200.

105. Siffert, R.S. The role of alkaline phosphatse in osteogenesis. *J. Exp. Med.* **1951**, *93*, 415–426.

106. Nakamura, T.; Nakamura-Takahashi, A.; Kasahara, M.; Yamaguchi, A.; Azuma, T. Tissue-nonspecific alkaline phosphatase promotes the osteogenic differentiation of osteoprogenitor cells. *Biochem. Biophys. Res. Commun.* **2020**, *524*, 702–709, doi:10.1016/j.bbrc.2020.01.136.

107. Narisawa, S.; Yadav, M.C.; Millán, J.L. In vivo overexpression of tissue-nonspecific alkaline phosphatase increases skeletal mineralization and affects the phosphorylation status of osteopontin. *J. Bone Miner. Res.* **2013**, *28*, 1587–1598, doi:10.1002/jbmr.1901.

108. Narisawa, S.; Fröhlander, N.; Millán, J.L. Inactivation of two mouse alkaline phosphatase genes and establishment of a model of infantile hypophosphatasia. *Dev. Dyn.* **1997**, *208*, 432–446, doi:10.1002/(SICI)1097-0177(199703)208:3<432::AID-AJA13>3.0.CO;2-1.

109. Waymire, K.G.; Mahuren, J.D.; Jaje, J.M.; Guilarte, T.R.; Coburn, S.P.; MacGregor, G.R. Mice lacking tissue non–specific alkaline phosphatase die from seizures due to defective metabolism of vitamin B–6. *Nat. Genet.* **1995**, *11*, 45–51, doi:10.1038/ng0995-45.

110. Liu, W.; Zhang, L.; Xuan, K.; Hu, C.; Li, L.; Zhang, Y.; Jin, F.; Jin, Y. Alkaline phosphatase controls lineage switching of mesenchymal stem cells by regulating the lrp6/gsk3β complex in hypophosphatasia. *Theranostics* **2018**, *8*, 5575–5592, doi:10.7150/thno.27372.

111. Nakamura-Takahashi, A.; Miyake, K.; Watanabe, A.; Hirai, Y.; Iijima, O.; Miyake, N.; Adachi, K.; Nitahara-Kasahara, Y.; Kinoshita, H.; Noguchi, T.; et al. Treatment of hypophosphatasia by muscle-directed expression of bone-targeted alkaline phosphatase via self-complementary AAV8 vector. *Mol. Ther. - Methods Clin. Dev.* **2016**, *3*, 15059, doi:10.1038/mtm.2015.59.

112. Canty, E.G.; Kadler, K.E. Procollagen trafficking, processing and fibrillogenesis. *J. Cell Sci.* **2005**, *118*, 1341–1353, doi:10.1242/jcs.01731.

113. Alford, A.I.; Kozloff, K.M.; Hankenson, K.D. Extracellular matrix networks in bone remodeling. *Int. J. Biochem. Cell Biol.* **2015**, *65*, 20–31, doi:10.1016/j.biocel.2015.05.008.

114. Chen, Q.; Shou, P.; Zhang, L.; Xu, C.; Zheng, C.; Han, Y.; Li, W.; Huang, Y.; Zhang, X.; Shao, C.; et al. An osteopontin-integrin interaction plays a critical role in directing adipogenesis and osteogenesis by mesenchymal stem cells. *Stem Cells* **2014**, *32*, 327–337, doi:10.1002/stem.1567.

115. Ryoo, H.; Lee, M.; Kim, Y. Critical molecular switches involved in BMP-2-induced osteogenic differentiation of mesenchymal cells. *Gene* **2006**, *366*, 51–57, doi:10.1016/j.gene.2005.10.011.

116. Lee, M.; Kim, Y.; Kim, H.; Park, H.; Kang, A.; Kyung, H.; Sung, J.; Wozney, J.M.; Kim, H.; Ryoo, H. BMP-2-induced Runx2 Expression Is Mediated by Dlx5, and TGF-?1 Opposes the BMP-2-induced Osteoblast Differentiation by Suppression of Dlx5 Expression. *J. Biol. Chem.* **2003**, *278*, 34387–34394, doi:10.1074/jbc.M211386200.

117. Samee, N.; Geoffroy, V.; Marty, C.; Schiltz, C.; Vieux-Rochas, M.; Levi, G.; De Vernejoul, M.C. Dlx5, a positive regulator of osteoblastogenesis, is essential for osteoblast-osteoclast coupling. *Am. J. Pathol.* **2008**, *173*, 773–780, doi:10.2353/ajpath.2008.080243.

118. Acampora, D.; Merlo, G.R.; Paleari, L.; Zerega, B.; Postiglione, M.P.; Mantero, S.; Bober, E.; Barbieri, O.; Simeone, A.; Levi, G. Craniofacial , vestibular and bone defects in mice lacking the Distal-less- related gene Dlx5. *Development* **1999**, *126*, 3795–3809.

119. Robledo, R.F.; Rajan, L.; Li, X.; Lufkin, T. The D1x5 and D1x6 homeobox genes are essential for craniofacial, axial, and appendicular skeletal development. *Genes Dev.* **2002**, *16*, 1089–1101, doi:10.1101/gad.988402.

120. Muraglia, A.; Perera, M.; Verardo, S.; Liu, Y.; Cancedda, R.; Quarto, R.; Corte, G. DLX5 overexpression

impairs osteogenic differentiation of human bone marrow stromal cells. *Eur. J. Cell Biol.* **2008**, *87*, 751–761, doi:10.1016/j.ejcb.2008.04.004.

121. Collin-Osdoby, P.; Rothe, L.; Anderson, F.; Nelson, M.; Maloney, W.; Osdoby, P. Receptor activator of NF-kappa B and osteoprotegerin expression by human microvascular endothelial cells, regulation by inflammatory cytokines, and role in human osteoclastogenesis. *J. Biol. Chem.* **2001**, *276*, 20659–20672, doi:10.1074/jbc.M010153200.

122. Oshita, K.; Yamaoka, K.; Udagawa, N.; Fukuyo, S.; Sonomoto, K.; Maeshima, K.; Kurihara, R.; Nakano, K.; Saito, K.; Okada, Y.; et al. Human mesenchymal stem cells inhibit osteoclastogenesis through osteoprotegerin production. *Arthritis Rheum.* **2011**, *63*, 1658–1667, doi:10.1002/art.30309.

123. Min, H.; Morony, S.; Sarosi, I.; Dunstan, C.R.; Capparelli, C.; Scully, S.; Van, G.; Kaufman, S.; Kostenuik, P.J.; Lacey, D.L.; et al. Osteoprotegerin reverses osteoporosis by inhibiting endosteal osteoclasts and prevents vascular calcification by blocking a process resembling osteoclastogenesis. *J. Exp. Med.* **2000**, *192*, 463–474, doi:10.1084/jem.192.4.463.

124. Mizuno, A.; Amizuka, N.; Irie, K.; Murakami, A.; Fujise, N.; Kanno, T.; Sato, Y.; Nakagawa, N.; Yasuda, H.; Mochizuki, S.; et al. Severe osteoporosis in mice lacking osteoclastogenesis inhibitory factor/osteoprotegerin. *Biochem. Biophys. Res. Commun.* **1998**, *247*, 610–615, doi:10.1006/bbrc.1998.8697.

125. Palumbo, S.; Li, W.J. Osteoprotegerin enhances osteogenesis of human mesenchymal stem cells. *Tissue Eng. - Part A* **2013**, *19*, 2176–2187, doi:10.1089/ten.tea.2012.0550.

126. Zoch, M.L.; Clemens, T.L.; Riddle, R.C. New Insights into the Biology of Osteocalcin. *Bone* **2017**, *82*, 42–49, doi:10.1016/j.bone.2015.05.046.New.

127. Chen, J.K.; Shapiro, H.S.; Wrana, J.L.; Reimers, S.; Heersche, J.N.; Sodek, J. Localization of bone sialoprotein (BSP) expression to sites of mineralized tissue formation in fetal rat tissues by in situ hybridization. *Matrix* **1991**, *11*, 133–143, doi:10.1016/s0934-8832(11)80217-9.

128. Hunter, G.K.; Goldberg, H.A. Nucleation of hydroxyapatite by bone sialoprotein. *Proc. Natl. Acad. Sci.* **1993**, *90*, 8562–8565.

129. Gordon, J.A.R.; Tye, C.E.; Sampaio, A. V; Underhill, T.M.; Hunter, G.K.; Goldberg, H.A. Bone sialoprotein expression enhances osteoblast differentiation and matrix mineralization in vitro. *Bone* **2007**, *41*, 462–473, doi:10.1016/j.bone.2007.04.191.

130. Bouet, G.; Bouleftour, W.; Juignet, L.; Linossier, M.T.; Thomas, M.; Vanden-Bossche, A.; Aubin, J.E.; Vico, L.; Marchat, D.; Malaval, L. The impairment of osteogenesis in bone sialoprotein (BSP) knockout calvaria cell cultures is cell density dependent. *PLoS One* **2015**, *10*, 1–17, doi:10.1371/journal.pone.0117402.

131. Bouleftour, W.; Boudiffa, M.; Wade-Gueye, N.M.; Bouët, G.; Cardelli, M.; Laroche, N.; Vanden-Bossche, A.; Thomas, M.; Bonnelye, E.; Aubin, J.E.; et al. Skeletal development of mice lacking bone sialoprotein (BSP)--impairment of long bone growth and progressive establishment of high trabecular bone mass. *PLoS One* **2014**, *9*, e95144, doi:10.1371/journal.pone.0095144.

132. Malaval, L.; Wade-Guéye, N.M.; Boudiffa, M.; Fei, J.; Zirngibl, R.; Chen, F.; Laroche, N.; Roux, J.-P.; Burt-Pichat, B.; Duboeuf, F.; et al. Bone sialoprotein plays a functional role in bone formation and osteoclastogenesis. *J. Exp. Med.* **2008**, *205*, 1145–1153, doi:10.1084/jem.20071294.

133. Thysen, S.; Cailotto, F.; Lories, R. Osteogenesis induced by frizzled-related protein (FRZB) is linked to the netrin-like domain. *Lab. Investig.* **2016**, *96*, 570–580, doi:10.1038/labinvest.2016.38.

134. Lories, R.J.U.; Peeters, J.; Bakker, A.; Tylzanowski, P.; Derese, I.; Schrooten, J.; Thomas, J.T.; Luvten, F.P. Articular cartilage and biomechanical properties of the long bones in Frzb-knockout mice. *Arthritis Rheum.* **2007**, *56*, 4095–4103, doi:10.1002/art.23137.

135. Macdonald, B.T.; Joiner, D.M.; Oyserman, S.M.; Sharma, P.; Steven, A.; He, X.; Hauschka, P. V Bone mass is inversely proportional to Dkk1 levels in mice. *Bone* **2010**, *41*, 331–339, doi:10.1016/j.bone.2007.05.009.For.

136. Li, X.; Liu, P.; Liu, W.; Maye, P.; Zhang, J.; Zhang, Y.; Hurley, M.; Guo, C.; Boskey, A.; Sun, L.; et al. Dkk2 has a role in terminal osteoblast differentiation and mineralized matrix formation. *Nat. Genet.* **2005**, *37*, 945–952, doi:10.1038/ng1614.

137. Gao, R.; Zhan, L.; Meng, C.; Zhang, N.; Chang, S.; Yao, R.; Li, C. Homeobox B7 promotes the osteogenic differentiation potential of mesenchymal stem cells by activating RUNX2 and transcript of BSP. *Int. J. Clin. Exp. Med.* **2015**, *8*, 10459–10470.

138. Gersch, R.P.; Lombardo, F.; McGovern, S.C.; Hadjiargyrou, M. Reactivation of Hox gene expression during bone regeneration. *J. Orthop. Res. Off. Publ. Orthop. Res. Soc.* **2005**, *23*, 882–890, doi:10.1016/j.orthres.2005.02.005.

139. Bathaie, S.Z.; Faridi, N.; Nasimian, A.; Heidarzadeh, H.; Tamanoi, F. *How Phytochemicals Prevent Chemical Carcinogens and/or Suppress Tumor Growth?*; 1st ed.; Elsevier Inc., 2015; Vol. 37; ISBN 9780128038765.

140. Day, T.F.; Guo, X.; Garrett-Beal, L.; Yang, Y. Wnt/β-catenin signaling in mesenchymal progenitors controls osteoblast and chondrocyte differentiation during vertebrate skeletogenesis. *Dev. Cell* **2005**, *8*, 739–750, doi:10.1016/j.devcel.2005.03.016.

141. Qiu, W.; Andersen, T.E.; Bollerslev, J.; Mandrup, S.; Abdallah, B.M.; Kassem, M. Patients With High Bone Mass Phenotype Exhibit Enhanced Osteoblast Differentiation and Inhibition of Adipogenesis of Human Mesenchymal Stem Cells. *J. Bone Miner. Reasearchsearch* **2007**, *22*, 1720–1731, doi:10.1359/JBMR.070721.

142. Rawadi, G.; Vayssière, B.; Dunn, F.; Baron, R.; Roman-Roman, S. BMP-2 controls alkaline phosphatase expression and osteoblast mineralization by a Wnt autocrine loop. *J. bone Miner. Res. Off. J. Am. Soc. Bone Miner. Res.* **2003**, *18*, 1842–1853, doi:10.1359/jbmr.2003.18.10.1842.

143. Hill, T.P.; Später, D.; Taketo, M.M.; Birchmeier, W.; Hartmann, C. Canonical Wnt/β-catenin signaling prevents osteoblasts from differentiating into chondrocytes. *Dev. Cell* **2005**, *8*, 727–738, doi:10.1016/j.devcel.2005.02.013.

144. Cho, Y.-D.; Kim, W.-J.; Yoon, W.-J.; Woo, K.-M.; Baek, J.-H.; Lee, G.; Kim, G.-S.; Ryoo, H.-M. Wnt3a stimulates Mepe, Matrix extracellular phosphoglycoprotein, expression directly by the activation of the canonical Wnt signaling pathway and indirectly through the stimulation of autocrine Bmp-2 expression. *J. Cell. Physiol.* **2012**, *227*, 2287–2296, doi:10.1002/jcp.24038.

145. Li, Y.; Yuan, J.; Rothzerg, E.; Wu, X.; Xu, H.; Zhu, S.; Xu, J. Molecular structure and the role of high-temperature requirement protein 1 in skeletal disorders and cancers. *Cell Prolif.* **2020**, *53*, 1–9, doi:10.1111/cpr.12746.

146. Kawai, M.; Breggia, A.C.; Demambro, V.E.; Shen, X.; Canalis, E.; Bouxsein, M.L.; Beamer, W.G.; Clemmons, D.R.; Rosen, C.J. The heparin-binding domain of IGFBP-2 has insulin-like growth factor binding-independent biologic activity in the growing skeleton. *J. Biol. Chem.* **2011**, *286*, 14670–14680, doi:10.1074/jbc.M110.193334.

147. Rauch, A.; Haakonsson, A.K.; Madsen, J.G.S.; Larsen, M.; Forss, I.; Madsen, M.R.; Van Hauwaert, E.L.; Wiwie, C.; Jespersen, N.Z.; Tencerova, M.; et al. Osteogenesis depends on commissioning of a network of stem cell transcription factors that act as repressors of adipogenesis. *Nat. Genet.* **2019**, *51*, 716–727, doi:10.1038/s41588-019-0359-1.

148. Rosset, E.M.; Bradshaw, A.D. SPARC/osteonectin in mineralized tissue. *Matrix Biol.* **2016**, *52–54*, 78–87, doi:https://doi.org/10.1016/j.matbio.2016.02.001.

149. Tanaka, K.; Kaji, H.; Yamaguchi, T.; Kanazawa, I.; Canaff, L.; Hendy, G.N.; Sugimoto, T. Involvement of the Osteoinductive Factors, Tmem119 and BMP-2, and the ER Stress Response PERK–eIF2α–ATF4 Pathway in the Commitment of Myoblastic into Osteoblastic Cells. *Calcif. Tissue Int.* **2014**, *94*, 454–464, doi:10.1007/s00223-013-9828-1.

150. Olvera, D.; Stolzenfeld, R.; Marini, J.C.; Caird, M.S.; Kozloff, K.M. Low Dose of Bisphosphonate Enhances Sclerostin Antibody-Induced Trabecular Bone Mass Gains in Brtl/+ Osteogenesis Imperfecta Mouse Model. *J. Bone Miner. Res.* **2018**, *33*, 1272–1282, doi:10.1002/jbmr.3421.

151. Lampert, F.M.; Kutscher, C.; Stark, G..; Finkenzeller, nd G. Overexpression of Hif-1 a in Mesenchymal Stem Cells. *J. Cell. Biochem.* **2016**, *768*, 760–768, doi:10.1002/jcb.25361.

152. Cao, X.; Chen, D. The BMP signaling and in vivo bone formation. *Gene* **2009**, *357*, 1–8, doi:10.1016/j.gene.2005.06.017.The.

153. Tsialogiannis, E.; Polyzois, I.; Tang, Q.O.; Pavlou, G.; Tsiridis, E.; Heliotis, M.; Tsiridis, E. Targeting bone morphogenetic protein antagonists: In vitro and in vivo evidence of their role in bone metabolism. *Expert Opin. Ther. Targets* **2009**, *13*, 123–137, doi:10.1517/14728220802637725.

154. Asserson, D.B.; Orbay, H.; Sahar, D.E. Review of the pathways involved in the osteogenic differentiation of adipose-derived stem cells. *J. Craniofac. Surg.* **2019**, *30*, 703–708, doi:10.1097/SCS.0000000000005447.

155. Fujii, M.; Takeda, K.; Imamura, T.; Aoki, H.; Sampath, T.K.; Enomoto, S.; Kawabata, M.; Kato, M.; Ichijo, H.; Miyazono, K. Roles of Bone Morphogenetic Protein Type I Receptors and Smad Proteins in Osteoblast and Chondroblast Differentiation. *Mol. Biol. Cell* **1999**, *10*, 3801–3813.

156. Wu, X. Bin; Li, Y.; Schneider, A.; Yu, W.; Rajendren, G.; Iqbal, J.; Yamamoto, M.; Alam, M.; Brunet, L.J.; Blair, H.C.; et al. Impaired osteoblastic differentiation, reduced bone formation, and severe osteoporosis in noggin-overexpressing mice. *J. Clin. Invest.* **2003**, *112*, 924–934, doi:10.1172/JCI15543.

157. Groppe, J.; Greenwald, J.; Wiater, E.; Rodriguez-Leon, J.; Economides, A.N.; Kwiatkowski, W.; Affolter,

M.; Vale, W.W.; Belmonte, J.C.I.; Choe, S. Structural basis of BMP signalling inhibition by the cystine knot protein Noggin. *Nature* **2002**, *420*, 636–642, doi:10.1038/nature01245.

158. Chen, C.; Uludağ, H.; Wang, Z.; Jiang, H. Noggin suppression decreases BMP-2-induced osteogenesis of human bone marrow-derived mesenchymal stem cells In Vitro. *J. Cell. Biochem.* **2012**, *113*, 3672–3680, doi:https://doi.org/10.1002/jcb.24240.

159. Makhdom, A.M.; Hamdy, R.C. The Role of Growth Factors on Acceleration of Bone Regeneration During Distraction Osteogenesis. *Tissue Eng. Part B Rev.* **2013**, *19*, 442–453, doi:10.1089/ten.teb.2012.0717.

160. Wang, C.; Xiao, F.; Gan, Y.; Yuan, W.; Zhai, Z.; Jin, T.; Chen, X.; Zhang, X. Improving Bone Regeneration Using Chordin siRNA Delivered by pH-Responsive and Non-Toxic Polyspermine Imidazole-4,5-Imine. *Cell. Physiol. Biochem.* **2018**, *46*, 133–147, doi:10.1159/000488416.

161. Dudarić, L.; Cvek, S.Z.; Cvijanović, O.; Šantić, V.; Marić, I.; Crnčević-Orlić, Ž.; Bobinac, D. Expression of the BMP-2, -4 and-7 and their antagonists gremlin, chordin, noggin and follistatin during ectopic osteogenesis. *Coll. Antropol.* **2013**, *37*, 1291–128.

162. Zhang, D.; Ferguson, C.M.; O'Keefe, R.J.; Puzas, J.E.; Rosier, R.N.; Reynolds, P.R. A Role for the BMP Antagonist Chordin in Endochondral Ossification. *J. Bone Miner. Res.* **2002**, *17*, 293–300, doi:https://doi.org/10.1359/jbmr.2002.17.2.293.

163. Hu, K.; Sun, H.; Gui, B.; Sui, C. Gremlin-1 suppression increases BMP-2-induced osteogenesis of human mesenchymal stem cells. *Mol Med Rep* **2017**, *15*, 2186–2194, doi:10.3892/mmr.2017.6253.

164. Rowan, S.C.; Jahns, H.; Mthunzi, L.; Piouceau, L.; Cornwell, J.; Doody, R.; Frohlich, S.; Callanan, J.J.; McLoughlin, P. Gremlin 1 depletion in vivo causes severe enteropathy and bone marrow failure. *J. Pathol.* **2020**, *251*, 117–122, doi:https://doi.org/10.1002/path.5450.

165. Zhang, W.; Luo, Q.; Shi, Q.; Zhang, B.; Bi, Y.; Luo, X.; Jiang, W.; Su, Y.; Shen, J.; Kim, S.H.; et al. TGF B/ BMP Type I Receptors ALK1 and ALK2 Are Essential for BMP9-induced Osteogenic Signaling in Mesenchymal Stem. *J. Biol. Chem.* **2010**, *285*, 29588–29598, doi:10.1074/jbc.M110.130518.

166. Wang, J.H.; Liu, Y.Z.; Yin, L.J.; Chen, L.; Huang, J.; Liu, Y.; Zhang, R.X.; Zhou, L.Y.; Yang, Q.J.; Luo, J.Y.; et al. BMP9 and COX-2 form an important regulatory loop in BMP9-induced osteogenic differentiation of mesenchymal stem cells. *Bone* **2013**, *57*, 311–321, doi:10.1016/j.bone.2013.08.015.

167. Xie, C.; Ming, X.; Wang, Q.; Schwarz, E.M.; Guldberg, R.E.; O'Keefe, R.J.; Zhang, X. COX-2 from the injury milieu is critical for the initiation of periosteal progenitor cell mediated bone healing. *Bone* **2008**, *43*, 1075–1083, doi:10.1016/j.bone.2008.08.109.

168. Rice, R.; Rice, D.P.C.; Olsen, B.R.; Thesleff, I. Progression of calvarial bone development requires Foxc1 regulation of Msx2 and Alx4. *Dev. Biol.* **2003**, *262*, 75–87, doi:10.1016/S0012-1606(03)00355-5.

169. Kume, T.; Deng, K.Y.; Winfrey, V.; Gould, D.B.; Walter, M.A.; Hogan, B.L.M. The forkhead/winged helix gene Mf1 is disrupted in the pleiotropic mouse mutation congenital hydrocephalus. *Cell* **1998**, *93*, 985–996, doi:10.1016/S0092-8674(00)81204-0.

170. Mirzayans, F.; Lavy, R.; Penner-Chea, J.; Berry, F.B. Initiation of Early Osteoblast Differentiation Events through the Direct Transcriptional Regulation of Msx2 by FOXC1. *PLoS One* **2012**, *7*, 1–8, doi:10.1371/journal.pone.0049095.

171. Hopkins, A.; Mirzayans, F.; Berry, F. Foxc1 Expression in Early Osteogenic Differentiation Is Regulated by BMP4-SMAD Activity. *J. Cell. Biochem.* **2016**, *117*, 1707–1717, doi:10.1002/jcb.25464.

172. Karner, C.M.; Long, F. Wnt signaling and cellular metabolism in osteoblasts. *Cell. Mol. Life Sci.* **2017**, *74*, 1649–1657, doi:10.1007/s00018-016-2425-5.

173. Riddle, R.C.; Diegel, C.R.; Leslie, J.M.; van Koevering, K.K.; Faugere, M.C.; Clemens, T.L.; Williams, B.O. Lrp5 and Lrp6 Exert Overlapping Functions in Osteoblasts during Postnatal Bone Acquisition. *PLoS One* **2013**, *8*, doi:10.1371/journal.pone.0063323.

174. Laine, C.M.; Joeng, K.S.; Campeau, P.M.; Tarkkonen, K.; Grover, M.; Lu, J.T.; Pekkinen, M.; Wessman, M.; Heino, T.J.; Nieminen-, V. WNT1 Mutations in Early-onset Osteoporosis and Osteogenesis Imperfecta. *N. Engl. J. Med.* **2013**, *368*, 1809–1816, doi:10.1056/NEJMoa1215458.WNT1.

175. Zheng, H.F.; Tobias, J.H.; Duncan, E.; Evans, D.M.; Eriksson, J.; Paternoster, L.; Yerges-Armstrong, L.M.; Lehtimäki, T.; Bergström, U.; Kähönen, M.; et al. WNT16 influences bone mineral density, cortical bone thickness, bone strength, and osteoporotic fracture risk. *PLoS Genet.* **2012**, *8*, doi:10.1371/journal.pgen.1002745.

176. Deregowski, V.; Gazzerro, E.; Priest, L.; Rydziel, S.; Canalis, E. Notch 1 overexpression inhibits osteoblastogenesis by suppressing Wnt/β-catenin but not bone morphogenetic protein signaling. *J. Biol. Chem.* **2006**, *281*, 6203–6210, doi:10.1074/jbc.M508370200.

177. Nishimura, I.; Hisanaga, R.; Sato, T.; Arano, T.; Nomoto, S. Effect of osteogenic differentiation medium

on proliferation and differentiation of human mesenchymal stem cells in three- dimensional culture with radial fl ow bioreactor. *Regen. Ther.* **2015**, *2*, 24–31, doi:10.1016/j.reth.2015.09.001.

178. Chung, C.H.; Golub, E.E.; Forbes, E.; Tokuoka, T.; Shapiro, I.M. Mechanism of action of beta-glycerophosphate on bone cell mineralization. *Calcif. Tissue Int.* **1992**, *51*, 305–311, doi:10.1007/BF00334492.

179. Prockop, D.J.; Kivirikko, K.I. COLLAGENS : Molecular Biology , Diseases , and Potentials. *Annu. Rev. Biochem.* **1995**, *64*, 403–434.

180. Hamidouche, Z.; Haÿ, E.; Vaudin, P.; Charbord, P.; Schüle, R.; Marie, P.J.; Fromigué, O. FHL2 mediates dexamethasone-induced mesenchymal cell differentiation into osteoblasts by activating Wnt/beta-catenin signaling-dependent Runx2 expression. *FASEB J. Off. Publ. Fed. Am. Soc. Exp. Biol.* **2008**, *22*, 3813–3822, doi:10.1096/fj.08-106302.

181. Rungby, J.; Kassem, M.; Eriksen, E.F.; Danscher, G. The Von Kossa reaction for calcium deposits : silver lactate staining increases sensitivity and reduces background. *Histochem. J.* **1993**, *25*, 446–451.

182. Puchtler, H.; Meloan, S.N.; Terry, M.S. On the History and Mechanisms of Alizarin and Alizarin Red S Stains for Calcium. *J. Histochem. Cytochem.* **1969**, *17*, 110–124.

183. Bab, I.; Ashton, B.A.; Syftestad, G.T.; Owen, M.E. International Assessment of an in vivo Diffusion Chamber Method as a Quantitative Assay for Osteogenesis. *Calcif. Tissue Int.* **1984**, *36*, 77–82.

184. Cai, R.; Nakamoto, T.; Hoshiba, T.; Kawazoe, N.; Chen, G. Control of Simultaneous Osteogenic and Adipogenic Differentiation of Mesenchymal Stem Cells. *J. Stem Cell Res. Ther.* **2014**, *4*, doi:10.4172/2157-7633.1000223.

185. Vieira, N.M.; Zucconi, E.; Secco, M.; Suzuki, M.F.; Bartolini, P.; Vainzof, M.; Zatz, M. Human Multipotent Mesenchymal Stromal Cells from Distinct Sources Show Different In Vivo Potential to Differentiate into Muscle Cells When Injected in Dystrophic Mice. *Stem Cell Rev. Reports* **2010**, *6*, 560–566, doi:10.1007/s12015-010-9187-5.

186. BIEBACK, K.; KERN, S.; KLÜTER, H.; HERMANN EICHLER Critical Parameters for the Isolation of Mesenchymal Stem Cells from Umbilical Cord Blood. *Stem Cells* **2004**, *22*, 625–634.

187. Waterman, R.S.; Tomchuck, S.L.; Henkle, S.L.; Betancourt, A.M. A New Mesenchymal Stem Cell (MSC) Paradigm : Polarization into a Pro-Inflammatory MSC1 or an Immunosuppressive MSC2 Phenotype. *PLoS One* **2010**, *5*, e10088, doi:10.1371/journal.pone.0010088.

188. Elashrya, M.I.; Gegnawa, S.T.; Klymiuka, M.C.; Wenischb, S.; Arnhold, S. Influence of mechanical fluid shear stress on the osteogenic differentiation protocols for equine adipose tissue-derived mesenchymal stem cells. *Elsevier* **2019**, 1–10, doi:10.1016/j.acthis.2019.02.002.

189. Li, J.E.J.; Kawazoe, N.; Chen, G. Gold nanoparticles with different charge and moiety induce differential cell response on mesenchymal stem cell osteogenesis. *Elsevier* **2015**, *54*, 226–236, doi:10.1016/j.biomaterials.2015.03.001.

190. SOTIROPOULOU, P.A.; PEREZ, S.A.; SALAGIANNI, M.; BAXEVANIS, C.N.; PAPAMICHAIL, M. Technology Development Characterization of the Optimal Culture Conditions for Clinical Scale Production of Human Mesenchymal Stem Cells. *Stem Cells* **2006**, *24*, 462–471, doi:10.1634/stemcells.2004-0331.

191. Rada, T.; Reis, R.L.; Gomes, M.E. Distinct Stem Cells Subpopulations Isolated from Human Adipose Tissue Exhibit Different Chondrogenic and Osteogenic Differentiation Potential. *Stem Cell Rev. Reportsm cell* **2011**, *7*, 64–76, doi:10.1007/s12015-010-9147-0.

192. Meuleman, N.; Tondreau, T.; Delforge, A.; Dejeneffe, M.; Massy, M.; Meuleman, N.; Delforge, A.; Massy, M.; Bron, D. Human marrow mesenchymal stem cell culture : serum-free medium allows better expansion than classical a-MEM medium. *Eur. J. Heamatology* **2006**, *76*, 309–316, doi:10.1111/j.1600-0609.2005.00611.x.

193. Sasaki, M.; Abe, R.; Fujita, Y.; Ando, S.; Inokuma, D.; Shimizu, H. Mesenchymal Stem Cells Are Recruited into Wounded Skin and Contribute to Wound Repair by Transdifferentiation into Multiple Skin Cell Type. *J. Immunol.* **2008**, *180*, 2581–2587, doi:10.4049/jimmunol.180.4.2581.

194. Bunnell, B.A.; Flaat, M.; Gagliardi, C.; Patel, B.; Ripoll, C. Adipose-derived Stem Cells: Isolation, Expansion and Differentiation. *Methods Mol. Biol.* **2008**, *45*, 115–120, doi:10.1016/j.ymeth.2008.03.006.Adipose-derived.

195. Xu, L.; Liu, Y.; Sun, Y.; Wang, B.; Xiong, Y.; Lin, W.; Wei, Q.; Wang, H.; He, W.; Wang, B.; et al. Tissue source determines the differentiation potentials of mesenchymal stem cells: A comparative study of human mesenchymal stem cells from bone marrow and adipose tissue. *Stem Cell Res. Ther.* **2017**, *8*, 1–11, doi:10.1186/s13287-017-0716-x.

196. Shen, C.; Yang, C.; Xu, S.; Zhao, H. Comparison of osteogenic differentiation capacity in mesenchymal stem cells derived from human amniotic membrane (AM), umbilical cord (UC), chorionic membrane

(CM), and decidua (DC). *Cell Biosci.* **2019**, *9*, 1–11, doi:10.1186/s13578-019-0281-3.

197. Topoluk, N.; Hawkins, R.; Tokish, J.; Mercuri, J. Amniotic Mesenchymal Stromal Cells Exhibit Preferential Osteogenic and Chondrogenic Differentiation and Enhanced Matrix Production Compared With Adipose Mesenchymal Stromal Cells. *Am. J. Sports Med.* **2017**, *176*, 139–148, doi:10.1016/j.physbeh.2017.03.040.

198. Sun, Q.; Nakata, H.; Yamamoto, M.; Kasugai, S.; Kuroda, S. Comparison of gingiva-derived and bone marrow mesenchymal stem cells for osteogenesis. *J. Cell. Mol. Med.* **2019**, *23*, 7592–7601, doi:10.1111/jcmm.14632.

199. Pérez-Silos, V.; Camacho-Morales, A.; Fuentes-Mera, L. Mesenchymal Stem Cells Subpopulations: Application for Orthopedic Regenerative Medicine. *Stem Cells Int.* **2016**, *2016*, 3187491, doi:10.1155/2016/3187491.

200. McLeod, C.M.; Mauck, R.L. On the origin and impact of mesenchymal stem cell heterogeneity: new insights and emerging tools for single cell analysis. *Eur. Cell. Mater.* **2017**, *34*, 217–231, doi:10.22203/eCM.v034a14.

201. Contentin, R.; Demoor, M.; Concari, M.; Desancé, M.; Audigié, F.; Branly, T.; Galéra, P. Comparison of the Chondrogenic Potential of Mesenchymal Stem Cells Derived from Bone Marrow and Umbilical Cord Blood Intended for Cartilage Tissue Engineering. *Stem Cell Rev. Reports* **2020**, *16*, 126–143, doi:10.1007/s12015-019-09914-2.

202. Barboni, B.; Russo, V.; Curini, V.; Martelli, A.; Berardinelli, P.; Mauro, A.; Mattioli, M.; Marchisio, M.; Bonassi Signoroni, P.; Parolini, O.; et al. Gestational stage affects amniotic epithelial cells phenotype, methylation status, immunomodulatory and stemness properties. *Stem Cell Rev. Reports* **2014**, *10*, 725–741, doi:10.1007/s12015-014-9519-y.

203. Xin, T.Y.; Yu, T.T.; Yang, R.L. DNA methylation and demethylation link the properties of mesenchymal stem cells: Regeneration and immunomodulation. *World J. Stem Cells* **2020**, *12*, 351–358, doi:10.4252/wjsc.v12.i5.351.

204. Murphy, J.M.; Dixon, K.; Beck, S.; Fabian, D.; Feldman, A.; Barry, F. Reduced chondrogenic and adipogenic activity of mesenchymal stem cells from patients with advanced osteoarthritis. *Arthritis Rheum.* **2002**, *46*, 704–713, doi:10.1002/art.10118.

205. He, J.; Jiang, B.; Dai, Y.; Hao, J.; Zhou, Z.; Tian, Z.; Wu, F.; Gu, Z. Regulation of the osteoblastic and chondrocytic differentiation of stem cells by the extracellular matrix and subsequent bone formation modes. *Biomaterials* **2013**, *34*, 6580–6588, doi:https://doi.org/10.1016/j.biomaterials.2013.05.056.

206. He, J.; Guo, J.; Jiang, B.; Yao, R.; Wu, Y.; Wu, F. Directing the osteoblastic and chondrocytic differentiations of mesenchymal stem cells: matrix vs. induction media. *Regen. Biomater.* **2017**, *4*, 269—279, doi:10.1093/rb/rbx008.

207. Gungordu, H.I.; Bao, M.; van Helvert, S.; Jansen, J.A.; Leeuwenburgh, S.C.G.; Walboomers, X.F. Effect of mechanical loading and substrate elasticity on the osteogenic and adipogenic differentiation of mesenchymal stem cells. *J. Tissue Eng. Regen. Med.* **2019**, *13*, 2279–2290, doi:10.1002/term.2956.

208. Castrén, E.; Sillat, T.; Oja, S.; Noro, A.; Laitinen, A.; Konttinen, Y.T.; Lehenkari, P.; Hukkanen, M.; Korhonen, M. Osteogenic differentiation of mesenchymal stromal cells in two-dimensional and three-dimensional cultures without animal serum. *Stem Cell Res. Ther.* **2015**, *6*, 167, doi:10.1186/s13287-015-0162-6.

209. Cimino, M.; Gonçalves, R.M.; Barrias, C.C.; Martins, M.C.L. Xeno-Free Strategies for Safe Human Mesenchymal Stem/Stromal Cell Expansion: Supplements and Coatings. *Stem Cells Int.* **2017**, *2017*, 6597815, doi:10.1155/2017/6597815.

210. Okajcekova, T.; Strnadel, J.; Pokusa, M.; Zahumenska, R.; Janickova, M.; Halasova, E.; Skovierova, H. A Comparative In Vitro Analysis of the Osteogenic Potential of Human Dental Pulp Stem Cells Using Various Differentiation Conditions. *Int. J. Mol. Sci.* **2020**, *21*, doi:10.3390/ijms21072280.

211. Walter, S.G.; Randau, T.M.; Hilgers, C.; Haddouti, E.-M.; Masson, W.; Gravius, S.; Burger, C.; Wirtz, D.C.; Schildberg, F.A. Molecular and Functional Phenotypes of Human Bone Marrow-Derived Mesenchymal Stromal Cells Depend on Harvesting Techniques. *Int. J. Mol. Sci.* **2020**, *21*, doi:10.3390/ijms21124382.

212. Musina, R.A.; Beckchanova, E.S.; Belyavskii, A. V; Sukhikh, G.T. Differentiation Potential of Mesenchymal Stem Cells of Different Origin. *Cell Technol. Biol. Med.* **2006**, *2*, 147–151.

213. Mohamed-Ahmed, S.; Fristad, I.; Lie, S.A.; Suliman, S.; Mustafa, K.; Vindenes, H.; Idris, S.B. Adipose-derived and bone marrow mesenchymal stem cells: A donor-matched comparison. *Stem Cell Res. Ther.* **2018**, *9*, 1–15, doi:10.1186/s13287-018-0914-1.

214. Szöke, K.; Daňková, J.; Buzgo, M.; Amler, E.; Brinchmann, J.E.; Østrup, E. The effect of medium composition on deposition of collagen type 1 and expression of osteogenic genes in mesenchymal

stem cells derived from human adipose tissue and bone marrow. *Process Biochem.* **2017**, *59*, 321–328, doi:10.1016/j.procbio.2016.10.011.

215. Niel, G.V.A.N.; Raposo, A. Intestinal Epithelial Cells Secrete Exosome-like Vesicles. *Gastroenterology* **2001**, *121*, 337–349, doi:10.1053/gast.2001.26263.

216. Kraitchman, D.L.; Tatsumi, M.; Gilson, W.D.; Ishimori, T.; Kedziorek, D.; Walczak, P.; Segars, W.P.; Chen, H.H.; Fritzges, D.; Izbudak, I.; et al. Dynamic imaging of allogeneic mesenchymal stem cells trafficking to myocardial infarction. *Circulation* **2005**, *112*, 1451–1461, doi:10.1161/CIRCULATIONAHA.105.537480.

217. Toma, C.; Wagner, W.R.; Bowry, S.; Schwartz, A.; Villanueva, F. Fate of culture-expanded mesenchymal stem cells in the microvasculature: in vivo observations of cell kinetics. *Circ. Res.* **2009**, *104*, 398–402, doi:10.1161/CIRCRESAHA.108.187724.

218. Kallmeyer, K.; André-Lévigne, D.; Baquié, M.; Krause, K.-H.; Pepper, M.S.; Pittet-Cuénod, B.; Modarressi, A. Fate of systemically and locally administered adipose-derived mesenchymal stromal cells and their effect on wound healing. *Stem Cells Transl. Med.* **2020**, *9*, 131–144, doi:10.1002/sctm.19-0091.

219. Rojas, M.; Xu, J.; Woods, C.R.; Mora, A.L.; Spears, W.; Roman, J.; Brigham, K.L. Bone marrow-derived mesenchymal stem cells in repair of the injured lung. *Am. J. Respir. Cell Mol. Biol.* **2005**, *33*, 145–152, doi:10.1165/rcmb.2004-0330OC.

220. Ortiz, L.A.; Gambelli, F.; McBride, C.; Gaupp, D.; Baddoo, M.; Kaminski, N.; Phinney, D.G. Mesenchymal stem cell engraftment in lung is enhanced in response to bleomycin exposure and ameliorates its fibrotic effects. *Proc. Natl. Acad. Sci. U. S. A.* **2003**, *100*, 8407–8411, doi:10.1073/pnas.1432929100.

221. Bruno, S.; Grange, C.; Deregibus, M.C.; Calogero, R.A.; Saviozzi, S.; Collino, F.; Morando, L.; Busca, A.; Falda, M.; Bussolati, B.; et al. Mesenchymal stem cell-derived microvesicles protect against acute tubular injury. *J. Am. Soc. Nephrol.* **2009**, *20*, 1053–1067, doi:10.1681/ASN.2008070798.

222. Bruno, S.; Grange, C.; Collino, F.; Deregibus, M.C.; Cantaluppi, V.; Biancone, L.; Tetta, C.; Camussi, G. Microvesicles derived from mesenchymal stem cells enhance survival in a lethal model of acute kidney injury. *PLoS One* **2012**, *7*, e33115, doi:10.1371/journal.pone.0033115.

223. Arslan, F.; Lai, R.C.; Smeets, M.B.; Akeroyd, L.; Choo, A.; Aguor, E.N.E.; Timmers, L.; van Rijen, H. V; Doevendans, P.A.; Pasterkamp, G.; et al. Mesenchymal stem cell-derived exosomes increase ATP levels, decrease oxidative stress and activate PI3K/Akt pathway to enhance myocardial viability and prevent adverse remodeling after myocardial ischemia/reperfusion injury. *Stem Cell Res.* **2013**, *10*, 301–312, doi:10.1016/j.scr.2013.01.002.

224. Bian, S.; Zhang, L.; Duan, L.; Wang, X.; Min, Y.; Yu, H. Extracellular vesicles derived from human bone marrow mesenchymal stem cells promote angiogenesis in a rat myocardial infarction model. *J. Mol. Med. (Berl).* **2014**, *92*, 387–397, doi:10.1007/s00109-013-1110-5.

225. Teng, X.; Chen, L.; Chen, W.; Yang, J.; Yang, Z.; Shen, Z. Mesenchymal Stem Cell-Derived Exosomes Improve the Microenvironment of Infarcted Myocardium Contributing to Angiogenesis and Anti-Inflammation. *Cell. Physiol. Biochem. Int. J. Exp. Cell. Physiol. Biochem. Pharmacol.* **2015**, *37*, 2415–2424, doi:10.1159/000438594.

226. van Koppen, A.; Joles, J.A.; van Balkom, B.W.M.; Lim, S.K.; de Kleijn, D.; Giles, R.H.; Verhaar, M.C. Human Embryonic Mesenchymal Stem Cell-Derived Conditioned Medium Rescues Kidney Function in Rats with Established Chronic Kidney Disease. *PLoS One* **2012**, *7*, 1–12, doi:10.1371/journal.pone.0038746.

227. Reis, L.A.; Borges, F.T.; Simões, M.J.; Borges, A.A.; Sinigaglia-Coimbra, R.; Schor, N. Bone marrow-derived mesenchymal stem cells repaired but did not prevent gentamicin-induced acute kidney injury through paracrine effects in rats. *PLoS One* **2012**, *7*, e44092–e44092, doi:10.1371/journal.pone.0044092.

228. Zhou, Y.; Xu, H.; Xu, W.; Wang, B.; Wu, H.; Tao, Y.; Zhang, B.; Wang, M.; Mao, F.; Yan, Y.; et al. Exosomes released by human umbilical cord mesenchymal stem cells protect against cisplatin-induced renal oxidative stress and apoptosis in vivo and in vitro. *Stem Cell Res. Ther.* **2013**, *4*, 34, doi:10.1186/scrt194.

229. Bonafede, R.; Scambi, I.; Peroni, D.; Potrich, V.; Boschi, F.; Benati, D.; Bonetti, B.; Mariotti, R. Exosome derived from murine adipose-derived stromal cells: Neuroprotective effect on in vitro model of amyotrophic lateral sclerosis. *Exp. Cell Res.* **2016**, *340*, 150–158, doi:10.1016/j.yexcr.2015.12.009.

230. Zhang, Y.; Chopp, M.; Meng, Y.; Katakowski, M.; Xin, H.; Mahmood, A.; Xiong, Y. Effect of exosomes derived from multipluripotent mesenchymal stromal cells on functional recovery and neurovascular plasticity in rats after traumatic brain injury. *J. Neurosurg.* **2015**, *122*, 856–867,

doi:10.3171/2014.11.JNS14770.

231. Kim, D.; Nishida, H.; An, S.Y.; Shetty, A.K.; Bartosh, T.J.; Prockop, D.J. Chromatographically isolated CD63+CD81+ extracellular vesicles from mesenchymal stromal cells rescue cognitive impairments after TBI. *Proc. Natl. Acad. Sci. U. S. A.* **2016**, *113*, 170–175, doi:10.1073/pnas.1522297113.

232. Gennai, S.; Monsel, A.; Hao, Q.; Park, J.; Matthay, M.A.; Lee, J.W. Microvesicles Derived From Human Mesenchymal Stem Cells Restore Alveolar Fluid Clearance in Human Lungs Rejected for Transplantation. *Am. J. Transplant. Off. J. Am. Soc. Transplant. Am. Soc. Transpl. Surg.* **2015**, *15*, 2404–2412, doi:10.1111/ajt.13271.

233. Monsel, A.; Zhu, Y.; Gennai, S.; Hao, Q.; Hu, S.; Rouby, J.-J.; Rosenzwajg, M.; Matthay, M.A.; Lee, J.W. Therapeutic Effects of Human Mesenchymal Stem Cell-derived Microvesicles in Severe Pneumonia in Mice. *Am. J. Respir. Crit. Care Med.* **2015**, *192*, 324–336, doi:10.1164/rccm.201410-1765OC.

234. Aliotta, J.M.; Pereira, M.; Wen, S.; Dooner, M.S.; Del Tatto, M.; Papa, E.; Goldberg, L.R.; Baird, G.L.; Ventetuolo, C.E.; Quesenberry, P.J.; et al. Exosomes induce and reverse monocrotaline-induced pulmonary hypertension in mice. *Cardiovasc. Res.* **2016**, *110*, 319–330, doi:10.1093/cvr/cvw054.

235. Zhang, B.; Wang, M.; Gong, A.; Zhang, X.; Wu, X.; Zhu, Y.; Shi, H.; Wu, L.; Zhu, W.; Qian, H.; et al. HucMSC-Exosome Mediated-Wnt4 Signaling Is Required for Cutaneous Wound Healing. *Stem Cells* **2015**, *33*, 2158–2168, doi:10.1002/stem.1771.

236. Zhang, B.; Wu, X.; Zhang, X.; Sun, Y.; Yan, Y.; Shi, H.; Zhu, Y.; Wu, L.; Pan, Z.; Zhu, W.; et al. Human umbilical cord mesenchymal stem cell exosomes enhance angiogenesis through the Wnt4/β-catenin pathway. *Stem Cells Transl. Med.* **2015**, *4*, 513–522, doi:10.5966/sctm.2014-0267.

237. Nakamura, Y.; Miyaki, S.; Ishitobi, H.; Matsuyama, S.; Nakasa, T.; Kamei, N.; Akimoto, T.; Higashi, Y.; Ochi, M. Mesenchymal-stem-cell-derived exosomes accelerate skeletal muscle regeneration. *FEBS Lett.* **2015**, *589*, 1257–1265, doi:10.1016/j.febslet.2015.03.031.

238. Qi, X.; Zhang, J.; Yuan, H.; Xu, Z.; Li, Q.; Niu, X.; Hu, B.; Wang, Y.; Li, X. Exosomes secreted by human-induced pluripotent stem cell-derived mesenchymal stem cells repair critical-sized bone defects through enhanced angiogenesis and osteogenesis in osteoporotic rats. *Int. J. Biol. Sci.* **2016**, *12*, 836–849, doi:10.7150/ijbs.14809.

239. Zhang, S.; Chu, W.C.; Lai, R.C.; Lim, S.K.; Hui, J.H.P.; Toh, W.S. Exosomes derived from human embryonic mesenchymal stem cells promote osteochondral regeneration. *Osteoarthr. Cartil.* **2016**, *24*, 2135–2140, doi:10.1016/j.joca.2016.06.022.

240. Zhang, B.; Yin, Y.; Lai, R.C.; Tan, S.S.; Choo, A.B.H.; Lim, S.K. Mesenchymal stem cells secrete immunologically active exosomes. *Stem Cells Dev.* **2014**, *23*, 1233–1244, doi:10.1089/scd.2013.0479.

241. Tan, C.Y.; Lai, R.C.; Wong, W.; Dan, Y.Y.; Lim, S.-K.; Ho, H.K. Mesenchymal stem cell-derived exosomes promote hepatic regeneration in drug-induced liver injury models. *Stem Cell Res. Ther.* **2014**, *5*, 76, doi:10.1186/scrt465.

242. Steele, D.G.; Bramblett, C.A. *The Anatomy and Biology of the Human Skeleton*; 1988;

243. Walmsley, G.G.; Mcardle, A.; Tevlin, R.; Momeni, A.; Atashroo, D.; Hu, M.S.; Feroze, A.H.; Wong, V.W.; Lorenz, P.H.; Longaker, M.T.; et al. Nanotechnology in bone tissue engineering. *Nanomedicine* **2015**, *11*, 1253–1263, doi:10.1016/j.nano.2015.02.013.Nanotechnology.

244. Carbone, E.J.; Jiang, T.; Nelson, C.; Henry, N. Small molecule delivery through nanofibrous scaffolds for musculoskeletal regenerative engineering. *Nonomedicine* **2015**, *10*, 1691–1699, doi:10.1016/j.nano.2014.05.013.Small.

245. Kneser, U.; Schaefer, D.J.; Polykandriotis, E.; Horch, R.E. Tissue engineering of bone: the reconstructive surgeon's point of view. *J. Cell Mol. Med.* **2006**, *10*, 7–19.

246. William, B.; Jr, G.D.L.; Einhorn, T.A.; Koval, K.; Mckee, M.; Smith, W.; Sanders, R.; Watson, T. Bone Grafts and Bone Graft Substitutes in Orthopaedic Trauma Surgery A Critical Analysis. *J. Bone Jt. Surg.* **2007**, *89*, 649–658.

247. Lo, K.W.-H.; Ulery, B.D.; Ashe, K.M.; Laurencin, C.T. Studies of Bone Morphogenetic Protein based Surgical Repair. *Adv. Drug Deliv. Rev.* **2013**, *64*, 1277–1291, doi:10.1016/j.addr.2012.03.014.Studies.

248. Wei, G.; Ma, P.X. Structure and properties of nano-hydroxyapatite / polymer composite scaffolds for bone tissue engineering. *Elsevier* **2009**, *25*, 4749–4757, doi:10.1016/j.biomaterials.2003.12.005.

249. Salgado, J.; Coutinho, O.P.; Reis, R.L. Bone Tissue Engineering : State of the Art and Future Trends. *Macromol. Biosci.* **2004**, *4*, 743–765, doi:10.1002/mabi.200400026.

250. Wang, A.; Tang, Z.; Park, I.-H.; Zhu, Y.; Patel, S.; Daley, G.Q.; Song, L. Induced Pluripotent Stem Cells for Neural Tissue Engineering. *Biomaterials* **2012**, *32*, 5023–5032, doi:10.1016/j.biomaterials.2011.03.070.Induced.

251. Gamblin, A.L.; Brennan, M.A.; Renaud, A.; Yagita, H.; Lézot, F.; Heymann, D.; Trichet, V.; Layrolle, P.

Bone tissue formation with human mesenchymal stem cells and biphasic calcium phosphate ceramics: The local implication of osteoclasts and macrophages. *Biomaterials* **2014**, *35*, 9660–9667, doi:10.1016/j.biomaterials.2014.08.018.

252. Brennan, M.A.; Renaud, A.; Amiaud, J.; Rojewski, M.T.; Schrezenmeier, H.; Heymann, D.; Trichet, V.; Layrolle, P. Pre-clinical studies of bone regeneration with human bone marrow stromal cells and biphasic calcium phosphate. *Stem Cell Res. Ther.* **2014**, *5*, 1–15, doi:10.1186/scrt504.

253. Brennan, M.A.; Renaud, A.; Guilloton, F.; Mebarki, M.; Trichet, V.; Sensebé, L.; Deschaseaux, F.; Chevallier, N.; Layrolle, P. Inferior In Vivo Osteogenesis and Superior Angiogeneis of Human Adipose Tissue: A Comparison with Bone Marrow-Derived Stromal Stem Cells Cultured in Xeno-Free Conditions. *Stem Cells Transl. Med.* **2017**, *6*, 2160–2172, doi:10.1002/sctm.17-0133.

254. Diao, Y.; Ma, Q.; Cui, F.; Zhong, Y. Human umbilical cord mesenchymal stem cells : Osteogenesis in vivo as seed cells for bone tissue engineering. *J. Biomed. Mater. Res.* **2008**, *91A*, 123–131, doi:10.1002/jbm.a.32186.

255. Perez, R.A.; Mestres, G. Role of pore size and morphology in musculo-skeletal tissue regeneration. *Mater. Sci. Eng. C* **2016**, *61*, 922–939, doi:10.1016/j.msec.2015.12.087.

256. Brien, F.J.O. Biomaterials & scaffolds for tissue engineering. *Mater. Today* **2011**, *14*, 88–95, doi:10.1016/S1369-7021(11)70058-X.

257. Wen, Y.; Xun, S.; Haoye, M.; Baichuan, S.; Peng, C.; Xuejian, L.; Kaihong, Z.; Xuan, Y.; Jiang, P. 3D Printing Porous Ceramic Scaffold for Bone Tissue Engineering: A Review. *Biomater. Sci.* **2017**, *5*, 1690–1698, doi:10.1039/C7BM00315C.

258. Sozen, T.; Ozisik, L.; Calik Basaran, N. An overview and management of osteoporosis. *Eur. J. Rheumatol.* **2017**, *4*, 46–56, doi:10.5152/eurjrheum.2016.048.

259. Lippuner, K. The future of osteoporosis treatment - a research update. *Swiss Med. Wkly.* **2012**, *142*, w13624, doi:10.4414/smw.2012.13624.

260. Roos, J.C.; Cox, T.M. Giant osteoclast formation and long-term oral bisphosphonate therapy. *N. Engl. J. Med.* 2009, *360*, 1676–1678.

261. Wang, Z.; Goh, J.; Das De, S.; Ge, Z.; Ouyang, H.; Chong, J.S.W.; Low, S.L.; Lee, E.H. Efficacy of bone marrow-derived stem cells in strengthening osteoporotic bone in a rabbit model. *Tissue Eng.* **2006**, *12*, 1753–1761, doi:10.1089/ten.2006.12.1753.

262. Hsiao, F.S.-H.; Cheng, C.-C.; Peng, S.-Y.; Huang, H.-Y.; Lian, W.-S.; Jan, M.-L.; Fang, Y.-T.; Cheng, E.C.-H.; Lee, K.-H.; Cheng, W.T.-K.; et al. Isolation of therapeutically functional mouse bone marrow mesenchymal stem cells within 3 h by an effective single-step plastic-adherent method. *Cell Prolif.* **2010**, *43*, 235–248, doi:10.1111/j.1365-2184.2010.00674.x.

263. Wyles, C.C.; Houdek, M.T.; Behfar, A.; Sierra, R.J. Mesenchymal stem cell therapy for osteoarthritis : current perspectives. *Stem Cells Cloning Adv. Appl.* **2015**, *8*, 117–124.

264. Bert, J.M.; Gasser, S.I. Approach to the Osteoarthritic Knee in the Aging Athlete: Debridement to Osteotomy. *Arthrosc. J. Arthrosc. Relat. Surg.* **2002**, *18*, 107–110, doi:10.1053/jars.2002.36513.

265. Eder, C.; Schmidt-Bleek, K.; Geissler, S.; Sass, F.A.; Maleitzke, T.; Pumberger, M.; Perka, C.; Duda, G.N.; Winkler, T. Mesenchymal stromal cell and bone marrow concentrate therapies for musculoskeletal indications: a concise review of current literature. *Mol. Biol. Rep.* **2020**, doi:10.1007/s11033-020-05428-0.

266. Marcucio, R.S.; Nauth, A.; Giannoudis, P. V; Bahney, C.; Piuzzi, N.S.; Muschler, G.; Miclau 3rd, T. Stem Cell Therapies in Orthopaedic Trauma. *J. Orthop. Trauma* **2015**, *29 Suppl 1*, S24–S27, doi:10.1097/BOT.0000000000000459.

267. Šponer, P.; Filip, S.; Kučera, T.; Brtková, J.; Urban, K.; Palička, V.; Kočí, Z.; Syka, M.; Bezrouk, A.; Syková, E. Utilizing Autologous Multipotent Mesenchymal Stromal Cells and β-Tricalcium Phosphate Scaffold in Human Bone Defects: A Prospective, Controlled Feasibility Trial. *Biomed Res. Int.* **2016**, *2016*, 2076061, doi:10.1155/2016/2076061.

268. Liebergall, M.; Schroeder, J.; Mosheiff, R.; Gazit, Z.; Yoram, Z.; Rasooly, L.; Daskal, A.; Khoury, A.; Weil, Y.; Beyth, S. Stem cell-based therapy for prevention of delayed fracture union: a randomized and prospective preliminary study. *Mol. Ther.* **2013**, *21*, 1631–1638, doi:10.1038/mt.2013.109.

269. Giannotti, S.; Bottai, V.; Ghilardi, M.; Dell'osso, G.; Fazzi, R.; Trombi, L.; Petrini, M.; Guido, G. Treatment of pseudoarthrosis of the upper limb using expanded mesenchymal stem cells: a pilot study. *Eur. Rev. Med. Pharmacol. Sci.* **2013**, *17*, 224–227.

270. Giannotti, S.; Trombi, L.; Bottai, V.; Ghilardi, M.; D'Alessandro, D.; Danti, S.; Dell'Osso, G.; Guido, G.; Petrini, M. Use of autologous human mesenchymal stromal cell/fibrin clot constructs in upper limb non-unions: long-term assessment. *PLoS One* **2013**, *8*, e73893, doi:10.1371/journal.pone.0073893.

271. Dufrane, D.; Docquier, P.-L.; Delloye, C.; Poirel, H.A.; André, W.; Aouassar, N. Scaffold-free Three-dimensional Graft From Autologous Adipose-derived Stem Cells for Large Bone Defect Reconstruction: Clinical Proof of Concept. *Medicine (Baltimore).* **2015**, *94*, e2220, doi:10.1097/MD.0000000000002220.

272. Marcacci, M.; Kon, E.; Moukhachev, V.; Lavroukov, A.; Kutepov, S.; Quarto, R.; Mastrogiacomo, M.; Cancedda, R. Stem cells associated with macroporous bioceramics for long bone repair: 6- to 7-year outcome of a pilot clinical study. *Tissue Eng.* **2007**, *13*, 947–955, doi:10.1089/ten.2006.0271.

273. Quarto, R.; Mastrogiacomo, M.; Cancedda, R.; Kutepov, S.M.; Mukhachev, V.; Lavroukov, A.; Kon, E.; Marcacci, M. Repair of large bone defects with the use of autologous bone marrow stromal cells. *N. Engl. J. Med.* 2001, *344*, 385–386.

274. Bajada, S.; Harrison, P.E.; Ashton, B.A.; Cassar-Pullicino, V.N.; Ashammakhi, N.; Richardson, J.B. Successful treatment of refractory tibial nonunion using calcium sulphate and bone marrow stromal cell implantation. *J. Bone Joint Surg. Br.* **2007**, *89*, 1382–1386, doi:10.1302/0301-620X.89B10.19103.

275. Dessels, C.; Durandt, C.; Pepper, M.S.; Dessels, C.; Durandt, C.; Pepper, M.S. Comparison of human platelet lysate alternatives using expired and freshly isolated platelet concentrates for adipose-derived stromal cell expansion Comparison of human platelet lysate alternatives using expired and freshly isolated platelet concentrates . *Platelets* **2018**, 1–12, doi:10.1080/09537104.2018.1445840.

276. van Vollenstee, F.A.; Dessels, C.; Kallmeyer, K.; de Villiers, D.; Potgieter, M.; Durandt, C.; Pepper, M.S. Isolation and Characterization of Adipose-Derived Stromal Cells. In *Stem Cell Processing*; Pham, P. Van, Ed.; Springer International Publishing: Cham, 2016; pp. 131–161 ISBN 978-3-319-40073-0.

277. Ambele, M.A.; Dessels, C.; Durandt, C.; Pepper, M.S. Genome-wide analysis of gene expression during adipogenesis in human adipose-derived stromal cells reveals novel patterns of gene expression during adipocyte differentiation. *Stem Cell Res.* **2016**, *16*, 725–734, doi:10.1016/j.scr.2016.04.011.

278. Durandt, C.; Vollenstee, F.A. Van; Dessels, C.; Kallmeyer, K.; Villiers, D. De; Murdoch, C.; Potgieter, M.; Pepper, M.S. Novel flow cytometric approach for the detection of adipocyte subpopulations during adipogenesis. *J. Lipid Res.* **2016**, *57*, 729–742, doi:10.1194/jlr.D065664.

279. de Villiers, D.; Potgieter, M.; Ambele, M.A.; Adam, L.; Durandt, C.; Pepper, M.S. The Role of Reactive Oxygen Species in Adipogenic Differentiation. In Proceedings of the Stem Cells: Biology and Engineering; Van Pham, P., Ed.; Springer International Publishing: Cham, 2018; pp. 125–144.

280. Ambele, M.A.; Pepper, M.S. Identification of transcription factors potentially involved in human adipogenesis in vitro. *Mol. Genet. Genomic Med.* **2017**, *5*, 210–222, doi:10.1002/mgg3.269.

281. Dzobo, K.; Turnley, T.; Wishart, A.; Rowe, A.; Kallmeyer, K.; Vollenstee, F.A. Van; Thomford, N.E.; Dandara, C.; Chopera, D.; Pepper, M.S.; et al. Fibroblast-Derived Extracellular Matrix Induces Chondrogenic Differentiation in Human Adipose-Derived Mesenchymal Stromal / Stem Cells in Vitro. *Int. J. Mol. Sci.* **2016**, *17*, doi:10.3390/ijms17081259.

282. Van Vollenstee, F.A.; Jackson, C.; Hoffmann, D.; Potgieter, M.; Durandt, C.; Pepper, M.S. Human adipose derived mesenchymal stromal cells transduced with GFP lentiviral vectors : assessment of immunophenotype and differentiation capacity in vitro. *Cytotechnology* **2016**, *68*, 2117–2128, doi:10.1007/s10616-016-9945-6.

283. Stenderup, K.; Justesen, J.; Clausen, C.; Kassem, M. Aging is associated with decreased maximal life span and accelerated senescence of bone marrow stromal cells. *Bone* **2003**, *33*, 919–926, doi:10.1016/j.bone.2003.07.005.

284. Mueller, S.M.; Glowacki, J. Age-related decline in the osteogenic potential of human bone marrow cells cultured in three-dimensional collagen sponges. *J. Cell. Biochem.* **2001**, *82*, 583–590, doi:10.1002/jcb.1174.

285. Bacakova, L.; Zarubova, J.; Travnickova, M.; Musilkova, J.; Pajorova, J.; Slepicka, P.; Kasalkova, N.S.; Svorcik, V.; Kolska, Z.; Motarjemi, H.; et al. Stem cells: their source, potency and use in regenerative therapies with focus on adipose-derived stem cells – a review. *Biotechnol. Adv.* **2018**, *36*, 1111–1126, doi:https://doi.org/10.1016/j.biotechadv.2018.03.011.

286. Louwen, F.; Ritter, A.; Kreis, N.N.; Yuan, J. Insight into the development of obesity: functional alterations of adipose-derived mesenchymal stem cells. *Obes. Rev. an Off. J. Int. Assoc. Study Obes.* **2018**, *19*, 888–904, doi:10.1111/obr.12679.

287. Si, Z.; Wang, X.; Sun, C.; Kang, Y.; Xu, J.; Wang, X.; Hui, Y. Adipose-derived stem cells: Sources, potency, and implications for regenerative therapies. *Biomed. Pharmacother.* **2019**, *114*, 108765, doi:10.1016/j.biopha.2019.108765.

288. Markarian, C.F.; Frey, G.Z.; Silveira, M.D.; Chem, E.M.; Milani, A.R.; Ely, P.B.; Horn, A.P.; Nardi, N.B.; Camassola, M. Isolation of adipose-derived stem cells: a comparison among different methods. *Biotechnol. Lett.* **2014**, *36*, 693–702, doi:10.1007/s10529-013-1425-x.

289. Priya, N.; Sarcar, S.; Majumdar, A. Sen; SundarRaj, S. Explant culture: a simple, reproducible, efficient and economic technique for isolation of mesenchymal stromal cells from human adipose tissue and lipoaspirate. *J. Tissue Eng. Regen. Med.* **2012**, *12*, 181–204, doi:10.1002/term.

290. Cottrill, A.; Samadi, Y.; Marra, K. Adipose stem cells and donor demographics: Impact of anatomic location, donor sex, race, BMI, and health. In; Kokai, L., Marra, K., Rubin, J.P.B.T.-S.P. of A.S.C., Eds.; Academic Press, 2022; pp. 149–163 ISBN 978-0-12-819376-1.

291. Prockop, D.J. Collagens: Molecular Biology, Diseases, and Potentials for Therapy. *Annu. Rev. Biochem.* **1995**, *64*, 403–434, doi:10.1146/annurev.biochem.64.1.403.

292. Song, I.-H.; Caplan, A.I.; Dennis, J.E. In vitro dexamethasone pretreatment enhances bone formation of human mesenchymal stem cells in vivo. *J. Orthop. Res. Off. Publ. Orthop. Res. Soc.* **2009**, *27*, 916–921, doi:10.1002/jor.20838.

293. Song, I.-H.; Caplan, A.I.; Dennis, J.E. Dexamethasone inhibition of confluence-induced apoptosis in human mesenchymal stem cells. *J. Orthop. Res. Off. Publ. Orthop. Res. Soc.* **2009**, *27*, 216–221, doi:10.1002/jor.20726.

294. Wang, H.; Pang, B.; Li, Y.; Zhu, D.; Pang, T.; Liu, Y. Dexamethasone has variable effects on mesenchymal stromal cells. *Cytotherapy* **2012**, *14*, 423–430, doi:10.3109/14653249.2011.652735.

295. Franceschi, R.T.; Iyer, B.S. Relationship between collagen synthesis and expression of the osteoblast phenotype in MC3T3-E1 cells. *J. bone Miner. Res. Off. J. Am. Soc. Bone Miner. Res.* **1992**, *7*, 235–246, doi:10.1002/jbmr.5650070216.

296. Langenbach, F.; Handschel, J. Effects of dexamethasone, ascorbic acid and β-glycerophosphate on the osteogenic differentiation of stem cells in vitro. *Stem Cell Res. Ther.* **2013**, *4*, doi:10.1186/scrt328.

297. Donnenberg, A.D.; Meyer, E.M.; Rubin, J.P.; Donnenberg, V.S. The cell-surface proteome of cultured adipose stromal cells. *Cytom. Part A* **2015**, *87*, 665–674, doi:10.1002/cyto.a.22682.

298. Matta, C.; Szűcs-Somogyi, C.; Kon, E.; Robinson, D.; Neufeld, T.; Altschuler, N.; Berta, A.; Hangody, L.; Veréb, Z.; Zákány, R. Osteogenic differentiation of human bone marrow-derived mesenchymal stem cells is enhanced by an aragonite scaffold. *Differentiation.* **2019**, *107*, 24–34, doi:10.1016/j.diff.2019.05.002.

299. Sordi, M.B.; Curtarelli, R.B.; da Silva, I.T.; Fongaro, G.; Benfatti, C.A.M.; de Souza Magini, R.; Cabral da Cruz, A.C. Effect of dexamethasone as osteogenic supplementation in in vitro osteogenic differentiation of stem cells from human exfoliated deciduous teeth. *J. Mater. Sci. Mater. Med.* **2021**, *32*, 1, doi:10.1007/s10856-020-06475-6.

300. Jaiswal, N.; Haynesworth, S.E.; Caplan, A.I.; Bruder, S.P. Osteogenic differentiation of purified, culture-expanded human mesenchymal stem cells in vitro. *J. Cell. Biochem.* **1997**, *64*, 295–312, doi:10.1002/(SICI)1097-4644(199702)64:2<295::AID-JCB12>3.0.CO;2-I.

301. van der Valk, J.; Brunner, D.; De Smet, K.; Fex Svenningsen, A.; Honegger, P.; Knudsen, L.E.; Lindl, T.; Noraberg, J.; Price, A.; Scarino, M.L.; et al. Optimization of chemically defined cell culture media--replacing fetal bovine serum in mammalian in vitro methods. *Toxicol. In Vitro* **2010**, *24*, 1053–1063, doi:10.1016/j.tiv.2010.03.016.

302. van der Valk, J.; Bieback, K.; Buta, C.; Cochrane, B.; Dirks, W.G.; Fu, J.; Hickman, J.J.; Hohensee, C.; Kolar, R.; Liebsch, M.; et al. Fetal Bovine Serum (FBS): Past - Present - Future. *ALTEX* **2018**, *35*, 99–118, doi:10.14573/altex.1705101.

303. Dessels, C.; Durandt, C.; Pepper, M.S. Comparison of human platelet lysate alternatives using expired and freshly isolated platelet concentrates for adipose-derived stromal cell expansion Comparison of human platelet lysate alternatives using expired and freshly isolated platelet concentrates . *Platelets* **2019**, *30*, 356–367, doi:10.1080/09537104.2018.1445840.

304. Shih, D.T.-B.; Burnouf, T. Preparation, quality criteria, and properties of human blood platelet lysate supplements for ex vivo stem cell expansion. *N. Biotechnol.* **2015**, *32*, 199–211, doi:10.1016/j.nbt.2014.06.001.

305. Fekete, N.; Gadelorge, M.; Fürst, D.; Maurer, C.; Dausend, J.; Fleury-Cappellesso, S.; Mailänder, V.; Lotfi, R.; Ignatius, A.; Sensebé, L.; et al. Platelet lysate from whole blood-derived pooled platelet concentrates and apheresis-derived platelet concentrates for the isolation and expansion of human bone marrow mesenchymal stromal cells: production process, content and identification of active com. *Cytotherapy* **2012**, *14*, 540–554, doi:10.3109/14653249.2012.655420.

306. Ben Azouna, N.; Jenhani, F.; Regaya, Z.; Berraeis, L.; Ben Othman, T.; Ducrocq, E.; Domenech, J. Phenotypical and functional characteristics of mesenchymal stem cells from bone marrow: comparison of culture using different media supplemented with human platelet lysate or fetal bovine serum. *Stem Cell Res. Ther.* **2012**, *3*, 6, doi:10.1186/scrt97.

307.   Chen, C.-F.; Liao, H.-T. Platelet-rich plasma enhances adipose-derived stem cell-mediated angiogenesis in a mouse ischemic hindlimb model. *World J. Stem Cells* **2018**, *10*, 212–227, doi:10.4252/wjsc.v10.i12.212.

308.   Xu, Y.; Wang, X.; Liu, W.; Lu, W. Thrombin-activated platelet-rich plasma enhances osteogenic differentiation of human periodontal ligament stem cells by activating SIRT1-mediated autophagy. *Eur. J. Med. Res.* **2021**, *26*, 105, doi:10.1186/s40001-021-00575-x.

309.   Tavakolinejad, S.; Khosravi, M.; Mashkani, B.; Ebrahimzadeh Bideskan, A.; Sanjar Mossavi, N.; Parizadeh, M.R.S.; Hamidi Alamdari, D. The effect of human platelet-rich plasma on adipose-derived stem cell proliferation and osteogenic differentiation. *Iran. Biomed. J.* **2014**, *18*, 151–157, doi:10.6091/ibj.1301.2014.

310.   Arpornmaeklong, P.; Kochel, M.; Depprich, R.; Kübler, N.R.; Würzler, K.K. Influence of platelet-rich plasma (PRP) on osteogenic differentiation of rat bone marrow stromal cells. An in vitro study. *Int. J. Oral Maxillofac. Surg.* **2004**, *33*, 60–70, doi:https://doi.org/10.1054/ijom.2003.0492.

311.   Kasten, P.; Vogel, J.; Beyen, I.; Weiss, S.; Niemeyer, P.; Leo, A.; Lüginbuhl, R. Effect of Platelet-rich Plasma on the in vitro Proliferation and Osteogenic Differentiation of Human Mesenchymal Stem Cells on Distinct Calcium Phosphate Scaffolds: The Specific Surface Area Makes a Difference. *J. Biomater. Appl.* **2008**, *23*, 169–188, doi:10.1177/0885328207088269.

312.   Rubio-Azpeitia, E.; Andia, I. Partnership between platelet-rich plasma and mesenchymal stem cells: in vitro experience. *Muscles. Ligaments Tendons J.* **2014**, *4*, 52–62.

313.   Iudicone, P.; Fioravanti, D.; Bonanno, G.; Miceli, M.; Lavorino, C.; Totta, P.; Frati, L.; Nuti, M.; Pierelli, L. Pathogen-free, plasma-poor platelet lysate and expansion of human mesenchymal stem cells. *J. Transl. Med.* **2014**, *12*, 28, doi:10.1186/1479-5876-12-28.

314.   Jafar, H.; Abuarqoub, D.; Ababneh, N.; Hasan, M.; Al-Sotari, S.; Aslam, N.; Kailani, M.; Ammoush, M.; Shraideh, Z.; Awidi, A. hPL promotes osteogenic differentiation of stem cells in 3D scaffolds. *PLoS One* **2019**, *14*, e0215667.

315.   Shanbhag, S.; Mohamed-Ahmed, S.; Lunde, T.H.F.; Suliman, S.; Bolstad, A.I.; Hervig, T.; Mustafa, K. Influence of platelet storage time on human platelet lysates and platelet lysate-expanded mesenchymal stromal cells for bone tissue engineering. *Stem Cell Res. Ther.* **2020**, *11*, 351, doi:10.1186/s13287-020-01863-9.

316.   Karadjian, M.; Senger, A.-S.; Essers, C.; Wilkesmann, S.; Heller, R.; Fellenberg, J.; Simon, R.; Westhauser, F. Human Platelet Lysate Can Replace Fetal Calf Serum as a Protein Source to Promote Expansion and Osteogenic Differentiation of Human Bone-Marrow-Derived Mesenchymal Stromal Cells. *Cells* 2020, *9*.

317.   Xia, W.; Li, H.; Wang, Z.; Xu, R.; Fu, Y.; Zhang, X.; Ye, X.; Huang, Y.; Xiang, A.P.; Yu, W. Human platelet lysate supports ex vivo expansion and enhances osteogenic differentiation of human bone marrow-derived mesenchymal stem cells. *Cell Biol. Int.* **2011**, *35*, 639–643, doi:https://doi.org/10.1042/CBI20100361.

318.   Chevallier, N.; Anagnostou, F.; Zilber, S.; Bodivit, G.; Maurin, S.; Barrault, A.; Bierling, P.; Hernigou, P.; Layrolle, P.; Rouard, H. Osteoblastic differentiation of human mesenchymal stem cells with platelet lysate. *Biomaterials* **2010**, *31*, 270–278, doi:https://doi.org/10.1016/j.biomaterials.2009.09.043.

319.   Schallmoser, K.; Strunk, D. Generation of a pool of human platelet lysate and efficient use in cell culture. *Methods Mol. Biol.* **2013**, *946*, 349–362, doi:10.1007/978-1-62703-128-8_22.

320.   Cates, N.C.; Oakley, D.J.; Onwuemene, O.A. Therapeutic white blood cell and platelet depletions using the spectra OPTIA system continuous mononuclear cell protocol. *J. Clin. Apher.* **2018**, *33*, 580–585, doi:10.1002/jca.21644.

321.   Dheda, K.; Huggett, J.F.; Bustin, S.A.; Johnson, M.A.; Rook, G.; Zumla, A. Validation of housekeeping genes for normalizing RNA expression in real-time PCR. *Biotechniques* **2004**, *37*, 112–119, doi:10.2144/04371RR03.

322.   Svec, D.; Tichopad, A.; Novosadova, V.; Pfaffl, M.W.; Kubista, M. How good is a PCR efficiency estimate: Recommendations for precise and robust qPCR efficiency assessments. *Biomol. Detect. Quantif.* **2015**, *3*, 9–16, doi:https://doi.org/10.1016/j.bdq.2015.01.005.

323.   Koellensperger, E.; Bollinger, N.; Dexheimer, V.; Gramley, F.; Germann, G.; Leimer, U. Choosing the right type of serum for different applications of human adipose tissue-derived stem cells: Influence on proliferation and differentiation abilities. *Cytotherapy* **2014**, *16*, 789–799, doi:10.1016/j.jcyt.2014.01.007.

324.   Gstraunthaler, G.; Rauch, C.; Feifel; Lindl Preparation of Platelet Lysates for Mesenchymal Stem Cell Culture Media. *J Stem Cells Res, Rev Rep. J Stem Cells Res, Rev Rep* **2015**, *2*, 1021–1.

325. Castegnaro, S.; Chieregato, K.; Maddalena, M.; Albiero, E.; Visco, C.; Madeo, D.; Pegoraro, M.; Rodeghiero, F. Effect of platelet lysate on the functional and molecular characteristics of mesenchymal stem cells isolated from adipose tissue. *Curr. Stem Cell Res. Ther.* **2011**, *6*, 105–114, doi:10.2174/157488811795495440.

326. Camilleri, E.T.; Dudakovic, A.; Riester, S.M.; Galeano-Garces, C.; Paradise, C.R.; Bradley, E.W.; McGee-Lawrence, M.E.; Im, H.-J.; Karperien, M.; Krych, A.J.; et al. Loss of histone methyltransferase Ezh2 stimulates an osteogenic transcriptional program in chondrocytes but does not affect cartilage development. *J. Biol. Chem.* **2018**, *293*, 19001–19011, doi:10.1074/jbc.RA118.003909.

327. Riis, S.; Zachar, V.; Boucher, S.; Vemuri, M.C.; Pennisi, C.P.; Fink, T. Critical steps in the isolation and expansion of adipose-derived stem cells for translational therapy. *Expert Rev. Mol. Med.* **2015**, *17*, e11, doi:10.1017/erm.2015.10.

328. Panda, S.; Karanxha, L.; Goker, F.; Satpathy, A.; Taschieri, S.; Francetti, L.; Chandra Das, A.; Kumar, M.; Panda, S.; Del Fabbro, M. Autologous Platelet Concentrates in Treatment of Furcation Defects—A Systematic Review and Meta-Analysis. *Int. J. Mol. Sci.* **2019**, *20*.

329. Metlerska, J.; Fagogeni, I.; Nowicka, A. Efficacy of Autologous Platelet Concentrates in Regenerative Endodontic Treatment: A Systematic Review of Human Studies. *J. Endod.* **2019**, *45*, 20-30.e1, doi:https://doi.org/10.1016/j.joen.2018.09.003.

330. Mariani, E.; Pulsatelli, L. Platelet Concentrates in Musculoskeletal Medicine. *Int. J. Mol. Sci.* **2020**, *21*.

331. Fortunato, L.; Bennardo, F.; Buffone, C.; Giudice, A. Is the application of platelet concentrates effective in the prevention and treatment of medication-related osteonecrosis of the jaw? A systematic review. *J. Cranio-Maxillofacial Surg.* **2020**, *48*, 268–285, doi:https://doi.org/10.1016/j.jcms.2020.01.014.

332. Astori, G.; Amati, E.; Bambi, F.; Bernardi, M.; Chieregato, K.; Schäfer, R.; Sella, S.; Rodeghiero, F. Platelet lysate as a substitute for animal serum for the ex-vivo expansion of mesenchymal stem/stromal cells: present and future. *Stem Cell Res. Ther.* **2016**, *7*, 93, doi:10.1186/s13287-016-0352-x.

333. Scherer, S.S.; Tobalem, M.; Vigato, E.; Heit, Y.; Modarressi, A.; Hinz, B.; Pittet, B.; Pietramaggiori, G. Nonactivated versus thrombin-activated platelets on wound healing and fibroblast-to-myofibroblast differentiation in vivo and in vitro. *Plast. Reconstr. Surg.* **2012**, *129*, 46e-54e, doi:10.1097/PRS.0b013e3182362010.

334. Maumus, M.; Peyrafitte, J.A.; D'Angelo, R.; Fournier-Wirth, C.; Bouloumié, A.; Casteilla, L.; Sengenès, C.; Bourin, P. Native human adipose stromal cells: Localization, morphology and phenotype. *Int. J. Obes.* **2011**, *35*, 1141–1153, doi:10.1038/ijo.2010.269.

335. Patrikoski, M.; Juntunen, M.; Boucher, S.; Campbell, A.; Vemuri, M.C.; Mannerström, B.; Miettinen, S. Development of fully defined xeno-free culture system for the preparation and propagation of cell therapy-compliant human adipose stem cells. *Stem Cell Res. Ther.* **2013**, *4*, doi:10.1186/scrt175.

336. Riis, S.; Nielsen, F.M.; Pennisi, C.P.; Zachar, V.; Fink, T. Comparative Analysis of Media and Supplements on Initiation and Expansion of Adipose-Derived Stem Cells. *Stem Cells Transl. Med.* **2016**, *5*, 314–324, doi:10.5966/sctm.2015-0148.

337. Tobita, M.; Tajima, S.; Mizuno, H. Adipose tissue-derived mesenchymal stem cells and platelet-rich plasma: stem cell transplantation methods that enhance stemness. *Stem Cell Res. Ther.* **2015**, *6*, 215, doi:10.1186/s13287-015-0217-8.

338. Liao, H.T.; James, I.B.; Marra, K.G.; Rubin, J.P. The Effects of Platelet-Rich Plasma on Cell Proliferation and Adipogenic Potential of Adipose-Derived Stem Cells. *Tissue Eng. Part A* **2015**, *21*, 2714–2722, doi:10.1089/ten.tea.2015.0159.

339. Haubner, F.; Muschter, D.; Schuster, N.; Pohl, F.; Ahrens, N.; Prantl, L.; Gassner, H.G. Platelet-rich plasma stimulates dermal microvascular endothelial cells and adipose derived stem cells after external radiation. *Clin. Hemorheol. Microcirc.* **2015**, *61*, 279–290, doi:10.3233/CH-151982.

340. Januszyk, M.; Rennert, R.C.; Sorkin, M.; Maan, Z.N.; Wong, L.K.; Whittam, A.J.; Whitmore, A.; Duscher, D.; Gurtner, G.C. Evaluating the Effect of Cell Culture on Gene Expression in Primary Tissue Samples Using Microfluidic-Based Single Cell Transcriptional Analysis. **2015**, 540–550, doi:10.3390/microarrays4040540.

341. Woodford-Thomas, T.; Thomas, M.L. The leukocyte common antigen, CD45 and other protein tyrosine phosphatases in hematopoietic cells. *Semin. Cell Biol.* **1993**, *4*, 409–418, doi:https://doi.org/10.1006/scel.1993.1049.

342. Park, T.I.-H.; Feisst, V.; Brooks, A.E.S.; Rustenhoven, J.; Monzo, H.J.; Feng, S.X.; Mee, E.W.; Bergin, P.S.; Oldfield, R.; Graham, E.S.; et al. Cultured pericytes from human brain show phenotypic and functional differences associated with differential CD90 expression. *Sci. Rep.* **2016**, *6*, 26587,

doi:10.1038/srep26587.

343. Guo, J.; Nguyen, A.; Banyard, D.A.; Fadavi, D.; Toranto, J.D.; Wirth, G.A.; Paydar, K.Z.; Evans, G.R.D.; Widgerow, A.D. Stromal vascular fraction: A regenerative reality? Part 2: Mechanisms of regenerative action. *J. Plast. Reconstr. Aesthetic Surg.* **2016**, *69*, 180–188, doi:https://doi.org/10.1016/j.bjps.2015.10.014.

344. Pierantozzi, E.; Badin, M.; Vezzani, B.; Curina, C.; Randazzo, D.; Petraglia, F.; Rossi, D.; Sorrentino, V. Human pericytes isolated from adipose tissue have better differentiation abilities than their mesenchymal stem cell counterparts. *Cell Tissue Res.* **2015**, *361*, 769–778, doi:10.1007/s00441-015-2166-z.

345. Dubey, N.K.; Mishra, V.K.; Dubey, R.; Tsai, F.; Deng, W. Revisiting the Advances in Isolation , Characterization and Secretome of Adipose-Derived Stromal / Stem Cells. *Int. J. Mol. Sci.* **2018**, *19*, 1–23, doi:10.3390/ijms19082200.

346. Bora, P.; Majumdar, A.S. Adipose tissue-derived stromal vascular fraction in regenerative medicine: a brief review on biology and translation. *Stem Cell Res. Ther.* **2017**, *8*, 145, doi:10.1186/s13287-017-0598-y.

347. Skubis, A.; Gola, J.; Sikora, B.; Hybiak, J.; Paul-Samojedny, M.; Mazurek, U.; Łos, M.J. Impact of Antibiotics on the Proliferation and Differentiation of Human Adipose-Derived Mesenchymal Stem Cells. *Int. J. Mol. Sci.* **2017**, *18*, 2522, doi:10.3390/ijms18122522.

348. Gupta, P.; Hall, G.N.; Geris, L.; Luyten, F.P.; Papantoniou, I. Human Platelet Lysate Improves Bone Forming Potential of Human Progenitor Cells Expanded in Microcarrier-Based Dynamic Culture. *Stem Cells Transl. Med.* **2019**, *8*, 810–821, doi:10.1002/sctm.18-0216.

349. Shanbhag, S.; Suliman, S.; Mohamed-Ahmed, S.; Kampleitner, C.; Hassan, M.N.; Heimel, P.; Dobsak, T.; Tangl, S.; Bolstad, A.I.; Mustafa, K. Bone regeneration in rat calvarial defects using dissociated or spheroid mesenchymal stromal cells in scaffold-hydrogel constructs. *Stem Cell Res. Ther.* **2021**, *12*, 575, doi:10.1186/s13287-021-02642-w.

350. Qiu, G.; Wu, H.; Huang, M.; Ma, T.; Schneider, A.; Oates, T.W.; Weir, M.D.; Xu, H.H.K.; Zhao, L. Novel calcium phosphate cement with biofilm-inhibition and platelet lysate delivery to enhance osteogenesis of encapsulated human periodontal ligament stem cells. *Mater. Sci. Eng. C* **2021**, *128*, 112306, doi:https://doi.org/10.1016/j.msec.2021.112306.

351. Chignon-Sicard, B.; Kouidhi, M.; Yao, X.; Delerue-Audegond, A.; Villageois, P.; Peraldi, P.; Ferrari, P.; Rival, Y.; Piwnica, D.; Aubert, J.; et al. Platelet-rich plasma respectively reduces and promotes adipogenic and myofibroblastic differentiation of human adipose-derived stromal cells via the TGFβ signalling pathway. *Sci. Rep.* **2017**, *7*, 2954, doi:10.1038/s41598-017-03113-0.

352. Fink, T.; Zachar, V. Adipogenic differentiation of human mesenchymal stem cells. *Methods Mol. Biol.* **2011**, *698*, 243–251, doi:10.1007/978-1-60761-999-4_19.

353. Langenbach, F.; Handschel, J. Effects of dexamethasone, ascorbic acid and β-glycerophosphate on the osteogenic differentiation of stem cells in vitro. *Stem Cell Res. Ther.* **2013**, *4*, 117, doi:10.1186/scrt328.

354. Bustin, S.A.; Benes, V.; Garson, J.A.; Hellemans, J.; Huggett, J.; Kubista, M.; Mueller, R.; Nolan, T.; Pfaffl, M.W.; Shipley, G.L.; et al. The MIQE Guidelines: Minimum Information for Publication of Quantitative Real-Time PCR Experiments. *Clin. Chem.* **2009**, *55*, 611–622, doi:10.1373/clinchem.2008.112797.

Appendix A: Consent Forms

PATIENT INFORMATION LEAFLET AND INFORMED CONSENT FORM
(Each patient must receive, read and understand this document before the start of the study)

STUDY TITLE
The isolation, characterisation and differentiation of mesenchymal stem cells from adipose tissue.

Mesenchymal stromal/stem cells isolated from voluntarily donated adipose (fat) tissue will be used in various studies. The current studies are listed below. The isolated cells may also be used in future studies. Permission to use the cells in future experiments/studies will be obtained from the Ethics Committee at the Faculty of Health Sciences, University of Pretoria before the cells are used.

1. Do adipose-derived stromal cells possess endocytic function?

2. The role of Pref-1 in *in vitro* adipogenic differentiation of mesenchymal stromal/stem cells (MSCs)

3. Characterization of adipose-derived stromal cell heterogeneity

4. Comparison of the effect of human platelet lysate and foetal bovine serum on adipose-derived stem cell characteristics in culture

5. Is HIV-1 able to infect mesenchymal stromal/ stem cells (MSC)?

6. Effects of reactive oxygen species on adipogenesis.

7. Human alternatives to foetal bovine serum for the expansion of human adipose-derived stem cells

8. In vitro adipose derived stromal cell myogenic differentiation

9. Development of a high throughput screening assay to evaluate compound libraries for the modulation of adipogenesis

10. The role of Solute Carrier Family 7 Member 8 in adipogenesis in vitro and murine model of obesity

11. In vitro osteogenic differentiation of mesenchymal stem cells

12. Immunomodulatory properties of adipocyte derived stromal/stem cells cultured in human platelet lysate

Dear Patient/Participant: _____

INTRODUCTION

You are invited to participate in a research study that is being carried out by the Department of Immunology at the University of Pretoria. This information leaflet is to help you to decide if you would like to participate. Before you agree to take part in this study you should fully understand what is involved. If you have any questions, which are not fully explained in this leaflet, do not hesitate to ask the investigator. You should not agree to take part unless you are completely happy about all the procedures involved. Your personal health will not be compromised by the procedures. These procedures have already been discussed with your doctor beforehand.

THE PURPOSE OF THE STUDY

Researchers at the University of Pretoria would like to investigate the healing properties of adult stem cells for possible future application in regenerative medicine. Regenerative medicine refers to experimental (current status) medicine where researchers try to replace, improve or restore the function of cells that do not function optimally in the body. Adult stem cells are present in various tissues in the body, including fat (adipose) tissue. These adult stem cells could potentially be used to cure patients with various kinds of injuries or diseases. In order to use these cells to cure humans in the future, researchers must first study their characteristics, behaviour, growth and interactions with other cells and/or organisms in the body. This is done by isolating these cells from the fat (adipose) tissue and perform experiments in the laboratory (tissue culture) and/or using experimental animal models.

These adult stem cells can also be used to investigate the process of fat formation. Scientists are able to mimic the formation of fat cells using adult stem cells isolated from fat (adipose) tissue. Obesity is becoming an increasing problem worldwide and in order to find solutions to combat obesity it is important to understand the biological processes involved in the formation of fat. It is also important to understand the interactions of infectious organisms, like HIV and *Mycobacterium tuberculosis* (organism that cause tuberculosis in humans), with stem cells in order to provide safe treatment options in the future. It is therefore important that researchers also investigate the interactions between these infectious organisms and stem cells by performing experiments in the laboratory as well as using experimental animal models. Investigations will be performed on cellular (intact cells) and molecular (investigating the effect on various treatments/exposures to the genetic footprint of cells) levels. For molecular studies we will need to isolate genetic material (DNA and RNA) from your cells.

Many of the experiments that researchers perform require the isolation of genetic material, also known as DNA and RNA, from cells. Genetic material contains information about the cell that only can be revealed if researchers perform specialized tests on the genetic material. These tests are often needed in order to completely understand the characteristics of cells. Genetic information also allows researchers to look into what effect infectious agents, such as *Mycobacterium tuberculosis* (cause tuberculosis in humans) and HIV, might have on these cells. In addition, molecular biology tests (tests that make use of DNA or RNA) are often the most sensitive tests available to detect if cells are infected with bacteria (such as *Mycobacterium tuberculosis)* and/or viruses (such as HIV).

Isolation, Characterisation and Differentiation of MSCs from **adipose tissue**

No unethical procedures will be used when collecting the samples and performing the experiments.

ADIPOSE TISSUE COLLECTION

During various normal plastic surgery operations, adipose tissue (fat) will be excised (cut out) or aspirated (sucked out), and discarded. This adipose tissue, does not serve a purpose to the patient's body anymore, but could serve as a valuable source of stem cells for researchers in the field of regenerative medicine. No additional fat will be collected for the study. Only the fat that the doctor planned to aspirate/cut away during the procedures discussed with you during the consultation visits will be collected.

There will be no added risks or discomfort with the collection of the adipose tissue other than normally associated with the specific procedure the patient will experience during normal operative procedures.

CONFIDENTIALITY

Each participant's sample will be assigned a specific code and this code will be used from there on in all research studies. Certain information, including race, ethnicity, gender and medical history, may be important for scientific reasons. This information will be linked to the sample code and not to your identity. Research reports and articles in scientific journals will not include any information that may identify you.

In some isolated cases it might however be important for the doctors or researchers involved in the study to convey medical information to medical personnel or appropriate Research Ethics committees. In such a case, you by signing this document, give permission to the investigator to release your medical records to regulatory health authorities or an appropriate Research Ethics committee. If necessary, these medical professionals will discuss the results with your doctor and everyone will act in your best interest.

ETHICAL APPROVAL

The protocol involved for this study was submitted to the Research Ethics Committee. This study has received written approval from the Research Ethics Committee of the Faculty of Health Sciences at the University of Pretoria. The study is structured in accordance with the Declaration of Helsinki, which deals with the recommendations of guiding doctors in biomedical research involving humans.

You are also welcome to contact the Faculty of Health Sciences Ethics Committee at the University of Pretoria if you have any concerns or questions. Their contact details are:

The Research Ethics Office:
Tel: 012 - 354 1330 or 012 - 354 1677
Fax: 012 - 354 1367

RIGHTS OF THE PARTICIPANT

Your participation in this study is entirely voluntary and you can refuse to participate or withdraw consent at any time without stating any reason. Your withdrawal will not affect your access to medical care or the quality of medical care that you will receive. Your participation or withdrawal from the study would not affect you in any way.

FINANCIAL GAIN OR LOSS

There will be no financial gain or loss to you, should you participate or withdraw from the study. This research could potentially lead to future profitable treatments. However, you will not have access to these profits. There will be no additional financial costs for you to participate in the study.

> **The participant has no legal remedy and will not share in any financial gain that may be derived from the study**

INFORMATION AND CONTACT PERSON

If at any time you would like to find out more information or have any questions regarding the study, please do not hesitate to contact the researchers.
Dr. C. Durandt: 012 -319 2101
Prof. M.S. Pepper: 012 420 3845 or 012 420 5317

PERSONAL/MEDICAL INFORMATION

The information below may be important for scientific reasons. This information will be linked to the sample code and not to your identity.

Gender: _____

Ethnicity: _____

Date of Birth: _____

Weight: _____

Height: _____

Waste Circumference: _____

Do you smoke? YES ☐ NO ☐

Are you suffering from:

Diabetes YES ☐ NO ☐

Cardiovascular disease YES ☐ NO ☐

Hypertension YES ☐ NO ☐

Isolation, Characterisation and Differentiation of MSCs from **adipose tissue**

INFORMED CONSENT

WHAT IS EXPECTED?

I confirm that the person asking my consent to take part in this study has told me about the nature, process, risks, discomforts and benefits of the study. I have also received, read and understood the above written information regarding the study. I am aware that the results of the study, including personal details, will be anonymously processed into research reports. I am participating willingly. I have had time to ask questions and have no objection to participate in the study. I understand that there is no penalty should I wish to discontinue with the study and my withdrawal will not affect my access to medical care or the quality of medical care I will receive.

I also understand that certain laboratory tests may require the isolation of genetic material, also known as DNA and RNA and give herewith permission that the researchers may extract RNA/DNA from cells isolated from the adipose tissue.

YES	NO

I hereby give the researchers permission to perform routine HIV, hepatitis B and hepatitis C tests on the adipose tissue donated. Testing for these infectious agents is important for our work as we only like to work with tissue that is negative for these infections. If the researchers detect HIV or hepatitis B or C in the sample, the codified sample details will be sent to _____, who will notify you. If you do not wish us to test your tissue for HIV or hepatitis B or hepatitis C, or if you do not wish to know the results of these tests, we will not be able to include you in the study. In the case on an HIV positive result, you will be counselled and treated by qualified medical personnel.

YES	NO

I have received a copy of this informed consent agreement.

Participant full names (print):_____

Participant signature: _____ Date: _____

Investigator full names (print):_____

Investigator signature:_____ Date:_____

Witness full names (print):_____

Witness signature:_____ Date:_____

Witness full names (print):_____

Witness signature:_____ Date:_____

Isolation, Characterisation and Differentiation of MSCs from **adipose tissue**

Informed Consent Form - Updated 12 July 2017   Page **6** of **6**

Appendix B: Compensation experiment (FBS)

It is important to set up compensation experiments before doing a multi-colour immunophenotyping panel as fluorochromes have a wide fluorescence emission spectrum and the emitted fluorescence may spill-over in more than one channel which may lead to false positive results. In a compensation experiment, single fluorochrome tubes are run and the level of spectral spill over is measured. This spectral spill over is then removed from the respective channel. A colour compensation matrix is then calculated by the software to determine how much spill over should be removed from each channel.

Unstained Cells
First control for autofluorescence
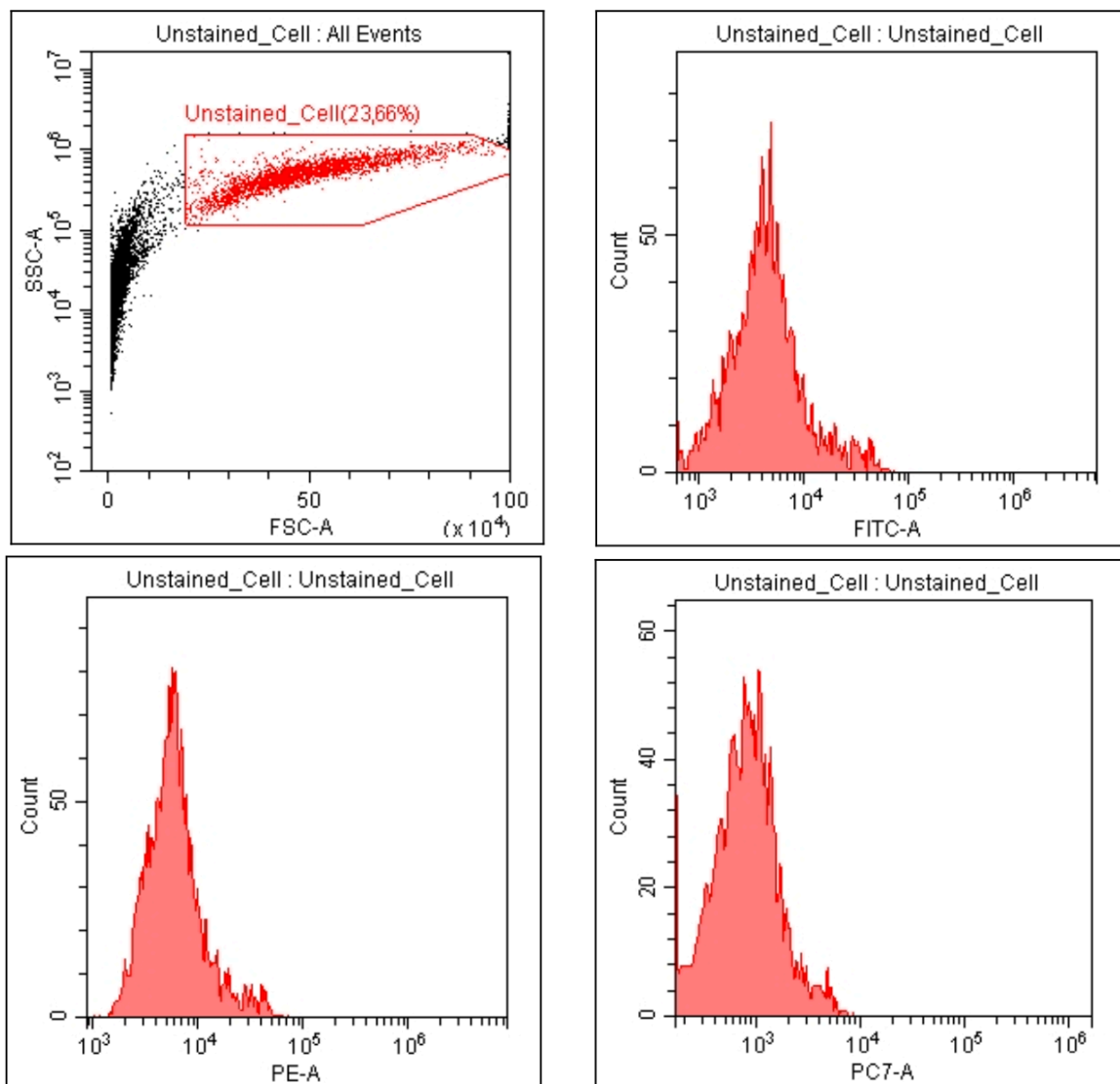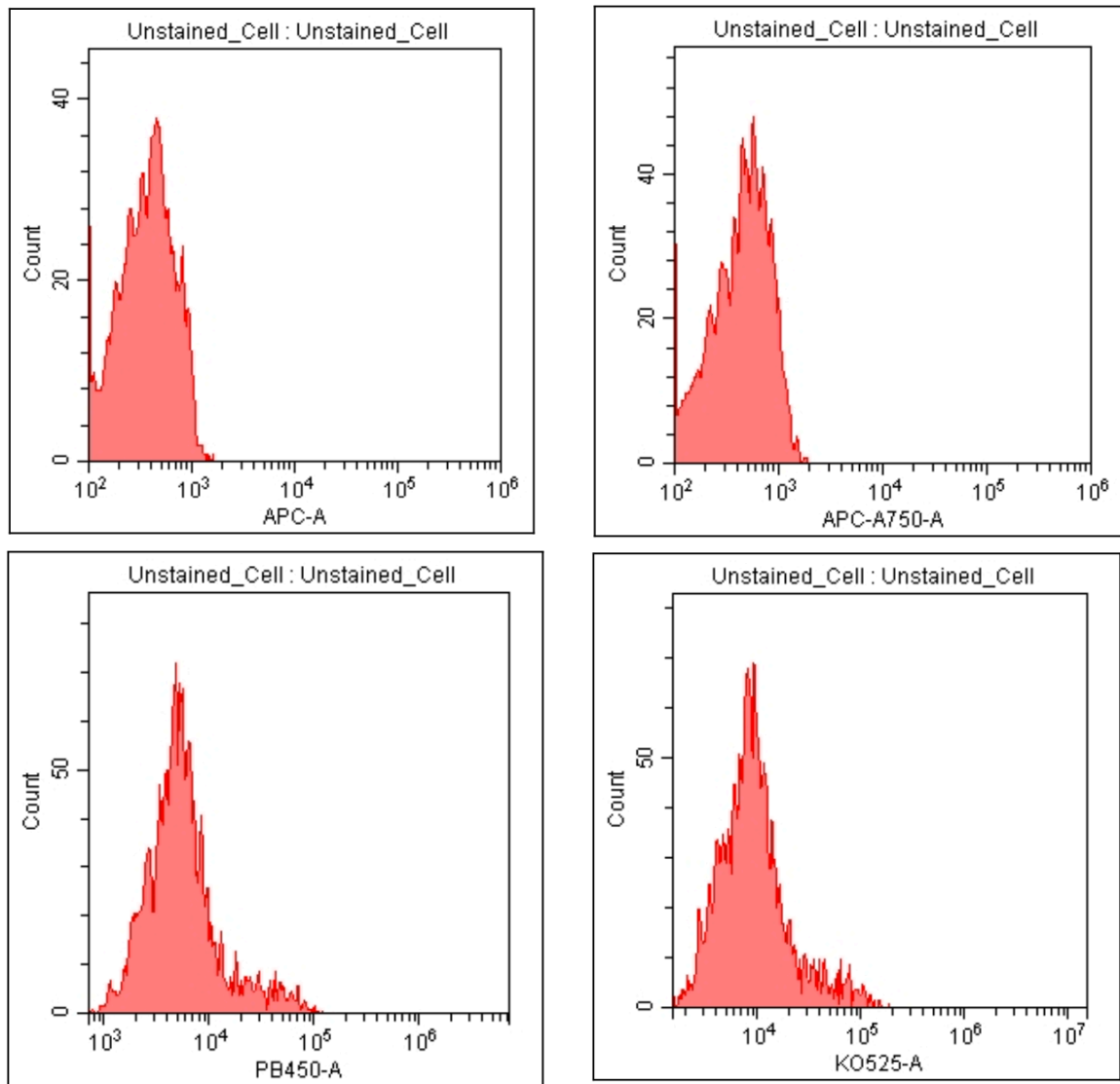
Figure B1. Colour compensation experiment set up to detect and correct for autofluorescence of cells.

Unstained Beads
Second control for autofluorescence
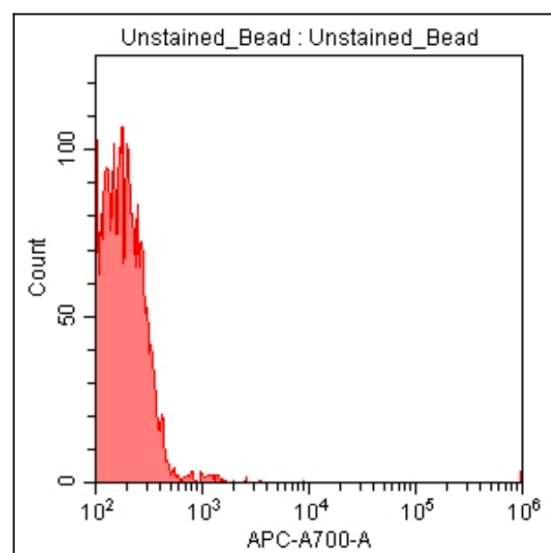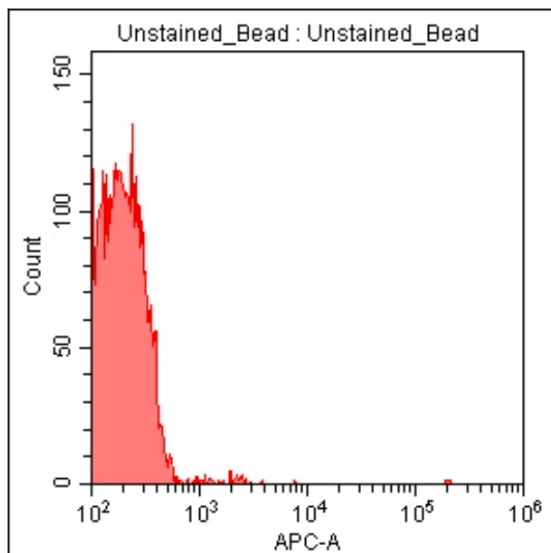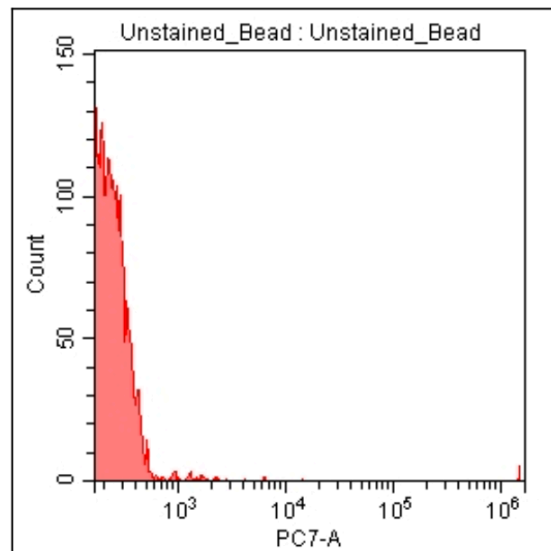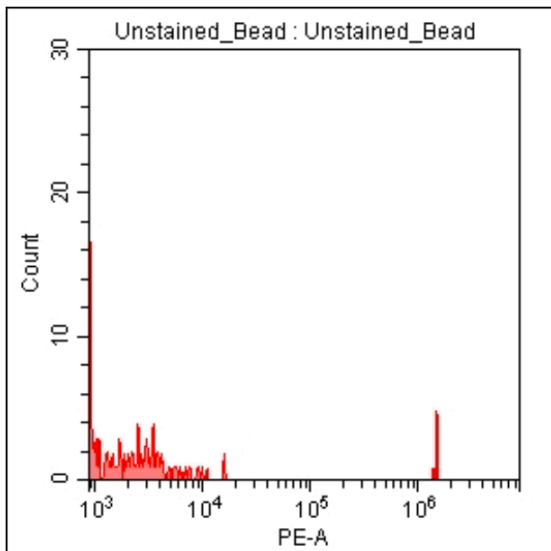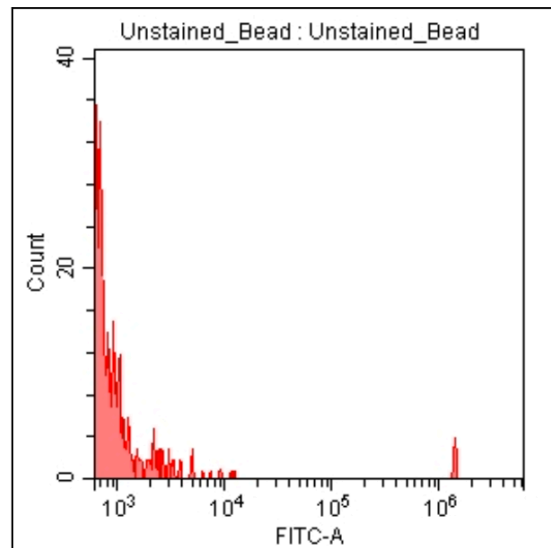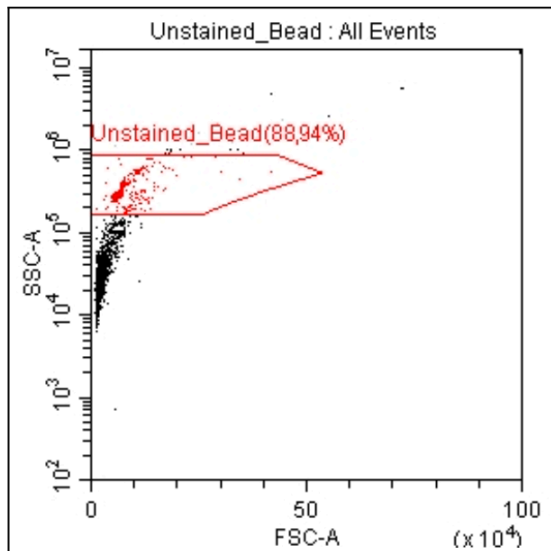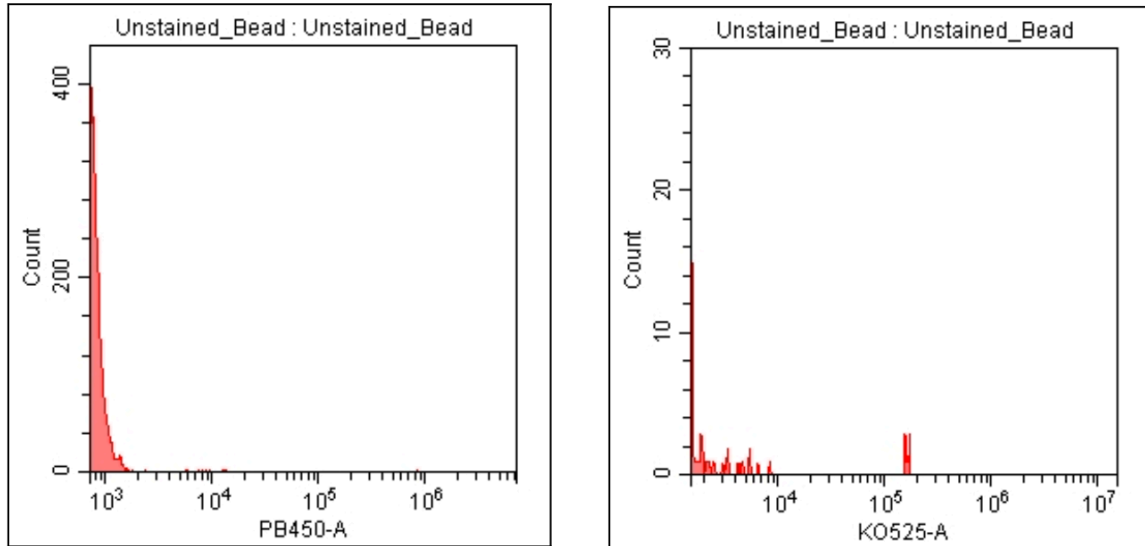
Figure B2. Colour compensation experiment set up to detect and correct for autofluorescence of beads.

FITC (FL1) channel:
To determine the spillover of FITC (conjugate) into the other fluorescence channels
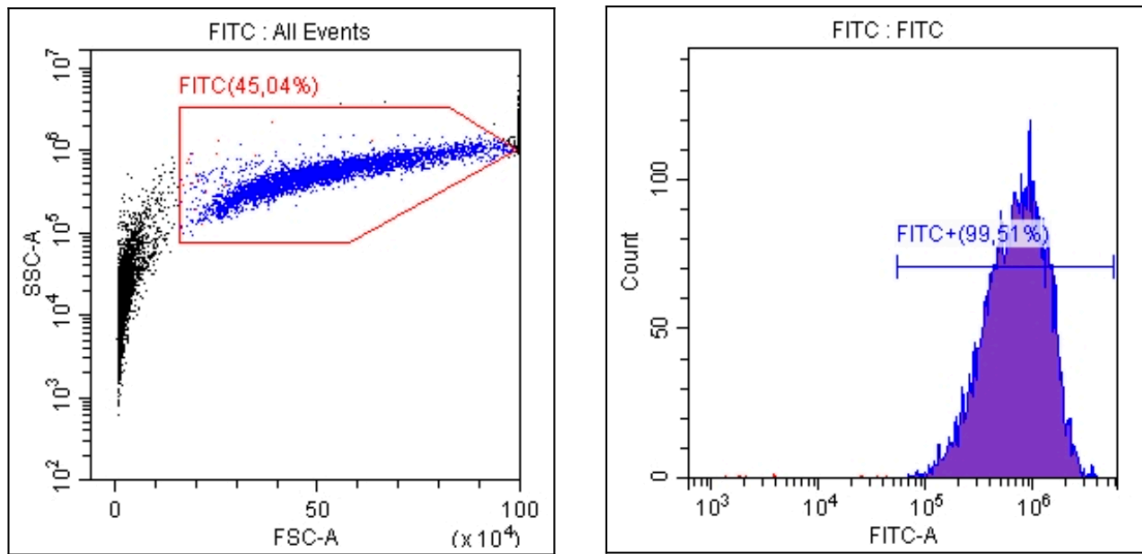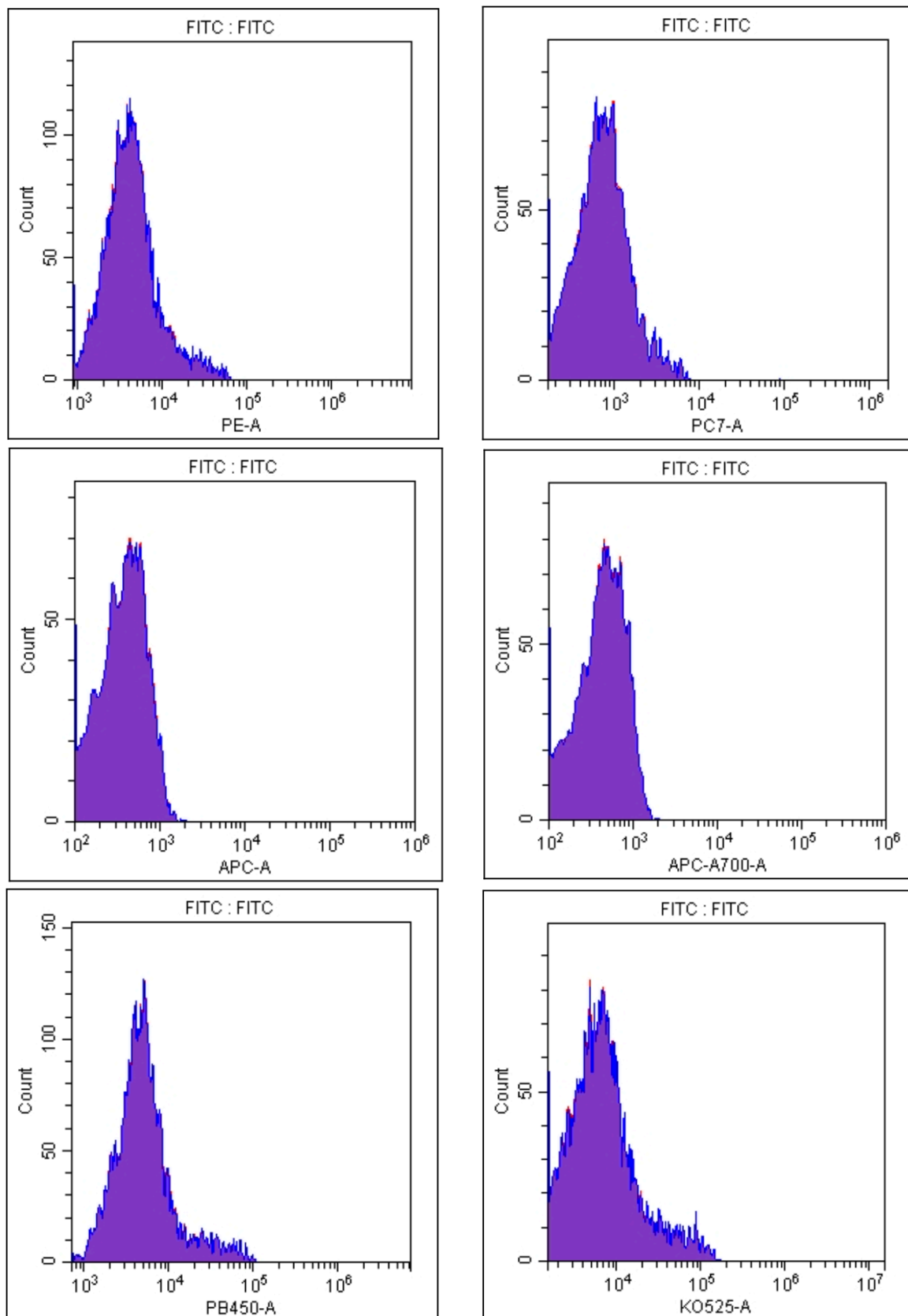
Figure B3. Colour compensation experiment set up to detect and correct for spill over of FITC into other channels.

PE (FL2 channel)
To determine the spillover of PE (conjugate) into the other fluorescence channels
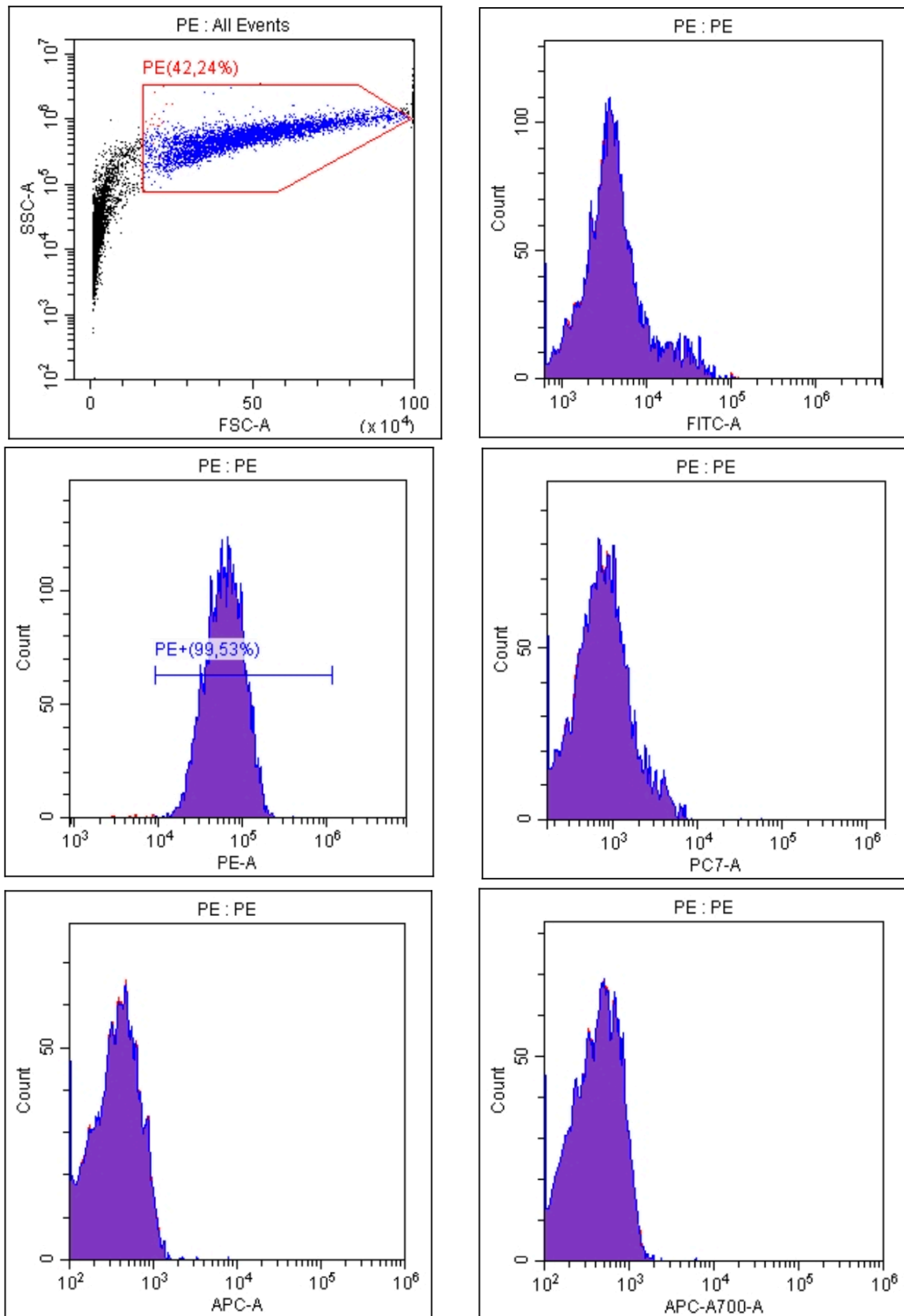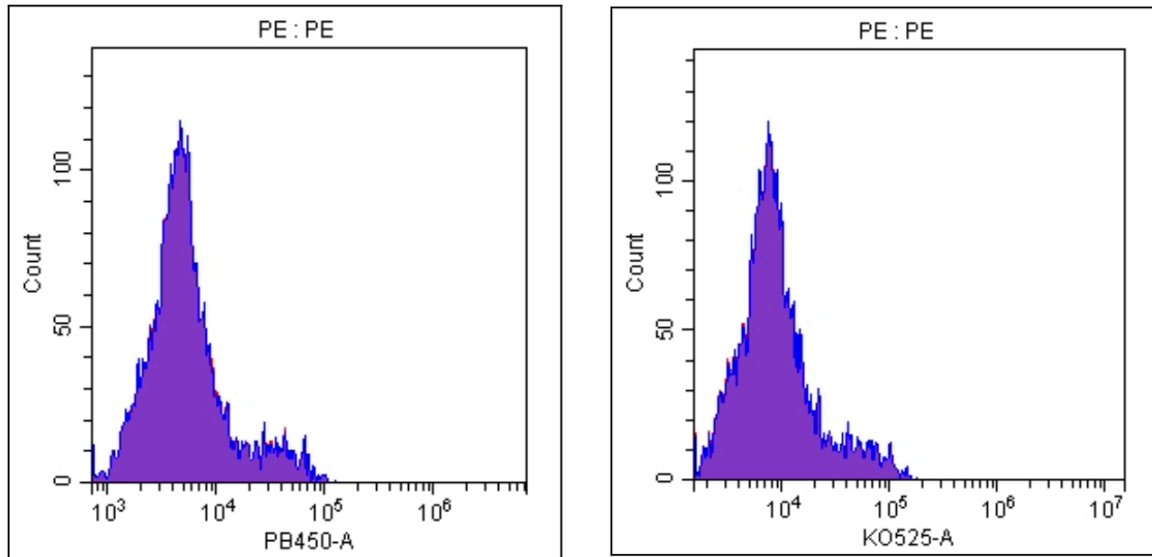
Figure B4. Colour compensation experiment set up to detect and correct for spill over of PE into other channels.

PC7 (FL3 channel)

To determine the spillover of PC7 (conjugate) into the other fluorescence channels
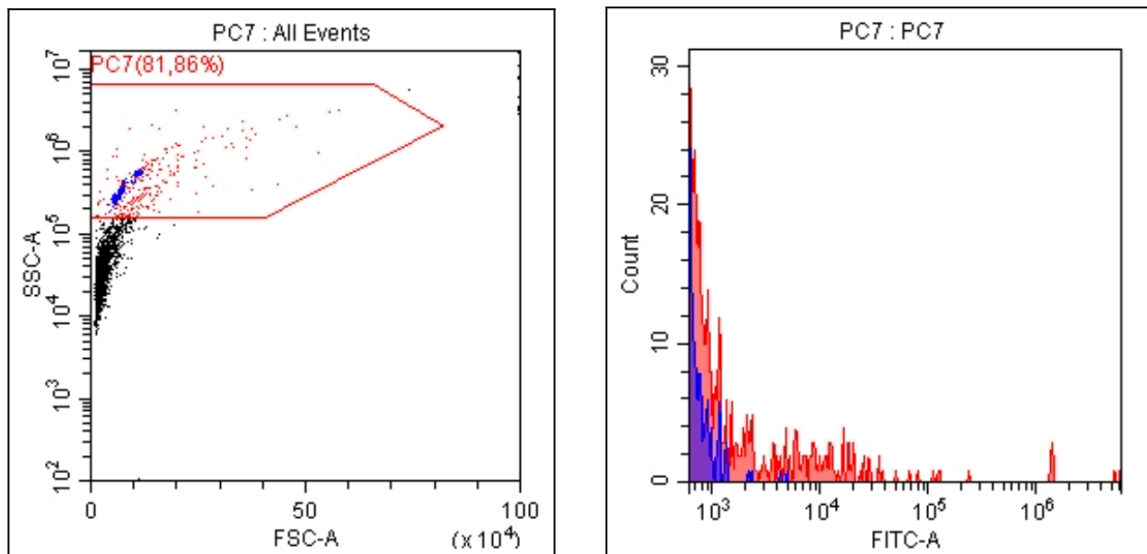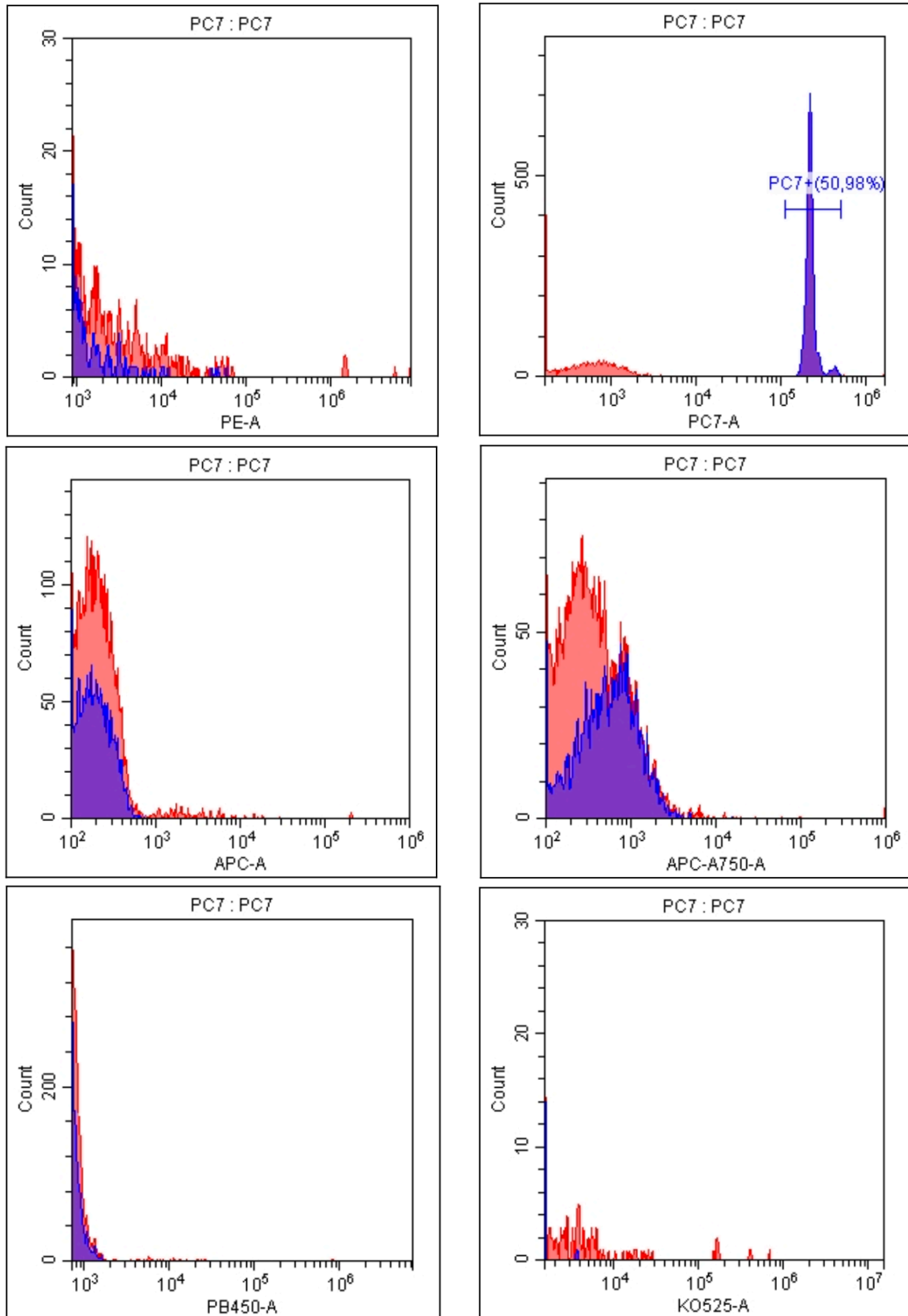
Figure B5. Colour compensation experiment set up to detect and correct for spill over of PC7 into other channels.

APC (FL6 channel)

To determine the spillover of APC (conjugate) into the other fluorescence channels
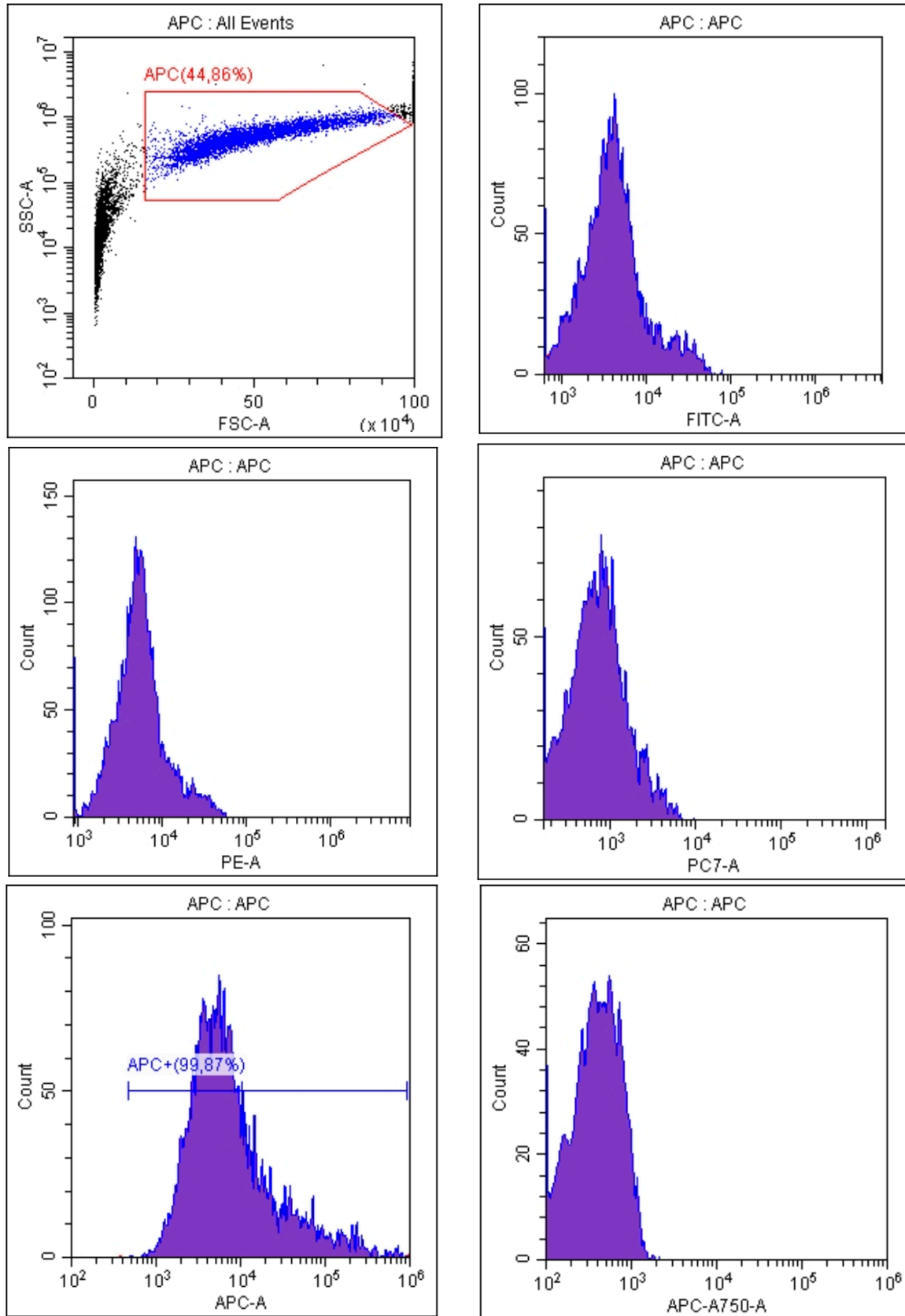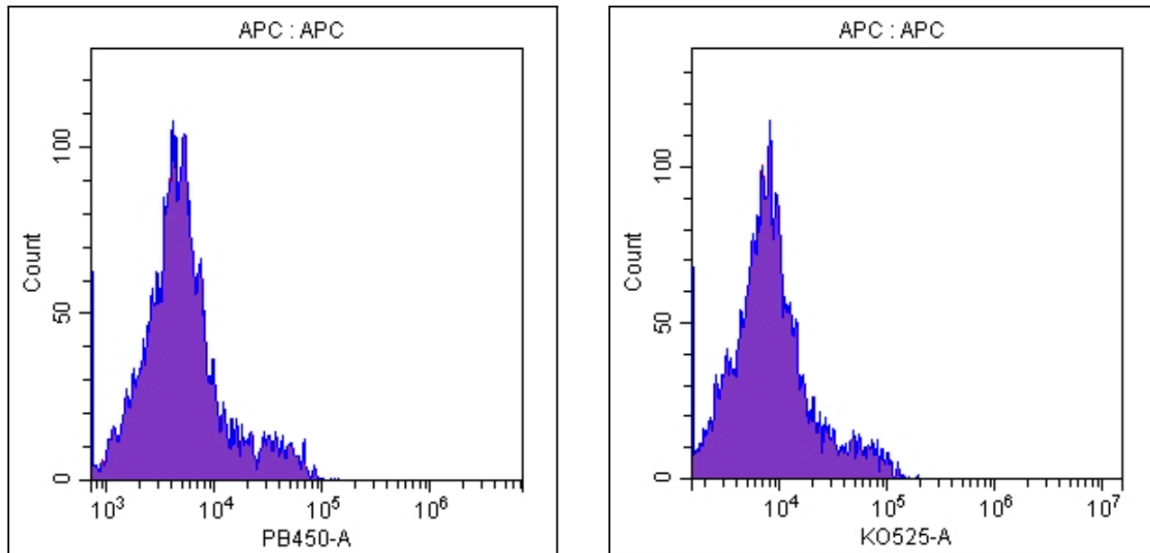
Figure B6. Colour compensation experiment set up to detect and correct for spill over of APC into other channels.

APC-A750 (FL8 channel)

To determine the spillover of APC-A750 (conjugate) into the other fluorescence channels
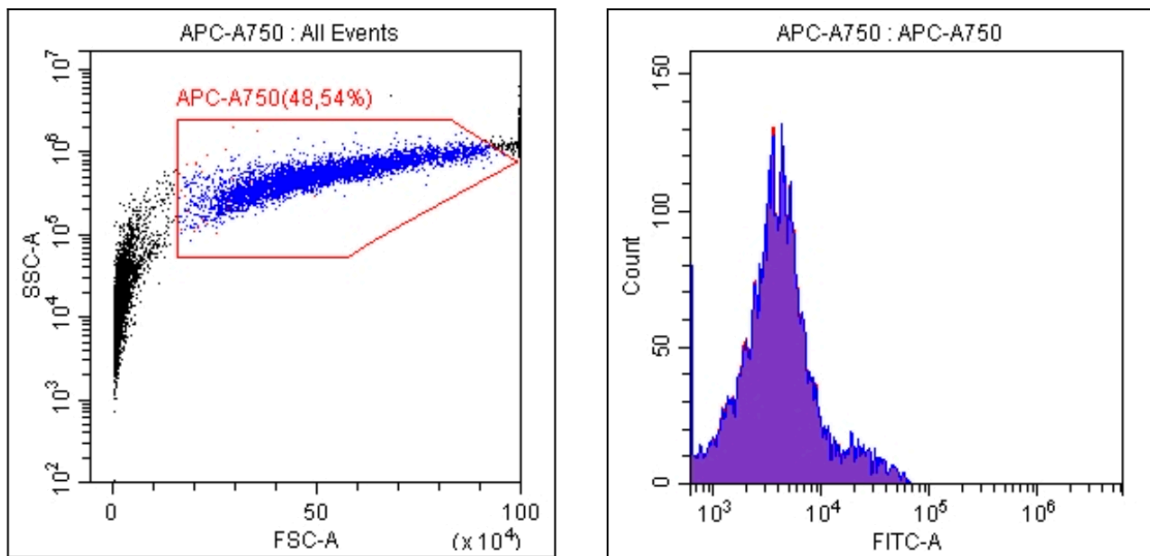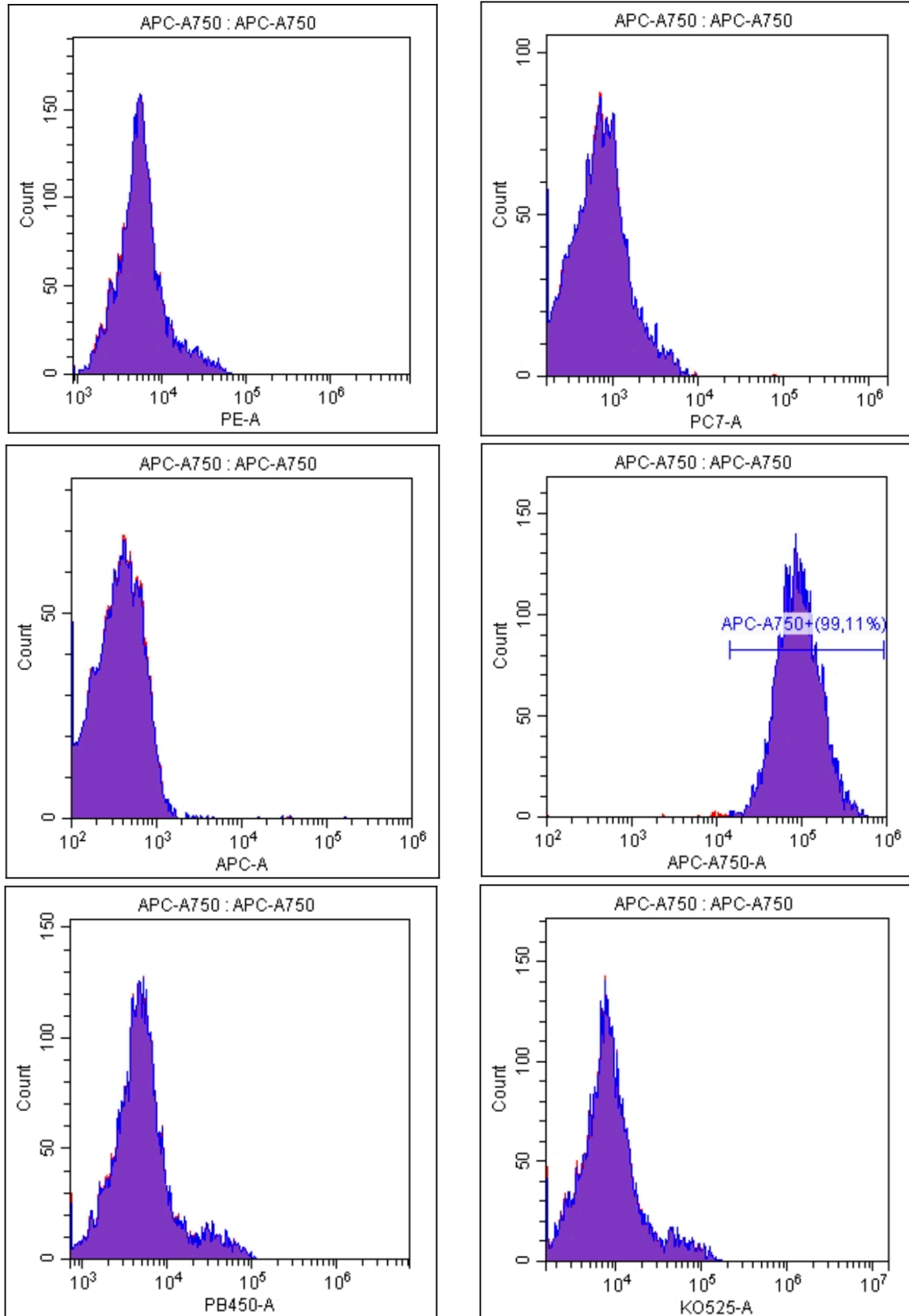
Figure B7. Colour compensation experiment set up to detect and correct for spill over of APC-A750 into other channels.

PB450 (FL9 channel)
To determine the spillover of PB450 (conjugate) into the other fluorescence channels
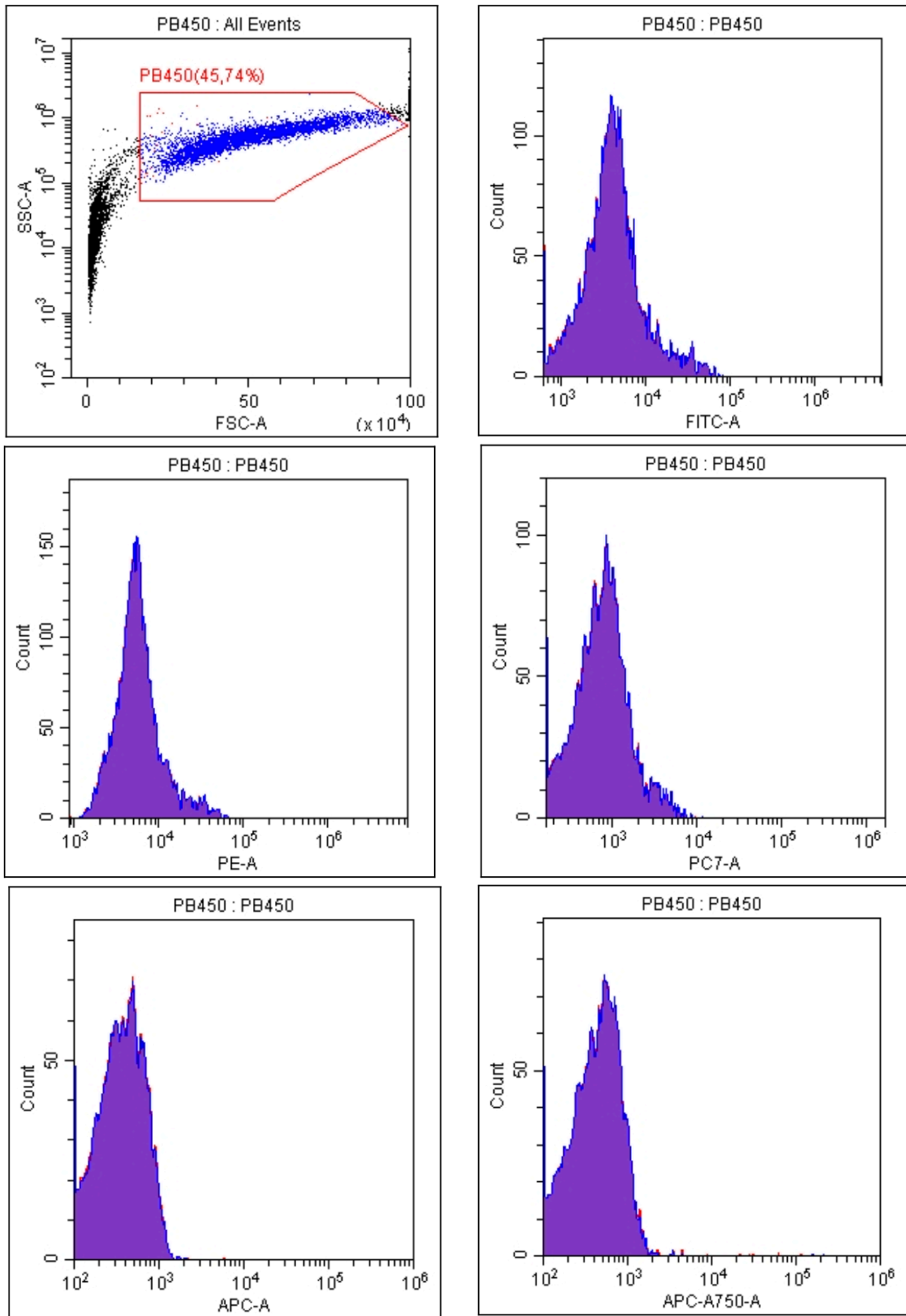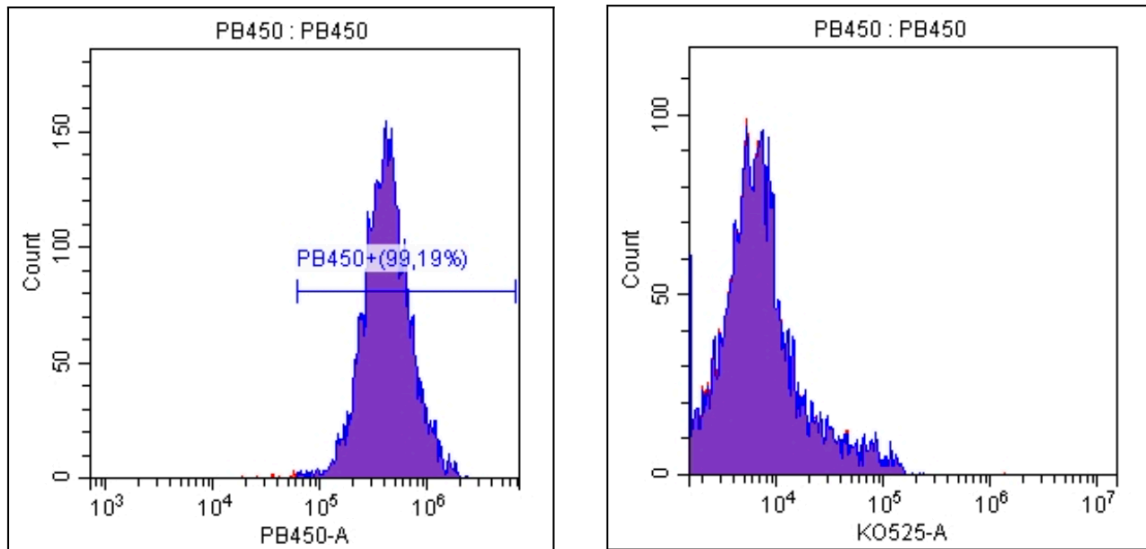
Figure B8. Colour compensation experiment set up to detect and correct for spill over of PB into other channels.

KO (FL10 channel)
To determine the spillover of KO (conjugate) into the other fluorescence channels
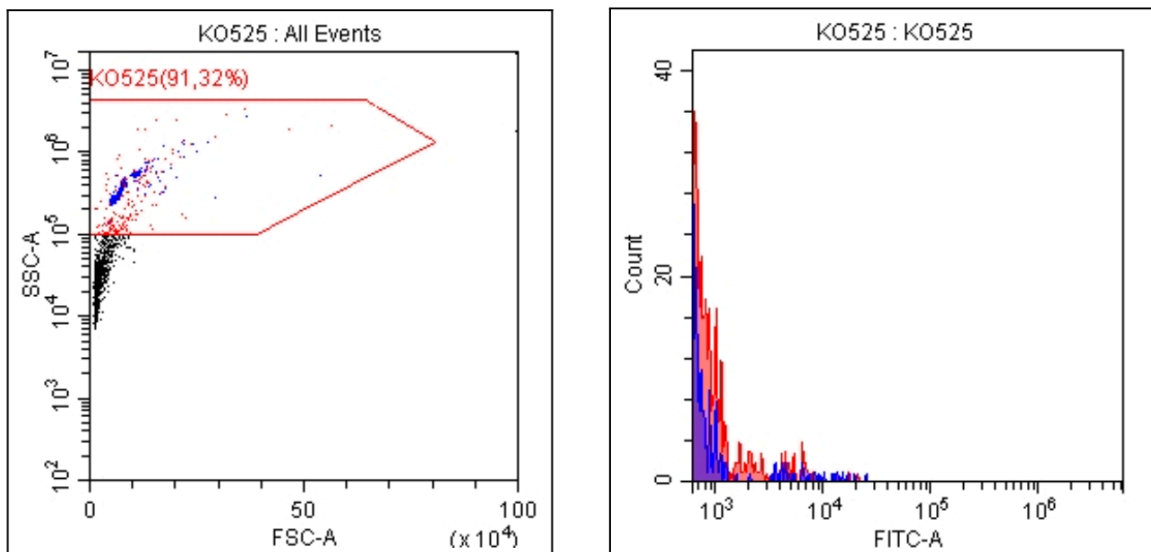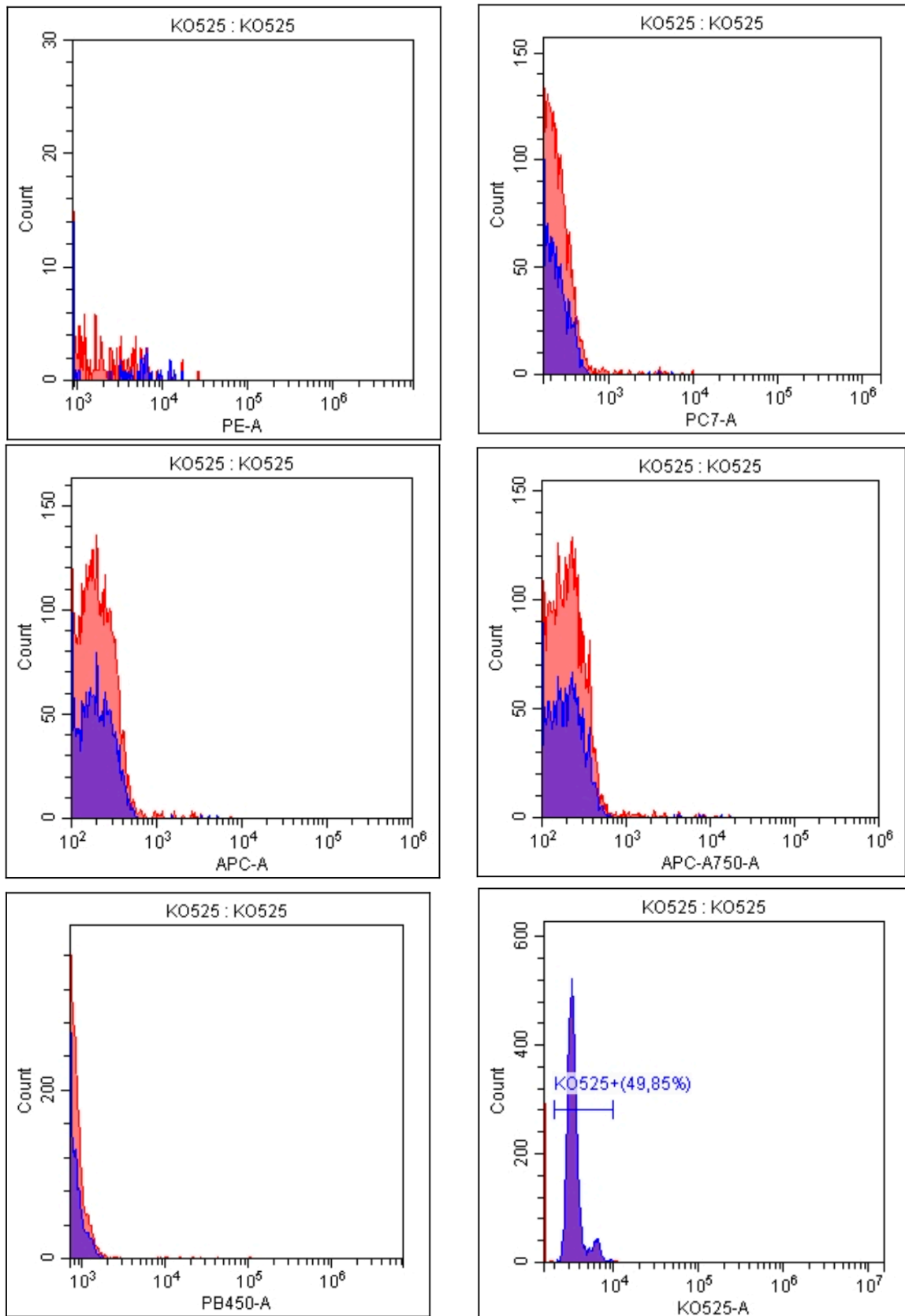
Figure B9. Colour compensation experiment set up to detect and correct for spill over of KO into other channels.

Appendix C: Osteogenic Media Calculations and Assay

Calculations

Preparation of Osteogenic Differentiation Medium 1

Recipe table

Chemical	Molar mass	Required concentration	Stock solution
Ascorbate-2-phosphate	322.05 g/mol	155.26 μM	Powder
B-glycerophosphate	306.11 g/mol	10 mM	Powder
Dexamethasone	392.46 g/mol	10 nM	1 mM

Calculations

Ascorbate-2-phosphate
Need: 50mg/L = 0.05g/L
Moles per litre = concentration (grams per litre) ÷ molecular weight (grams per mole)
M = 0.05g/L ÷ 322.05g/mol = 0.00015526 mol/L = **155.26 μM**

m = CMV
  = 155.26 μM x 322.05g/mol x 0.25
  = 0.01250037 g

B-glycerophosphate
m = CMV
m = 0.01 M x 306.11 g/mol x **0.25L**
m = 0.765275 g

Dexamethasone
Make a **stock solution**: 0.001M/ 1mM
m=CMV
m= 0.001 M x 392.46 g/mol x 0.01 L (10ml)
m= 0.0039246 g
m=3.9246 mg
Dissolve in 100% ethanol
What to add to differentiation medium:

$C_1V_1 = C_2V_2$ $C_1V_1 = C_2V_2$
0.001M x V_1 = 1 x 10^{-8} M x **250** ml   0.001M x V_1 = 1 x 10^{-8} M x **500** ml
V_1 = 0.0025 ml V_1 = 5 ul
V_1= 2.5 ul

Preparation of Osteogenic Differentiation Medium 2

Recipe table

Chemical	Molar mass	Required concentration	Stock solution
Ascorbate-2-phosphate	322.05 g/mol	0.06 mM	Powder
B-glycerophosphate	306.11 g/mol	10 mM	Powder
Dexamethasone	392.46 g/mol	0.1 µM	1 mM

Calculations

Ascorbate-2-phosphate
m = CMV
m = 0.00006 M x 322.05 g/mol x 0.25 L
m = 0.00483075 g
m = 4.83 mg

B-glycerophosphate
m = CMV
m = 0.01 M x 306.11 g/mol x **0.25L**
m = 0.765275 g

Dexamethasone
Make a **stock solution**: 0.001M/ 1mM
m=CMV
m= 0.001 M x 392.46 g/mol x 0.01 L (10ml)
m= 0.0039246 g
m=3.9246 mg
Dissolve in 100% ethanol

What to add to differentiation medium:

$C_1V_1 = C_2V_2$

$0.001M \times V_1 = 1 \times 10^{-7} M \times \textbf{250}$ ml

$V_1 = 0.025$ ml

$V_1 = 25$ ul

$C_1V_1 = C_2V_2$

$0.001M \times V_1 = 1 \times 10^{-7} M \times \textbf{500}$ ml

$V_1 = 50$ ul

Preparation of Osteogenic Differentiation Medium 3

Recipe table

Chemical	Molar mass	Required concentration	Stock solution
Ascorbate-2-phosphate	322.05 g/mol	0.2 mM	Powder
B-glycerophosphate	306.11 g/mol	10 mM	Powder
Dexamethasone	392.46 g/mol	50 nM	1mM

Calculations

Ascorbate-2-phosphate

m = CMV

m = 0.0002 M x 322.05 g/mol x 0.25 L

m = 0.0161025 g

m = 16.1025 mg

B-glycerophosphate

m = CMV

m = 0.01 M x 306.11 g/mol x **0.25L**

m = 0.765275 g

Dexamethasone

Make a **stock solution**: 0.001M/ 1mM

m=CMV

m= 0.001 M x 392.46 g/mol x 0.01 L

m= 0.0039246 g

m=3.9246 mg

Dissolve in 100% ethanol

What to add to differentiation medium:

$C_1V_1 = C_2V_2$

$0.001M \times V_1 = 5 \times 10^{-8} M \times \textbf{250}$ ml

$V_1 = 0.0125$ ml

$V_1 = 12.5$ ul

$C_1V_1 = C_2V_2$

$0.001M \times V_1 = 5 \times 10^{-8}$ M $\times$ **500** ml

$V_1 = 25$ ul

ALP Buffer

10x Stock Solutions

4 nitrophenylphosphate (50 mM)

m = CMV

    = 0.05 M $\times$ 219.09 g/M $\times$ 50 ml

    =0.547725 g

MgCl hexahydrate (5mM)

m = CMV

    =0.005 M $\times$ 203.31 g/M $\times$ 50 ml

    =0.051 g

Triton X-100

No stock solution

Tris-HCL (500mM)

m = CMV

    = 0.5 M $\times$ 157.60 g/M $\times$ 50 ml

    = 3.94 g

For Experiment

For 36ml:

4 nitrophenyl phosphate (5 mM)	Triton X-100 (0.1%)
$C_1V_1 = C_2V_2$	$V_1 = 0.1\% \times 36$ mL
$V_1 = \dfrac{5mM \times 36mL}{50\ mM}$	$V_1 = 0.036$ mL $\times$ 1000 ul/mL
$V_1 = 3.6$ mL	$V_1 = 36$ ul
MgCl hexahydrate (0.5mM)	**Tris-HCL (50 mM)**
$C_1V_1 = C_2V_2$	$C_1V_1 = C_2V_2$
$V_1 = \dfrac{0.5mM \times 36mL}{5\ mM}$	$V_1 = \dfrac{50mM \times 36mL}{500\ mM}$
$V_1 = 3.6$ mL	$V_1 = 3.6$ mL

Total = 3.6 mL + 3.6 mL +3.6 mL + 0.036 mL

= 10.836 mL (Add 25.2 mL od ddH$_2$O for a final volume of 36 mL)
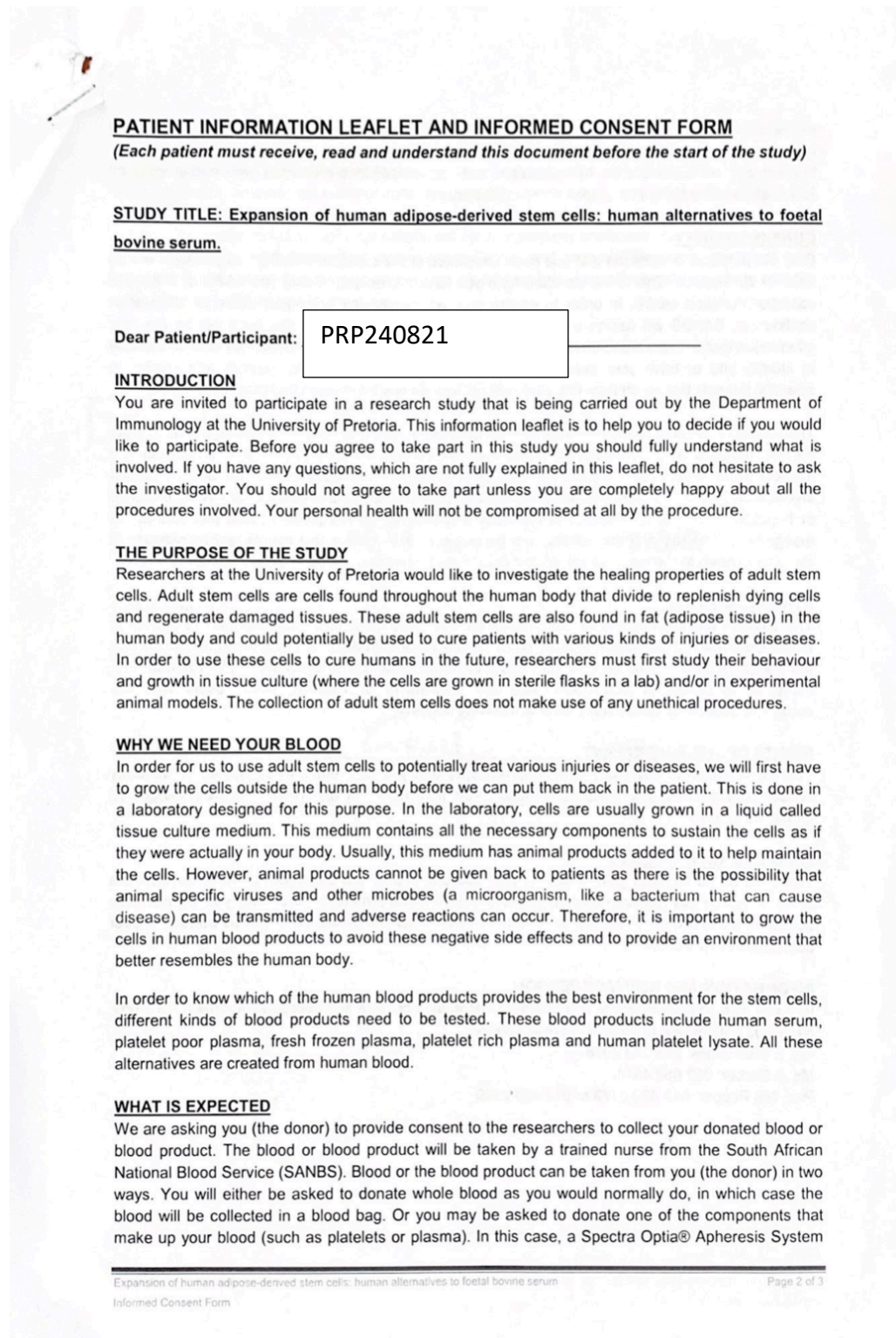
ARS Stain

Need a 2% Stain:

For 50 mL add 1 g of ARS powder to 50mL of dH$_2$O.

Appendix D: PRP Consent, Pre-donation Results and Post-donation Results

PATIENT INFORMATION LEAFLET AND INFORMED CONSENT FORM
(Each patient must receive, read and understand this document before the start of the study)

STUDY TITLE: Expansion of human adipose-derived stem cells: human alternatives to foetal bovine serum.

Dear Patient/Participant: PRP240821

INTRODUCTION
You are invited to participate in a research study that is being carried out by the Department of Immunology at the University of Pretoria. This information leaflet is to help you to decide if you would like to participate. Before you agree to take part in this study you should fully understand what is involved. If you have any questions, which are not fully explained in this leaflet, do not hesitate to ask the investigator. You should not agree to take part unless you are completely happy about all the procedures involved. Your personal health will not be compromised at all by the procedure.

THE PURPOSE OF THE STUDY
Researchers at the University of Pretoria would like to investigate the healing properties of adult stem cells. Adult stem cells are cells found throughout the human body that divide to replenish dying cells and regenerate damaged tissues. These adult stem cells are also found in fat (adipose tissue) in the human body and could potentially be used to cure patients with various kinds of injuries or diseases. In order to use these cells to cure humans in the future, researchers must first study their behaviour and growth in tissue culture (where the cells are grown in sterile flasks in a lab) and/or in experimental animal models. The collection of adult stem cells does not make use of any unethical procedures.

WHY WE NEED YOUR BLOOD
In order for us to use adult stem cells to potentially treat various injuries or diseases, we will first have to grow the cells outside the human body before we can put them back in the patient. This is done in a laboratory designed for this purpose. In the laboratory, cells are usually grown in a liquid called tissue culture medium. This medium contains all the necessary components to sustain the cells as if they were actually in your body. Usually, this medium has animal products added to it to help maintain the cells. However, animal products cannot be given back to patients as there is the possibility that animal specific viruses and other microbes (a microorganism, like a bacterium that can cause disease) can be transmitted and adverse reactions can occur. Therefore, it is important to grow the cells in human blood products to avoid these negative side effects and to provide an environment that better resembles the human body.

In order to know which of the human blood products provides the best environment for the stem cells, different kinds of blood products need to be tested. These blood products include human serum, platelet poor plasma, fresh frozen plasma, platelet rich plasma and human platelet lysate. All these alternatives are created from human blood.

WHAT IS EXPECTED
We are asking you (the donor) to provide consent to the researchers to collect your donated blood or blood product. The blood or blood product will be taken by a trained nurse from the South African National Blood Service (SANBS). Blood or the blood product can be taken from you (the donor) in two ways. You will either be asked to donate whole blood as you would normally do, in which case the blood will be collected in a blood bag. Or you may be asked to donate one of the components that make up your blood (such as platelets or plasma). In this case, a Spectra Optia® Apheresis System

will be used to take the blood product we need and put the remaining components of your blood back into your body. This procedure will not affect your health in any way.

The consent will also allow the researchers to use your blood/blood product to grow and study adult stem cells under different conditions in the laboratory.

CONFIDENTIALITY

Only the personal information that you have completed in the standard SANBS questionnaire will be kept for our records. This is the standard form you fill out when you donate your blood at a SANBS collection/donation centre. In order to ensure your anonymity and keep your personal information confidential, SANBS will assign a specific code to each participant and this code will be the only information that the researchers will have to identify your blood or blood product. No one will be able to identify you or have your personal information. Any research reports, outputs and articles in scientific journals that result from this study will not include any information that may identify you.

The testing of blood or blood products that are donated by you (the donor) will undergo routine tests for HIV, hepatitis B, and hepatitis C. These tests will be performed by SANBS and, if necessary, a medical professional from SANBS will contact your doctor to discuss the results and all parties involved will act in your best interest. Any blood/blood products that test positive for HIV, hepatitis B, or hepatitis C will not be included in the study and SANBS will not provide these products to the researchers. The researchers will thus not be aware of any positive test results and the donor will remain unknown to the researchers. All test results will be handled exclusively by SANBS.

ETHICAL APPROVAL

The protocol and addendums to the protocol for this study have been submitted to the Research Ethics Committee. This study has received written approval from the ethics committee of SANBS and the Research Ethics Committee of the Faculty of Health Sciences at the University of Pretoria. The study is structured in accordance with the Declaration of Helsinki, which deals with the recommendations for biomedical research involving humans.

RIGHTS OF THE PARTICIPANT

Your participation in this study is entirely voluntary and you can refuse to participate or withdraw consent at any time without stating any reason. Your participation or withdrawal from the study will not affect you in any way.

FINANCIAL GAIN OR LOSS

There will be no financial gain or loss to your account, should you participate or withdraw from the study. Although this research could potentially lead to future profitable treatments, you will not have access to these profits. There will be no additional financial compensation to you as a result of your participation in the study.

INFORMATION AND CONTACT PERSON

If at any time you would like to find out more information or have any questions regarding the study, please do not hesitate to contact the researchers.

Ms. E Wolmarans: 072 242 2018

Ms. A Gerber: 082 559 4514

Prof. MS Pepper: 012 420 2179 or 012 420 2190

INFORMED CONSENT

I hereby confirm that the investigator asking for my consent to take part in this study has told me about the nature, process, risks, discomforts, and benefits of the study. I have also received, read and understood the Information Leaflet and Informed Consent regarding this study. I am aware that the results of the study, including personal details, will be anonymously processed into research reports. I am participating willingly. I have had time to ask questions and have no objection to participating in this study. I understand that there is no penalty should I wish to discontinue with the study and my withdrawal will not affect me in any way.

I hereby give consent to donate whole blood/blood product to the present study.

YES ✗	NO

Participant full names (print): PRP240821

Participant signature: _____ Date: 2₆/08/2021

Investigator full names (print): Jamie Mollentze

Investigator signature: _Mollentze_ Date: 24/08/2021

Witness full names (print): Caroline P Strydom

Witness signature: _____ Date: 23.8.2021

PATIENT INFORMATION LEAFLET AND INFORMED CONSENT FORM
(Each patient must receive, read and understand this document before the start of the study)

STUDY TITLE: Expansion of human adipose-derived stem cells: human alternatives to foetal bovine serum.

Dear Patient/Participant: _____ | PRP260821 | _____

INTRODUCTION
You are invited to participate in a research study that is being carried out by the Department of Immunology at the University of Pretoria. This information leaflet is to help you to decide if you would like to participate. Before you agree to take part in this study you should fully understand what is involved. If you have any questions, which are not fully explained in this leaflet, do not hesitate to ask the investigator. You should not agree to take part unless you are completely happy about all the procedures involved. Your personal health will not be compromised at all by the procedure.

THE PURPOSE OF THE STUDY
Researchers at the University of Pretoria would like to investigate the healing properties of adult stem cells. Adult stem cells are cells found throughout the human body that divide to replenish dying cells and regenerate damaged tissues. These adult stem cells are also found in fat (adipose tissue) in the human body and could potentially be used to cure patients with various kinds of injuries or diseases. In order to use these cells to cure humans in the future, researchers must first study their behaviour and growth in tissue culture (where the cells are grown in sterile flasks in a lab) and/or in experimental animal models. The collection of adult stem cells does not make use of any unethical procedures.

WHY WE NEED YOUR BLOOD
In order for us to use adult stem cells to potentially treat various injuries or diseases, we will first have to grow the cells outside the human body before we can put them back in the patient. This is done in a laboratory designed for this purpose. In the laboratory, cells are usually grown in a liquid called tissue culture medium. This medium contains all the necessary components to sustain the cells as if they were actually in your body. Usually, this medium has animal products added to it to help maintain the cells. However, animal products cannot be given back to patients as there is the possibility that animal specific viruses and other microbes (a microorganism, like a bacterium that can cause disease) can be transmitted and adverse reactions can occur. Therefore, it is important to grow the cells in human blood products to avoid these negative side effects and to provide an environment that better resembles the human body.

In order to know which of the human blood products provides the best environment for the stem cells, different kinds of blood products need to be tested. These blood products include human serum, platelet poor plasma, fresh frozen plasma, platelet rich plasma and human platelet lysate. All these alternatives are created from human blood.

WHAT IS EXPECTED
We are asking you (the donor) to provide consent to the researchers to collect your donated blood or blood product. The blood or blood product will be taken by a trained nurse from the South African National Blood Service (SANBS). Blood or the blood product can be taken from you (the donor) in two ways. You will either be asked to donate whole blood as you would normally do, in which case the blood will be collected in a blood bag. Or you may be asked to donate one of the components that make up your blood (such as platelets or plasma). In this case, a Spectra Optia® Apheresis System

will be used to take the blood product we need and put the remaining components of your blood back into your body. This procedure will not affect your health in any way.

The consent will also allow the researchers to use your blood/blood product to grow and study adult stem cells under different conditions in the laboratory.

CONFIDENTIALITY

Only the personal information that you have completed in the standard SANBS questionnaire will be kept for our records. This is the standard form you fill out when you donate your blood at a SANBS collection/donation centre. In order to ensure your anonymity and keep your personal information confidential, SANBS will assign a specific code to each participant and this code will be the only information that the researchers will have to identify your blood or blood product. No one will be able to identify you or have your personal information. Any research reports, outputs and articles in scientific journals that result from this study will not include any information that may identify you.

The testing of blood or blood products that are donated by you (the donor) will undergo routine tests for HIV, hepatitis B, and hepatitis C. These tests will be performed by SANBS and, if necessary, a medical professional from SANBS will contact your doctor to discuss the results and all parties involved will act in your best interest. Any blood/blood products that test positive for HIV, hepatitis B, or hepatitis C will not be included in the study and SANBS will not provide these products to the researchers. The researchers will thus not be aware of any positive test results and the donor will remain unknown to the researchers. All test results will be handled exclusively by SANBS.

ETHICAL APPROVAL

The protocol and addendums to the protocol for this study have been submitted to the Research Ethics Committee. This study has received written approval from the ethics committee of SANBS and the Research Ethics Committee of the Faculty of Health Sciences at the University of Pretoria. The study is structured in accordance with the Declaration of Helsinki, which deals with the recommendations for biomedical research involving humans.

RIGHTS OF THE PARTICIPANT

Your participation in this study is entirely voluntary and you can refuse to participate or withdraw consent at any time without stating any reason. Your participation or withdrawal from the study will not affect you in any way.

FINANCIAL GAIN OR LOSS

There will be no financial gain or loss to your account, should you participate or withdraw from the study. Although this research could potentially lead to future profitable treatments, you will not have access to these profits. There will be no additional financial compensation to you as a result of your participation in the study.

INFORMATION AND CONTACT PERSON

If at any time you would like to find out more information or have any questions regarding the study, please do not hesitate to contact the researchers.

Ms. E Wolmarans: 072 242 2018

Ms. A Gerber: 082 559 4514

Prof. MS Pepper: 012 420 2179 or 012 420 2190

INFORMED CONSENT

I hereby confirm that the investigator asking for my consent to take part in this study has told me about the nature, process, risks, discomforts, and benefits of the study. I have also received, read and understood the Information Leaflet and Informed Consent regarding this study. I am aware that the results of the study, including personal details, will be anonymously processed into research reports. I am participating willingly. I have had time to ask questions and have no objection to participating in this study. I understand that there is no penalty should I wish to discontinue with the study and my withdrawal will not affect me in any way.

I hereby give consent to donate whole blood/blood product to the present study.

YES	NO
☒	☐

Participant full names (print): PRP240821

Participant signature: _____ 08/2021

Investigator full names (print): Jamie Mollentze

Investigator signature: _Mollentze_ Date: 26/08/2021

Witness full names (print): C Stydom

Witness signature: _____ Date: 26.8.2021

PATIENT INFORMATION LEAFLET AND INFORMED CONSENT FORM
(Each patient must receive, read and understand this document before the start of the study)

STUDY TITLE: Expansion of human adipose-derived stem cells: human alternatives to foetal bovine serum.

PRP070721

Dear Patient/Participant: _____ _____

INTRODUCTION

You are invited to participate in a research study that is being carried out by the Department of Immunology at the University of Pretoria. This information leaflet is to help you to decide if you would like to participate. Before you agree to take part in this study you should fully understand what is involved. If you have any questions, which are not fully explained in this leaflet, do not hesitate to ask the investigator. You should not agree to take part unless you are completely happy about all the procedures involved. Your personal health will not be compromised at all by the procedure.

THE PURPOSE OF THE STUDY

Researchers at the University of Pretoria would like to investigate the healing properties of adult stem cells. Adult stem cells are cells found throughout the human body that divide to replenish dying cells and regenerate damaged tissues. These adult stem cells are also found in fat (adipose tissue) in the human body and could potentially be used to cure patients with various kinds of injuries or diseases. In order to use these cells to cure humans in the future, researchers must first study their behaviour and growth in tissue culture (where the cells are grown in sterile flasks in a lab) and/or in experimental animal models. The collection of adult stem cells does not make use of any unethical procedures.

WHY WE NEED YOUR BLOOD

In order for us to use adult stem cells to potentially treat various injuries or diseases, we will first have to grow the cells outside the human body before we can put them back in the patient. This is done in a laboratory designed for this purpose. In the laboratory, cells are usually grown in a liquid called tissue culture medium. This medium contains all the necessary components to sustain the cells as if they were actually in your body. Usually, this medium has animal products added to it to help maintain the cells. However, animal products cannot be given back to patients as there is the possibility that animal specific viruses and other microbes (a microorganism, like a bacterium that can cause disease) can be transmitted and adverse reactions can occur. Therefore, it is important to grow the cells in human blood products to avoid these negative side effects and to provide an environment that better resembles the human body.

In order to know which of the human blood products provides the best environment for the stem cells, different kinds of blood products need to be tested. These blood products include human serum, platelet poor plasma, fresh frozen plasma, platelet rich plasma and human platelet lysate. All these alternatives are created from human blood.

WHAT IS EXPECTED

We are asking you (the donor) to provide consent to the researchers to collect your donated blood or blood product. The blood or blood product will be taken by a trained nurse from the South African National Blood Service (SANBS). Blood or the blood product can be taken from you (the donor) in two ways. You will either be asked to donate whole blood as you would normally do, in which case the blood will be collected in a blood bag. Or you may be asked to donate one of the components that make up your blood (such as platelets or plasma). In this case, a Spectra Optia® Apheresis System

37154861

173

will be used to take the blood product we need and put the remaining components of your blood back into your body. This procedure will not affect your health in any way.

The consent will also allow the researchers to use your blood/blood product to grow and study adult stem cells under different conditions in the laboratory.

CONFIDENTIALITY

Only the personal information that you have completed in the standard SANBS questionnaire will be kept for our records. This is the standard form you fill out when you donate your blood at a SANBS collection/donation centre. In order to ensure your anonymity and keep your personal information confidential, SANBS will assign a specific code to each participant and this code will be the only information that the researchers will have to identify your blood or blood product. No one will be able to identify you or have your personal information. Any research reports, outputs and articles in scientific journals that result from this study will not include any information that may identify you.

The testing of blood or blood products that are donated by you (the donor) will undergo routine tests for HIV, hepatitis B, and hepatitis C. These tests will be performed by SANBS and, if necessary, a medical professional from SANBS will contact your doctor to discuss the results and all parties involved will act in your best interest. Any blood/blood products that test positive for HIV, hepatitis B, or hepatitis C will not be included in the study and SANBS will not provide these products to the researchers. The researchers will thus not be aware of any positive test results and the donor will remain unknown to the researchers. All test results will be handled exclusively by SANBS.

ETHICAL APPROVAL

The protocol and addendums to the protocol for this study have been submitted to the Research Ethics Committee. This study has received written approval from the ethics committee of SANBS and the Research Ethics Committee of the Faculty of Health Sciences at the University of Pretoria. The study is structured in accordance with the Declaration of Helsinki, which deals with the recommendations for biomedical research involving humans.

RIGHTS OF THE PARTICIPANT

Your participation in this study is entirely voluntary and you can refuse to participate or withdraw consent at any time without stating any reason. Your participation or withdrawal from the study will not affect you in any way.

FINANCIAL GAIN OR LOSS

There will be no financial gain or loss to your account, should you participate or withdraw from the study. Although this research could potentially lead to future profitable treatments, you will not have access to these profits. There will be no additional financial compensation to you as a result of your participation in the study.

INFORMATION AND CONTACT PERSON

If at any time you would like to find out more information or have any questions regarding the study, please do not hesitate to contact the researchers.
Ms. E Wolmarans: 072 242 2018
Ms. A Gerber: 082 559 4514
Prof. MS Pepper: 012 420 2179 or 012 420 2190

174

INFORMED CONSENT

I hereby confirm that the investigator asking for my consent to take part in this study has told me about the nature, process, risks, discomforts, and benefits of the study. I have also received, read and understood the Information Leaflet and Informed Consent regarding this study. I am aware that the results of the study, including personal details, will be anonymously processed into research reports. I am participating willingly. I have had time to ask questions and have no objection to participating in this study. I understand that there is no penalty should I wish to discontinue with the study and my withdrawal will not affect me in any way.

I hereby give consent to donate whole blood/blood product to the present study.

YES ☒   NO ☐

PRP070721

Participant full names (print): _____

Participant signature: _____ Date: 7/7/21

Investigator full names (print): Jamie Mollentze

Investigator signature: Mollentze Date: 7/7/2021

Witness full names (print): Caroline Styelam

Witness signature: _____ Date: 7/7/ 2021

DOB: 05/12/1962
Gender: male
Weight: 117kg.
Bloodgroup: OPOS
Ethnic: White

175

LANCET LABORATORIES
PATHOLOGY RESULT

Key to Diagnostic Excellence

Page : 1/1

Patient Name	:	**PRP240821**	Lab Name	: Central
Lab Ref	:		Dr. Ref No.	: NOT AVAILABLE
Age/Sex/DOB	:		Spec No.	: 0823:HR05852R
ID Num.	:		Collection Date	: 23/08/21 1700
Contact Nos	:		Receive Date	: 23/08/21 1703
Email	:		Report Date	: 24/08/21 1155

Report for Doctor
Sa National Blood Services
10 Eden Road
Pinetown - 3610

Other Doctors
Submit Dr : Sa National Blood Services

Guarantor Information
Name :
Contact Nos :
Email :
MedAid : CLIENT

Tests: CAL/P4 cor./MG, FBC

Haematology

FULL BLOOD COUNT

ERYTHROCYTE COUNT		5.51 x10^12/L		4.5	-	6.5
HAEMOGLOBIN		16.1 g/dL		13.8	-	18.8
HAEMATOCRIT		0.46 L/L		0.40	-	0.56
MCV		83.7 fL		79	-	100
MCH		29.3 pg		27	-	35
MCHC		35.0 g/dL		32	-	36
RDW		13.3 %		11.0	-	16.0
LEUCOCYTE COUNT		7.15 x 10^9/L		4.0	-	12.0
Neutrophils	52.2%	3.73 x 10^9/L		2.0	-	7.5
Lymphocytes	37.9%	2.71 x 10^9/L		1.0	-	4.0
Monocytes	6.9%	0.49 x 10^9/L		0.2	-	1.0
Eosinophils	2.3%	0.16 x 10^9/L		0.0	-	0.5
Basophils	0.7%	0.05 x 10^9/L		0.0	-	0.3
NEUTRO/LYMPH RATIO(NLR)		1.38				
PLATELETS		254 x 10^9/L		150	-	450

COMMENT:
Normal red cell indices,
Absolute leucocyte values are normal,
Platelets are adequate.

For consultation by referring doctors only, please call:
Dr Prushini Moodley 031 3086519
Dr Nicole Holland +2711 358 0800

Biochemistry

MINERAL AND BONE METABOLISM

S-CALCIUM Total	2.40 mmol/L		2.10	-	2.55
S-MAGNESIUM	0.85 mmol/L		0.66	-	1.07
S-PHOSPHATE inorganic	1.38 mmol/L		0.87	-	1.45

COMMENT:
Normal calcium and phosphate.

S-ALBUMIN	49 g/L		35	-	50

For consultation by referring doctors only, please call:
Dr Kogie Reddi +2711 3580977
Dr Thavan Padayachi 031 3086547

176

AMPATH
LABORATORIES

Drs Du Buisson, Kramer, Swart, Bouwer Inc.
Registration number: 2007/018337/21
PR0520003200411

Pathology Report

24hr Contact No. 012 678 0700

Patient:

PRP260821

Age: 27 Sex: M
H: None C: 0833898000
dj.cloete05@gmail.com

Ref By: Dr SANBS Spec. Doner Services
Folio:

Doctor:
Dr SANBS Spec. Doner Services
Dr Neo Moleli
Unitas lifestyle Suite 17
Lyttelton 0157

COPY REPORT
Req: 41074182
Specimen: 0825:AS08615R

Guarantor:
Mr Detlef J Cloete
15 Murati Avenue
9 Murati Corner
Centurion 0157
W: 0343121166 C: 0833898000
Private Patient

Collected:2021-08-25 14:32
Received: 2021-08-25 14:47
Printed: 2021-08-26 14:55
Batch: PATIENT RESULTS STD

Ordered: Full Blood Count, Potassium, Calcium, Magnesium, Phosphate
Sample: E01 EDTA Haematology (1), S01 SST (1)

Test	ABN	Result	Reference Range	Unit
Full Blood Count				
Haemoglobin		15.1	14.3-18.3	g/dl
Red Cell Count		5.97	4.89-6.11	10 12/L
Haematocrit		46.7	43.0-55.0	%
MCV	L	78.2	79.1-98.9	fl
MCH	L	25.3	27.0-32.0	pg
MCHC		32.3	31.0-37.0	g/dl
RDW		13.9	10.0-16.3	%
White Cell Count		5.57	3.92-9.88	10 9/L
Neutrophils Abs		2.62	2.00-7.50	10 9/L
Lymphocytes Abs		2.30	1.00-4.00	10 9/L
Monocytes Abs		0.48	0.18-1.00	10 9/L
Eosinophils Abs		0.12	0.00-0.45	10 9/L
Basophils Abs		0.03	0.00-0.20	10 9/L
Immature Granulocytes Abs		0.02	0.00-0.10	10 9/L
Neut:Lymph ratio		1.00		
Platelet Count		301	150-450	10 9/L
Mean Platelet Volume		10.8	7.1-11.0	fl
FBC Comment		.		

The red cells appear hypochromic, microcytic with elliptocytes present.
Suggest iron studies if clinically indicated.

Potassium		4.7	3.5-5.1	mmol/l
Calcium				
Calcium Corrected		2.44	2.15-2.50	mmol/l
Albumin		44	35-52	g/l
Magnesium		0.90	0.66-1.07	mmol/l
Phosphate		1.27	0.78-1.42	mmol/l

Please contact your medical practitioner to discuss these results.

Page 1 of 1

```
RUN DATE: 31/08/21              BBK/LAB SYSTEM                        PAGE 1
RUN TIME: 1419         LAB SPECIMEN INTERNAL INQUIRY
RUN USER: LM4078
```

PATIENT: BB DONOR 04110797	ACCT #: Z83430220	LOC:	U #:
	AGE/SX: 25/M	ROOM:	REG: 28/07/21
REG DR: Unkown,U	DOB:	BED:	DIS:
	STATUS: BB DON	TLOC:	

```
SPEC#: 0824:LB00322R    ORD FOR: 24/08/21-1202   STATUS: COMP        REQ #: 19149685
                        COLL: 24/08/21-1202      SUBM DR: Unkown,U
                        RECV: 24/08/21-1202      PT AGE AT COLL: 25

ENTERED:  24/08/21-1202    ENT BY: LM4078         OTHR DR:
COLL BY:                   RCV BY: LM4078
LAST RPTD:      -          WKLD FN:
LAST ACT: 25/08/21-0705    BAR CD#: 441657.
ORDERED:  FBC_PRE
```

(PRP240821) – Pre-Collection

```
COL CATEG:
ORD SITE: GBT001
RCV SITE: GBT001                      TRANSIT SITE:
                                POINT OF TESTING
PERFORM SITE               RCV DEPT   DATE-TIME   USR    AT SITE
GAL003 25/08/21-0704                                     GAL003 25/08/21-0704
```

Test	Result	Flag	Reference
PLT	256.00		180-450 x10^3ul
	Ent:25/08-0704 autoins, Ver: 25/08-0705 MK9272		
	Method: Advia 2120		Analyzer: GL3_ADV01
HGB	15.70		12.5-18.0 g/dl
	Ent:25/08-0704 autoins, Ver: 25/08-0705 MK9272		
	Method: Advia 2120		Analyzer: GL3_ADV01
HCT	46.90		38-54 %
	Ent:25/08-0704 autoins, Ver: 25/08-0705 MK9272		
	Method: Advia 2120		Analyzer: GL3_ADV01
RBC	5.73		4.2-6.1 x10^3/ul
	Ent:25/08-0704 autoins, Ver: 25/08-0705 MK9272		
	Method: Advia 2120		Analyzer: GL3_ADV01
WBC	6.88		4.0-12.6 x10^3/ul
	Ent:25/08-0704 autoins, Ver: 25/08-0705 MK9272		
	Method: Advia 2120		Analyzer: GL3_ADV01
MCV	81.90		80-99 fl
	Ent:25/08-0704 autoins, Ver: 25/08-0705 MK9272		
	Method: Advia 2120		Analyzer: GL3_ADV01
MCH	27.40		27-31 pg
	Ent:25/08-0704 autoins, Ver: 25/08-0705 MK9272		
	Method: Advia 2120		Analyzer: GL3_ADV01
MCHC	33.50		32-37 g/dl
	Ent:25/08-0704 autoins, Ver: 25/08-0705 MK9272		
	Method: Advia 2120		Analyzer: GL3_ADV01
COMMENTS	NP		
	Ent:24/08-1202 AutoDft, Ver: 24/08-1202 AutoDft		
	Method:		

*** End of Report ***

```
RUN DATE: 31/08/21                    BBK/LAB SYSTEM                          PAGE 1
RUN TIME: 1419                  LAB SPECIMEN INTERNAL INQUIRY
RUN USER: LM4078
```

PATIENT: BB DONOR 04110797	ACCT #: Z83430220	LOC:	U #:
	AGE/SX: 25/M	ROOM:	REG: 28/07/21
REG DR: Unkown,U	DOB:	BED:	DIS:
	STATUS: BB DON	TLOC:	

```
SPEC#: 0824:LB00324R    ORD FOR: 24/08/21-1203   STATUS:   COMP          REQ #: 19149691
                           COLL: 24/08/21-1203   SUBM DR: Unkown,U
                           RECV: 24/08/21-1203   PT AGE AT COLL: 25

ENTERED:   24/08/21-1203   ENT BY:  LM4078        OTHR DR:
COLL BY:                   RCV BY:  LM4078
LAST RPTD:         -       WKLD FN:
LAST ACT:  25/08/21-0705   BAR CD#: 441658.
ORDERED:   FBC Post
COL CATEG:
ORD SITE: GBT001                           TRANSIT SITE:
RCV SITE: GBT001
                           POINT OF TESTING
PERFORM SITE                 RCV DEPT   DATE-TIME     USR     AT SITE
GAL003 25/08/21-0705                                         GAL003 25/08/21-0705
```

(PRP240821) – Post-Collection

Test	Result	Flag	Reference
PLT	195.00		180-450 x10^3ul
	Ent:25/08-0705 autoins, Ver: 25/08-0705 MK9272		
	Method: Advia 2120		Analyzer: GL3_ADV01
HGB	16.00		12.5-18.0 g/dl
	Ent:25/08-0705 autoins, Ver: 25/08-0705 MK9272		
	Method: Advia 2120		Analyzer: GL3_ADV01
HCT	45.30		38-54 %
	Ent:25/08-0705 autoins, Ver: 25/08-0705 MK9272		
	Method: Advia 2120		Analyzer: GL3_ADV01
RBC	5.52		4.2-6.1 x10^3/ul
	Ent:25/08-0705 autoins, Ver: 25/08-0705 MK9272		
	Method: Advia 2120		Analyzer: GL3_ADV01
WBC	7.46		4.0-12.6 x10^3/ul
	Ent:25/08-0705 autoins, Ver: 25/08-0705 MK9272		
	Method: Advia 2120		Analyzer: GL3_ADV01
MCV	82.20		80-99 fl
	Ent:25/08-0705 autoins, Ver: 25/08-0705 MK9272		
	Method: Advia 2120		Analyzer: GL3_ADV01
MCH	28.90		27-31 pg
	Ent:25/08-0705 autoins, Ver: 25/08-0705 MK9272		
	Method: Advia 2120		Analyzer: GL3_ADV01
MCHC	35.20		32-37 g/dl
	Ent:25/08-0705 autoins, Ver: 25/08-0705 MK9272		
	Method: Advia 2120		Analyzer: GL3_ADV01
COMMENTS	NP		
	Ent:24/08-1203 AutoDft, Ver: 24/08-1203 AutoDft		
	Method:		

```
                         *** End of Report ***
```

```
RUN DATE: 31/08/21              BBK/LAB SYSTEM                        PAGE 1
RUN TIME: 1419          LAB SPECIMEN INTERNAL INQUIRY
RUN USER: LM4078
```

PATIENT: RPPP #34861867	ACCT #: Z83828749	LOC:	U #:
	AGE/SX: 25/M	ROOM:	REG: 24/08/21
REG DR: Unkown,U	DOB:	BED:	DIS:
	STATUS: BB UNIT	TLOC:	

```
SPEC#: 0824:LB00387R    ORD FOR: 24/08/21-1324  STATUS:  COMP        REQ #: 19150296
                        COLL: 24/08/21-1324  SUBM DR: Unkown,U
                        RECV: 24/08/21-1324  PT AGE AT COLL: 25

ENTERED:   24/08/21-1325   ENT BY: LM4078        OTHR DR:
COLL BY:                   RCV BY: LM4078                        (PRP240821) –
LAST RPTD:       -         WKLD FN:                              Post-Collection
LAST ACT:  25/08/21-1540   BAR CD#: 441765.                      Analysis
ORDERED:   RPROD
COL CATEG:
ORD SITE: GBT001                          TRANSIT SITE:
RCV SITE: GBT001
                          POINT OF TESTING
PERFORM SITE                 RCV DEPT   DATE-TIME      USR    AT SITE
GAL003 25/08/21-0930                                          GAL003 25/08/21-0930
```

Test	Result	Flag	Reference
WCC PRODUCT	0.00		0-5 x10^6
	Ent:*25/08-1102 BT7888*, Ver: *25/08-1102 BT7888*		
	Method: *Advia 2120*		
PLT COUNT PROD	1386.00		1000-3000 x10^3/ul
	Ent:*25/08-0930 autoins*, Ver: *25/08-0954 BT7888*		
	Method: *Advia 2120*		Analyzer: *GL3_ADV01*
PRODVOL	200		200-800 ML
	Ent:*25/08-1102 BT7888*, Ver: *25/08-1102 BT7888*		
	Method: *Manual*		
STERILITY	NP		
	Ent:*24/08-1325 AutoDft*, Ver: *24/08-1325 AutoDft*		
	Method:		
ANO2	NP		Negative CFU
	Ent:*24/08-1325 AutoDft*, Ver: *24/08-1325 AutoDft*		
	Method:		
ANO2_BATCH	NP		CFU
	Ent:*24/08-1325 AutoDft*, Ver: *24/08-1325 AutoDft*		
	Method:		
O2	NP		Negative CFU
	Ent:*24/08-1325 AutoDft*, Ver: *24/08-1325 AutoDft*		
	Method:		
O2_Batch	NP		CFU
	Ent:*24/08-1325 AutoDft*, Ver: *24/08-1325 AutoDft*		
	Method:		
PH	6.8		6.4-10.4 pH
	Ent:*25/08-1540 BT7888*, Ver: *25/08-1540 BT7888*		
	Method: *pH Meter*		
COMMENTS	NP		
	Ent:*24/08-1325 AutoDft*, Ver: *24/08-1325 AutoDft*		
	Method:		

```
              Continued on next page ...
```

RUN DATE: 31/08/21   BBK/LAB SYSTEM   PAGE 1
RUN TIME: 1357   LAB SPECIMEN INTERNAL INQUIRY
RUN USER: LM4078

```
PATIENT: BB DONOR 02613663        ACCT #: Z30347381   LOC:          U #:
                                  AGE/SX: 27/M        ROOM:         REG: 14/05/10
REG DR:  Unkown,U                 DOB:                BED:          DIS:
                                  STATUS: BB DON      TLOC:
```

```
SPEC#: 0826:LB00256R   ORD FOR: 26/08/21-1455  STATUS:  COMP        REQ #: 19157545
                       COLL: 26/08/21-1455     SUBM DR: Unkown,U
                       RECV: 26/08/21-1455     PT AGE AT COLL: 27


ENTERED:   26/08/21-1455   ENT BY:  LM4078        OTHR DR:
COLL BY:                   RCV BY:  LM4078
LAST RPTD:      -          WKLD FN:
LAST ACT:   27/08/21-0740  BAR CD#: 442767.
ORDERED:    FBC_PRE
COL CATEG:
ORD SITE: GBT001                              TRANSIT SITE:
RCV SITE: GBT001
                             POINT OF TESTING
PERFORM SITE                 RCV DEPT   DATE-TIME    USR    AT SITE
GAL003 27/08/21-0736                                        GAL003 27/08/21-0736
```

(PRP260821) – Pre-Collection

Test	Result	Flag	Reference
PLT	254.00		180-450 x10^3ul
	Ent:27/08-0736 autoins, Ver: 27/08-0740 MK9272		
	Method: Advia 2120		Analyzer: GL3_ADV01
HGB	14.10		12.5-18.0 g/dl
	Ent:27/08-0736 autoins, Ver: 27/08-0740 MK9272		
	Method: Advia 2120		Analyzer: GL3_ADV01
HCT	44.70		38-54 %
	Ent:27/08-0736 autoins, Ver: 27/08-0740 MK9272		
	Method: Advia 2120		Analyzer: GL3_ADV01
RBC	5.49		4.2-6.1 x10^3/ul
	Ent:27/08-0736 autoins, Ver: 27/08-0740 MK9272		
	Method: Advia 2120		Analyzer: GL3_ADV01
WBC	5.50		4.0-12.6 x10^3/ul
	Ent:27/08-0736 autoins, Ver: 27/08-0740 MK9272		
	Method: Advia 2120		Analyzer: GL3_ADV01
MCV	81.40		80-99 fl
	Ent:27/08-0736 autoins, Ver: 27/08-0740 MK9272		
	Method: Advia 2120		Analyzer: GL3_ADV01
MCH	25.70	L	27-31 pg
	Ent:27/08-0740 MK9272, Ver: 27/08-0740 MK9272		
	Method: Advia 2120		
MCHC	31.50	L	32-37 g/dl
	Ent:27/08-0740 MK9272, Ver: 27/08-0740 MK9272		
	Method: Advia 2120		
COMMENTS	NP		
	Ent:26/08-1455 AutoDft, Ver: 26/08-1455 AutoDft		
	Method:		

*** End of Report ***

RUN DATE: 31/08/21   BBK/LAB SYSTEM   PAGE 1
RUN TIME: 1357   LAB SPECIMEN INTERNAL INQUIRY
RUN USER: LM4078

PATIENT: BB DONOR 02613663	ACCT #: Z30347381	LOC:	U #:
	AGE/SX: 27/M	ROOM:	REG: 14/05/10
REG DR: Unkown,U	DOB:	BED:	DIS:
	STATUS: BB DON	TLOC:	

SPEC#: 0826:LB00257R   ORD FOR: 26/08/21-1456   STATUS: COMP   REQ #: 19157554
                      COLL: 26/08/21-1456   SUBM DR: Unkown,U
                      RECV: 26/08/21-1456   PT AGE AT COLL: 27

ENTERED: 26/08/21-1456   ENT BY: LM4078   OTHR DR:
COLL BY: RCV BY: LM4078
LAST RPTD: -   WKLD FN:
LAST ACT: 27/08/21-0740   BAR CD#: 442775.
ORDERED: FBC Post
COL CATEG:
ORD SITE: GBT001   TRANSIT SITE:
RCV SITE: GBT001

(PRP260821) – Post-Collection

POINT OF TESTING

PERFORM SITE	RCV DEPT	DATE-TIME	USR	AT SITE
GAL003 27/08/21-0736				GAL003 27/08/21-0736

Test	Result	Flag	Reference
PLT	227.00		180-450 x10^3ul
	Ent:27/08-0736 autoins, Ver: 27/08-0740 MK9272		
	Method: Advia 2120		Analyzer: GL3_ADV01
HGB	13.90		12.5-18.0 g/dl
	Ent:27/08-0736 autoins, Ver: 27/08-0740 MK9272		
	Method: Advia 2120		Analyzer: GL3_ADV01
HCT	46.30		38-54 %
	Ent:27/08-0736 autoins, Ver: 27/08-0740 MK9272		
	Method: Advia 2120		Analyzer: GL3_ADV01
RBC	5.67		4.2-6.1 x10^3/ul
	Ent:27/08-0736 autoins, Ver: 27/08-0740 MK9272		
	Method: Advia 2120		Analyzer: GL3_ADV01
WBC	7.41		4.0-12.6 x10^3/ul
	Ent:27/08-0736 autoins, Ver: 27/08-0740 MK9272		
	Method: Advia 2120		Analyzer: GL3_ADV01
MCV	81.60		80-99 fl
	Ent:27/08-0736 autoins, Ver: 27/08-0740 MK9272		
	Method: Advia 2120		Analyzer: GL3_ADV01
MCH	24.50	L	27-31 pg
	Ent:27/08-0740 MK9272, Ver: 27/08-0740 MK9272		
	Method: Advia 2120		
MCHC	30.00	L	32-37 g/dl
	Ent:27/08-0740 MK9272, Ver: 27/08-0740 MK9272		
	Method: Advia 2120		
COMMENTS	NP		
	Ent:26/08-1456 AutoDft, Ver: 26/08-1456 AutoDft		
	Method:		

*** End of Report ***

PATIENT: RPPP #34861744   ACCT #: Z83865057   LOC: U #:
                                 AGE/SX: 27/M   ROOM: REG: 26/08/21
REG DR: Unkown,U   DOB: BED: DIS:
                                 STATUS: BB UNIT   TLOC:

SPEC#: 0826:LB00330R   ORD FOR: 26/08/21-1730   STATUS: COMP   REQ #: 19158536
                          COLL: 26/08/21-1730   SUBM DR: Unkown,U
                          RECV: 26/08/21-1730   PT AGE AT COLL: 27

ENTERED: 26/08/21-1730   ENT BY: LM4078   OTHR DR:
COLL BY: RCV BY: LM4078
LAST RPTD: -   WKLD FN: (PRP260821) –
LAST ACT: 27/08/21-1306   BAR CD#: 442848.   Post-Collection
ORDERED: RPROD   Analysis
COL CATEG:
ORD SITE: GBT001   TRANSIT SITE:
RCV SITE: GBT001
                           POINT OF TESTING
PERFORM SITE   RCV DEPT   DATE-TIME   USR   AT SITE
GAL003 27/08/21-0949   GAL003 27/08/21-0949

Test	Result	Flag	Reference
WCC PRODUCT	0.00		0-5 x10^6
	Ent:27/08-1306 BT7888, Ver: 27/08-1306 BT7888		
	Method: Advia 2120		
PLT COUNT PROD	1480.00		1000-3000 x10^3/ul
	Ent:27/08-0949 autoins, Ver: 27/08-1022 BT7888		
	Method: Advia 2120		Analyzer: GL3_ADV01
PRODVOL	250		200-800 ML
	Ent:27/08-1306 BT7888, Ver: 27/08-1306 BT7888		
	Method: Manual		
STERILITY	NP		
	Ent:26/08-1730 AutoDft, Ver: 26/08-1730 AutoDft		
	Method:		
ANO2	NP		Negative CFU
	Ent:26/08-1730 AutoDft, Ver: 26/08-1730 AutoDft		
	Method:		
ANO2_BATCH	NP		CFU
	Ent:26/08-1730 AutoDft, Ver: 26/08-1730 AutoDft		
	Method:		
O2	NP		Negative CFU
	Ent:26/08-1730 AutoDft, Ver: 26/08-1730 AutoDft		
	Method:		
O2_Batch	NP		CFU
	Ent:26/08-1730 AutoDft, Ver: 26/08-1730 AutoDft		
	Method:		
PH	6.8		6.4-10.4 pH
	Ent:27/08-1306 BT7888, Ver: 27/08-1306 BT7888		
	Method: pH Meter		
COMMENTS	NP		
	Ent:26/08-1730 AutoDft, Ver: 26/08-1730 AutoDft		
	Method:		

Continued on next page ...

```
PATIENT: BB DONOR 381287          ACCT #: Z23414586    LOC:          U #:
                                  AGE/SX: 58/M         ROOM:         REG: 01/10/08
REG DR:  Unkown,U                 DOB:                 BED:          DIS:
                                  STATUS: BB DON       TLOC:
```

```
SPEC#: 0707:LB00111R    ORD FOR: 07/07/21-1013   STATUS:  COMP        REQ #: 19017779
                        COLL: 07/07/21-1013   SUBM DR: Unkown,U
                        RECV: 07/07/21-1013   PT AGE AT COLL: 58

ENTERED:    07/07/21-1014   ENT BY:  LM4078        OTHR DR:
COLL BY:                    RCV BY:  LM4078
LAST RPTD:         -        WKLD FN:
LAST ACT:   07/07/21-1522   BAR CD#: 423100.
ORDERED:    FBC_PRE
COL CATEG:
ORD SITE: GBT001
RCV SITE: GBT001                        TRANSIT SITE:

PERFORM SITE                    POINT OF TESTING
                        RCV DEPT   DATE-TIME    USR    AT SITE
GAL003 07/07/21-1420                                  GAL003 07/07/21-1420
```

(PRP070721) –
Pre-Collection

Test	Result	Flag	Reference
PLT	291.00		180-450 x10^3ul
	Ent:07/07-1420 autoins, Ver: 07/07-1522 KM8060		
	Method: Advia 2120		Analyzer: GL3_ADV01
HGB	12.60		12.5-18.0 g/dl
	Ent:07/07-1420 autoins, Ver: 07/07-1522 KM8060		
	Method: Advia 2120		Analyzer: GL3_ADV01
HCT	39.20		38-54 %
	Ent:07/07-1420 autoins, Ver: 07/07-1522 KM8060		
	Method: Advia 2120		Analyzer: GL3_ADV01
RBC	4.60		4.2-6.1 x10^3/ul
	Ent:07/07-1420 autoins, Ver: 07/07-1522 KM8060		
	Method: Advia 2120		Analyzer: GL3_ADV01
WBC	4.63		4.0-12.6 x10^3/ul
	Ent:07/07-1420 autoins, Ver: 07/07-1522 KM8060		
	Method: Advia 2120		Analyzer: GL3_ADV01
MCV	85.20		80-99 fl
	Ent:07/07-1420 autoins, Ver: 07/07-1522 KM8060		
	Method: Advia 2120		Analyzer: GL3_ADV01
MCH	27.30		27-31 pg
	Ent:07/07-1420 autoins, Ver: 07/07-1522 KM8060		
	Method: Advia 2120		Analyzer: GL3_ADV01
MCHC	32.00		32-37 g/dl
	Ent:07/07-1420 autoins, Ver: 07/07-1522 KM8060		
	Method: Advia 2120		Analyzer: GL3_ADV01
COMMENTS	NP		
	Ent:07/07-1014 AutoDft, Ver: 07/07-1014 AutoDft		
	Method:		

RUN DATE: 08/07/21
RUN TIME: 1615
RUN USER: CS4477

BBK/LAB SYSTEM
LAB SPECIMEN INTERNAL INQUIRY

PAGE 1

PATIENT: BB DONOR 381287

REG DR: Unkown,U

ACCT #: Z23414586   LOC: U #:
AGE/SX: 58/M   ROOM: REG: 01/10/08
DOB: BED: DIS:
STATUS: BB DON   TLOC:

SPEC#: 0707:LB00112R   ORD FOR: 07/07/21-1014   STATUS: COMP   REQ #: 19017781
                         COLL: 07/07/21-1014   SUBM DR: Unkown,U
                         RECV: 07/07/21-1014   PT AGE AT COLL: 58

ENTERED: 07/07/21-1015   ENT BY: LM4078   OTHR DR:
COLL BY: RCV BY: LM4078
LAST RPTD: -   WKLD FN:
LAST ACT: 07/07/21-1521   BAR CD#: 423101.
ORDERED: FBC Post
COL CATEG:
ORD SITE: GBT001   TRANSIT SITE:
RCV SITE: GBT001

                                    POINT OF TESTING
PERFORM SITE   RCV DEPT   DATE-TIME   USR   AT SITE
GAL003 07/07/21-1420   GAL003 07/07/21-1420

(PRP070721) – Post-Collection

| Test	Result	Flag	Reference
PLT	264.00		180-450 x10^3ul
	Ent:*07/07-1420 autoins*, Ver: *07/07-1521 KM8060*		
	Method: *Advia 2120*		Analyzer: *GL3_ADV01*
HGB	13.00		12.5-18.0 g/dl
	Ent:*07/07-1420 autoins*, Ver: *07/07-1521 KM8060*		
	Method: *Advia 2120*		Analyzer: *GL3_ADV01*
HCT	41.00		38-54 %
	Ent:*07/07-1420 autoins*, Ver: *07/07-1521 KM8060*		
	Method: *Advia 2120*		Analyzer: *GL3_ADV01*
RBC	4.80		4.2-6.1 x10^3/ul
	Ent:*07/07-1420 autoins*, Ver: *07/07-1521 KM8060*		
	Method: *Advia 2120*		Analyzer: *GL3_ADV01*
WBC	5.18		4.0-12.6 x10^3/ul
	Ent:*07/07-1420 autoins*, Ver: *07/07-1521 KM8060*		
	Method: *Advia 2120*		Analyzer: *GL3_ADV01*
MCV	85.40		80-99 fl
	Ent:*07/07-1420 autoins*, Ver: *07/07-1521 KM8060*		
	Method: *Advia 2120*		Analyzer: *GL3_ADV01*
MCH	27.10		27-31 pg
	Ent:*07/07-1420 autoins*, Ver: *07/07-1521 KM8060*		
	Method: *Advia 2120*		Analyzer: *GL3_ADV01*
MCHC	31.70	L	32-37 g/dl
	Ent:*07/07-1521 KM8060*, Ver: *07/07-1521 KM8060*		
	Method: *Advia 2120*		
COMMENTS	NP		
	Ent:*07/07-1015 AutoDft*, Ver: *07/07-1015 AutoDft*		
	Method:		

*** End of Report ***

Appendix E: Compensation Experiment (Human Alternatives)

The importance of doing compensation experiments were described in Appendix B. Compensation experiments were repeated for each of the human alternatives as the presence of the different human alternative affect the expression of different markers differently and the cells have different autofluorescence.

Unstained Cells
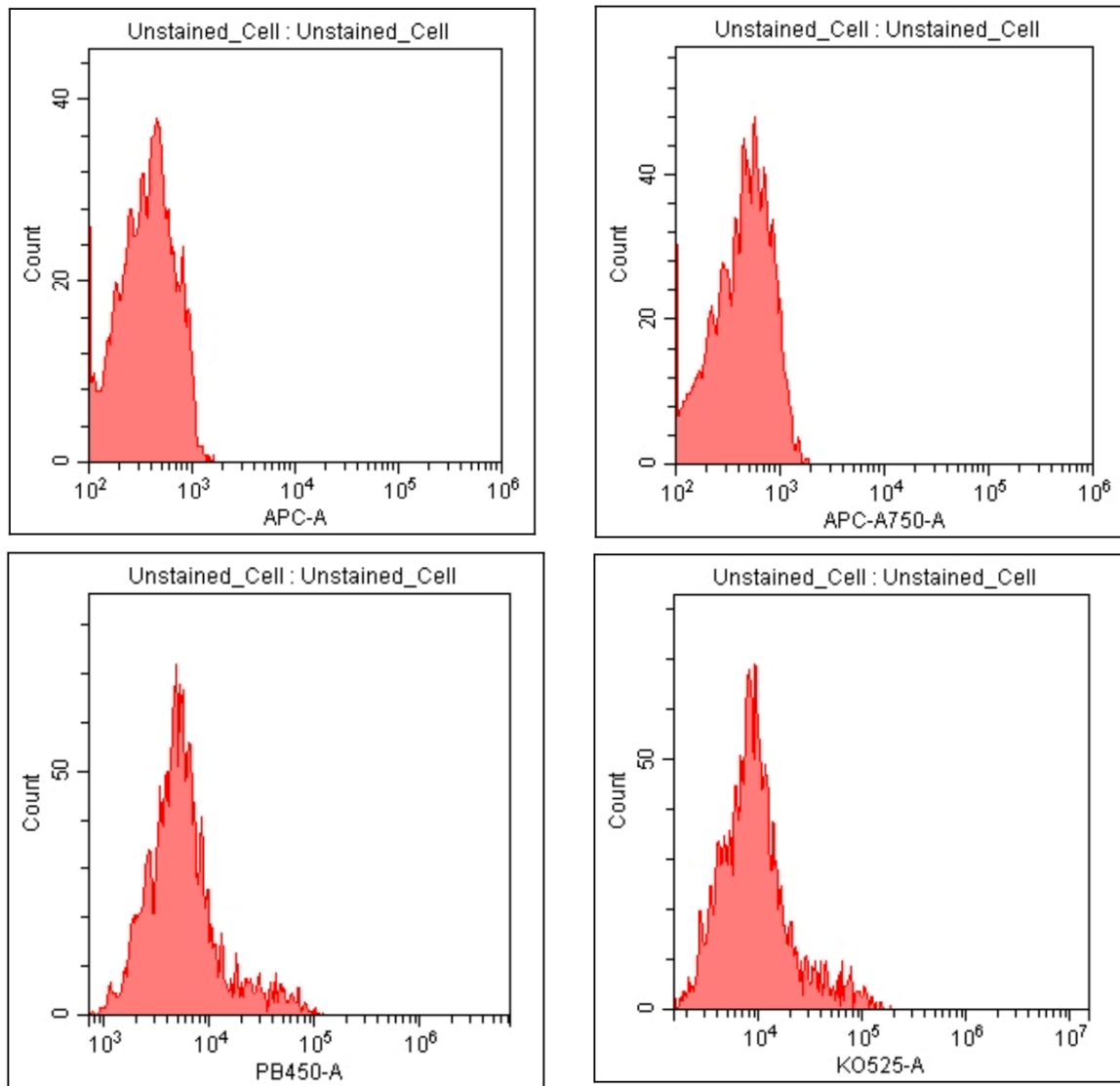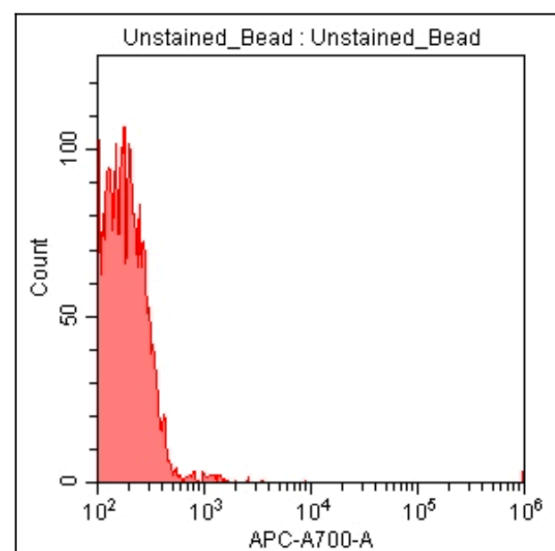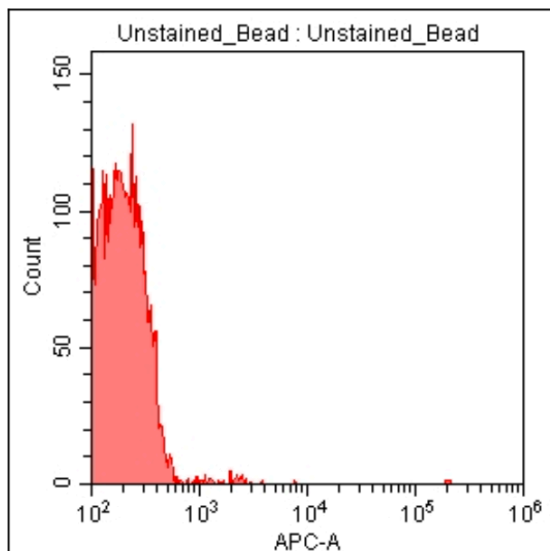First control for autofluorescence
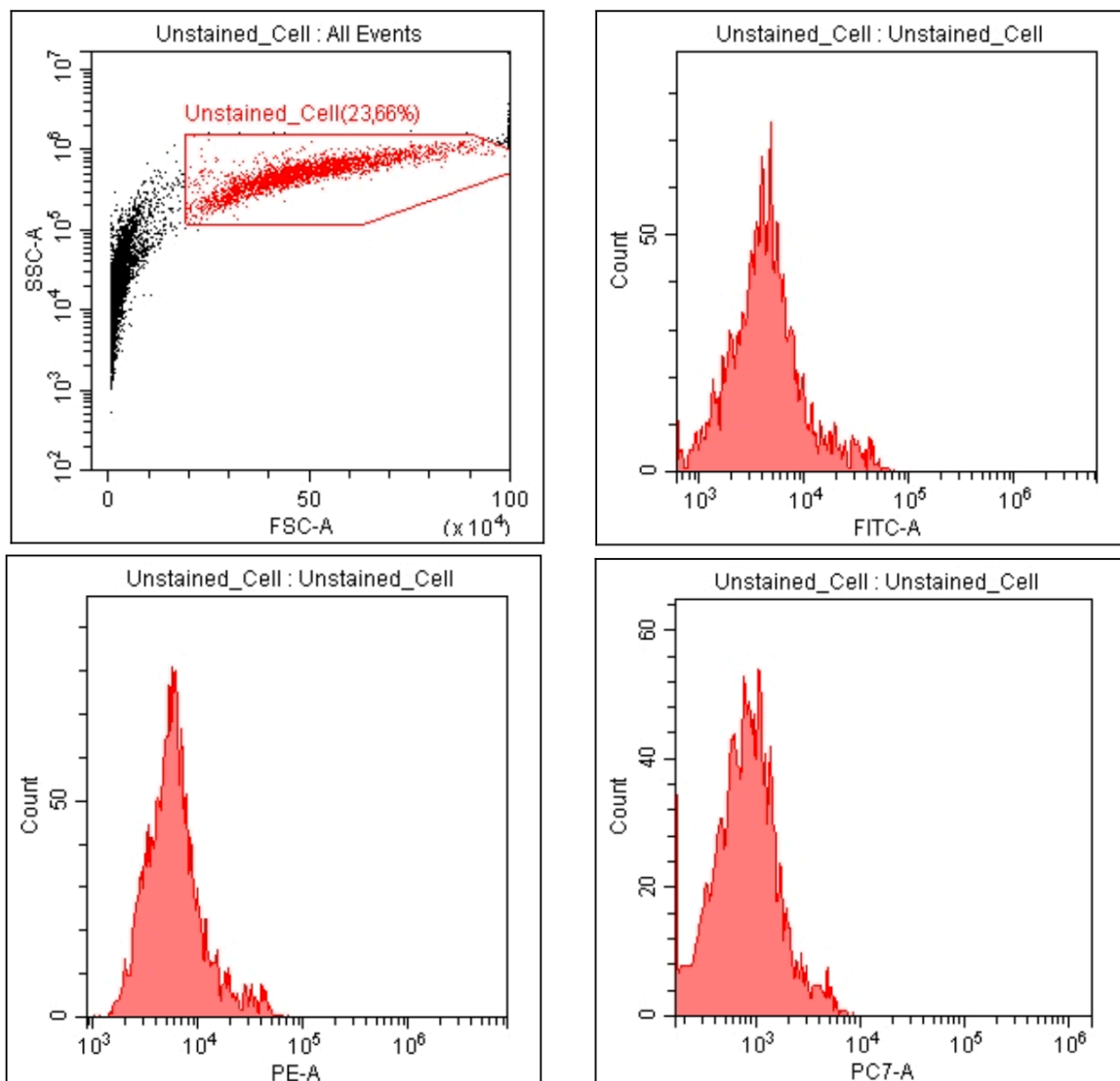
Figure E1. Colour compensation experiment set up to detect and correct for autofluorescence of unstained cells.

Unstained Beads
Second control for autofluorescence
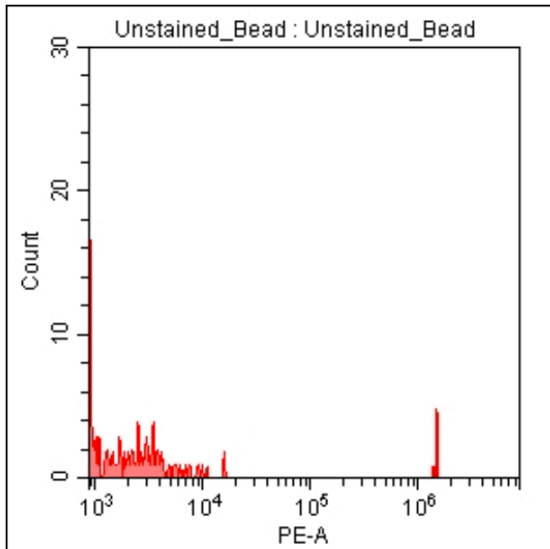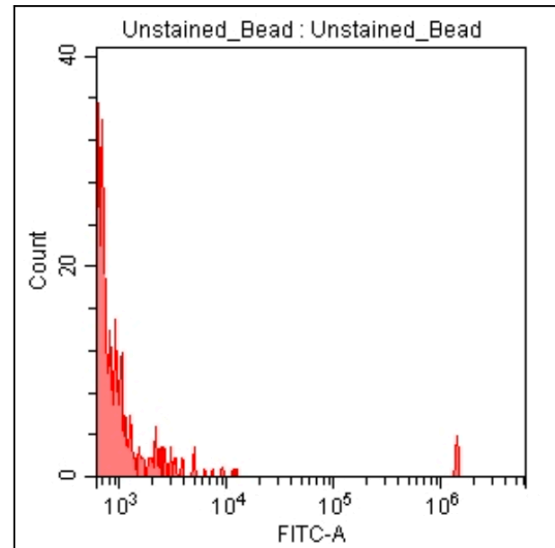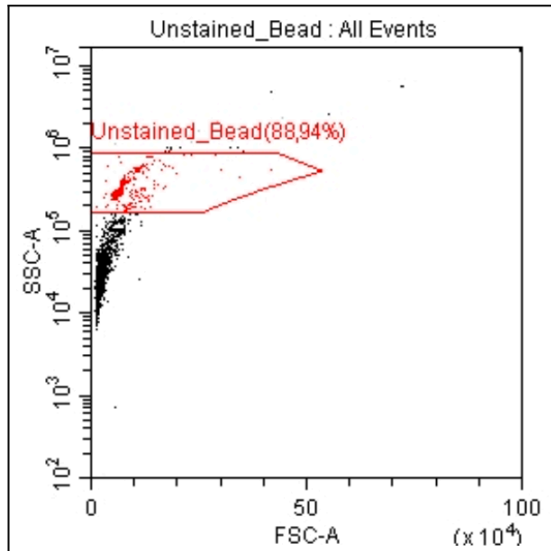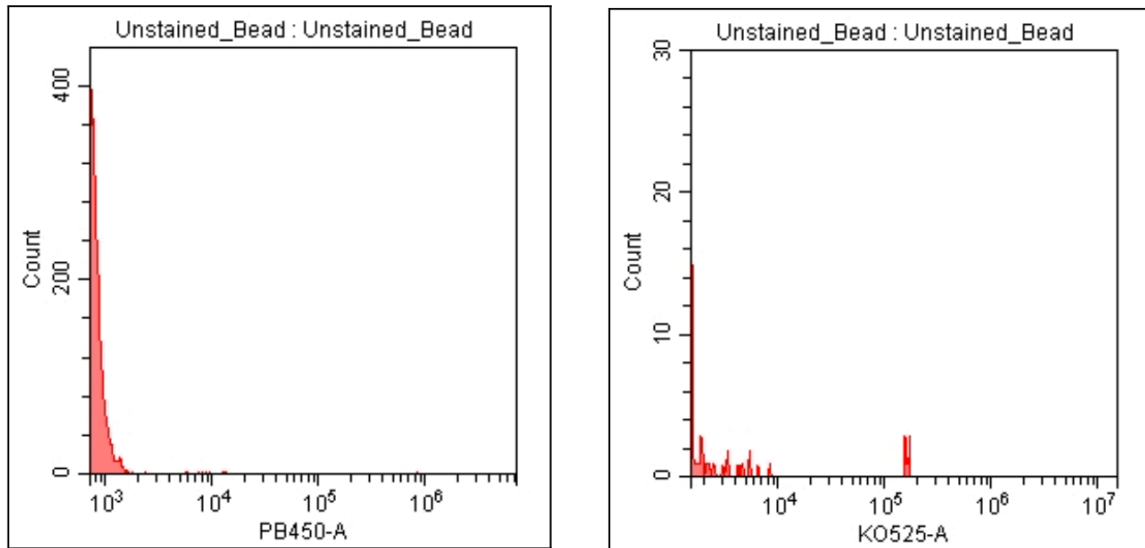
Figure E2. Colour compensation experiment set up to detect and correct for autofluorescence of beads.

FITC (FL1) channel:

To determine the spillover of FITC (conjugate) into the other fluorescence channels
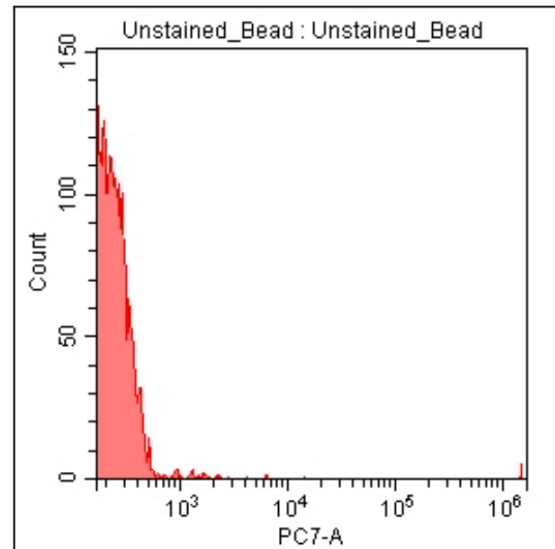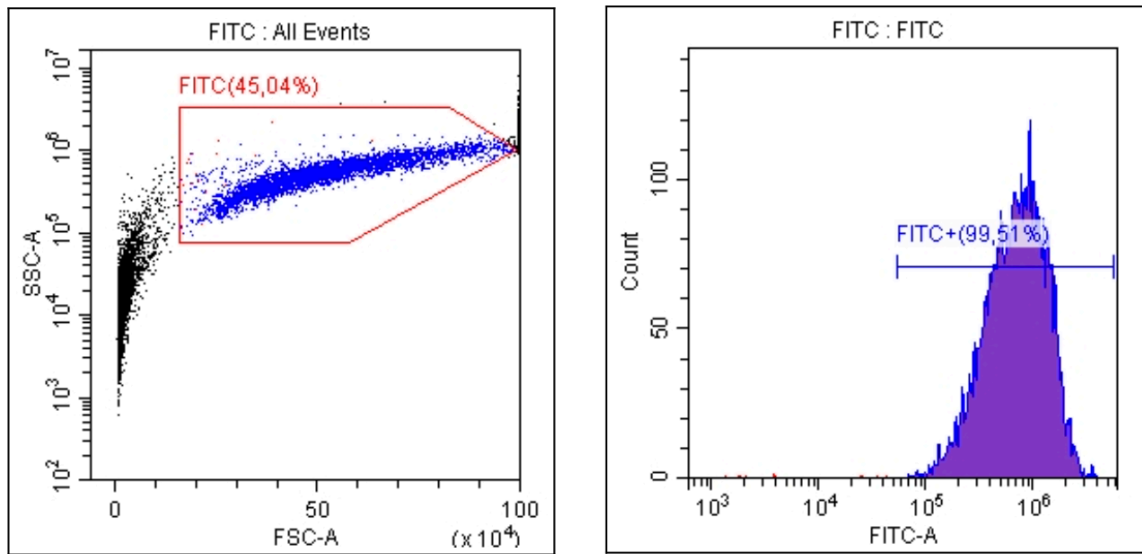
Figure E3. Colour compensation experiment set up to detect and correct for spill over from FITC into other channels.

PE (FL2 channel)
To determine the spillover of PE (conjugate) into the other fluorescence channels

Figure E4. Colour compensation experiment set up to detect and correct for spill over from PE into other channels.

PC7 (FL3 channel)
To determine the spillover of PC7 (conjugate) into the other fluorescence channels

Figure E5. Colour compensation experiment set up to detect and correct for spill over from PC7 into other channels.

To determine the spillover of APC (conjugate) into the other fluorescence channels
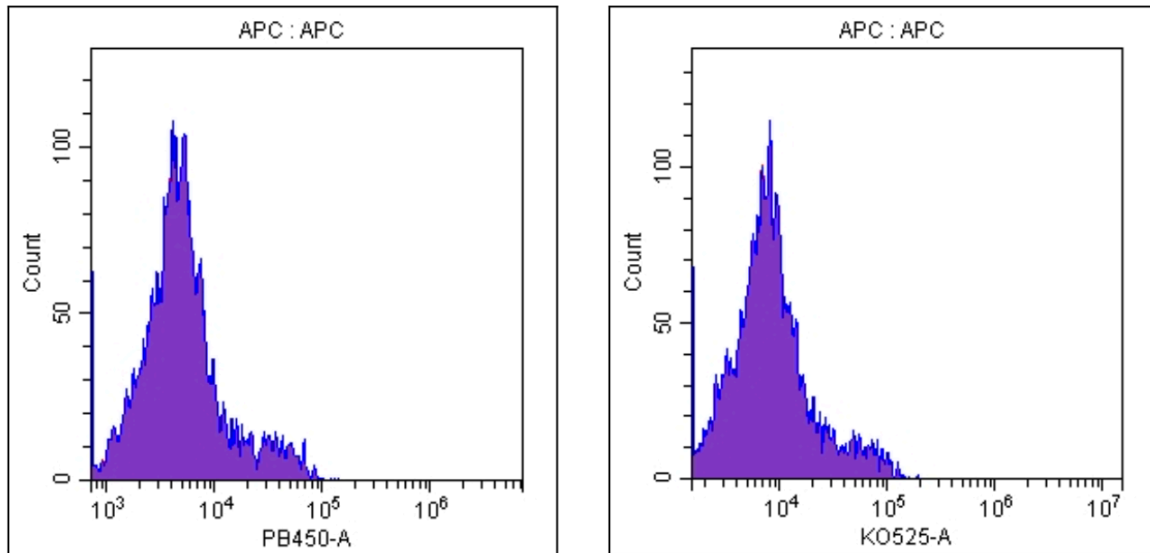
Figure E6. Colour compensation experiment set up to detect and correct for spill over from APC into other channels.

APC-A750 (FL8 channel)

To determine the spillover of APC-A750 (conjugate) into the other fluorescence channels
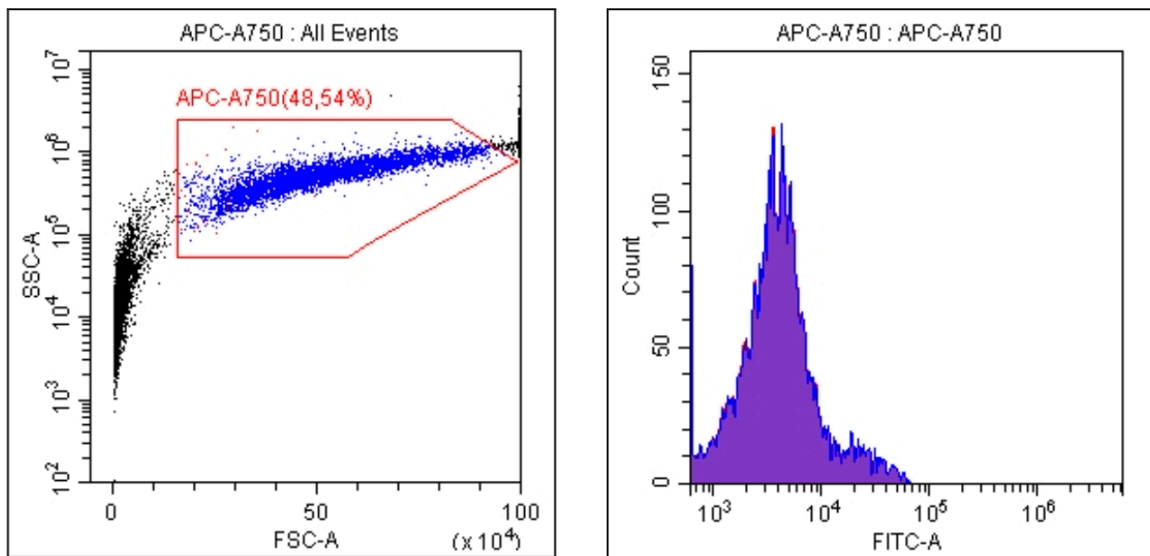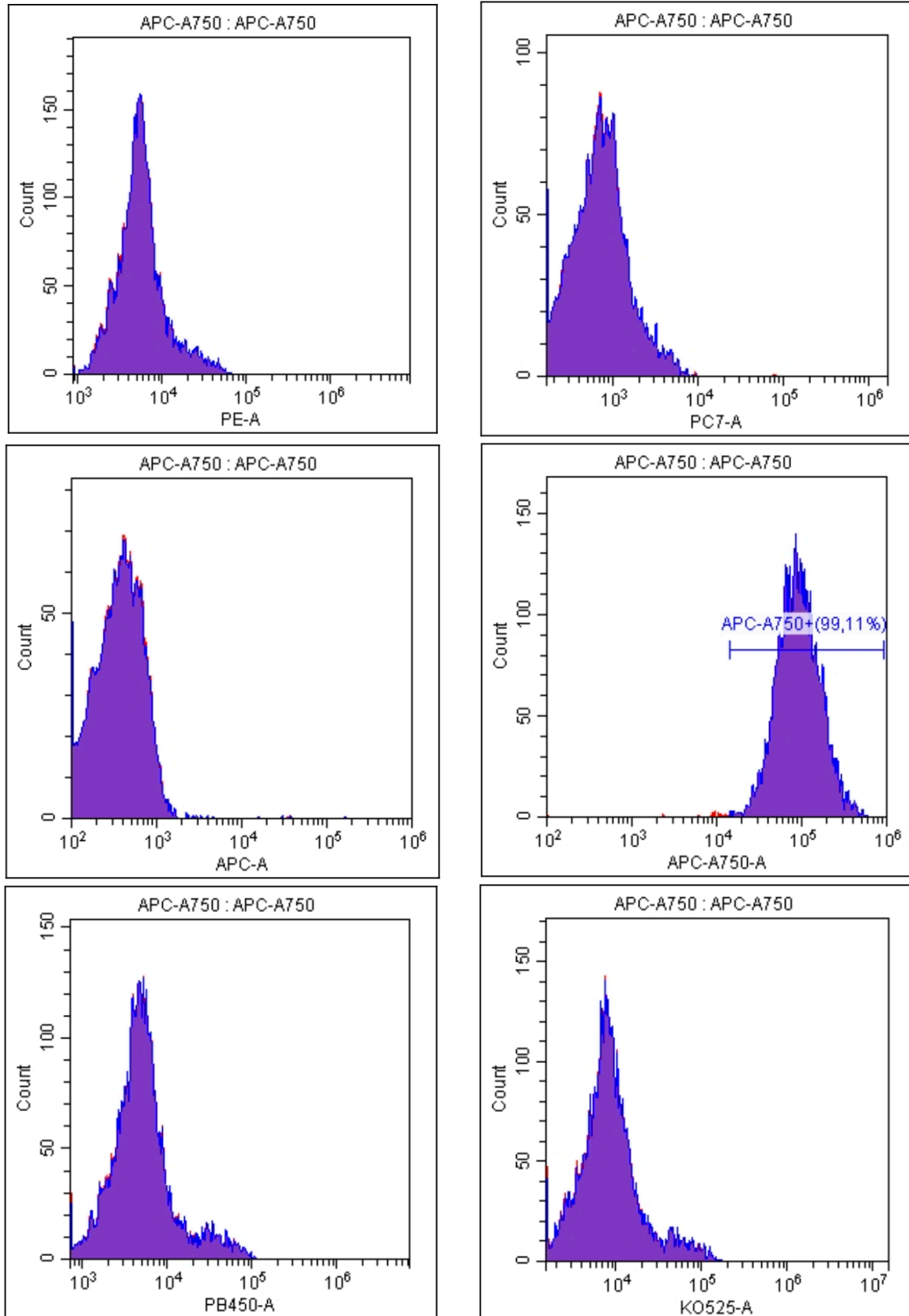
Figure E7. Colour compensation experiment set up to detect and correct for spill over from APC-A750 into other channels.

PB450 (FL9 channel)
To determine the spillover of PB450 (conjugate) into the other fluorescence channels
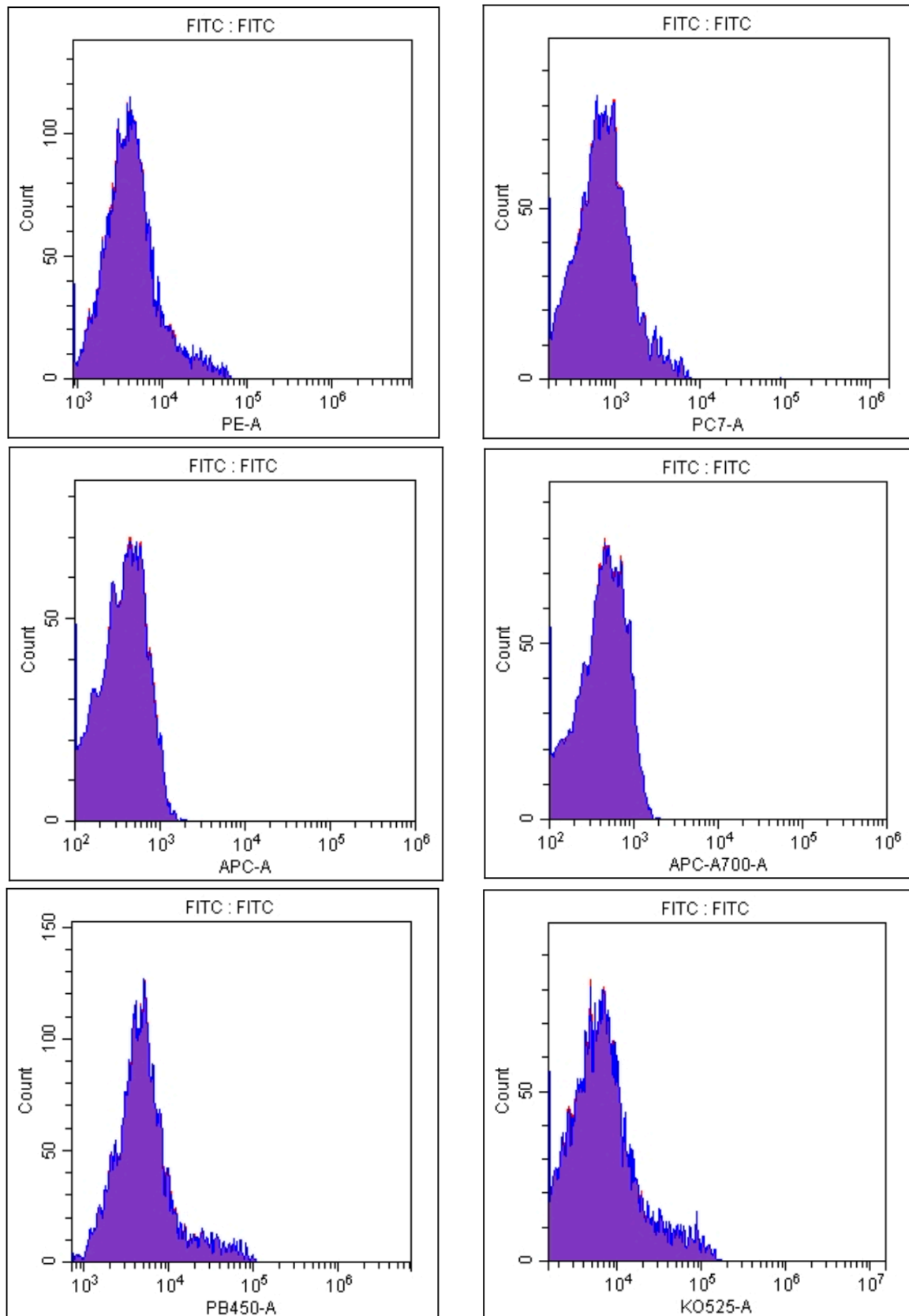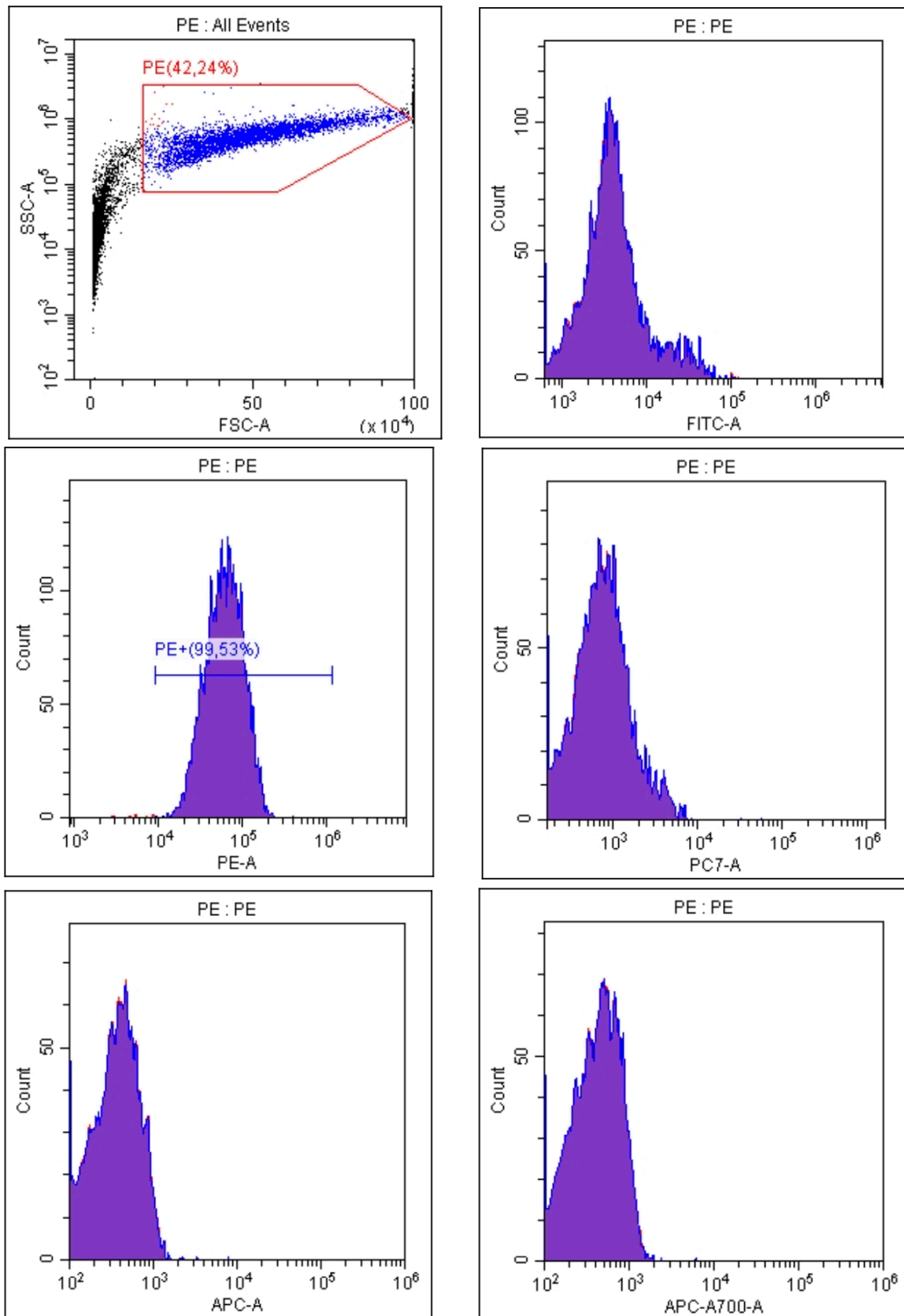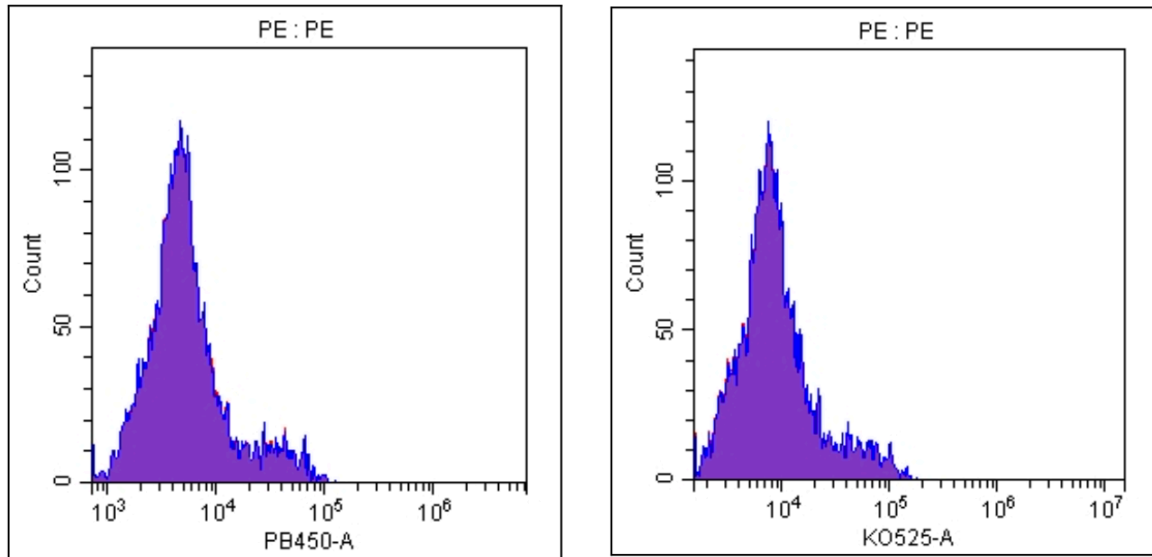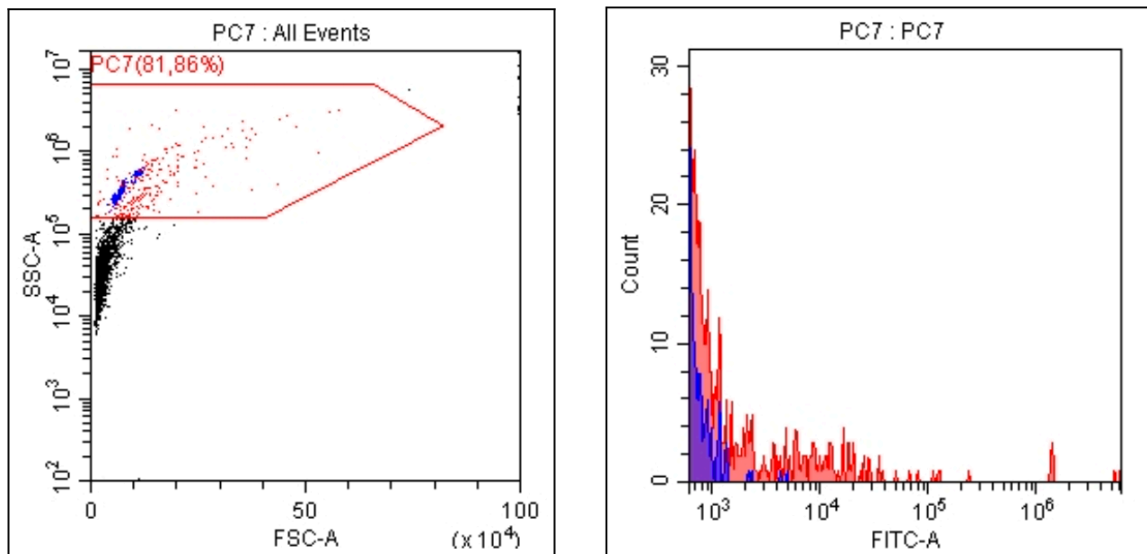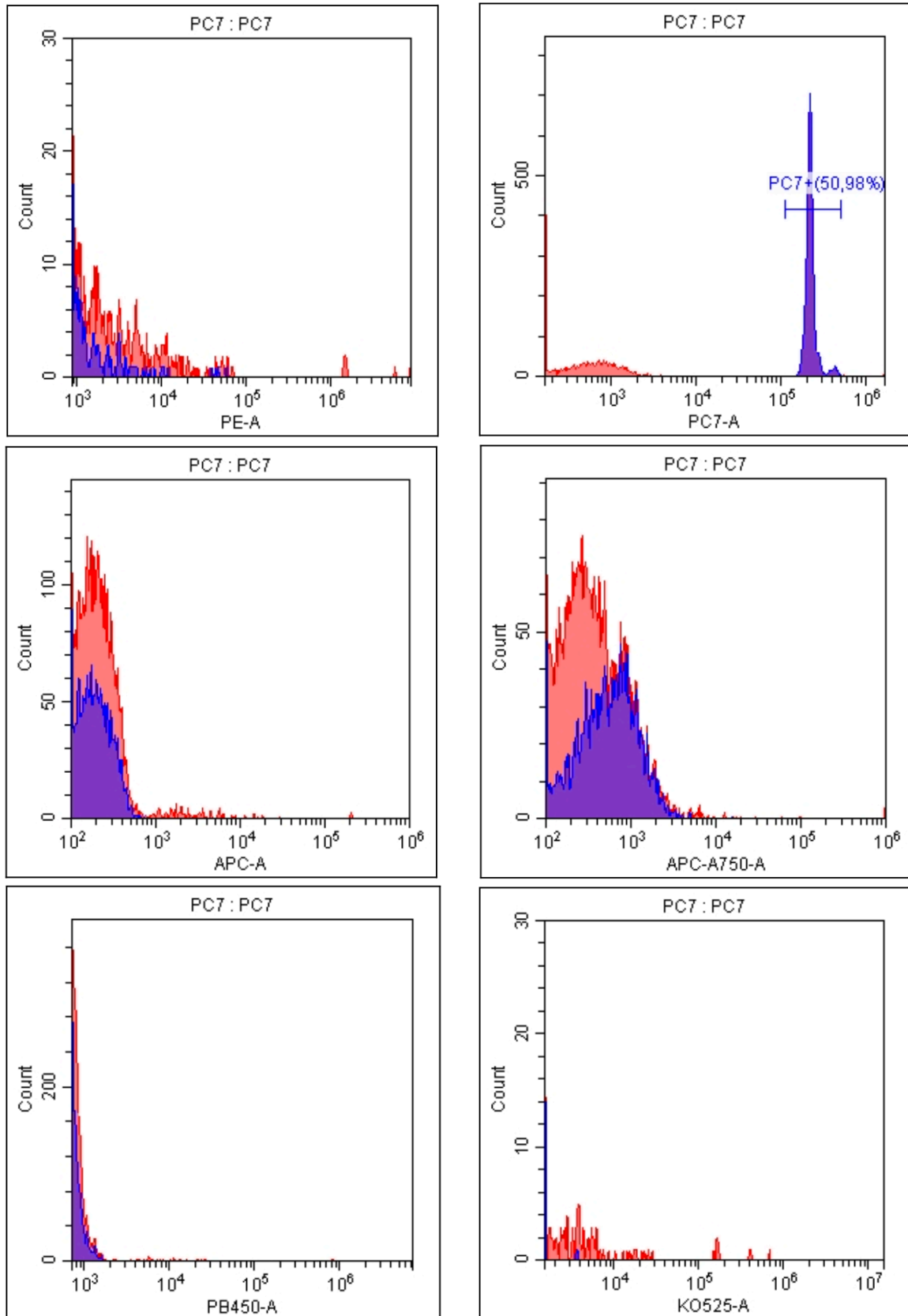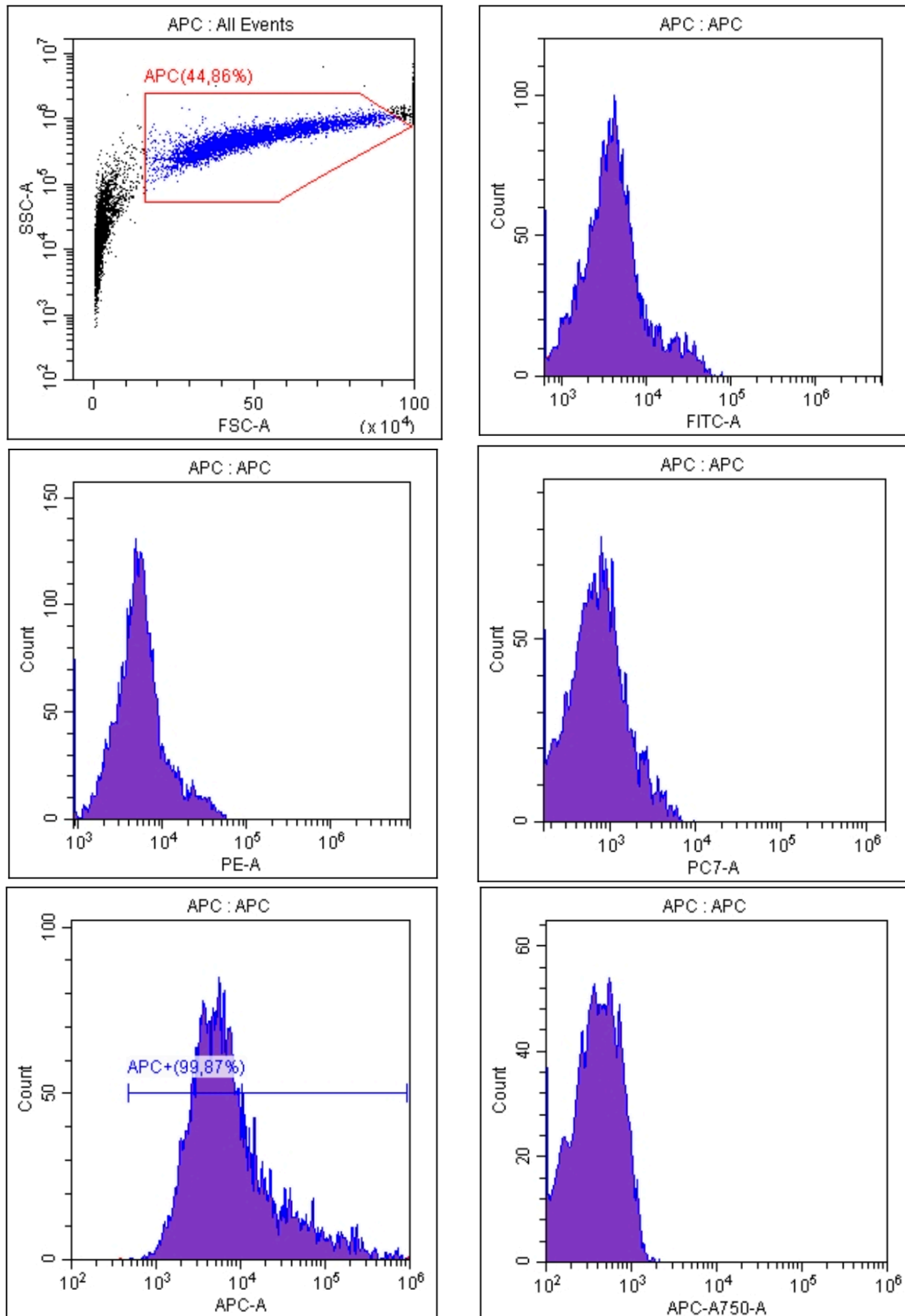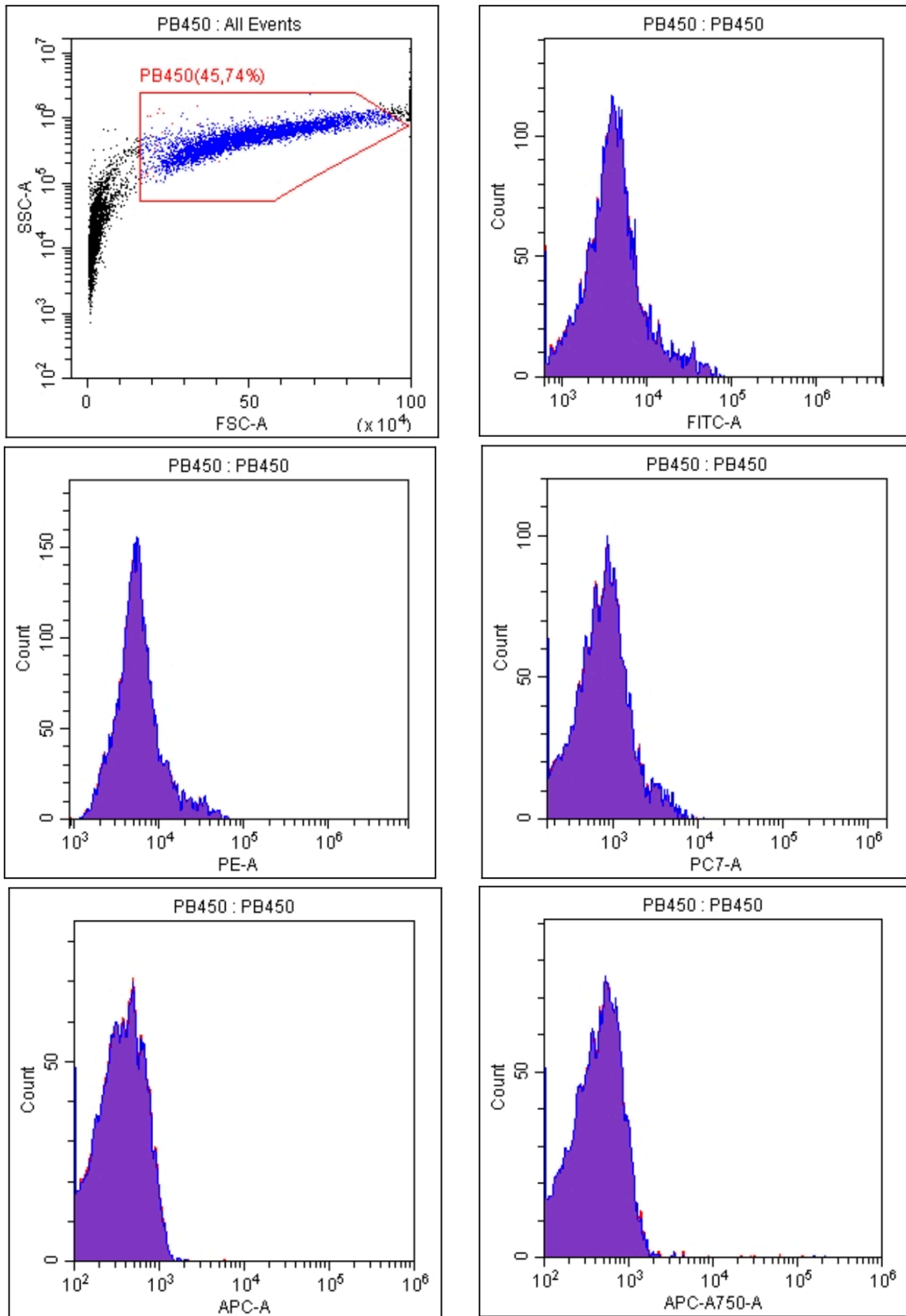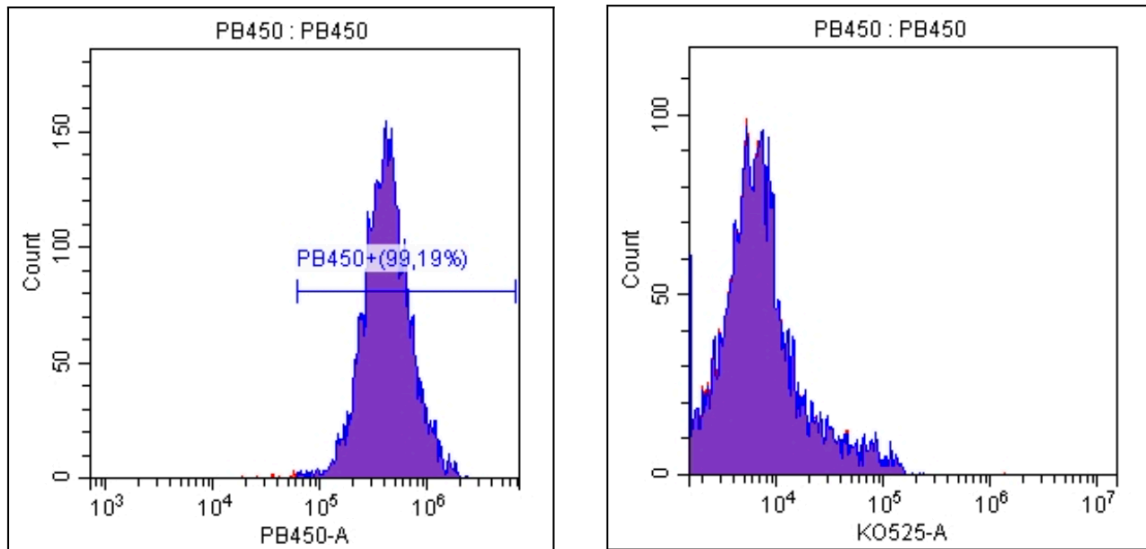
Figure E8. Colour compensation experiment set up to detect and correct for spill over from PB into other channels.

KO(FL10 channel)

To determine the spillover of KO (conjugate) into the other fluorescence channels
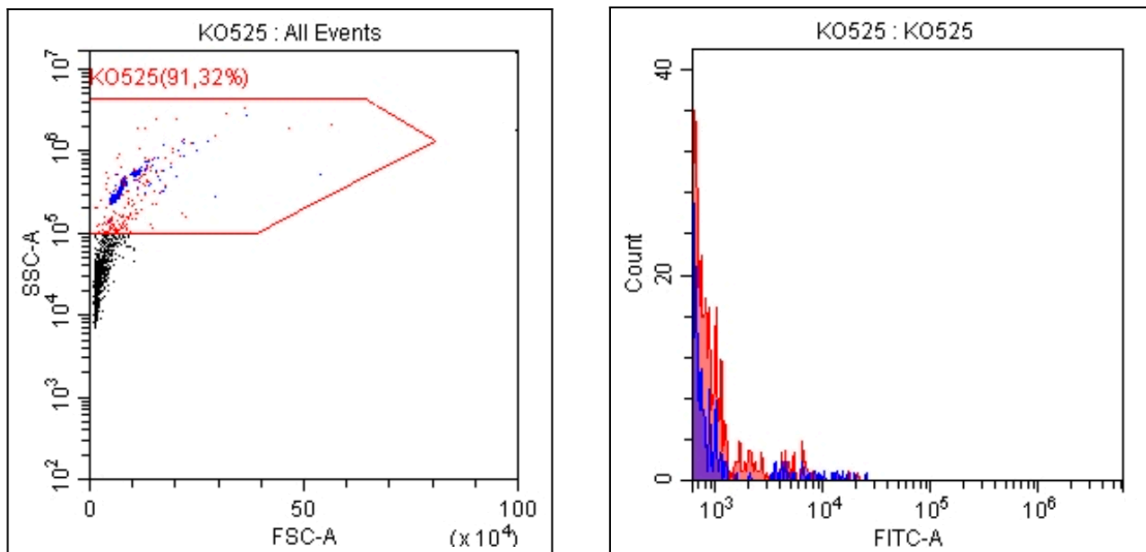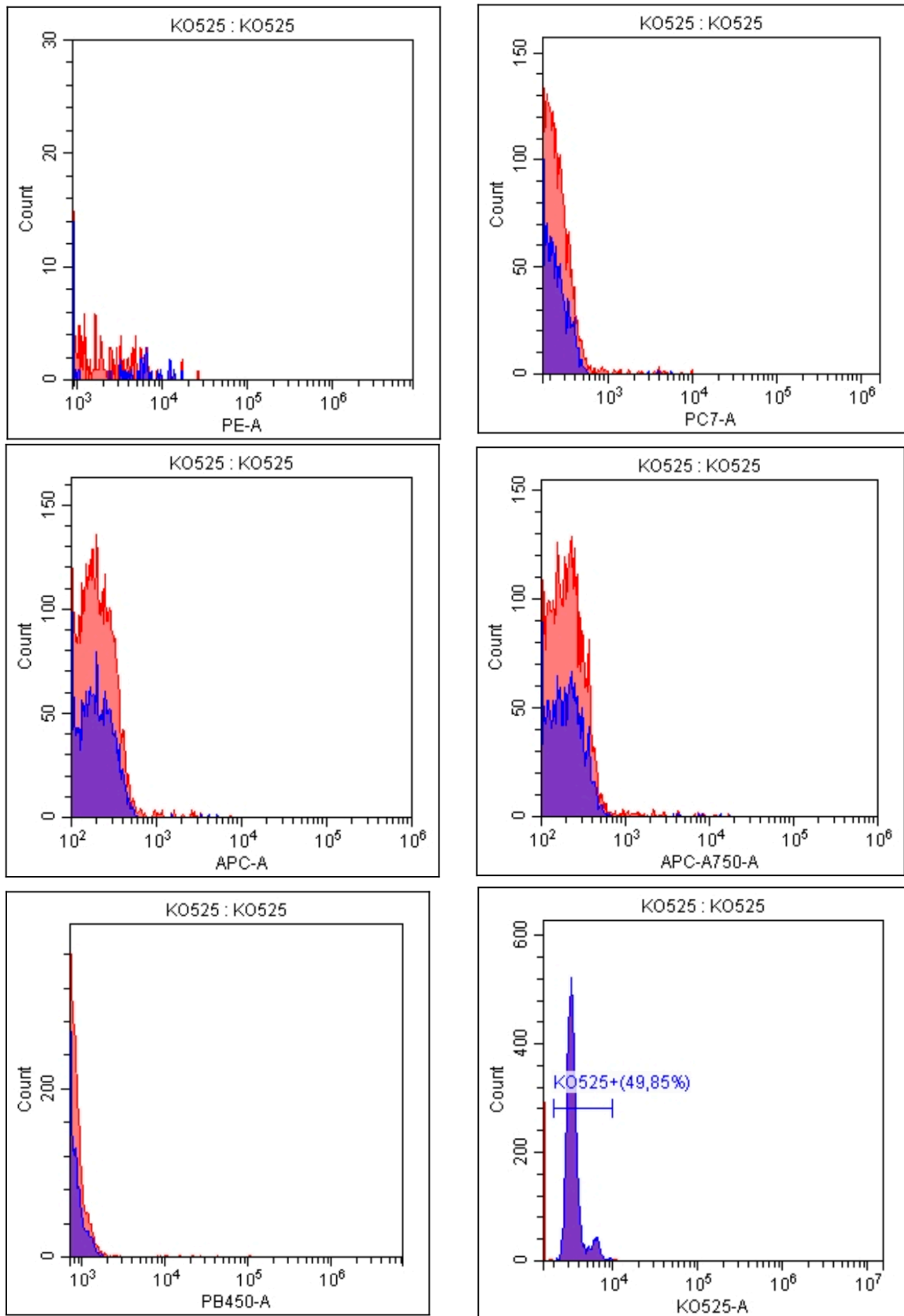
Figure E9. Colour compensation experiment set up to detect and correct for spill over from KO into other channels.

Appendix F: Minimum Information for Publication of Quantitative Real-Time PCR Experiments

Bustin et al. 2009 describe a set of guidelines that should be used for qPCR experiments [354]. When these guidelines are followed, data can be considered reliable. This study aimed to adhere to the MIQE guidelines as far as possible. All information labelled by the MIQE guidelines as 'essential' has been included in this document.

Experimental Design

Please refer to Chapter 5, section 5.2.8. – 5.2.11.

Definition of control and experimental groups and the numbers in each group

Three ASC biological replicates were used for each experimental group, and each replicate was run in triplicate for FBS and pHPL experiments. For PRP experiments, three ASC biological replicates and well as three donor PRP biological replicates were used, and each replicate was run in triplicate. For the controls, no induction medium was added, the cells were only maintained in the respective CGM. For experimental groups, cells were exposed to induction medium described in Chapter 5 section 5.2.5.

Sample

Description

RNA was isolated at the 4 timepoints (day 0, 7, 14, 21) throughout the differentiation process from both non-induced (control) and induced samples.

Microdissection or macrodissection

The samples were not subjected to micro- or macrodissection.

Processing

Please refer to Chapter 5, section 5.2.8. – 5.2.11.

If frozen -how and how quickly?

Please refer to Chapter 5 section 5.2.8.

If fixed -how and how quickly?

Samples for RT-qPCR were not fixed.

Storage

RNA extraction was performed immediately after trypsinisation (0.25% Trypsin/EDTA). The extracted RNA was then stored at -80°C until cDNA could be synthesised. cDNA was stored at -20°C until it was used for RT-qPCR.

Nucleic Acid Extraction

Total RNA was isolated from samples as described in Chapter 5 section 5.2.8.

DNAse or RNase treatment

Samples were not treated with DNase or RNase.

Contamination assessment

During the cDNA experiments, NRTs controls were generated. The reference gene TBP was used in the RT-qPCR reaction mix to determine if there was any genomic DNA (gDNA) contamination (Figure F1).
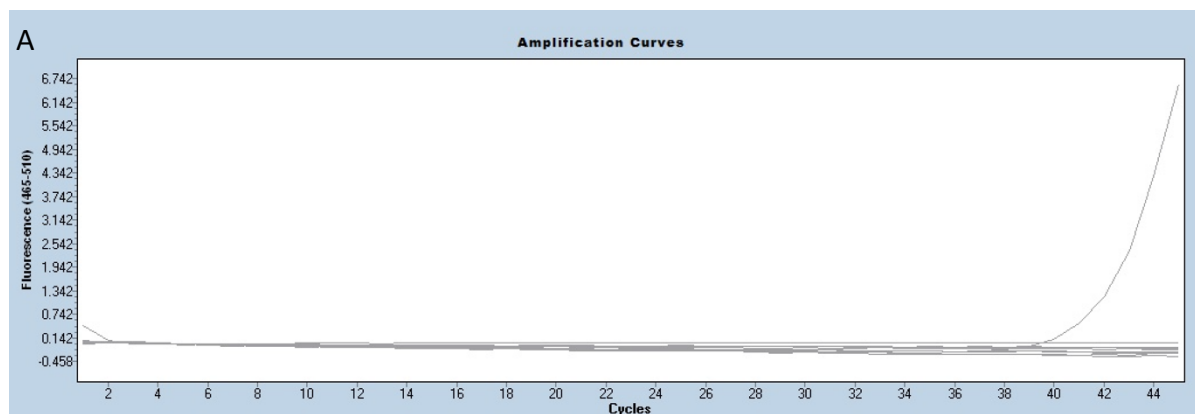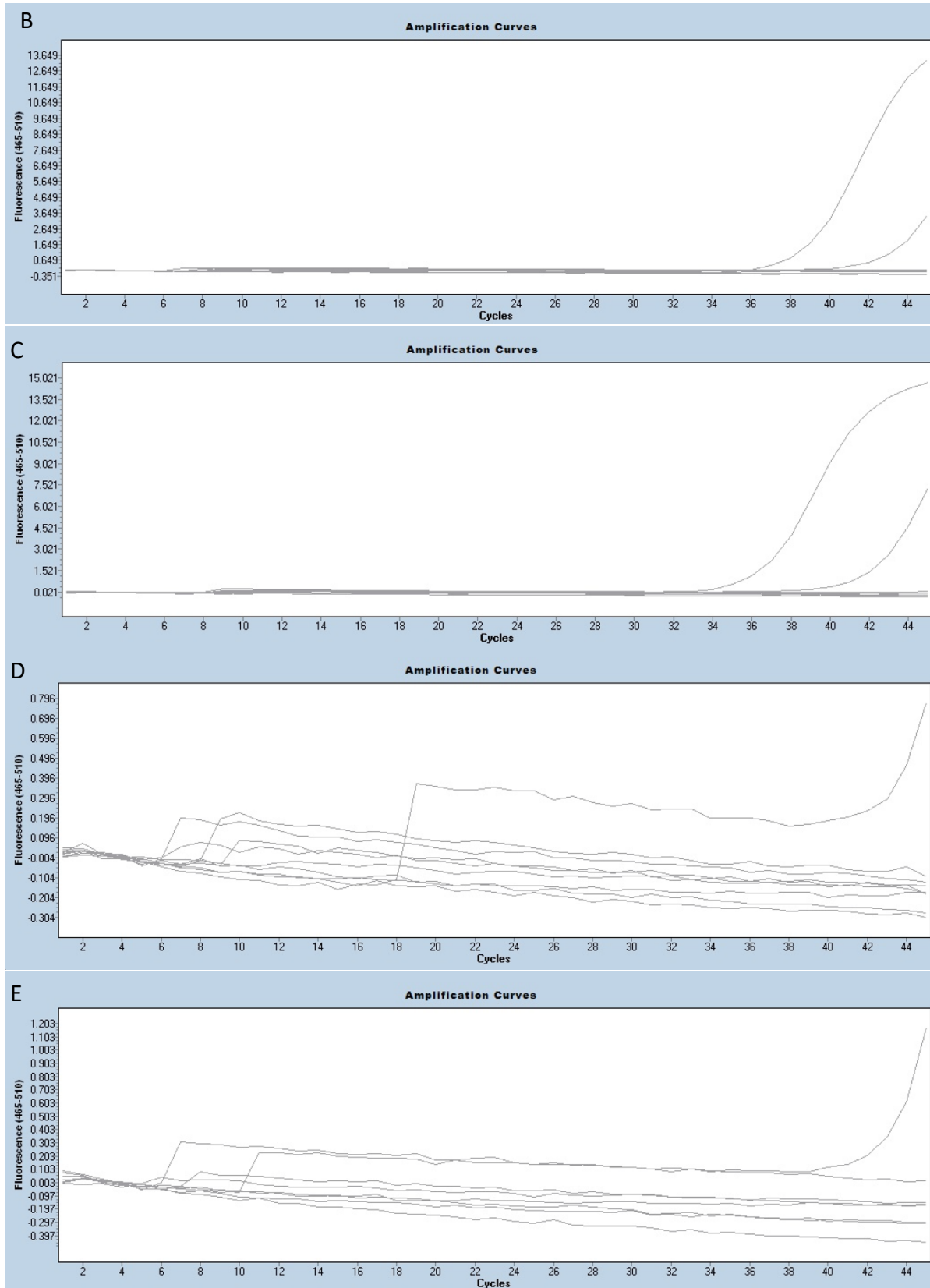
Figure F1. Amplification Curves for respective NRT controls.
A-E show FBS, pHPL, PRP070721, PRP240821 and PRP260821 respectively, amplification curves using the TBP gene to detect the presence of any gDNA using 2ng/ul of template. In some cases, there was amplification of NRT samples at 35 or more cycles indicating small to negligible amount of gDNA contamination.

Little to no gDNA contamination was seen in the samples. Some gDNA contamination was seen in FBS, pHPL and PRP070721 samples (Figure F1, B-C). In the instances where amplification was seen, it was only seen in one of the three technical repeats and not across all three repeats The amplification of the gDNA in these samples occurred at a Ct of 35 or greater.

Nucleic acid quantification, purity, and integrity

Please see Chapter 5 section 5.2.8.- 5.2.11 for sample preparation and instruments used to determine quantity, purity, and integrity of samples. Table F1 summarizes to concentrations, purity and integrity values for samples used in this study.

Table F1. Total RNA concentration, purity and integrity values for samples used in this study.

Culture	Timepoint	Non-induced(NI) /Induced(I)	NanoDrop® ND 1000 spectrophotometer			Tapestation ®2200		
			Concentration (ng/ul)	A260/280	A260/230	Concentration (ng/ul)	28S/18S (Area)	RINe
					FBS			
A150221-01A	0		179.49	2.06	2.14	115	2.2	10
A311019-01A	0		107.71	2.04	2.1			
A311019-02T	0		50.47	2.05	1.54			
A150221-01A	7	NI	433.75	1.94	0.79	62.9	0.4	9.5
A150221-01A	7	I	336.54	1.86	0.73	151	0.2	9.5
A311019-01A	7	NI	534.53	1.63	0.28	26.6	0.3	9.3
A311019-01A	7	I	613.45	1.65	0.32	309	3.1	9.6
A311019-02T	7	NI	381.09	1.87	0.98	334	3	9.8
A311019-02T	7	I	571.4	1.7	0.35	355	3	9.6
A150221-01A	14	NI	68.96	2.06	1.59	100	2.6	9.9
A150221-01A	14	I	201.72	1.93	1.42	205	2.9	9.8
A311019-01A	14	NI	107.98	1.99	1.52			
A311019-01A	14	I	125.71	2	1.79			
A311019-02T	14	NI	134.97	2.04	2.04	171	3	9.9
A311019-02T	14	I	200.21	2.06	1.53			
A150221-01A	21	NI	138.78	2.04	1.95			
A150221-01A	21	I	213.68	2.06	2.15			
A311019-01A	21	NI	120.11	2.11	2.03	90.1	3.1	10
A311019-01A	21	I	172.68	2.05	2.17			
A311019-02T	21	NI	190.15	2.06	1.83			

A311019-02T	21	I	205.19	2.06	2.07	277	3.5	9.8
pHPL								
A311019-01A	0		72.46	2.15	2.21			
A311019-02T	0		35.44	2.16	1.51			
A280621-01R	0		176.73	2.08	1.91	277	3	10
A150221-01A	7	NI	40	2.17	2.11			
A150221-01A	7	I	95.07	2.1	2.23			
A311019-01A	7	NI	98.91	2.9	2.94	66.6	2.7	10
A311019-01A	7	I	11.29	2.11	0.45	16.8	2.1	9.6
A311019-02T	7	NI	64.25	2.12	2.15			
A311019-02T	7	I	14	2.51	0.03	44.5	2.1	9.4
A280621-01R	7	NI	65.8	2.02	2.14			
A280621-01R	7	I	239.02	2.06	2.1	449	1.9	9.6
A150221-01A	14	NI	64.6	2.05	1.81			
A150221-01A	14	I	34.69	1.97	1.88			
A311019-01A	14	NI	12.11	1.74	1.58	35.4	2	9.4
A311019-01A	14	I	1.41	3.34	0.07	8.28		3.7*
A311019-02T	14	NI	18.89	1.65	0.82	36.5	2.1	9.9
A311019-02T	14	I	8.73	1.75	0.47	6.45		8
A280621-01R	14	NI	119.78	2.03	1.97	150	2.5	9.8
A280621-01R	14	I	476.59	2.02	1.84	342	3.2	9.8
A150221-01A	21	NI	33.04	1.95	0.36			
A150221-01A	21	I	253.83	2.06	1.11			
A311019-01A	21	NI	65.68	2.09	1.23			
A311019-01A	21	I	35.9	2.09	0.65	4.5		2.7*
A311019-02T	21	NI	47.95	2.05	1.41	50.5	2.3	9.8

A311019-02T	21	I	22.37	1.79	1.2	5.52	1.5	6.1*
A280621-01R	21	NI	136.55	2.1	2.18			
A280621-01R	21	I	147.1	2.1	2.12			
PRP070721								
A280621-01R	0		103,95	0.75	1.13	117	3.2	10
A311019-01A	0		63.1	2.09	1.62			
A311019-02T	0		43.49	0.07	1.61	22	2.4	10
A280621-01R	7	NI	224.78	2.07	2.17			
A280621-01R	7	I	519.2	2.07	2.18			
A311019-01A	7	NI	303.15	2.04	1.62	181	2.9	9.7
A311019-01A	7	I	312.89	2.05	1.89			
A311019-02T	7	NI	227.26	2.06	1.93			
A311019-02T	7	I	294.45	2.05	2.15	269	3.2	9.9
A280621-01R	14	NI	189.39	2	1.81			
A280621-01R	14	I	267.52	2.07	1.99			
A311019-01A	14	NI	205.69	2.07	2.11	419	3.3	9.8
A311019-01A	14	I	313.81	2.05	2.2	402	3	9.4
A311019-02T	14	NI	159.56	2.06	1.87			
A311019-02T	14	I	146.93	2.05	1.86			
A280621-01R	21	NI	174.47	2.1	2.16			
A280621-01R	21	I	525.98	2.06	2.16			
A311019-01A	21	NI	294.82	2.07	2.17			
A311019-01A	21	I	179.51	2.08	2.13			
A311019-02T	21	NI	106.29	2.08	1.43	64.9	2.1	9.5
A311019-02T	21	I	147.38	2.12	1.95	168	2.9	9.5
PRP240821								

A280621-01R	0		263.7	2.01	0.8	574	3.4	10
A311019-01A	0		214.02	1.98	0.79	277	4	10
A311019-02T	0		136.46	1.99	0.72	71	3.3	10
A280621-01R	7	NI	200.7	2.06	2.11			
A280621-01R	7	I	432.55	2.03	2.28	743	3.7	9.7
A311019-01A	7	NI	236.86	2.08	2.3	247	2.7	9.6
A311019-01A	7	I	286.53	2.07	2.38			
A311019-02T	7	NI	214.13	2.11	2.33			
A311019-02T	7	I	141.58	2.07	2.05			
A280621-01R	14	NI	549.06	2.1	2.27	676	2.8	9.2
A280621-01R	14	I	167.14	2.11	2.24			
A311019-01A	14	NI	251.32	2.05	2.21			
A311019-01A	14	I	14.12	3.51	1.31			
A311019-02T	14	NI	173.15	2.09	2.08			
A311019-02T	14	I	336.46	2.05	2.23	382	3.3	9.7
A280621-01R	21	NI	904.31	2.11	2.27	309	2.7	9.6
A280621-01R	21	I	401.28	2.04	2			
A311019-01A	21	NI	296.97	2.09	1.54			
A311019-01A	21	I	161	2.09	1.62	79.6	2.8	9.4
A311019-02T	21	NI	84.48	2.12	1.83			
A311019-02T	21	I	52.2	1.9	1.23			
PRP260821								
A280621-01R	0		276.86	1.79	0.6	13.2	2.3	10
A311019-01A	0		141.82	1.72	0.33	7.76	2.3	10
A311019-02T	0		97.49	1.7	0.27	6.64	1.9	10
A280621-01R	7	NI	73.51	2.07	2.38	63.4	2.4	10

A280621-01R	7	I	182.11	2.11	2.42			
A311019-01A	7	NI	96.45	2.1	2.03			
A311019-01A	7	I	231.96	2.08	2.26	258	2.8	9.9
A311019-02T	7	NI	66.24	2.17	2.23			
A311019-02T	7	I	196.17	2.08	2.18			
A280621-01R	14	NI	167.33	2.12	2.28	161	2.2	9.3
A280621-01R	14	I	56.08	2.09	2.14			
A311019-01A	14	NI	51.69	2.24	2.12			
A311019-01A	14	I	23.98	2.25	1.24	37.4	2.3	9.4
A311019-02T	14	NI	64.4	2.2	2.09			
A311019-02T	14	I	141.17	2.09	2			
A280621-01R	21	NI	224.16	2.08	2.02			
A280621-01R	21	I	229.64	2.08	2.04	121	3	9.5
A311019-01A	21	NI	52.65	1.92	0.82	25.4	2.1	9.8
A311019-01A	21	I	97.04	2.08	1.62			
A311019-02T	21	NI	121.48	2.04	1.91	28.4	2.4	9.8
A311019-02T	21	I	157.83	2.04	1.92			

*Any sample with a RIN^e value lower than 6.5, together with its counterpart (e.g. pHPL sample A311019-01A Day 14 I had a RIN^e value of 3.7 therefore this sample together with sample A311019-01A Day 14 NI was excluded from downstream experiments).

Inhibition testing

No inhibition testing was performed.

Reverse Transcription

Please see Chapter 5 section 5.2.10 for details regarding the synthesis of cDNA. To convert mRNA isolated from cells to cDNA the SensiFastTM cDNA synthesis kit (Bioline, London, England) was used. Information provided by the kit: *"one unit catalyses the incorporation of 1 nmol of dTTP into acid- soluble material in 10 min at 370C in 50nM Tris-HCL, pH8.6, 40nm KCl, 1mM MnSO4, 1 mM DTT, and 0.5 mM [3H]TTP, using 200 µM oligo(dT)12- 18-primed poly(A)n as template."*

cDNA quantification and purity

Please see Chapter 5 sections 5.2.8, 5.2.9 and 5.2.10 regarding the synthesis of cDNA and the determination of purity and integrity. The NanoDrop® ND 1000 spectrophotometer was used to determine the concentration(ng/ul), A260/A280 ratio and A260/230 for cDNA.

Quantitation cycle (Cq) values with and without reverse transcriptase (RT)

NRTs were produced for 10% of samples. These samples were selected for at random. The reference gene TBP was used for the detection of gDNA contamination using a template concentration of 2ng/ul. The results obtained is summarised in Table F2, while the results are visually represented in Figure F1.

Table F2. Cq values of NRT control sample.

Medium Supplementation	Culture	Timepoint	Non-induced(NI) /Induced(I)	Cq (Average of three technical repeates)
FBS	A150221-01A	0		40
	A311019-02T	0		ND
	A311019-02T	21	I	ND
pHPL	A311019-01A	0		ND
	A311019-01A	7	NI	40
	A280621-01R	7	I	38.4
PRP070721	A280621-01R	0		36.01
	A311019-01A	7	NI	ND

	A280621-01R	14	NI	40
PRP240821	A311019-02T	7	NI	ND
	A311019-02T	7	I	ND
	A280621-01R	14	NI	ND
PRP260821	A280621-01R	7	I	40
	A280621-01R	14	I	ND
	A311019-02T	14	I	ND

Cq=Ct=Crossing point; ND= Not detected.

cDNA Storage

Once the mRNA was converted to cDNA, the cDNA was stored at -20°C until used in RT-qPCR experiments.

qPCR target information

Please see chapter 5 section 5.2.11, Table 5.2 for the forward and reverse primer sequences for each gene of interest.

In silico specificity screen and primer locations

The NCBI Primer BLAST® tool was used to determine the specificity of the primers. Results from NCBI Primer BLAST® tool are displayed in Figure F2.

OCN

	Sequence (5'->3')	Length	Tm	GC%	Self complementarity	Self 3' com
Forward primer	ACCCTTCTTTCCTCTTCC	18	52.88	50.00	1.00	0.00
Reverse primer	CCCACAGATTCCTCTTCT	18	52.67	50.00	3.00	0.00

Products on target templates
>NM_001199662.1 Homo sapiens PMF1-BGLAP readthrough (PMF1-BGLAP), transcript variant 2, mRNA

```
product length = 111
Forward primer  1     ACCCTTCTTTCCTCTTCC   18
Template        884   ..................   901

Reverse primer  1     CCCACAGATTCCTCTTCT   18
Template        994   ..................   977
```

PPARγ

	Sequence (5'->3')	Length	Tm	GC%	Self complementarity	Self 3' com
Forward primer	CGTGGATCTCTCCGTAAT	18	53.11	50.00	4.00	2.00
Reverse primer	TGGATCTGTTCTTGTGAATG	20	53.21	40.00	4.00	0.00

Products on target templates
>NM_001354666.3 Homo sapiens peroxisome proliferator activated receptor gamma (PPARG), transcript variant 6, mRNA

```
product length = 124
Forward primer  1     CGTGGATCTCTCCGTAAT    18
Template        441   ..................    458

Reverse primer  1     TGGATCTGTTCTTGTGAATG  20
Template        564   ....................  545
```

FABP4

	Sequence (5'->3')	Length	Tm	GC%	Self complementarity	Self 3' com
Forward primer	ATCAACCACCATAAAGAGAAA	21	52.71	33.33	2.00	0.00
Reverse primer	ACCTTCAGTCCAGGTCAA	18	54.82	50.00	5.00	0.00

Products on target templates
>NM_001442.3 Homo sapiens fatty acid binding protein 4 (FABP4), mRNA

```
product length = 126
Forward primer  1     ATCAACCACCATAAAGAGAAA   21
Template        369   .....................   389

Reverse primer  1     ACCTTCAGTCCAGGTCAA   18
Template        494   .A................   477
```

TBP

	Sequence (5'->3')	Length	Tm	GC%	Self complementarity	Self 3' com
Forward primer	CCGAAACGCCGAATATAA	18	52.62	44.44	4.00	2.00
Reverse primer	GGACTGTTCTTCACTCTTG	19	52.94	47.37	3.00	0.00

Products on target templates
>NM_001172085.2 Homo sapiens TATA-box binding protein (TBP), transcript variant 2, mRNA

```
product length = 130
Forward primer  1     CCGAAACGCCGAATATAA   18
Template        602   ..................   619

Reverse primer  1     GGACTGTTCTTCACTCTTG   19
Template        731   ...................   713
```

GUSB

	Sequence (5'->3')	Length	Tm	GC%	Self complementarity	Self 3' com
Forward primer	GATCGCTCACACCAAATC	18	53.57	50.00	4.00	0.00
Reverse primer	TCGTGATACCAAGAGTAGTAG	21	53.71	42.86	6.00	1.00

Products on target templates
>XM_047420289.1 PREDICTED: Homo sapiens glucuronidase beta (GUSB), transcript variant X6, mRNA

```
product length = 132
Forward primer  1     GATCGCTCACACCAAATC   18
Template        707   ..................   724

Reverse primer  1     TCGTGATACCAAGAGTAGTAG   21
Template        838   .....................   818
```

YWHAZ

	Sequence (5'->3')	Length	Tm	GC%	Self complementarity	Self 3' com
Forward primer	TGACATTGGGTAGCATTAAC	20	53.27	40.00	4.00	2.00
Reverse primer	GCACCTGACAAATAGAAAGA	20	53.22	40.00	3.00	0.00

Products on target templates
>XM_017013811.2 PREDICTED: Homo sapiens tyrosine 3-monooxygenase/tryptophan 5-monooxygenase activation protein zeta (YWHAZ), transcript variant X4, mRNA

```
product length = 126
Forward primer  1      TGACATTGGGTAGCATTAAC   20
Template        2613   ....................   2632

Reverse primer  1      GCACCTGACAAATAGAAAGA   20
Template        2738   ....................   2719
```

Figure F2. *In silico* **primer BLAST results.**

The binding specificity of each primer was assessed using the NCBI Primer BLAST® tool.

Splice variants targeted

No splice variants were targeted.

Additional primer analysis

ALP

Table F3. Primer analysis of ALP primer used in the study.

Parameter	Optimal criteria for primer design for SYBR Green assay	Forward primer	Reverse primer	Accepted
Primer length	18 – 25 bases	20	20	Yes
PCR product size	100 – 150 bp	150		Yes
Melting temperature*	55°C - 60°C >5°C difference between forward and reverse primer	50.7	50.7	No
GC content	40% - 60%	45	45	Yes
GC clamp	More than 3 G's or C's should be avoided in the last 5 bases at the 3'end of the primer	3	2	Yes
Hairpin formation	3' end hairpin > -2kcal.mol^{-1} Internal hairpin > -3kcal.mol^{-1}	0.33	0.71	Yes
Internal annealing bases	< 4 bases	3	3	Yes
Self dimer	3' end hairpin > -5kcal.mol^{-1} Internal hairpin > -6kcal.mol^{-1}	-3.9	-3.14	Yes
Cross dimer/ Hetro-dimer	3' end hairpin > -5kcal.mol^{-1} Internal hairpin > -6kcal.mol^{-1}	-6.84		No
3' end sequence	3' end terminate with G or C	Yes	Yes	Yes
Cross homology	Specifically binds to target of interest	Yes	Yes	Yes

Table adapted from DNAbiotec® (Pty) Ltd Essential qPCR™ Short Course notes (2019). Calculations were done using OligoAnalyzer available on https://eu.idtdna.com/calc/analyzer.

Self-dimer:

Forward:


```
5'        GCAACTCTATCTTTGGTCTG
          | | |      : :     : : :
3'  GTCTGGTTTCTATCTCAACG
```
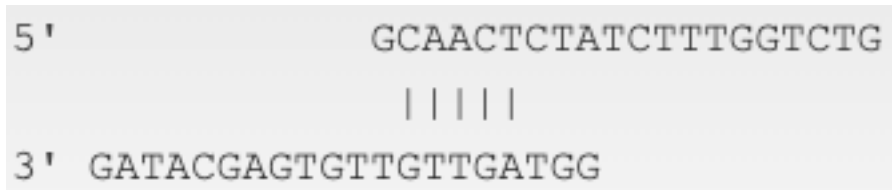
Reverse:


```
5' GGTAGTTGTTGTGAGCATAG
             :    | |    :
3'              GATACGAGTGTTGTTGATGG
```

Cross dimer:

```
5'                GCAACTCTATCTTTGGTCTG

                    | | | | |

3'   GATACGAGTGTTGTTGATGG
```
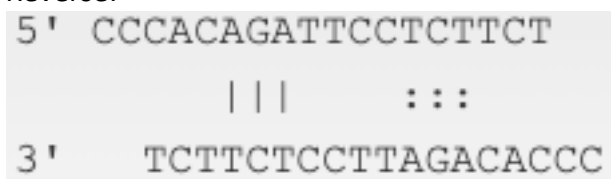
Osteocalcin (OCN)

Table F4. Primer analysis of OCN primer used in the study.

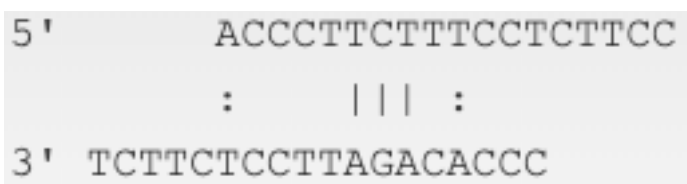| Parameter	Optimal criteria for primer design for SYBR Green assay	Forward primer	Reverse primer	Accepted
Primer length	18 – 25 bases	18	18	Yes
PCR product size	100 – 150 bp	111		Yes
Melting temperature	55°C - 60°C >5°C difference between forward and reverse primer	51.1	50.8	No
GC content	40% - 60%	50	50	Yes
GC clamp	More than 3 G's or C's should be avoided in the last 5 bases at the 3'end of the primer	3	2	Yes
Hairpin formation	3' end hairpin > -2kcal.mol^{-1} Internal hairpin > -3kcal.mol^{-1}	-	0.44	Yes
Internal annealing bases	< 4 bases	-	3	Yes
Self dimer	3' end hairpin > -5kcal.mol^{-1} Internal hairpin > -6kcal.mol^{-1}	-	-3.17	Yes
Cross dimer/ Hetro-dimer	3' end hairpin > -5kcal.mol^{-1} Internal hairpin > -6kcal.mol^{-1}	-3.17		Yes
3' end sequence	3' end terminate with G or C	Yes	No	No
Cross homology	Specifically binds to target of interest	Yes	Yes	Yes

Table adapted from DNAbiotec® (Pty) Ltd Essential qPCR™ Short Course notes (2019). Calculations were done using OligoAnalyzer available on https://eu.idtdna.com/calc/analyzer.

Self-dimer:

Reverse:

```
5' CCCACAGATTCCTCTTCT

        | | |        : : :

3'     TCTTCTCCTTAGACACCC
```

Cross dimer:

```
5'             ACCCTTCTTTCCTCTTCC

          :         | | |   :

3'  TCTTCTCCTTAGACACCC
```

```
5'  ACCCTTCTTTCCTCTTCC
            | | |
3'      TCTTCTCCTTAGACACCC
```

RUNX2

Table C5. Primer analysis of RUNX2 primer used in the study.

Parameter	Optimal criteria for primer design for SYBR Green assay	Forward primer	Reverse primer	Accepted
Primer length	18 – 25 bases	19	19	Yes
PCR product size	100 – 150 bp	117		Yes
Melting temperature	55°C - 60°C >5°C difference between forward and reverse primer	50.9	50.9	No
GC content	40% - 60%	47.4	47.4	Yes
GC clamp	More than 3 G's or C's should be avoided in the last 5 bases at the 3'end of the primer	3	2	Yes
Hairpin formation	3' end hairpin > -2kcal.mol^{-1} Internal hairpin > -3kcal.mol^{-1}	1.93	0.82	Yes
Internal annealing bases	< 4 bases	1	2	Yes
Self dimer	3' end hairpin > -5kcal.mol^{-1} Internal hairpin > -6kcal.mol^{-1}	-3.91	-3.61	Yes
Cross dimer/ Hetro-dimer	3' end hairpin > -5kcal.mol^{-1} Internal hairpin > -6kcal.mol^{-1}	-3.29		Yes
3' end sequence	3' end terminate with G or C	Yes	Yes	Yes
Cross homology	Specifically binds to target of interest	Yes	Yes	Yes

Table adapted from DNAbiotec® (Pty) Ltd Essential qPCR™ Short Course notes (2019). Calculations were done using OligoAnalyzer available on https://eu.idtdna.com/calc/analyzer.

Self-dimer:

Forward:
```
5'        ACCCATATCAGAGTTCCAG
       :    | | | |    :
3'  GACCTTGAGACTATACCCA
```

Reverse:
```
5'              GACCGTCTAAAGAGCAAAC
                     | |
3'  CAAACGAGAAATCTGCCAG
```

Cross dimer:

```
5'  ACCCATATCAGAGTTCCAG
                   | | |
3'            CAAACGAGAAATCTGCCAG
```

PPARγ

Table C6. Primer analysis of PPARγ primer used in the study.

Parameter	Optimal criteria for primer design for SYBR Green assay	Forward primer	Reverse primer	Accepted
Primer length	18 – 25 bases	18	20	Yes
PCR product size	100 – 150 bp	124		Yes
Melting temperature	55°C - 60°C >5°C difference between forward and reverse primer	50.9	50.1	No
GC content	40% - 60%	50	40	Yes
GC clamp	More than 3 G's or C's should be avoided in the last 5 bases at the 3'end of the primer	1	2	Yes
Hairpin formation	3' end hairpin > -2kcal.mol^{-1} Internal hairpin > -3kcal.mol^{-1}	-0.63	0.25	Yes
Internal annealing bases	< 4 bases	4	3	Yes
Self dimer	3' end hairpin > -5kcal.mol^{-1} Internal hairpin > -6kcal.mol^{-1}	-4.64	-4.62	Yes
Cross dimer/ Hetro-dimer	3' end hairpin > -5kcal.mol^{-1} Internal hairpin > -6kcal.mol^{-1}	-4.64		Yes
3' end sequence	3' end terminate with G or C	No	Yes	No
Cross homology	Specifically binds to target of interest	Yes	Yes	Yes

Table adapted from DNAbiotec® (Pty) Ltd Essential qPCR™ Short Course notes (2019). Calculations were done using OligoAnalyzer available on https://eu.idtdna.com/calc/analyzer.

Self-dimer:

Forward:
```
5'     CGTGGATCTCTCCGTAAT
           | | |      : : :
3'  TAATGCCTCTCTAGGTGC
```

Reverse:
```
5'                TGGATCTGTTCTTGTGAATG
                        | | | |
3'   GTAAGTGTTCTTGTCTAGGT
```

Cross dimer:

```
5'        CGTGGATCTCTCCGTAAT
          :   : :      | | |
3' GTAAGTGTTCTTGTCTAGGT
```
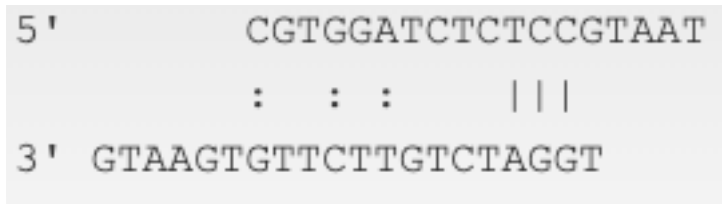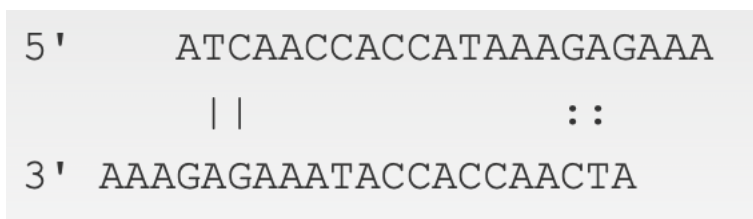
FABP4

Table C7. Primer analysis of FABP4 primer used in the study.

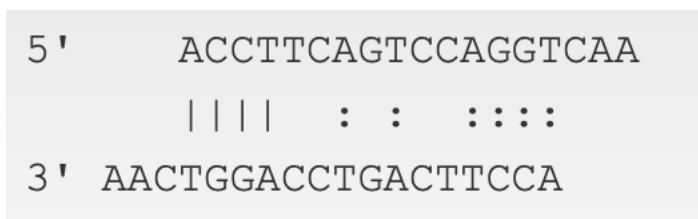| Parameter	Optimal criteria for primer design for SYBR Green assay	Forward primer	Reverse primer	Accepted
Primer length	18 – 25 bases	21	18	Yes
PCR product size	100 – 150 bp	126		Yes
Melting temperature	55°C - 60°C >5°C difference between forward and reverse primer	49.4	53	No
GC content	40% - 60%	33.3	50	No
GC clamp	More than 3 G's or C's should be avoided in the last 5 bases at the 3'end of the primer	1	2	Yes
Hairpin formation	3' end hairpin > -2kcal.mol^{-1} Internal hairpin > -3kcal.mol^{-1}	-15.8	-0.51	Yes
Internal annealing bases	< 4 bases	2	3	Yes
Self dimer	3' end hairpin > -5kcal.mol^{-1} Internal hairpin > -6kcal.mol^{-1}	-1.57	-6.01	Yes
Cross dimer/ Hetro-dimer	3' end hairpin > -5kcal.mol^{-1} Internal hairpin > -6kcal.mol^{-1}	-4.41		Yes
3' end sequence	3' end terminate with G or C	No	No	No
Cross homology	Specifically binds to target of interest	Yes	Yes	Yes

Table adapted from DNAbiotec® (Pty) Ltd Essential qPCR™ Short Course notes (2019). Calculations were done using OligoAnalyzer available on https://eu.idtdna.com/calc/analyzer.

Self-dimer:

Forward:

```
5'      ATCAACCACCATAAAGAGAAA
        | |                  : :
3' AAAGAGAAATACCACCAACTA
```

Reverse:

```
5'      ACCTTCAGTCCAGGTCAA
        | | | |   :   :    : : : :
3' AACTGGACCTGACTTCCA
```

Cross dimer:

```
5'  ATCAACCACCATAAAGAGAAA
        :   | | |     :     :     :
3'    AACTGGACCTGACTTCCA
```

TBP

Table C8. Primer analysis of TBP primer used in the study.

Parameter	Optimal criteria for primer design for SYBR Green assay	Forward primer	Reverse primer	Accepted
Primer length	18 – 25 bases	18	19	Yes
PCR product size	100 – 150 bp	130		Yes
Melting temperature	55°C - 60°C >5°C difference between forward and reverse primer	49.8	50.2	No
GC content	40% - 60%	44.4	47.4	Yes
GC clamp	More than 3 G's or C's should be avoided in the last 5 bases at the 3'end of the primer	0	2	Yes
Hairpin formation	3' end hairpin > -2kcal.mol^{-1} Internal hairpin > -3kcal.mol^{-1}	-0.46	0.3	Yes
Internal annealing bases	< 4 bases	2	2	Yes
Self dimer	3' end hairpin > -5kcal.mol^{-1} Internal hairpin > -6kcal.mol^{-1}	-3.91	-1.95	Yes
Cross dimer/ Hetro-dimer	3' end hairpin > -5kcal.mol^{-1} Internal hairpin > -6kcal.mol^{-1}	-3.52		Yes
3' end sequence	3' end terminate with G or C	No	Yes	No
Cross homology	Specifically binds to target of interest	Yes	Yes	Yes

Table adapted from DNAbiotec® (Pty) Ltd Essential qPCR™ Short Course notes (2019). Calculations were done using OligoAnalyzer available on https://eu.idtdna.com/calc/analyzer.

Self-dimer:

Forward:

```
5'  CCGAAACGCCGAATATAA
                  | | | |
3'          AATATAAGCCGCAAAGCC
```

Reverse:

```
5'    GGACTGTTCTTCACTCTTG
        : :  | |          : :  : :
3' GTTCTCACTTCTTGTCAGG
```

Cross dimer:

```
5'          CCGAAACGCCGAATATAA
            | | |    :  :
3' GTTCTCACTTCTTGTCAGG
```

GUSB

Table C9. Primer analysis of GUSB primer used in the study.

Parameter	Optimal criteria for primer design for SYBR Green assay	Forward primer	Reverse primer	Accepted
Primer length	18 – 25 bases	18	21	Yes
PCR product size	100 – 150 bp	132		Yes
Melting temperature	55°C - 60°C >5°C difference between forward and reverse primer	51	50.5	No
GC content	40% - 60%	50	42.9	Yes
GC clamp	More than 3 G's or C's should be avoided in the last 5 bases at the 3'end of the primer	1	2	Yes
Hairpin formation	3' end hairpin > -2kcal.mol^{-1} Internal hairpin > -3kcal.mol^{-1}	0.88	-0.05	Yes
Internal annealing bases	< 4 bases	2	3	Yes
Self dimer	3' end hairpin > -5kcal.mol^{-1} Internal hairpin > -6kcal.mol^{-1}	-4.62	-3.61	Yes
Cross dimer/ Hetro-dimer	3' end hairpin > -5kcal.mol^{-1} Internal hairpin > -6kcal.mol^{-1}	-4.87		Yes
3' end sequence	3' end terminate with G or C	Yes	Yes	Yes
Cross homology	Specifically binds to target of interest	Yes	Yes	Yes

Table adapted from DNAbiotec® (Pty) Ltd Essential qPCR™ Short Course notes (2019). Calculations were done using OligoAnalyzer available on https://eu.idtdna.com/calc/analyzer.

Self-dimer:

Forward:

```
5'          GATCGCTCACACCAAATC
            | | | |
3' CTAAACCACACTCGCTAG
```
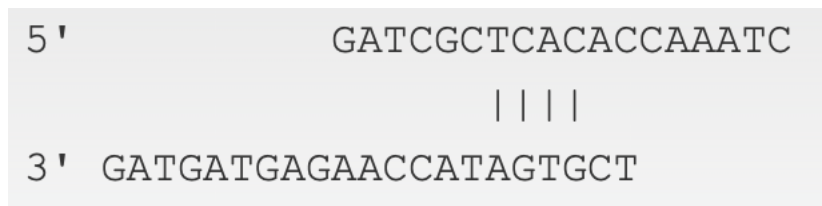
Reverse:

```
5'              TCGTGATACCAAGAGTAGTAG
                | |
3' GATGATGAGAACCATAGTGCT
```
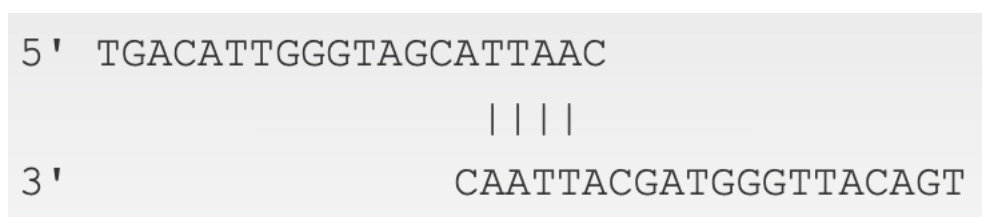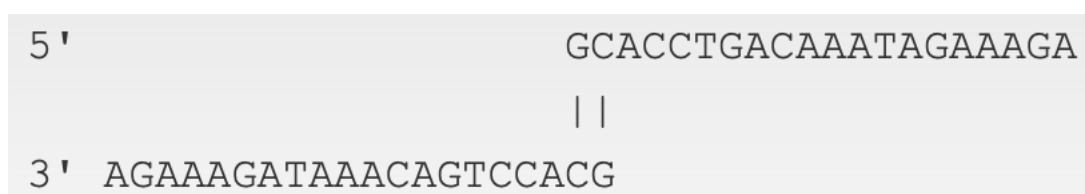
Cross dimer:

```
5'                GATCGCTCACACCAAATC
                         | | | |
3'  GATGATGAGAACCATAGTGCT
```

YWHAZ

Table C10. Primer analysis of YWHAZ primer used in the study.

Parameter	Optimal criteria for primer design for SYBR Green assay	Forward primer	Reverse primer	Accepted
Primer length	18 – 25 bases	20	20	Yes
PCR product size	100 – 150 bp			Yes
Melting temperature	55°C - 60°C >5°C difference between forward and reverse primer	50.2	50.1	No
GC content	40% - 60%	40	40	Yes
GC clamp	More than 3 G's or C's should be avoided in the last 5 bases at the 3'end of the primer	1	1	Yes
Hairpin formation	3' end hairpin > -2kcal.mol^{-1} Internal hairpin > -3kcal.mol^{-1}	0.14	0.92	Yes
Internal annealing bases	< 4 bases	2	3	Yes
Self dimer	3' end hairpin > -5kcal.mol^{-1} Internal hairpin > -6kcal.mol^{-1}	-4.85	-3.14	Yes
Cross dimer/ Hetro-dimer	3' end hairpin > -5kcal.mol^{-1} Internal hairpin > -6kcal.mol^{-1}	-4.41		Yes
3' end sequence	3' end terminate with G or C	Yes	Yes	Yes
Cross homology	Specifically binds to target of interest	Yes	Yes	Yes

Table adapted from DNAbiotec® (Pty) Ltd Essential qPCR™ Short Course notes (2019). Calculations were done using OligoAnalyzer available on https://eu.idtdna.com/calc/analyzer.

Self-dimer:

Forward:

```
5'  TGACATTGGGTAGCATTAAC
                    | | | |
3'            CAATTACGATGGGTTACAGT
```

Reverse:

```
5'                  GCACCTGACAAATAGAAAGA
                        | |
3'  AGAAAGATAAACAGTCCACG
```

Cross dimer:

```
5'          TGACATTGGGTAGCATTAAC
                 :   | | |
3'  AGAAAGATAAACAGTCCACG
```

qPCR Oligonucleotides

Primer sequences used in this study have been summarised in Chapter 5, section 5.2.11, Table 5.2.

Location and identity of any locations

There were no modifications.

Manufacture of oligonucleotides

Integrated DNA Technologies (IDT; Coralville, IA, USA) manufactured all oligonucleotides used in this study.

RT-qPCR protocol

The protocol used in this study is described in Chapter 5, section 5.2.11.

Polymerase identity and concentration

The LightCycler® 480 SYBR Green I Master Mix was used in this study. The polymerase in the master mix is FastStart™ Taq DNA polymerase (Roche, Basel, Switzerland), and the concentration was not indicated.

Buffer/kit identity and manufacturer

The LightCycler® 480 SYBR Green I Master Mix (Roche, Basel, Switzerland; Catalogue number: 04887352001) was used.

Additives

No additives were used.

Manufacture of plates/tubes and catalogue numbers

LightCycler® 480 Multiwell Plate 96 white plates (Roche, Basel, Switzerland; Catalogue 17 number: 04729692001) were used.
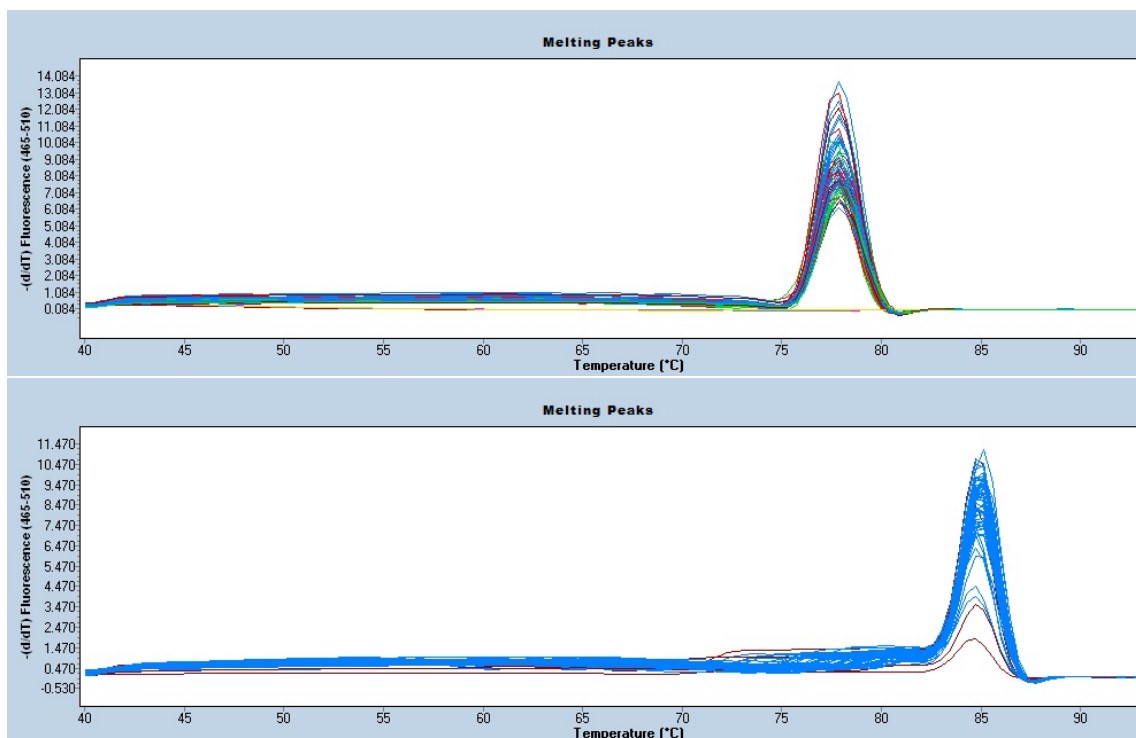
Manufacturer of qPCR instrument

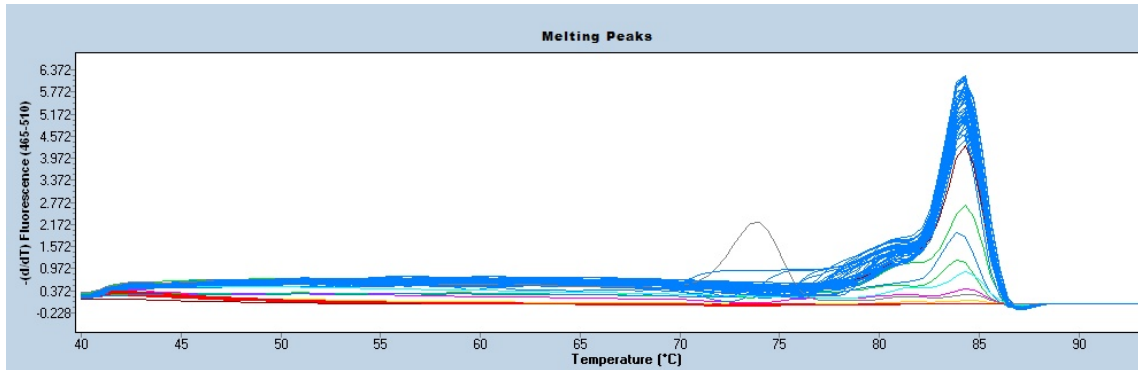The LightCycler® 480 II instrument was manufactured by Roche (Basel, Switzerland).

qPCR Validation

Specificity

The specificity of the primer binding to their targets was tested through the generation of melt curves. Melt curves can be visualised in Figure F3.
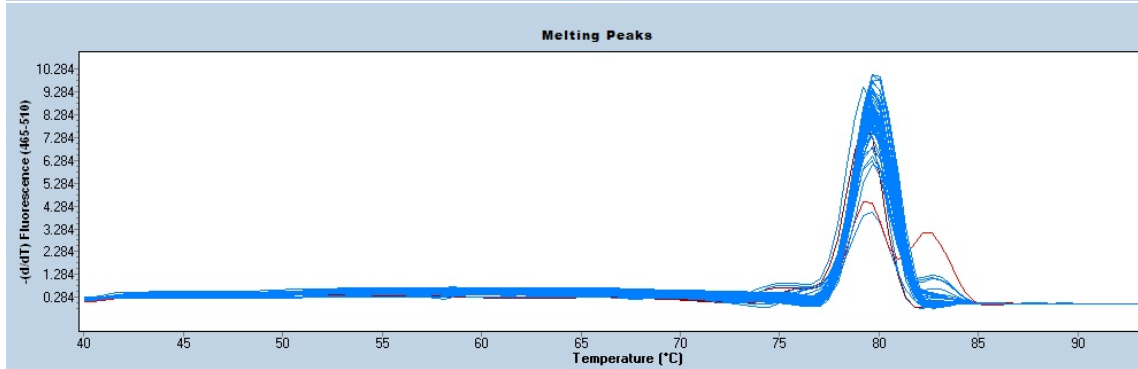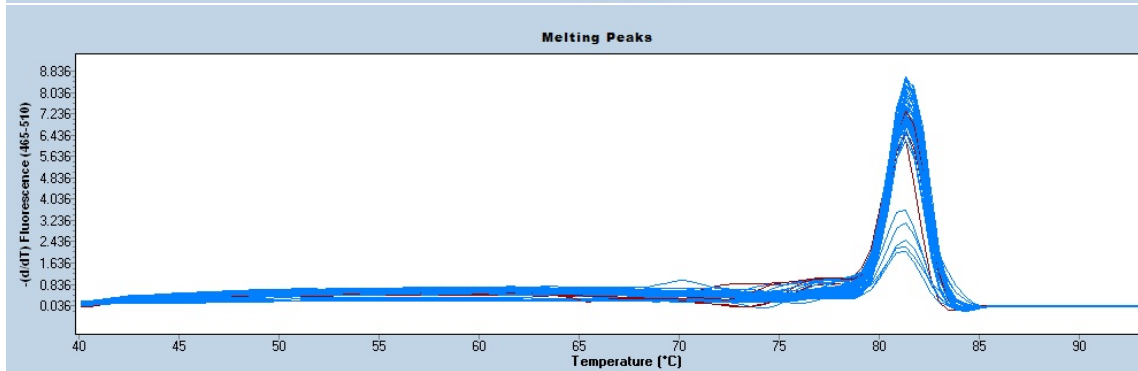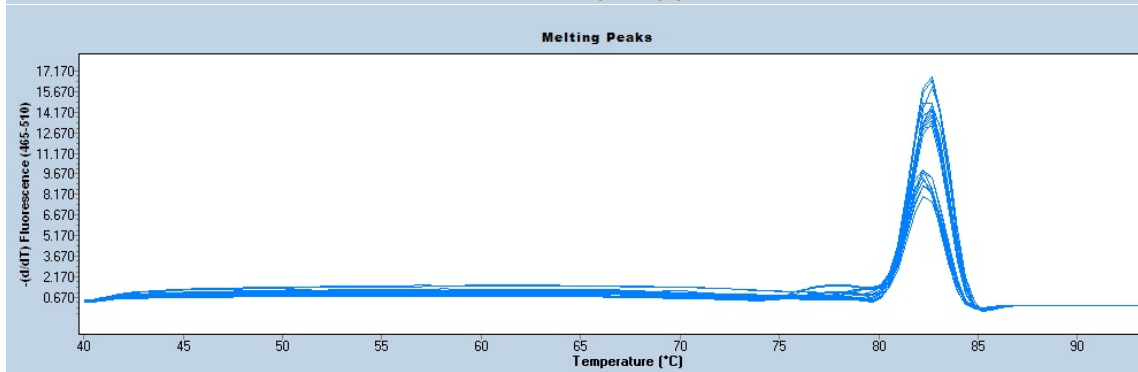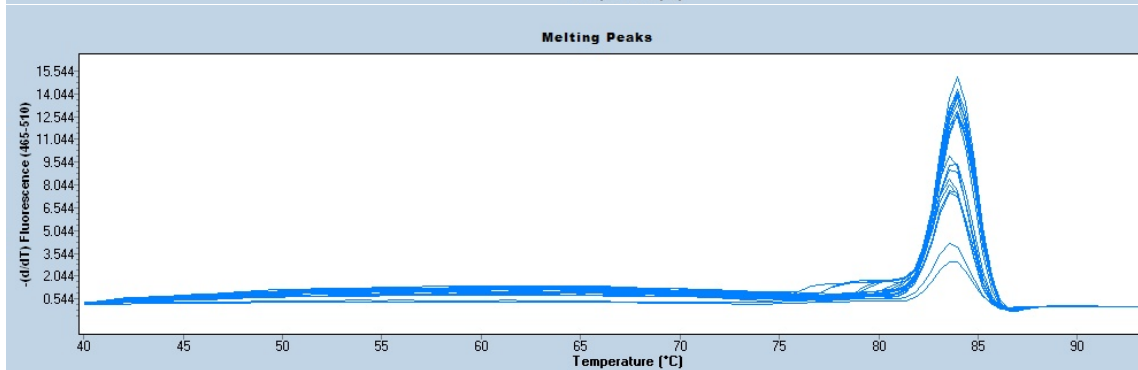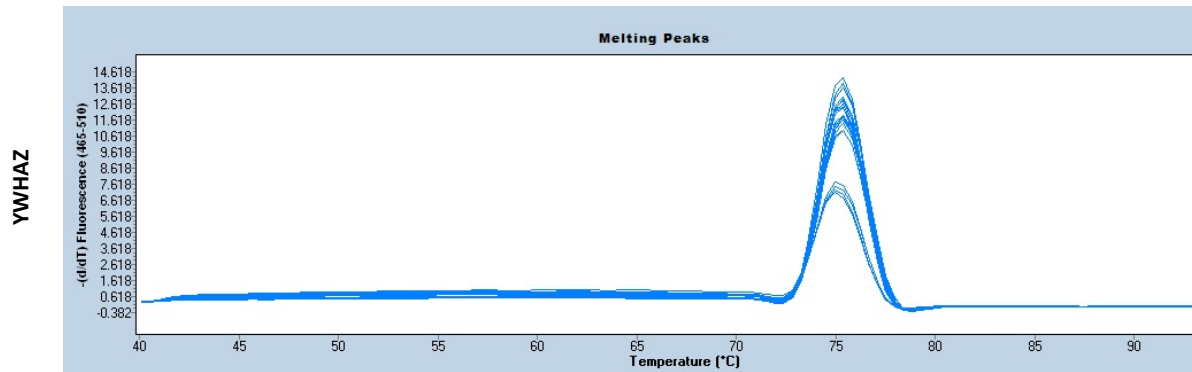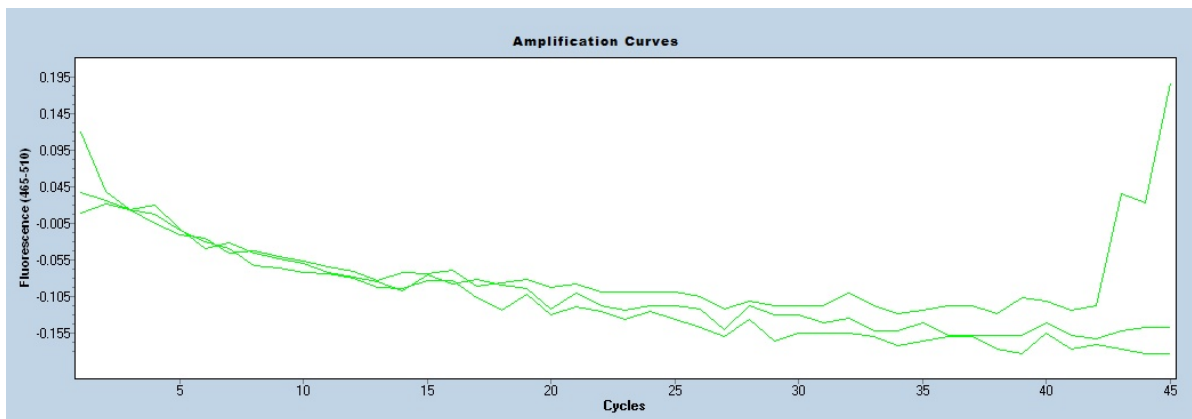
Figure F3. Melt curves of primers used in the study.
Melt curves were used to analyse the specificity of each primer binding to their binding target sites.

No template controls

No template controls were included on every plate for every target- and reference gene used in the study (Figure F4).

Figure F4. Representative Amplification Curves for No Template Control.
No template controls were included on every plate and were run in triplicate.

If amplification was detected in more than two of the three technical repeats, the plate was repeated.
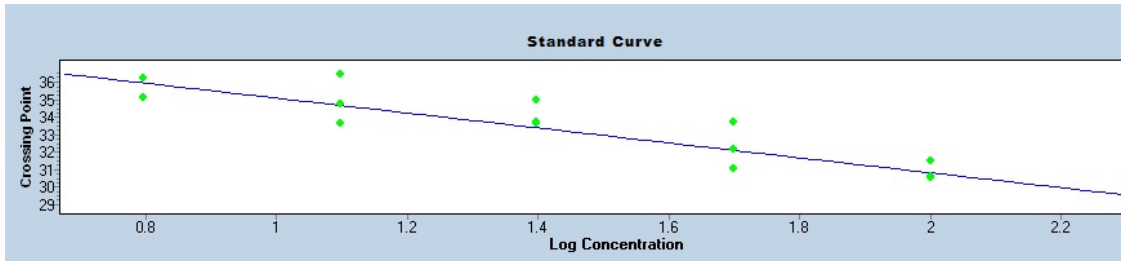
Standard curves

Standard curves were run for all genes in the study to determine the efficiency of each primer pair. The efficiency was then used to calculate relative gene expression. Figure F5 depicts the standard curves run in this study. Standards from standard curves was included on every plate and those standards had to fall on the standard curve graphs for the plate to be acceptable (Figure F6).
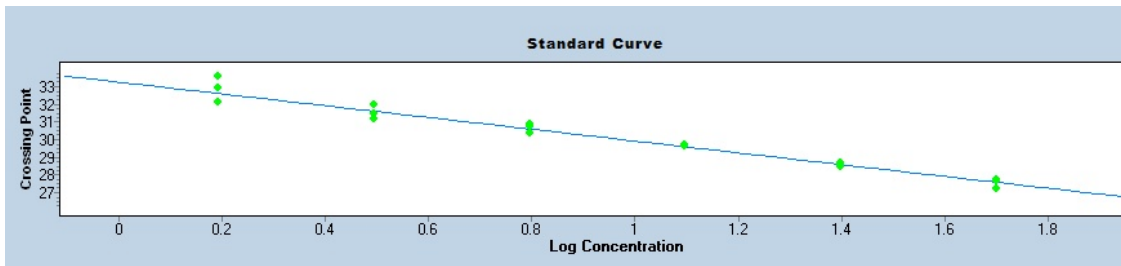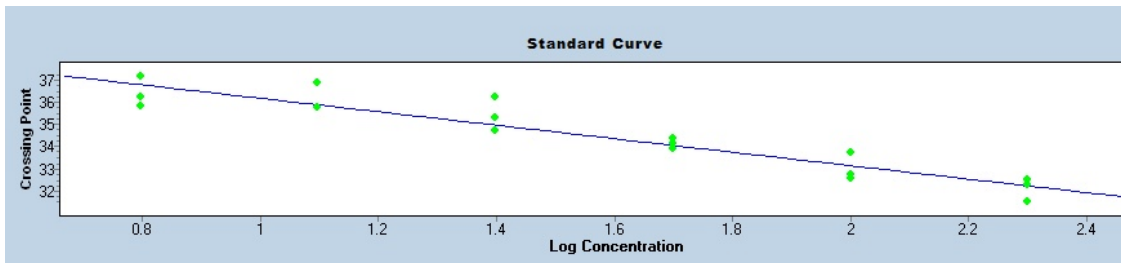
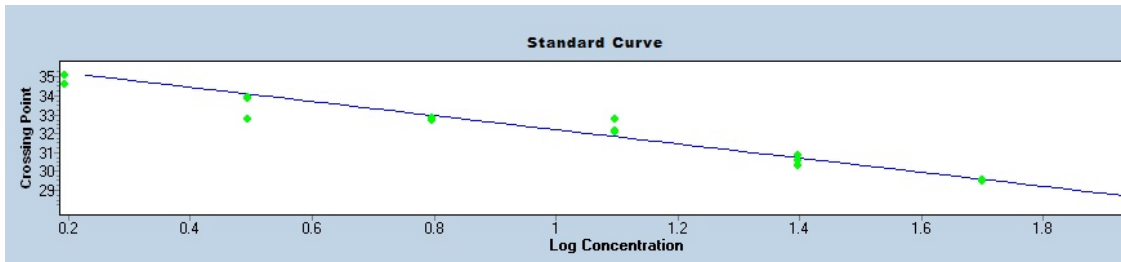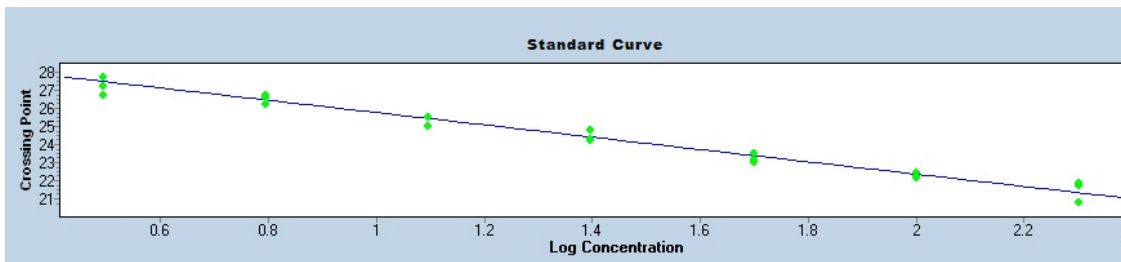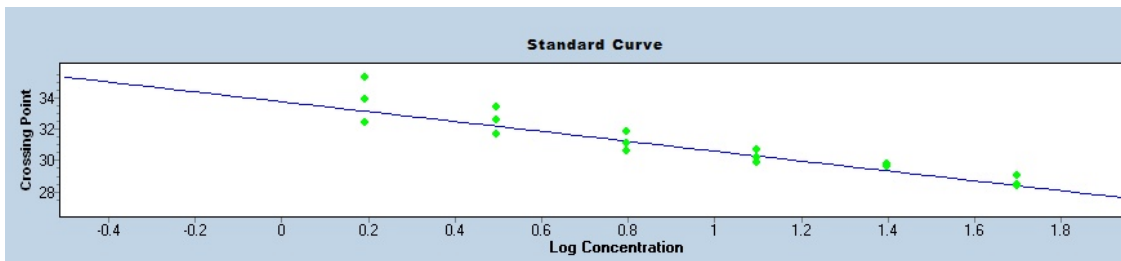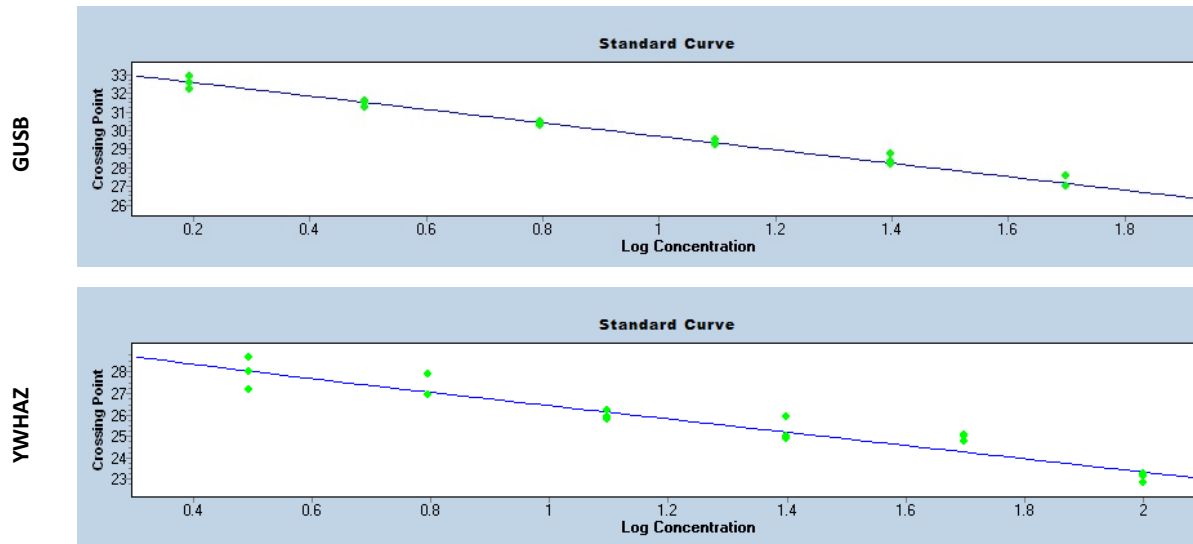**Figure F5. Standard curves for each target- and reference gene used in the study.**

Standard curves were run to determine the efficiency of each primer pair which was then used to calculate the relative gene expression.
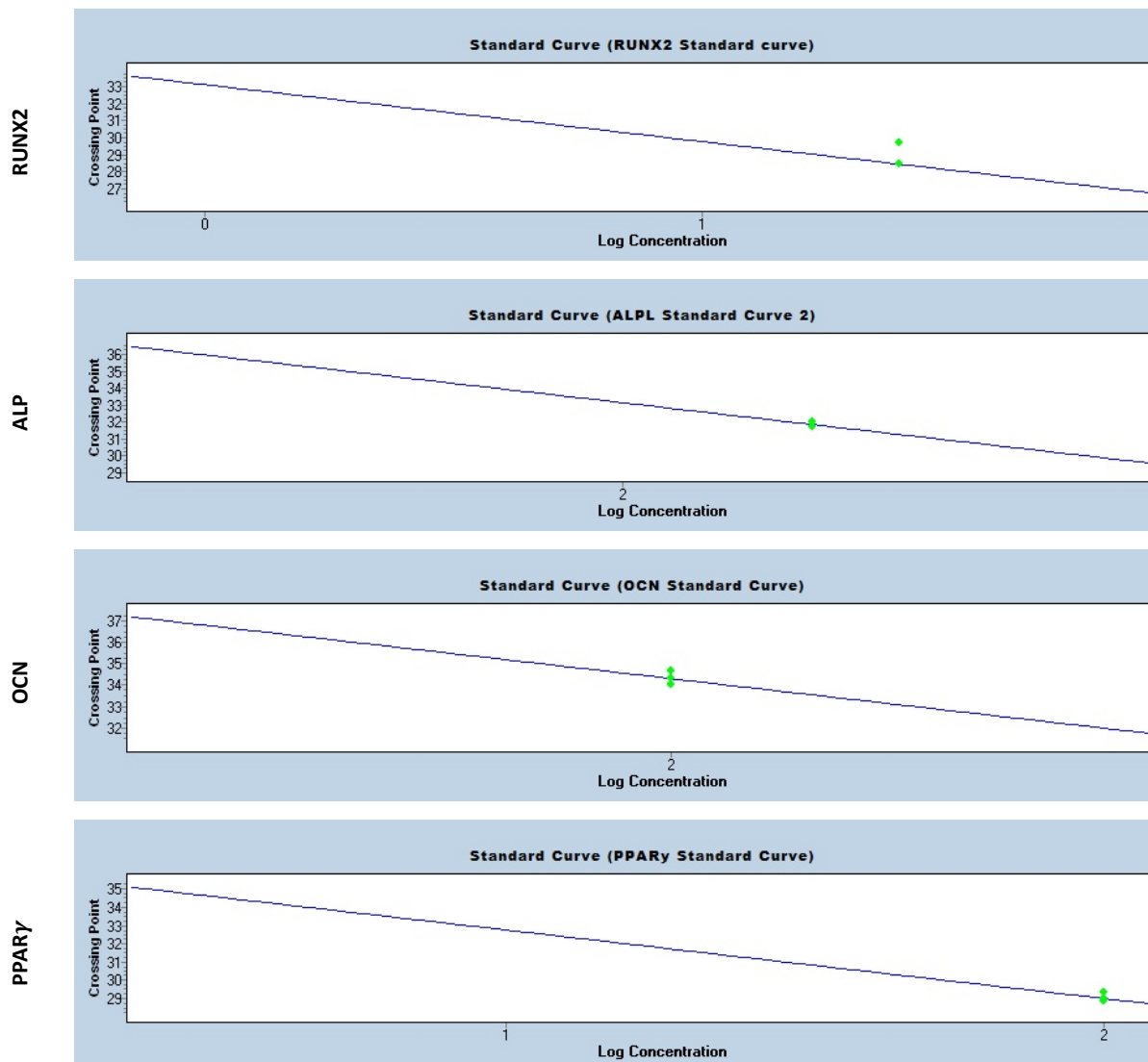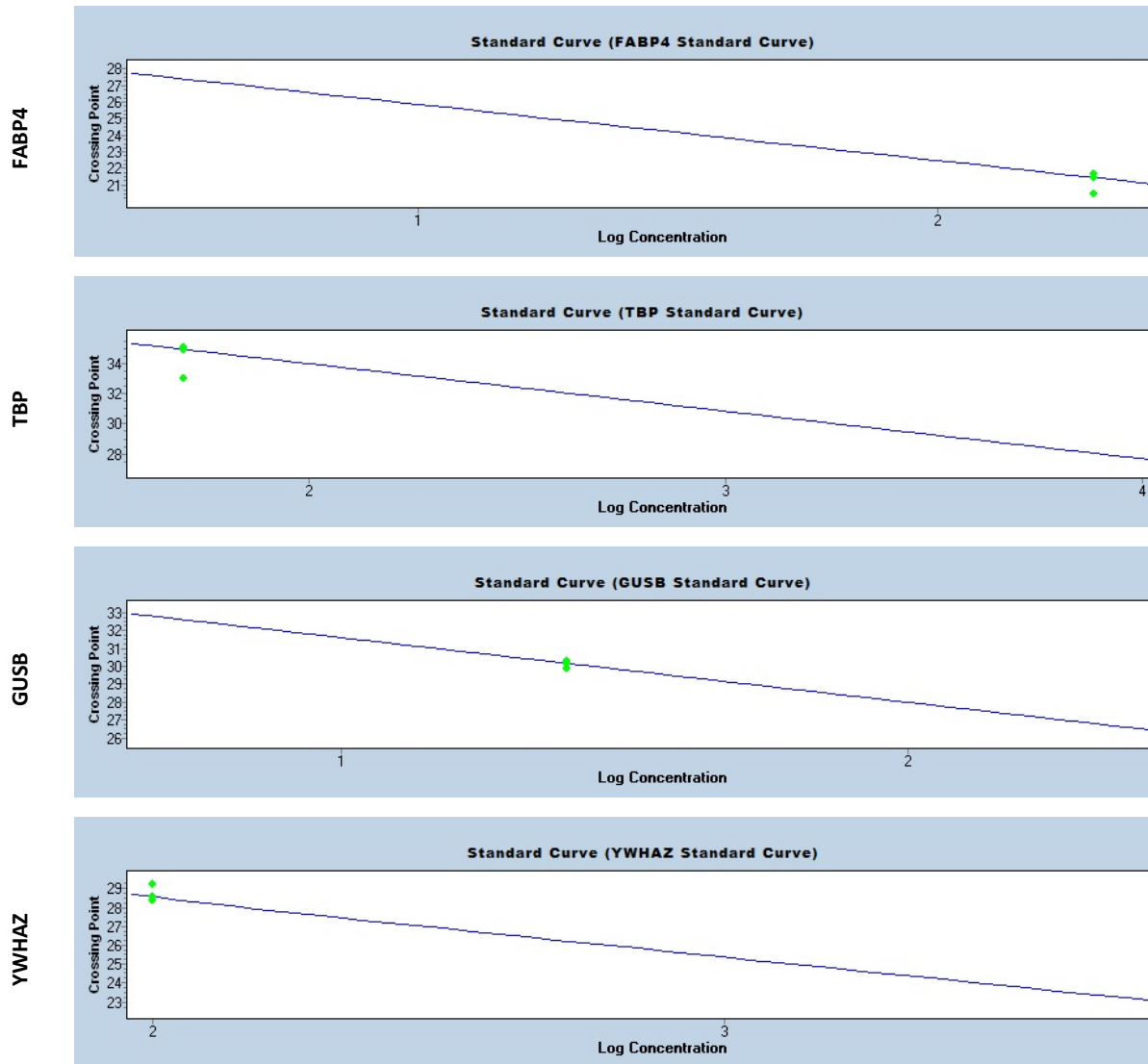
Figure F6. Representative images of standards run on experimental plates plotted on original standard curves.

Standards from standard curve experiments were run on each experimental plated to show that the conditions are comparable.

Evidence for limit of detection

Limit of detection was not performed.

If multiplex, efficiency and LOD for each assay

Multiplexing was not performed.

Data Analysis

qPCR analysis program

The LightCycler® Software (Version 1.5.1; Roche, Basel, Switzerland) was used to analyse data.

Quantitation cycle (Cq) method determination

The second derivative maximum method was used to determine the Cq-values (LightCycler®
Software and algorithms).

Outlier identification and disposition

No outliers identified.

Results of No Template Control (NTCs)

The Cq-values for the NTCs were ND (Not-detected). If at least two technical replicates amplified, the plate was re-run.

Justification of number and choice of reference genes

Three reference genes were used in this study: TBP, GUSB and YWHAZ. Reference genes were analysed in representative samples to determine if their expression was up or downregulated (Table F11). There was a slight up-regulation of reference genes in Day 21 samples and thus reference genes were ran at two time points (Day 7 and day 21, and the average Ct values were used for downstream analysis)

Table F11. Summary of Mean Cp for the 3 reference genes across multiple time points indicating suitability of reference genes

Sample number	Sample name	Condition	Day	NI	TBP (A) MeanCp	STD Cp	GUSB (B) MeanCp	STD Cp	YWAZ (C) MeanCp	STD Cp	ΔCt (A vs. B)	ΔCt (A vs. C)	ΔCt (B vs. C)
1	A150221-01A	FBS	0		25.7301935	0.13321461	22.9911711	0.03694415	19.5133999	0.04046452	2.73902246	6.21679362	3.47777116
8	A311019-02T	FBS	7	NI	26.1618342	0.20496412	22.7886815	0.14940181	20.6394519	0.8334067	3.37315264	5.5223823	2.14922966
9	A311019-02T	FBS	7	I	24.7524797	0.52026347	21.2989017	0.28546395	19.5298356	0.87795414	3.45357796	5.22264403	1.76906606
14	A311019-02T	FBS	14	NI	25.5428227	0.08383871	22.4163528	0.15774879	19.8025726	0.04947389	3.12646985	5.74025007	2.61378023
15	A311019-02T	FBS	14	I	25.2457346	0.5989449	22.5129817	0.0804652	19.1407104	0.41671256	2.73275289	6.10502411	3.37227122
16	A150221-01A	FBS	21	NI	25.4762427	0.25043689	23.6214432	0.06633348	19.2677901	0.35056378	1.85479948	6.20845255	4.35365307
17	A150221-01A	FBS	21	I	24.647768	0.26050731	22.7503425	0.13683559	19.0669968	0.11305974	1.89742553	5.5807712	3.68334568
66	A280621-01R	pHPL	0		24.9433464	0.7625542	21.8093377	0.06557392	18.6159384	0.18297832	3.13400869	6.32740795	3.19339927
67	A311019-01A	pHPL	7	NI	27.3693712	0.70211425	25.7907888	0.06182261	22.0165805	0.67089676	1.57858245	5.35279074	3.77420828
72	A280621-01R	pHPL	7	I	24.6398627	0.36116926	22.5519129	0.14659278	19.6811131	0.41730581	2.08794976	4.9587496	2.87079985
77	A280621-01R	pHPL	14	NI	25.7202892	0.2364826	22.2404961	0.27713398	20.3478067	0.33956075	3.47979305	5.3724825	1.89268945

228

78	A280621-01R	pHPL	14	I	28.2892619	0.47598923	24.5349091	0.02187088	22.2080893	0.83146506	3.75435286	6.08117258	2.32681971
83	A280621-01R	pHPL	21	NI	25.8679535	0.59156378	22.0761217	0.03985987	20.0914738	0.31824935	3.79183179	5.7764797	1.98464791
84	A280621-01R	pHPL	21	I	29.2341469	0.8339322	26.5818049	0.26923433	24.4489757	0.23185172	2.65234205	4.78517121	2.13282917
22	A280621-01R	PRP1	0		25.0646633	0.58924321	22.3978087	0.10779837	20.9716363	0.86081448	2.66685465	4.093027	1.42617234
25	A280621-01R	PRP1	7	NI	24.925458	0.25081028	21.990602	0.07668699	19.7252812	0.09146504	2.934856	5.20017683	2.26532083
26	A280621-01R	PRP1	7	I	25.0183464	0.2206534	23.9150775	0.08871236	19.7149191	0.54995028	1.10326889	5.30342726	4.20015836
33	A311019-01A	PRP1	14	NI	25.652697	0.28837344	22.5954613	0.1497299	19.9319249	0.28025968	3.05723564	5.72077209	2.66353646
34	A311019-01A	PRP1	14	I	31.8194397	0.93762176	27.5801104	0.03933793	25.0572069	0.81758299	4.23932923	6.76223271	2.52290347
39	A311019-01A	PRP1	21	NI	25.1595763	0.04432224	22.5512237	0.09980989	19.9637209	0.09027012	2.60835251	5.19585537	2.58750286
38	A280621-01R	PRP1	21	I	29.9914351	0.25787105	28.0957536	0.21261168	24.6209301	0.20812838	1.89568147	5.37050503	3.47482356
43	A280621-01R	PRP2	0		25.1896418	0.07030338	22.5794604	0.03036281	18.9461375	0.44245394	2.6101814	6.24350429	3.63332289
47	A280621-01R	PRP2	7	I	25.7855549	0.39615927	25.8738085	0.0527923	23.3976151	0.39607713	0.08825361	2.38793983	2.47619343
48	A311019-01A	PRP2	7	NI	24.5323074	0.81176826	22.0515089	0.09615275	21.4468802	1.70360059	2.48079852	3.08542719	0.60462868
52	A280621-01R	PRP2	14	NI	25.0296279	0.80968614	21.4302131	0.18175516	19.2450481	0.65114304	3.59941483	5.78457985	2.18516502
57	A311019-02T	PRP2	14	I	24.3529326	0.36207756	22.2966009	0.16768589	19.574852	0.13960382	2.05633173	4.77808057	2.72174885
58	A280621-01R	PRP2	21	NI	24.7573118	0.16964675	21.0730821	0.16583025	20.9221226	0.22556542	3.68422969	3.83518914	0.15095945
59	A280621-01R	PRP2	21	I	29.8169388	1.60456121	26.8032073	0.07515569	24.1829408	0.06210276	3.01373149	5.633998	2.62026651
85	A280621-01R	PRP3	0		28.4344303	0.2018182	24.7347779	0.003018	22.095978	0.36642374	3.69965236	6.3384523	2.63879994
90	A311019-01A	PRP3	7	NI	27.7735829	0.61430609	24.2482344	0.05801526	22.4569116	0.39787163	3.52534849	5.31667128	1.79132278
89	A280621-01R	PRP3	7	I	26.0785008	0.16268396	24.0131933	0.16092657	21.6378247	0.85908451	2.06530754	4.44067611	2.37536857
94	A280621-01R	PRP3	14	NI	29.8370575	4.45850831	32.8353864	0.18317373	28.8765006	0.55283858	2.99832887	0.96055685	3.95888572
99	A311019-02T	PRP3	14	I	26.6371015	0.14023516	23.0765297	0.07634653	22.6938426	0.2068151	3.56057183	3.94325889	0.38268706
100	A280621-01R	PRP3	21	NI	26.3938383	0.46115834	22.2266667	0.06506407	20.8610107	0.0530632	4.16717168	5.53282769	1.36565601
101	A280621-01R	PRP3	21	I	35.3203699	2.07358424	27.8995102	0.04315052	29.3891953	2.10454755	7.42085969	5.93117459	1.4896851
										Mean	2.94662347	5.17454014	2.48941767
										SD	1.18132357	1.19004992	1.01978418

Normalization method

Samples were first normalized to day 0 samples and then the induced samples were normalised to non-induced samples using the comparative CT method (Chapter 5, Section 5.2.11).

Number of biological repeats

Three ASC biological replicates were investigated. For PRP samples, three donors were also investigated against three ASC biological replicates.

Number and stage (RT or qPCR) of technical repeats

Three technical repeats were included on the qPCR plate using cDNA form the same sample.

Repeatability (Intra assay variability)

A SD of ≤ 1 between the technical replicates was considered repeatable.

Statistics

Please see Chapter 5, section 5.2.12.